CENTRO INTERNACIONAL DE ESTUDOS
DE DOUTORAMENTO E AVANZADOS
DA USC (CIEDUS)

TESIS DOCTORAL

LA TECNOLOGÍA LIDAR AL SERVICIO DE LA REPRESENTACIÓN DEL RELIEVE Y LA IDENTIFICACIÓN DE COBERTURAS DEL SUELO

ANEXOS

Sandra Buján Seoane

ESCOLA DE DOUTORAMENTO INTERNACIONAL
PROGRAMA DE DOCTORADO EN GESTIÓN SOSTENIBLE DE LA TIERRA Y EL TERRITORIO

LUGO
2018

USC
UNIVERSIDADE
DE SANTIAGO
DE COMPOSTELA

ANEXO A

Anexos del Capítulo 1. La representación del relieve

A.1 Principales algoritmos de filtrado (1996 - 2016).

En la Tabla A.1 se incluyen los principales algoritmos de filtrado desarrollados desde 1996 hasta 2016. Estos datos se emplearon para generar la Figura 1.2.

Tabla A.1: Listado de los principales algoritmos de filtrado desarrollados (1996 - 2016).

Algoritmo	Año	Tipo	Algoritmo	Año	Tipo
Arefi y Hahn (2005)	2005	Morfológico	Lodha et al. (2006)	2006	Híbrido
Axelsson (1999)	1999	Densificación	Lohmann et al. (2000)	2000	Morfológico
Bartels y Wei (2006)	2006	Segmentación	Lu et al. (2009)	2009	Híbrido
Bartels y Wei (2010)	2010	Híbrido	Maguya et al. (2013)	2013	Híbrido
Bretar y Chehata (2010)	2010	Híbrido	Meng et al. (2009)	2009	Híbrido
Briese et al. (2001)	2001	Densificación	Ming y Chen (2013)	2013	Densificación
Brovelli et al. (2002)	2002	Segmentación	Mongus y Žalik (2012)	2012	Híbrido
Chang (2010)(SMSM)	2010	Híbrido	Mongus y Žalik (2014)	2014	Híbrido
Chang (2010)(SSA)	2010	Híbrido	Nardinocchi et al. (2003)	2003	Segmentación
Chen et al. (2007)	2007	Morfológico	Pfeifer et al. (1998)	1998	Densificación
Chen et al. (2012a)	2012	Densificación	Pingel et al. (2013)	2013	Morfológico
Chen y Li (2012)	2012	Híbrido	Roggero (2001)	2001	Segmentación
Chen et al. (2013)	2013	Densificación	Schickler y Thorpe (2001)	2001	Densificación
Deng y Shi (2013)	2013	Híbrido	Schiewe (2001)	2001	Segmentación
Chen et al. (2016a)	2016	Densificación	Shan y Aparajithan (2005)	2005	Híbrido
Chen et al. (2016b)	2016	Segmentación	Shao y Chen (2008)	2008	Híbrido
Elmqvist et al. (2001)	2001	Densificación	Silván-Cárdenas y Wang (2006)	2006	Híbrido
Evans y Hudak (2007)	2007	Densificación	Sithole (2001)	2001	Densificación
Feng et al. (2009)	2009	Híbrido	Sithole (2005)	2005	Segmentación
Filin (2002)	2005	Segmentación	Sohn y Dowman (2002)	2002	Densificación
Forlani y Nardinocchi (2007)	2007	Segmentación	Su et al. (2015)	2015	Híbrido
Guan et al. (2014)	2014	Híbrido	Susaki (2012)	2012	Híbrido
Von Hansen y Vögtle (1999)	1999	Densificación	Tóvári y Pfeifer (2005)	2005	Segmentación
Haugerud y Harding (2001)	2001	Densificación	Véga et al. (2012)	2012	Híbrido
Hu et al. (2013)	2013	Híbrido	Vosselman (2000)	2000	Densificación
Hu et al. (2014)	2014	Densificación	Wack y Wimmer (2002)	2002	Densificación
Hu et al. (2015)	2015	Híbrido	Wang y Tseng (2004)	2004	Segmentación
Hui et al. (2016)	2016	Híbrido	Wang y Tseng (2010)	2010	Híbrido
Jahromi et al. (2011)	2011	Híbrido	Van de Woestyne et al. (2004)	2004	Segmentación
Kampa y Slatton (2004)	2004	Morfológico	Xiong et al. (2012)	2012	Densificación
Kilian et al. (1996)	1996	Morfológico	Yan et al. (2012)	2012	Híbrido
Kobler et al. (2007)	2007	Híbrido	Yuan et al. (2009)	2009	Híbrido
Kraus y Pfeifer (1998)	1998	Densificación	Yunfei et al. (2008)	2008	Híbrido
Krzystek (2003)	2003	Densificación	Zhang y Lin (2013)	2013	Híbrido
Lee y Younan (2003)	2003	Densificación	Zhang et al. (2003)	2003	Morfológico
Li (2013)	2013	Morfológico	Zhang et al. (2016)	2016	Densificación
Li et al. (2014)	2014	Morfológico	Zhao et al. (2016)	2016	Híbrido
Lin y Zhang (2014)	2014	Híbrido			

A.2 Integración de funciones de DTMofLabTe como complemento de otros algoritmos.

A continuación se incluye el principal resultado de la estancia de investigación realizada en el IERSE, Universidad de Azuay (Cuenca, Ecuador). Este trabajo, fue enviado a la revista *Journal of Photogrammetry, Remote Sensing and Geoinformation Science* y se encuentra pendiente de revisión. En él se demuestra como es posible combinar la función DebCloud con filtros existentes para mejorar el proceso de identificación de puntos terreno.

DebCloud
A New Tool for Improving LiDAR Data Filtering in Urban Areas

Sandra Buján[a], Chester. A. Sellers[b], Miguel Cordero[a] y David Miranda[a]

[a] LaboraTe, Departamento de Ingeniería Agroforestal. Instituto de Biodiversidad Agraria y Desarrollo Rural. Universidad de Santiago de Compostela. Escuela Politécnica Superior, C/Benigno Ledo s/n, 27002 Lugo, España; [b] Universidad de Azuay, Cuenca, Ecuador.

Identifying ground points from LiDAR data remains a challenge more than two decades after automatic filtering methods were first developed. The efficacy of filtering methods depends on both the physical characteristics of the environment and on the quality of the data used. Other limitations, affecting accessibility and usability, include the choice of filter and identification of optimal parameters. To address these problems, the existing filters have increased their level of complexity resulting in so-called hybrid methods. This study proposes the use (along with existing filters) of a debugging tool for non-ground points and a densification process to improve the filtering results for urban areas and to reduce the influence of parameters on the accuracy of the filtering process. These tools were tested in combination with the Iterative Robust Interpolation Filter (IRI) developed by Kraus y Pfeifer (1998) and implemented in the free FUSION software (McGaughey, 2018). The reference data analysed were acquired from the International Society of Photogrammetry and Remote Sensing (ISPRS). The results obtained were compared with those obtained in previous studies, by using the metrics proposed by Sithole y Vosselman (2004). For urban samples, the proposed hybrid method provided better results than the original IRI algorithm and the filter implemented in FUSION, yielding a Kappa coefficient of 91.6%. Finally, the proposed method is one the most accurate filters that has been tested with the ISPRS data.

Keywords: LiDAR ground identification, debugging and densification tools and hybrid method.

Introduction

More than half a century ago, Miller y Laflamme (1958) introduced the concept of the Digital Terrain Model (DTM)[1]. Since then, these models have been used in a wide range of applications, thanks to advances in geometry, photography, aviation, computing, Global Positioning Systems, cameras and sensors. By making geospatial information widely available, the authorities of different countries and the international scientific community have also contributed to widening the scope of DTM applications. Furthermore, these models are very important for forestry applications (González-Ferreiro et al., 2013b), natural resources modelling (Hladik y Alber, 2012), risk prevention and mitigation (Raber et al., 2007) and planning (Yan et al., 2015).

LiDAR technology has been recognized as a standard method of acquiring topographic data (Mongus y Žalik, 2012). LiDAR point clouds are composed of millions of georeferenced points representing both the terrain (ground points, P_g) and objects (non-ground points, P_{ng}). The filtering process, which seeks to identify the ground points automatically, is one of the main challenges faced in using this technology. Although many algorithms have been developed in recent years (Meng et al., 2010, Li et al., 2014, Hu et al., 2014), this problem has not been completely resolved (Zhang y Lin, 2013) and manual debugging of models remains common practice in commercial projects (Renslow, 2012).

Most filtering errors are due to the inability of filters to identify P_g in heterogeneous environments owing to either the presence of different objects (increase in commission errors) or the complexity of the terrain relief (increase in omission errors) (Aryal et al., 2017). In order to improve the filtering process, the complexity of the algorithms has been increased, resulting in so-called hybrid approaches. Most hybrid filters are derived from existing algorithms, which are modified to overcome some of their limitations. The modifications usually involve combining several of the existing methods (Silván-Cárdenas y Wang, 2006) or

[1] A DTM is simply a statistical representation of the continuous surface of the ground by a large number of selected points with known X, Y, Z coordinates in an arbitrary coordinate field.

adding a complementary process to an existing algorithm (Chang, 2010, Véga et al., 2012).

Finally, from the users' point of view, limitations associated with the accessibility and usability of the methods - rather than their efficacy - are also important. Thus, after the best filter has been identified, the values of the parameters that will minimize the filtering errors should be selected. For this purpose, good knowledge of the functioning and characteristics of the different filters available is required. However, such knowledge is difficult to acquire because most of the details of filtering algorithms are jealously safeguarded by their creators (Zhang y Lin, 2013). On the other hand, the effects of changes in parameters on the filtering results have not been widely studied.

Following the hybrid approach, this study proposes complementing the existing filtering algorithms with a debugging tool and a densification process. Our purpose is to improve the filtering accuracy by reducing commission errors in urban areas and also reducing the influence of parameters in the final accuracy. This approach was tested by using an adaptation of the Iterative Robust Interpolation algorithm (IRI) developed by Kraus y Pfeifer (1998), implemented in the free FUSION software (McGaughey, 2018) and the reference data of the International Society of Photogrammetry and Remote Sensing (ISPRS).

Methodology

LiDAR data

The LiDAR data used in this study were acquired during an aerial survey of the city of Stuttgart (Germany) with an Optech ALTM laser scanner system (in the second phase of the EuroSDR project). The data were published by *Working Group III/3* of ISPRS on its website (`http://www.itc.nl/isprswgIII-3/filtertest/`). The scanned area includes 15 reference areas, 9 urban areas (Sample 11 - 42) and 6 rural areas (Sample 51 - 71). However, in this study, we only used the urban samples. Each point was classified into either of two classes by combining

Tabla A.2: Characteristics of the ISPRS urban reference samples.

Sample - Characteristics	**Points**			**Density**	**Slope** (%)	
	P_g(outliers)	P_{ng}(outliers)	P_g/P_{ng}	(pts/ m^2)	Mean	Q90
S11 - Vegetation and buildings on hillside	21786 (9)	16224 (13)	1.3	0.93	53.8	100.0
S12 - Buildings and cars	26691 (37)	25428 (35)	1.0	0.95	11.9	26.8
S21 - Narrow bridge	10085 (0)	2875 (0)	3.5	0.89	7.5	17.2
S22 - Bridge and gangway	22504 (6)	10202 (17)	2.2	0.96	16.4	43.9
S23 - Large buildings and data gaps	13223 (0)	11872 (1)	1.1	0.82	24.2	60.4
S24 - Ramp	5434 (30)	2059 (1)	2.6	0.83	24.1	57.0
S31 - Large buildings	15556 (2)	13306 (14)	1.2	1.01	4.6	9.2
S41 - Outliers (multi-path error)	5602 (0)	5629 (116)	1.0	0.63	12.8	28.2
S42 - Railway station	12443 (0)	30027 (2)	0.4	0.91	6.8	15.5

semi-automatic and manual filtering techniques: ground (P_g coded as 0) and non-ground (P_{ng} coded as 1) (Vosselman, 2003). The characteristics of the reference samples are summarised in Table A.2. In addition to the number of P_g and P_{ng}, the table also includes the proportion of P_g relative to P_{ng}, the point density and the terrain slope (mean and the quantile of 90%).

In order to prevent errors in the filtering process, the low outliers (caused by the multi-path effect or by registration errors) were identified and removed from the point clouds by a process that combines the threshold method and a radial elimination method (Meng et al., 2010, Hu et al., 2014). The cells in columns P_g and P_{ng} in Table A.2 show the original number of ground and non-ground points before the outliers were removed. The number of outliers is shown in brackets.

Iterative Robust Interpolation filter

Following the definition proposed by Sohn y Dowman (2008), LiDAR data filtering consists of classifying N discrete points S=s_1, s_2,..., s_N as ground or objects, {g, ng}, where each point is defined by its coordinates s_i=(x_i, y_i, z_i) $\in$ R^3. The *Iterative Robust Interpolation* algorithm of Kraus y Pfeifer (1998), a hierarchical filtering method implemented in SCOP++ software (Pfeifer et al., 2001), approaches the problem of classifying LiDAR points by creating a reference surface $\varphi_t(x,y)$ from S and applying an interpolation method that uses linear prediction (kriging), where t represents the iteration number and φ_t is iteratively

modified by using a weighting function $\rho(v_i)$ and the differences between the elevation of s_i and its projection on φ_t (v_i=z_i-$\varphi_t(x_i,\ y_i)$).

In the first iteration, all points have the same weight s_i=(x_i, y_i, z_i, ρ_i=1) and the influence of each s_i is the same in creating $\varphi_{t=1}$. Theoretically, the probability that the points situated below φ_t correspond to ground is greater than that of the points situated above φ_t. On the basis of this idea, in successive iterations ρ_i was recalculated for each point, from the residuals v_i and the weighting function $\rho(v)$, so that the points with large negative residuals (residuals $< g$) were assigned the maximum weighting (i.e. a value of 1) whereas the weighting will decrease as the residuals approach the value of g+w, where the value assigned will be 0. Those points with the lowest weighting will have the least influence in creating φ_t, so that φ_t will be "attracted" by the points with the next highest weighting. Thus, the point representing objects will be iteratively assigned increasingly lower weighting so that φ_t will be displaced and will correspond to the actual ground relief (Pfeifer y Mandlburger, 2008). Parameters a and b define the slope of the weighting function, i.e. as the weighting function decreases until taking a value of 0, parameter g indicates where the function begins to decrease, whereas parameter w is used to establish the maximum threshold above which the points will not influence the generation of intermediate surfaces. The values of parameters a, b and w are fixed during the whole process, whereas the value of g varies automatically in each iteration depending on the residuals v_i. More details on the functioning of this algorithm can be found in Kraus y Pfeifer (1998), Pfeifer et al. (2001) and Pfeifer y Mandlburger (2008).

The FUSION software (v.3.7) (available free of charge here) implements an adapted version of the IRI algorithm under the name *GroundFilter*. There are several differences between this algorithm and the original IRI filter. First, the value of g remains fixed throughout the whole process. Second, all points that satisfy $v_i < g$ or $g < v_i < g$+w are considered P_g in the last iteration. Finally, the intermediate surfaces are calculated by assigning the average elevation of all points in that cell (cs) to each pixel. In this study, we modified the default values of g and w parameters and we also used a median filter (*/median* switch with m by m window) to smooth the intermediate surfaces and to reduce

the commission errors. Other parameters remained as default. See McGaughey (2018) for detailed analysis of the *GroundFilter* function.

The DebCloud function

If most P_{ng} corresponding to large buildings are removed from the point cloud before the application of filtering algorithms that involve generation of an initial reference surface, either from a sample (Mongus y Žalik, 2012) or from all points (Kraus y Pfeifer, 1998), it should be possible to reduce the commission errors in the surface, thus decreasing the size of the selection window in the case of algorithms that include a seed point selection process and improving the general accuracy of the filtering process. Following the studies of Chang (2010) and Véga et al. (2012), we developed and used the *DebCloud* function to produce a refined point cloud (S_D) by detecting and deleting the highest points in a local environment from the LiDAR data. Likewise, the function was programmed in the free software environment R (R Development Core Team, 2010) in an attempt to address the challenge of usability and accessibility of methods of processing LiDAR data.

The *DebCloud* function is defined by 3 variables: input LiDAR data (S); the maximum size of the area without P_g, usually identified from the lower side of the largest building in the area (c); and the maximum residual allowed (δ_h). In addition, this function is created in two steps: 1) automatic calculation of variables and 2) debugging of the point cloud. Figure A.1 includes the *DebCloud* code.

Step 1. Automatic calculation of variables The density (D), which represents the average point density, was calculated as (Eq. A.1)

$$D = NS/(max\ x_i - min\ x_i) \cdot (max\ y_i - min\ y_i) \qquad \text{(A.1)}$$

where D is the average point density of points, NS is the total number of points in S and x_i and y_i are the X and Y coordinates.

The minimum and maximum slope thresholds were then established (Sl_{min} and Sl_{max}) from the 65% and 90% quantiles of the cell values of slope surface (φ_{slope}). This surface was calculated from an initial DTM (φ_{DTM}) obtained by interpolating the lowest points (S_S). To select these points, a mobile window equal to c and longitudinal and transverse overlap equal to 50% were used. Finally, the penetrability was defined as the percentage of P_g relative to the total number of points in each cell (the cell size equal to $\sqrt{np/D}$, where np represents the count of points per cell necessary to calculate the penetrability, in this case $np = 8$). A point was considered P_g, if $\delta_i < 0.5$m, where δ_i represents the residual of each point and is calculated from the difference in elevation between S and φ_{DTM}. Empty cells were represented by NA.

DebCloud. Detecting and deleting the highest points in a local environment.

Inputs: Point cloud={S}, window size c, allowed maximum residual δ_h

Step 1. Automatic calculation of variables
- Calculate average density from {S} →D
- Select seed points in {S} → {S_S}, rasterize {S_S} → φ_{DTM}, calculate slope surface from φ_{DTM} → φ_{slope}, calculate Q65 from φ_{slope} → Sl_{min}, calculate Q90 from φ_{slope} → Sl_{max}
- Calculate point residuals from {S} and φ_{DTM}→ s_i=(x_i, y_i, z_i, δ_i)
- Calculate penetrability surface from s_i=(x_i, y_i, z_i, δ_i)→ φ_{PNT}

Step 2. Debugging the point cloud

Set L=1 and set O = 0.5

while $L \leq 2$ **do**
- **if** $L = 1$ **then** $C = c$ **else** $C = 0.75 \cdot c$ **end if**
- Define a square window, size=C → W_C, Define a square window, size=$1.5 \cdot C$ → W_W, Set $\overline{NS_W}=D \cdot (1.5 \cdot C)^2$
- Set geographical scope from {S} and W_W→ TRC=(x_{TRC}, y_{TRC}) and BLC=(x_{BLC}, y_{BLC})
- Displacement of W_W from BLC to TRC, overlap=O → Region list {R}
- **for all** {R} **do**
  - Available points in each region {S_W}
  - **if** $NS_W < 0.1 \cdot \overline{NS_W}$ **then** {S_W} $\xrightarrow{include}$ {S_D}, {S_W} ← Ø **else**
    - **while** {S_W} is not empty **do**
      - Highest point in {S_W} → s_{max}=(x_{max}, y_{max}, z_{max})
      - Available points in a W_C region centered in s_{max} {S_C},
      - Lowest point in {S_C} → s_{min}=(x_{min}, y_{min}, z_{min})
      - Slope between s_{min} and s_{max} → Sl
      - **if** z_{max}=z_{min} **or** $Sl \leq Sl_{min}$ **then** {S_W} $\xrightarrow{include}$ {S_D}, {S_W} ← Ø
      - **else if** $Sl \geq Sl_{max}$ **then** {s_{max}} $\xrightarrow{remove}$ {S_W} **else**
        - Lowest points in {S_C} ∩ cells whose $\varphi_{PNT} > 0$ → {S_R},
        - Rasterize {S_R} → $\varphi_{reference}$
        - Calculate residual from {s_{max}} and $\varphi_{reference}$→ s_{max}=(x_{max}, y_{max}, z_{max}, δ_{max})
        - **if** $\delta_{max} > \delta_h$ **then** {s_{max}} $\xrightarrow{remove}$ {S_W} **else**
          - {S_W} $\xrightarrow{include}$ {S_D}, {S_W} ← Ø
        - **end if**
      - **end if**
    - **end while**
  - **end if**
- **end for**
- Set L=(L + 1), Set Point cloud={S_D}

end while

Remove duplicated points in{S_D}

Return {S_D}

Figura A.1: DebCloud code.

Step 2. Debugging the point cloud Although this step was carried out at two levels (L), the same operations were used at both levels to produce the refined point cloud (S_D). In the first step, the size of analytical window (W_C) was defined on the basis of parameter c. At the first level, the size of W_C (C) is c, but at the second level this value was reduced by 25% in order to eliminate points corresponding to small objects. On the other hand, as the search window for the highest points (W_W) should include P_g and P_{ng}, a weighting coefficient of 1.5

was applied to the size of W_C in order to establish the size of W_W ($1.5 \cdot C$). The weighting coefficients were established by trial and error and checking the quality of results. In addition, the theoretical number of points that should be included in a window W_W was calculated as $N\bar{S}_W$ by multiplying D and $(1.5 \cdot C)^2$.

Then, the geographical scope was defined by the data zone plus an exterior buffer of $0.5 \cdot W_W$, to prevent the edge effect. W_W was then moved from the bottom left corner (BLC) to the top right corner (TRC), and a longitudinal and transverse overlap between windows equal to 50% was applied (O). In each position, all points that fell within the window W_W were selected (S_W). If the number of S_W ($\mathrm{N}S_W$) was lower than 10% of $N\bar{S}_W$, the debugging process was not required. S_W points were then selected and became part of the refined point cloud (S_D). New points were selected by moving W_W from left to right by $O \cdot W_W$ meters. Conversely, if $\mathrm{N}S_W \geq 0.1 \cdot N\bar{S}_W$, the highest point ($s_{max}$) in S_W was selected. In order to decide whether or not s_{max} was P_g, a local area defined by W_C and centred in s_{max} was considered. In this area, points neighbouring s_{max} were selected (S_C), and the lowest point was identified (s_{min}). Finally, the slope between s_{min} and s_{max} was calculated[2] (Sl).

Three situations were then considered: 1) if s_{min} and s_{max} elevations were the same or the slope between s_{min} and s_{max} was less than Sl_{min}, S_W points (including s_{max}) were considered P_g and therefore added to S_D. W_W was then moved one position, the new points were selected (S_W) and the number of S_W was evaluated again; 2) if the slope between s_{min} and s_{max} was greater than Sl_{max}, then s_{max} was removed from S_W, a new highest point was selected and the previous steps were repeated to check whether or not s_{max} was P_g; 3) finally, if $Sl_{min} < Sl < Sl_{max}$, a decision cannot be made on the basis of the slope and the difference in elevation relative to s_{max}, and therefore a reference surface[3] ($\varphi_{reference}$) was taken into account (δ_{max}). Then, if δ_{max} was greater than δ_h, as the in previous case, s_{max} was removed from S_W, and a new highest point

[2] $\mathrm{Sl}=\mathrm{z}_{max}\text{-}\mathrm{z}_{min}/\sqrt{(x_{max}-x_{min})^2 + (y_{max}-y_{min})^2}$

[3] $\varphi_{reference}$ is created by interpolating a set of lowest points (S_R), which are selected from S_C in the cells of φ_{PNT} whose penetrability > 0, and using the R code: lm(Z~(X+Y)^2+I(X^2) +I(Y^2),data= S_R) (in *scatter3d* function, *car* package v.2.1-2).

was selected. Otherwise, S_W points (including s_{max}) were considered P_g and added to S_D. W_W was then moved one position, the new points were selected (S_W) and the number of S_W was re-evaluated. At the second level, the above process was repeated considering the refined point cloud (S_D), obtained in the first level, as input data. Finally, a point can be selected several times due to overlapping between windows. In this case, the duplicated points in S_D were deleted.

Hybrid method: DebCloud and GroundFilter

The proposed hybrid method combines the *DebCloud* function, the *GroundFilter* function (an adaptation of the IRI filter by Kraus y Pfeifer (1998)) and a densification process. Figure A.2 shows an outline of the filtering process in the hybrid method. First, the original point cloud (S) was refined using the *DebCloud* function (after establishing the parameters c and δ_h), producing a refined point cloud (S_D). Second, the *GroundFilter* parameters (g, w, m and cs) were established, and this filter was run using the S_D as input data, producing ground point cloud (S_g). In order to correct omission errors, the ground points were interpolated using the *GridSurfaceCreate* function of FUSION software (φ_t) and the differences in elevation between each point of S and φ_t were calculated (residuals). All points with residual lower than or equal to δ_h were considered P_g and were added to S_g.

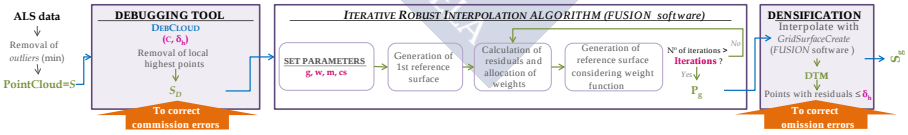

Figura A.2: Hybrid method flowchart.

Accuracy assessment and data analysis

We used the accuracy metrics proposed by Sithole y Vosselman (2004) for quantitative analysis of filter performance. Three types of errors were calculated for this purpose: Type I errors (*TIe* or omission

errors), Type II errors (*TIIe* or commission errors) and the total error (*Te*). In addition, in order to increase the robustness of the precision measurement and to guarantee that the concordance between the reference simple and the filtering results did not occur by chance, the Cohen's Kappa coefficient (K) (Cohen, 1960) was calculated.

To analyse the filtering results, we first fitted the *DebCloud* and *GroundFilter* parameters. The filtering results for the 9 reference urban samples for each of the combinations of parameters enabled both internal and external evaluation (Figure A.3). In the first case, we evaluated the efficacy of the debugging process by using the *DebCloud* function and examined the influence of the different parameters in the filtering results by considering the FUSION and hybrid methods. In the latter case, we tackled one of the limitations identified by users of filtering algorithms, i.e. selection of the parameters values so that application of the *DebCloud* function facilitates selection of the *GroundFilter* parameters. For external evaluation, we applied the evaluation paradigm used by Sithole y Vosselman (2004), so that our results were compared with those obtained in 14 previous studies.

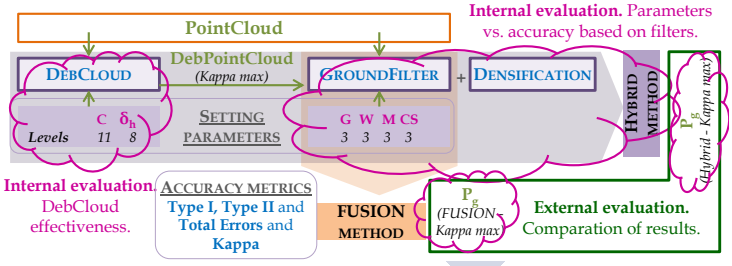

Figura A.3: Data analysis: internal and external assessment.

Results and discussion

We used the ISPRS reference LiDAR data (http://www.itc.nl/isprswgIII-3/filtertest/) to evaluate our results. Use of these data enabled us to check the efficacy of the debugging process and the influence of both debugging and densification processes on parameter selection (internal evaluation). We also compared our results with those

reported in the existing literature on the subject (external evaluation).

In order to obtain the filtering optimal parameters and to carry out the assessment, we first fitted the parameters of the *DebCloud* function (c and δ_h) and *GroundFilter* function (g, w, m and cs). The ranges for each parameter were as follows: $c \in$ [12,32] at intervals of 2m; $\delta_h \in$ [0.3,1] at intervals of 0.1m; $g \in$ [-2,-1] at intervals of 0.5m; $w \in$ [1.5,3.5] at intervals of 1m; $m \in$ [3,7] and $cs \in$ [1,5] at intervals of 2m. Finally, those parameters that maximized the Kappa coefficient were selected as optimal. Figure A.4 shows a graphical plot of the results of fitted process, which shows that the debugging process (hybrid method) homogenized the values of *GroundFilter* parameters relative to the case in which no debugging was used (FUSION method).

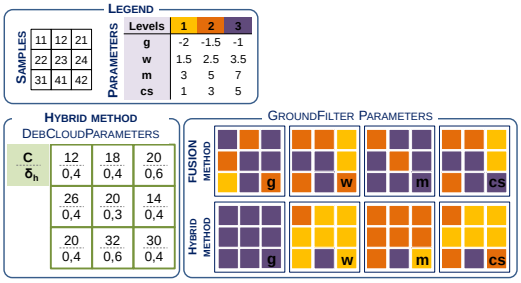

Figura A.4: Filtering optimal parameters for FUSION and hybrid methods.

Internal evaluation

Figure A.5 shows the quantitative results of internal evaluation and Figure A.6 shows the qualitative results of debugging process. Figure A.5a shows the number of original points (blue bars) and the refined points (pink bars) for each sample. It also includes the quantitative results (Te and K) obtained using the optimal parameters (Figure A.4). For almost 80% of the urban areas, the Kappa coefficient was $>$ 80%, indicating that the debugging process was effective. The efficacy of the debugging process is evident in the urban areas with simple relief and large buildings (Figures A.6c-A.6d and Figures A.6g-A.6h) or discontinuities in data (Figures A.6e-A.6f). However, the complexity of some scenes, as in sample 11 - in which vegetation coexists with buildings and steep slopes (mean slope $>$ 50%, Table A.2)- was the

main source of error in the debugging process (Te=21.7%) (Figures A.6a-A.6b).

Figure A.5b was created from the the Kappa coefficient of all combinations of parameters in the FUSION (green boxes) and hybrid methods (pink boxes). The interquartile range of K is lowest for those samples for which the *DebCloud* function was most effective. In terms of accuracy, small interquartile ranges indicate that variations in the parameters g, w, m and cs had little effect on the filtering accuracy. Thus, comparison of the results obtained with the FUSION and hybrid methods revealed that in general, except for sample 11, the range was much smaller for the hybrid method (Figure A.5b, pink boxes) than for the FUSION method (Figure A.5b, green boxes). We can therefore conclude that debugging the point cloud P_{ng} prior to filtering reduces the influence of the filtering parameters on the quality of filtering. These findings, together with the results shown in Figure A.4 (i.e. that an almost standard combination of parameters provided the best filtering results in different environments) demonstrate that use of the *DebCloud* function in combination with another filter may simplify the parameter selection and positively affect the efficiency, efficacy and usability of the filtering process.

External evaluation

Table A.3 shows the results of the original IRI algorithm of Kraus y Pfeifer (1998), included in the study of Sithole y Vosselman (2004), for the ISPRS urban reference samples. It also shows the quantitative and 3D qualitative (*Gph* column) results of the FUSION and hybrid methods. The global errors, included in the final row of Table A.3 were obtained by using all points classified incorrectly and correctly as P_g and P_{ng} in the urban reference samples (rather than the arithmetic average of the errors).

In almost 80% of the urban samples, the hybrid method yielded a Te value lower than 6% and K higher than 85%. For the whole set of urban samples, the Te and K values were 4.2% and 91.6%, respectively.

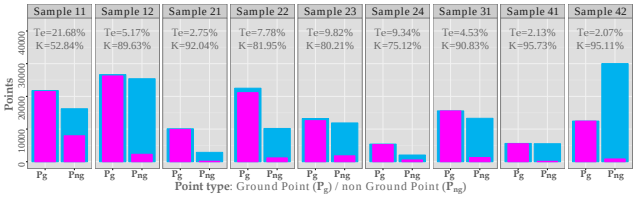

(a) Effectiveness of DebCloud function (original points in blue and refined-point cloud in pink).

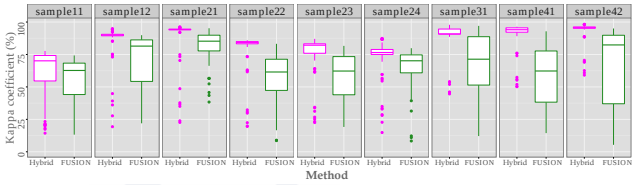

(b) Influence of the parameters in the filtering accuracy.

Figura A.5: Quantitative results of internal evaluation.

The values obtained using the hybrid method (K=91.6%) were about 5% and 3% higher than those obtained by respectively the IRI and FUSION methods. By contrast, at the individual level, the hybrid method produced better results than the IRI algorithm and the FUSION method for all reference samples. Moreover, comparison of the *TIIe* obtained with the FUSION and hybrid methods shows that one of the objectives of using the *DebCloud* function, i.e. reducing the commission errors, was achieved - without affecting the omission errors for most samples. If we extend the comparison to the results obtained with the IRI method, we see that the omission errors were larger. However, in both the study by Kraus y Pfeifer (1998) and in the other studies included in the comparison carried out by Sithole y Vosselman (2004), the aim was to minimize the *TIIe* values at the expense of increasing the *TIe* values, which negatively affected *Te*. Although the tendency in the most recently developed filtering methods (in the last decade) has been to minimize the *TIe* values (Table A.4), there are some exceptions, e.g. Lu et al. (2008). The idea of focusing on reducing the *TIIe* values arose as a result of different researchers considering that this type of error produces more negative effects in the final model than produced by omission errors. These effects will be more serious if points

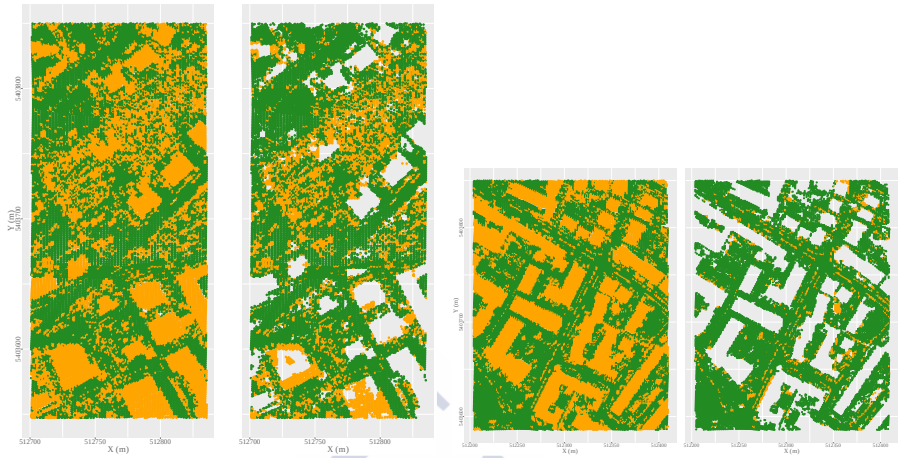

(a) Sample 11: S (b) S_D (c) Sample 12: S (d) S_D

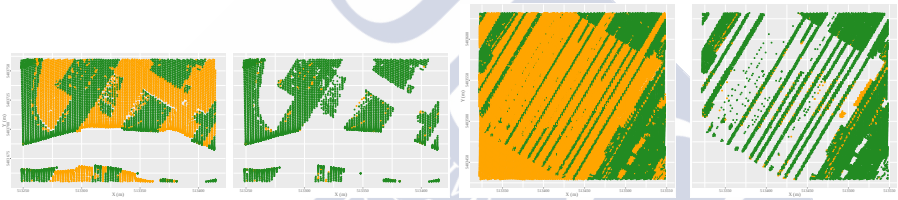

(e) Sample 41: S (f) S_D (g) Sample 42: S (h) S_D

Figura A.6: Qualitative results of internal evaluation (P_g-green points and P_{ng}-orange points).

wrongly classified as ground points actually correspond to buildings, as is common in urban areas. In addition, this effect will be much greater if such points are added during the selection of seed points. This consideration reinforces the importance of minimizing commission errors in urban zones.

Comparison of the accuracy indices obtained by using the hybrid method and those obtained in other studies (Table A.4) demonstrates the potential usefulness of the proposed hybrid method. The global Kappa coefficient is only surpassed by the values reported by Hu et al. (2014) (K=93.3%), Pingel et al. (2013) (K=92.9%) and Chang (2010) (K_{SSA}=92.2%), whereas the values obtained using the IRI algorithm

Tabla A.3: Comparison of error values (%) for each urban reference sample produced by the hybrid method and by the IRI filter and FUSION method. The orange cells indicate the best results across all the methods.

Sample	**IRI** (%)				**FUSION method** (%)					**Hybrid method** (%)				
	TIe	*TIIe*	*Te*	*K*	*TIe*	*TIIe*	*Te*	*K*	*Gph*[a]	*TIe*	*TIIe*	*Te*	*K*	*Gph*[a]
Sample 11	28.3	2.4	17.4	66.3	9.5	16.6	12.5	74.3	GF11	8.56	14.0	10.9	**77.7**	HM11
Sample 12	7.3	1.5	4.5	91.1	4.6	5.5	5.1	89.9	GF12	3.4	1.9	2.7	**94.6**	HM12
Sample 21	2.8	1.6	2.6	92.8	0.5	5.5	1.6	95.2	GF21	0.6	3.9	1.3	**96.2**	HM21
Sample 22	8.3	3.1	6.7	85.2	3.9	14.2	7.1	83.2	GF22	4.9	8.6	6.0	**86.0**	HM22
Sample 23	12.1	3.8	8.2	83.7	6.7	11.8	9.1	81.6	GF23	6.9	6.0	6.5	**87.0**	HM23
Sample 24	8.5	9.0	8.6	79.2	5.6	14.4	8.1	79.8	GF24	5.2	5.0	5.2	**87.4**	HM24
Sample 31	1.6	2.0	1.8	96.4	1.2	1.8	1.5	97.0	GF31	0.5	1.8	1.1	**97.9**	HM31
Sample 41	19.9	1.6	10.8	78.6	0.7	6.4	3.6	92.9	GF41	1.1	2.5	1.8	**96.4**	HM41
Sample 42	8.0	0.2	2.6	93.8	1.0	2.6	2.1	95.0	GF42	0.8	0.7	0.7	**98.2**	HM42
Urban[b]	*11.0*	*1.9*	*6.7*	*86.6*	*4.3*	*7.5*	*5.8*	*88.4*		***4.0***	***4.4***	***4.2***	***91.6***	

[a] 3D graph results. If the graphs cannot be visualized, WebGL should be enabled: instructions for Google Chrome here and for Firefox here.

[b] Using points from the urban samples.

and the FUSION method are lower than those obtained in respectively 11 and 10 of the studies included in Table A.4. As well as indicating the improvements in the filtering accuracy produced by the combined use of the *DebCloud* function and the *GroundFilter* algorithm, these values also show that the accuracy is comparable to that obtained in other recent studies.

The best results were achieved in the urban areas with large buildings (K_{S12}=94.6% and K_{S31}=97.9%), discontinuities in the bare-earth (K_{S41}=96.4% and K_{S42}=98.2%) and bridges (K_{S21}=96.2%). This is due to the efficacy of the debugging process in these areas (Figure A.5a and Figures A.6c-A.6h) and the balance achieved between the omission and commission errors (*TIe*=4.0% and *TIIe*=4.4%) relative to the results obtained with the IRI filter (*TIe*=11.0% and *TIIe*=1.9%) and the FUSION method (*TIe*=4.3% and *TIIe*=7.5%). Finally, the poorest results were obtained for sample 11 (K_{S11}=77.7%), as also observed for the debugging process (Figures A.6a-A.6b). Most filters analysed yielded poor results in this area due to the characteristics of the sample, i.e. vegetation and buildings on steep slopes (K_{IRI}=66.3%; K_{FUSION}=74.3%; $K_{SSA-Chang\ (2010)}$=78.1%; $K_{Pingelet\ al.\ (2013)}$=83.1%; $K_{Huet\ al.\ (2014)}$=82.9%).

Tabla A.4: Comparison of errors and K for all samples with 14 previous works from 2008 to 2016. The best filters are highlighted in orange.

Author	TIe	TIIe	Te	K
Lu et al. (2008)	20.2	3.5	12.4	75.4
Shao y Chen (2008)	6.4	3.3	5.0	90.1
Chang (2010) (SMSM)	2.3	6.9	4.4	91.1
Chang (2010) (SSA)	4.0	3.7	3.9	92.2
Mongus y Žalik (2012)	3.7	8.7	6.0	87.8
Yan et al. (2012)	16.8	2.8	10.3	79.6
Chen et al. (2013)	6.0	3.3	4.7	90.5
Li (2013)	6.0	4.4	5.3	89.4
Pingel et al. (2013)	2.9	4.3	3.5	92.9
Zhang y Lin (2013)	14.8	4.1	9.8	80.5
Hu et al. (2014)	2.5	4.3	3.3	93.3
Mongus y Žalik (2014)	3.4	6.1	4.7	90.6
Hui et al. (2016)	5.9	4.5	5.3	89.5
Zhang et al. (2016)	2.8	7.6	5.0	89.9
Hybrid method	4.0	4.4	4.2	91.6

Conclusions

Despite the large amount of resources invested in this field, identifying ground points from LiDAR data remains a challenge. The filtering efficacy depends on the characteristics of the environment and the methods used to construct the DTM, among other factors. Specifically, identifying ground points in complex environments, such as those characterised by the presence of buildings and vegetation on heterogeneous terrain, represents a challenge to the accuracy of filtering algorithms and also implies the need to carry out tedious fitting processes of parameters. We tackled this problem by using the *DebCloud* function to identify and eliminate local maximum points from LiDAR point cloud. By combining this function with filtering algorithms we aimed to 1) minimize the importance of parameter selection in the filtering process and 2) increase the filtering accuracy by reducing the commission errors. Achievement of these aims was verified by analysis of ISPRS urban

reference samples.

Internal evaluation was used to check whether the first objective was achieved. The accuracy of the filtering applied to the point clouds was evaluated by using different combinations of parameters. The filtering accuracy was found to be less dependent on the variations in parameters when the *DebCloud* function was used in combination with the *GroundFilter* function (hybrid method) than when only the *GroundFilter* function was used (FUSION method). Thus, the parameter fitting process and the internal evaluation of the showed that use of the *DebCloud* function in combination with another filter may simplify parameter selection, with positive effects on the efficiency, efficacy and usability of the method. On the other hand, external evaluation was conducted to check whether the second objective was achieved. For this purpose, the filtering results obtained using the IRI algorithm and the FUSION and hybrid methods were analysed and compared with each other and with the results of 14 previous studies. Taking into account the whole set of urban samples, the Te and K values were 4.2% and 91.6%, respectively. The hybrid method increased the Kappa coefficient of the IRI and *GroundFilter* algorithms by 5 and 3 percentage points respectively. It was also demonstrated that for most samples reduction of commission errors (one of the objectives of the *DebCloud* function) was successfully achieved, without affecting the omission errors. Finally, the proposed hybrid method was found to be one of the 4 most accurate filters developed to date.

Although the filtering results were improved by using the *GroundFilter* algorithm in the proposed hybrid method, some environments, such as that represented by *sample 11*, remained difficult to classify accurately. Modification of the *DebCloud* function, by e.g. identifying P_{ng} as a function of the probability of corresponding to ground points on the basis of the number of times that the points are detected as local maximum point, may improve the filtering accuracy in these zones.

Funding Information

This study was supported by the Land Laboratory Research Group (G.I.-1934-TB) (Universidade de Santiago de Compostela, Spain) and the University of Azuay (Cuenca, Ecuador) (Project No: 2016-53).

Acknowledgements

We are indebted to our colleagues at LaboraTe for their valuable and constructive suggestions. We are responsible for any remaining error.

A.3 Elección de parámetros óptimos.

En las siguientes tablas se incluyen los resultados del ajuste de parámetros. En negrita se marca la combinación de parámetros que ofrece el menor *Te* en la primera fase del ajuste de parámetros (donde variaban los parámetros C y C_S y permanecía constante el parámetro δ_h); y sombreado en malva se resalta la combinación de parámetros que ofrece el menor *Te* en la segunda fase (los parámetros C y C_S toman los valores que proporcionaron el menor *Te* en la fase anterior para cada muestra y varía el parámetro δ_h).

Tabla A.5: **Sample11**: Resultado del ajuste de parámetros (ver gráfico).

C_S	C	δ_h	TIe	TIIe	Te	K
3	12	0.5	10.75	14.36	12.29	74.88
3	14	0.5	10.57	12.24	11.28	77
3	16	0.5	10.35	14.4	12.08	75.3
3	18	0.5	9.99	16.9	12.94	73.44
3	20	0.5	10.33	17.63	13.45	72.38
3	22	0.5	10.08	18.3	13.59	72.05
3	24	0.5	9.62	22.5	15.12	68.72
3	26	0.5	9.74	23	15.4	68.13
3	28	0.5	9.72	24.46	16.01	66.79
3	30	0.5	9.74	22.34	15.11	68.74
3	32	0.5	9.12	27.89	17.13	64.27
4	12	0.5	12.66	11.06	11.98	75.7
4	14	0.4	15	7.96	12	75.86
4	**14**	**0.5**	**12.96**	**8.99**	**11.27**	**77.23**
4	14	0.6	11.53	9.72	10.76	78.18
4	14	0.7	10.8	10.55	10.69	78.26
4	14	0.8	9.59	12.06	10.65	78.26
4	16	0.5	12.16	10.17	11.31	77.07
4	18	0.5	11.87	11.68	11.79	76.04
4	20	0.5	12	13.48	12.63	74.27
4	22	0.5	11.59	14.1	12.66	74.17
4	24	0.5	11.31	17.44	13.93	71.45
4	26	0.5	11.37	18.31	14.33	70.59
4	28	0.5	11.82	17.92	14.42	70.45
4	30	0.5	11.76	16.9	13.95	71.44
4	32	0.5	11.37	21.82	15.83	67.37
5	12	0.5	15.23	9.33	12.71	74.38
5	14	0.5	15.74	7.39	12.17	75.58
5	16	0.5	15.25	7.96	12.14	75.57
5	18	0.5	14.77	9.35	12.46	74.88
5	20	0.5	14.6	10.08	12.67	74.42
5	22	0.5	14.58	10.97	13.04	73.63
5	24	0.5	14.42	13.22	13.91	71.79
5	26	0.5	14.59	13.76	14.24	71.11
5	28	0.5	14.62	13.65	14.2	71.19
5	30	0.5	14.46	12.97	13.83	71.97
5	32	0.5	14.64	17.23	15.74	67.92
6	12	0.5	17.24	8.3	13.43	73.07
6	14	0.5	17.82	6.42	12.95	74.1
6	16	0.5	17.4	6.87	12.91	74.17
6	18	0.5	16.79	7.82	12.96	74
6	20	0.5	16.48	8.59	13.11	73.66
6	22	0.5	16.76	8.27	13.14	73.63
6	24	0.5	16.49	9.75	13.61	72.61
6	26	0.5	16.71	9.88	13.79	72.25
6	28	0.5	17	9.78	13.92	72.02
6	30	0.5	16.93	9.09	13.59	72.71
6	32	0.5	16.66	11.75	14.56	70.63

Tabla A.6: **Sample12**: Resultado del ajuste de parámetros (ver gráfico).

C_S	C	δ_h	TIe	TIIe	Te	K
3	12	0.5	3.07	5.56	4.29	91.41
3	14	0.5	2.46	5	3.7	92.6
3	16	0.5	2.55	5.06	3.77	92.44
3	18	0.4	2.94	2.09	2.52	94.95
3	**18**	**0.5**	**2.33**	**2.65**	**2.49**	**95.02**
3	18	0.6	2.57	2.52	2.55	94.9
3	18	0.7	2.14	3.26	2.68	94.63
3	18	0.8	1.79	4.18	2.96	94.08
3	20	0.5	2.53	3.19	2.85	94.29
3	22	0.5	3.04	3.29	3.16	93.67
3	24	0.5	3.17	3.15	3.16	93.67
3	26	0.5	2.74	3.38	3.05	93.89
3	28	0.5	3	3.43	3.21	93.58
3	30	0.5	2.79	3.45	3.11	93.77
3	32	0.5	2.95	3.55	3.24	93.51
4	12	0.5	3.01	5.65	4.3	91.39
4	14	0.5	3.05	4.77	3.89	92.21
4	16	0.5	2.84	4.87	3.83	92.33
4	18	0.5	2.68	2.8	2.74	94.52
4	20	0.5	2.96	2.97	2.96	94.07
4	22	0.5	3.62	2.79	3.22	93.57
4	24	0.5	3.7	2.99	3.35	93.29
4	26	0.5	2.98	3.04	3.01	93.98
4	28	0.5	3.51	2.88	3.2	93.6
4	30	0.5	3.06	3.16	3.11	93.78
4	32	0.5	3.46	3.15	3.31	93.38
5	12	0.5	3.37	5.27	4.3	91.39
5	14	0.5	3.46	4.51	3.97	92.05
5	16	0.5	3.45	4.62	4.02	91.95
5	18	0.5	3.23	2.74	2.99	94.01
5	20	0.5	3.55	2.89	3.23	93.54
5	22	0.5	4.21	2.75	3.5	93
5	24	0.5	4.13	2.95	3.56	92.89
5	26	0.5	3.46	2.95	3.21	93.58
5	28	0.5	4.11	2.71	3.43	93.15
5	30	0.5	3.77	2.82	3.3	93.39
5	32	0.5	4.07	2.76	3.44	93.13
6	12	0.5	3.67	4.98	4.31	91.37
6	14	0.5	3.67	4.44	4.04	91.91
6	16	0.5	3.83	4.33	4.07	91.85
6	18	0.5	3.56	2.61	3.1	93.8
6	20	0.5	3.94	2.6	3.29	93.42
6	22	0.5	4.28	2.65	3.48	93.04
6	24	0.5	4.27	2.82	3.56	92.88
6	26	0.5	3.89	2.6	3.26	93.47
6	28	0.5	4.47	2.61	3.56	92.87
6	30	0.5	4.27	2.64	3.48	93.04
6	32	0.5	4.38	2.63	3.52	92.95

Tabla A.7: **Sample21**: Resultado del ajuste de parámetros (ver gráfico).

C_S	C	δ_h	TIe	TIIe	Te	K
3	12	0.5	0.32	3.65	1.06	96.91
3	14	0.5	0.26	3.76	1.03	96.97
3	16	0.5	0.24	4.14	1.1	96.77
3	18	0.5	0.35	3.97	1.15	96.64
3	20	0.5	0.46	3.17	1.06	96.92
3	22	0.5	0.29	3.58	1.02	97.02
3	24	0.5	0.25	3.72	1.02	97.02
3	26	0.4	0.53	3.06	1.09	96.83
3	**26**	**0.5**	**0.22**	**3.76**	**1**	**97.06**
3	26	0.6	0.11	4.94	1.18	96.52
3	26	0.7	0.26	4.56	1.21	96.44
3	26	0.8	0.19	5.91	1.46	95.7
3	28	0.5	0.18	4.28	1.09	96.81
3	30	0.5	0.18	4.14	1.06	96.9
3	32	0.5	0.18	4.14	1.06	96.9
4	12	0.5	0.33	3.58	1.05	96.93
4	14	0.5	0.33	3.51	1.03	96.98
4	16	0.5	0.33	3.9	1.12	96.73
4	18	0.5	0.23	4.17	1.1	96.77
4	20	0.5	0.43	3.55	1.12	96.74
4	22	0.5	0.28	3.93	1.09	96.82
4	24	0.5	0.33	3.76	1.09	96.82
4	26	0.5	0.26	3.79	1.04	96.95
4	28	0.5	0.25	4.07	1.1	96.79
4	30	0.5	0.21	3.9	1.03	96.99
4	32	0.5	0.21	3.97	1.04	96.95
5	12	0.5	0.33	3.62	1.06	96.91
5	14	0.5	0.33	3.62	1.06	96.91
5	16	0.5	0.23	4.28	1.13	96.7
5	18	0.5	0.34	3.93	1.13	96.68
5	20	0.5	0.34	3.9	1.13	96.71
5	22	0.5	0.3	3.93	1.1	96.77
5	24	0.5	0.34	3.93	1.13	96.68
5	26	0.5	0.26	3.97	1.08	96.84
5	28	0.5	0.26	3.97	1.08	96.84
5	30	0.5	0.39	3.51	1.08	96.85
5	32	0.5	0.39	3.51	1.08	96.85
6	12	0.5	0.38	3.62	1.1	96.8
6	14	0.5	0.38	3.62	1.1	96.8
6	16	0.5	0.33	3.9	1.12	96.73
6	18	0.5	0.32	3.93	1.12	96.73
6	20	0.5	0.32	3.93	1.12	96.73
6	22	0.5	0.34	3.9	1.13	96.71
6	24	0.5	0.34	3.9	1.13	96.71
6	26	0.5	0.29	3.93	1.1	96.79
6	28	0.5	0.29	3.93	1.1	96.79
6	30	0.5	0.26	3.97	1.08	96.84
6	32	0.5	0.26	3.97	1.08	96.84

Tabla A.8: **Sample22**: Resultado del ajuste de parámetros (ver gráfico).

C_S	C	δ_h	TIe	TIIe	Te	K
3	12	0.5	4.83	25.75	11.35	72.4
3	14	0.5	6.06	26.85	12.54	69.66
3	16	0.5	5.92	23.95	11.54	72.28
3	18	0.5	4.14	18.95	8.76	79.03
3	20	0.5	4.36	9.09	5.84	86.41
3	22	0.5	5.4	16.75	8.94	78.88
3	24	0.5	5.26	9.26	6.51	84.93
3	26	0.4	5.97	6.18	6.03	86.2
3	**26**	**0.5**	**4.82**	**6.89**	**5.47**	**87.39**
3	26	0.6	3.8	7.84	5.05	88.24
3	26	0.7	3.13	9.36	5.07	88.1
3	26	0.8	2.64	11.16	5.3	87.47
3	28	0.5	4.79	9.39	6.22	85.55
3	30	0.5	5.08	7.16	5.72	86.8
3	32	0.5	4.47	7.84	5.52	87.2
4	12	0.5	5.2	24.43	11.19	72.95
4	14	0.5	5.74	27.25	12.44	69.79
4	16	0.5	5.94	24.49	11.72	71.81
4	18	0.5	4.99	17.76	8.97	78.7
4	20	0.5	5.28	7.67	6.02	86.11
4	22	0.5	6.32	16.3	9.43	77.89
4	24	0.5	5.71	6.64	6	86.24
4	26	0.5	5.48	6.5	5.8	86.69
4	28	0.5	5.52	8.78	6.54	84.9
4	30	0.5	5.86	6.9	6.19	85.81
4	32	0.5	5.37	7.16	5.93	86.35
5	12	0.5	5.87	21.66	10.79	74.23
5	14	0.5	5.94	23.93	11.54	72.27
5	16	0.5	5.92	22.91	11.21	73.14
5	18	0.5	5.48	16.37	8.87	79.08
5	20	0.5	5.99	7.68	6.52	85.04
5	22	0.5	6.5	15.42	9.28	78.31
5	24	0.5	6.51	6.25	6.43	85.34
5	26	0.5	7.17	6.09	6.84	84.48
5	28	0.5	6.16	8.3	6.83	84.31
5	30	0.5	6.34	7.29	6.64	84.81
5	32	0.5	5.87	6.71	6.13	85.96
6	12	0.5	5.7	22.55	10.95	73.76
6	14	0.5	5.67	23.56	11.25	72.97
6	16	0.5	5.68	23.81	11.33	72.75
6	18	0.5	6.04	15.59	9.02	78.85
6	20	0.5	6.59	7.76	6.95	84.09
6	22	0.5	6.97	13.26	8.93	79.3
6	24	0.5	7.33	6.14	6.95	84.22
6	26	0.5	7.86	5.99	7.28	83.55
6	28	0.5	6.77	7.82	7.09	83.79
6	30	0.5	7.11	5.93	6.74	84.7
6	32	0.5	7.17	6.41	6.93	84.25

Tabla A.9: **Sample23**: Resultado del ajuste de parámetros (ver gráfico).

C_S	C	δ_h	TIe	TIIe	Te	K
3	12	0.5	6.44	32.26	18.65	62.1
3	14	0.5	7.1	27.67	16.83	65.89
3	16	0.5	7.61	13.54	10.41	79.06
3	18	0.5	7.57	9.24	8.36	83.22
3	20	0.5	7.76	6.81	7.31	85.35
3	22	0.5	6.78	5.17	6.02	87.94
3	24	0.4	9.23	4.56	7.02	85.96
3	**24**	**0.5**	**8.14**	**5.04**	**6.67**	**86.64**
3	24	0.6	5.49	5.86	5.67	88.64
3	24	0.7	5.01	6.93	5.92	88.11
3	24	0.8	4.98	7.67	6.25	87.45
3	26	0.5	7.96	5.23	6.67	86.65
3	28	0.5	8.64	5.12	6.98	86.04
3	30	0.5	9.44	5.1	7.38	85.23
3	32	0.5	10.54	5.14	7.99	84.04
4	12	0.5	7.71	30.5	18.49	62.48
4	14	0.5	10.78	23.83	16.95	65.79
4	16	0.5	8.02	12.42	10.1	79.7
4	18	0.5	8.86	9.56	9.19	81.57
4	20	0.5	7.76	8.13	7.93	84.09
4	22	0.5	8.02	4.25	6.23	87.53
4	24	0.5	9.64	4.2	7.07	85.87
4	26	0.5	9.42	4.21	6.96	86.09
4	28	0.5	9.35	4.25	6.94	86.12
4	30	0.5	11.16	4.3	7.92	84.18
4	32	0.5	12.51	4.34	8.64	82.75
5	12	0.5	8.18	28.58	17.83	63.88
5	14	0.5	8.57	26.22	16.92	65.78
5	16	0.5	9.11	12.25	10.59	78.73
5	18	0.5	9.11	10.24	9.64	80.66
5	20	0.5	8.68	7.7	8.22	83.53
5	22	0.5	9.89	3.82	7.02	85.98
5	24	0.5	11.4	3.73	7.77	84.48
5	26	0.5	10.61	3.73	7.36	85.31
5	28	0.5	10.94	3.75	7.54	84.95
5	30	0.5	12.77	3.79	8.52	82.99
5	32	0.5	14.37	3.78	9.36	81.34
6	12	0.5	9.14	25.98	17.1	65.41
6	14	0.5	9.51	24.86	16.77	66.11
6	16	0.5	11.14	10.88	11.02	77.92
6	18	0.5	9.97	9.7	9.84	80.28
6	20	0.5	9.95	8.04	9.05	81.88
6	22	0.5	10.1	3.54	6.99	86.03
6	24	0.5	12.12	3.57	8.08	83.88
6	26	0.5	11.59	3.54	7.78	84.46
6	28	0.5	11.98	3.58	8.01	84.02
6	30	0.5	14.21	3.54	9.16	81.74
6	32	0.5	15.61	3.53	9.89	80.29

Tabla A.10: **Sample24**: Resultado del ajuste de parámetros (ver gráfico).

C_S	C	δ_h	TIe	TIIe	Te	K
3	12	0.5	3.52	11.76	5.79	85.39
3	14	0.5	3.29	8.55	4.74	88.13
3	16	0.5	3.18	8.31	4.6	88.49
3	18	0.5	3.02	8.65	4.57	88.53
3	20	0.4	3.22	8.45	4.66	88.33
3	**20**	**0.5**	**2.74**	**9.18**	**4.52**	**88.62**
3	20	0.6	2.81	9.72	4.72	88.11
3	20	0.7	2.59	11.13	4.95	87.45
3	20	0.8	2.48	12.29	5.19	86.78
3	22	0.5	3.42	8.84	4.92	87.69
3	24	0.5	2.59	10.2	4.69	88.13
3	26	0.5	2.91	9.28	4.66	88.27
3	28	0.5	2.42	11.42	4.9	87.53
3	30	0.5	3.15	10.74	5.24	86.78
3	32	0.5	2.31	10.64	4.61	88.29
4	12	0.5	5.66	9.77	6.79	83.26
4	14	0.5	5.55	6.71	5.87	85.66
4	16	0.5	4.44	7.34	5.24	87.06
4	18	0.5	4.52	7.43	5.32	86.86
4	20	0.5	4.16	7.58	5.11	87.35
4	22	0.5	5.11	7.14	5.67	86.08
4	24	0.5	4.11	7.68	5.09	87.37
4	26	0.5	4.26	7.63	5.19	87.16
4	28	0.5	4.55	8.02	5.51	86.38
4	30	0.5	5.42	7.82	6.08	85.07
4	32	0.5	4.96	7.63	5.7	85.98
5	12	0.5	6.48	9.18	7.22	82.35
5	14	0.5	6.53	7	6.66	83.83
5	16	0.5	6.25	7.43	6.58	83.97
5	18	0.5	6.05	7.43	6.43	84.31
5	20	0.5	5.94	7.63	6.41	84.35
5	22	0.5	6.46	7.39	6.71	83.68
5	24	0.5	5.9	7.53	6.35	84.48
5	26	0.5	5.9	7.58	6.37	84.45
5	28	0.5	5.98	7.29	6.34	84.53
5	30	0.5	6.44	7.24	6.66	83.81
5	32	0.5	6.22	7.24	6.5	84.17
6	12	0.5	7.49	8.21	7.69	81.4
6	14	0.5	7.51	6.61	7.26	82.53
6	16	0.5	7.11	6.75	7.01	83.08
6	18	0.5	6.85	7.05	6.9	83.29
6	20	0.5	6.72	7.05	6.81	83.5
6	22	0.5	7.12	6.71	7.01	83.08
6	24	0.5	6.83	6.95	6.86	83.39
6	26	0.5	6.74	7	6.81	83.5
6	28	0.5	6.88	6.85	6.87	83.37
6	30	0.5	6.99	6.85	6.96	83.19
6	32	0.5	6.74	6.85	6.77	83.61

Tabla A.11: **Sample31**: Resultado del ajuste de parámetros (ver gráfico).

$\mathbf{C}_S$	**C**	δ_h	**TIe**	**TIIe**	**Te**	**K**
3	12	0.5	1.04	16.24	8.04	83.64
3	14	0.5	1.05	14.56	7.28	85.21
3	16	0.5	0.77	12.16	6.02	87.79
3	18	0.5	0.73	4.4	2.42	95.12
3	20	0.5	0.75	2.14	1.39	97.2
3	22	0.5	0.71	2.22	1.41	97.16
3	24	0.5	0.71	2.28	1.43	97.12
3	26	0.5	0.67	2.47	1.5	96.98
3	28	0.5	0.71	2.23	1.41	97.16
3	30	0.5	0.65	2.38	1.45	97.09
3	32	0.5	0.66	2.43	1.48	97.02
4	12	0.5	1.45	13.29	6.91	85.98
4	14	0.5	1.4	12.49	6.51	86.79
4	16	0.5	1.13	10.37	5.38	89.09
4	18	0.5	1.11	3.37	2.15	95.67
4	20	0.5	0.53	2.19	1.3	97.39
4	22	0.5	0.64	2.07	1.3	97.39
4	24	0.5	1.07	1.67	1.35	97.29
4	26	0.5	1.06	1.79	1.4	97.19
4	28	0.5	0.54	2.23	1.32	97.35
4	30	0.5	0.53	2.41	1.39	97.19
4	32	0.5	0.53	2.41	1.39	97.19
5	12	0.5	2.07	13.01	7.11	85.58
5	14	0.5	1.74	11.63	6.3	87.24
5	16	0.5	1.65	8.39	4.76	90.38
5	18	0.5	1.55	3.04	2.24	95.5
5	20	0.4	0.8	1.72	1.22	97.54
5	**20**	**0.5**	**0.56**	**2.09**	**1.27**	**97.45**
5	20	0.6	0.52	2.66	1.5	96.97
5	20	0.7	0.91	2.45	1.62	96.74
5	20	0.8	0.7	3.19	1.85	96.28
5	22	0.4	0.8	1.72	1.22	97.54
5	**22**	**0.5**	**0.56**	**2.09**	**1.27**	**97.45**
5	22	0.6	1.1	1.96	1.5	96.98
5	22	0.7	0.86	2.43	1.58	96.82
5	22	0.8	0.66	3.18	1.82	96.32
5	24	0.5	0.56	2.23	1.33	97.32
5	26	0.5	0.56	2.33	1.38	97.23
5	28	0.5	0.57	2.09	1.27	97.44
5	30	0.5	0.57	2.23	1.33	97.32
5	32	0.5	0.57	2.23	1.33	97.32
6	12	0.5	2.39	11.32	6.5	86.83
6	14	0.5	2.57	9.43	5.73	88.42
6	16	0.5	2.08	7.59	4.62	90.67
6	18	0.5	0.88	2.75	1.74	96.49
6	20	0.5	0.54	2.23	1.32	97.35
6	22	0.5	0.6	2.14	1.31	97.36
6	24	0.5	0.61	2.11	1.3	97.37
6	26	0.5	0.61	2.12	1.31	97.37
6	28	0.5	0.54	2.2	1.31	97.37
6	30	0.5	0.54	2.2	1.31	97.37
6	32	0.5	0.54	2.2	1.31	97.37

Tabla A.12: **Sample41**: Resultado del ajuste de parámetros (ver gráfico).

C_S	C	δ_h	TIe	TIIe	Te	K
3	12	0.5	5.77	55.25	30.31	39.14
3	14	0.5	4.66	33.59	19.01	61.89
3	16	0.5	3.62	31.51	17.45	65.01
3	18	0.5	3.43	12.75	8.05	83.88
3	20	0.5	3.52	6.51	5	89.99
3	22	0.5	3.82	3.25	3.54	92.93
3	24	0.5	8.5	2.63	5.59	88.83
3	26	0.5	2.23	1.38	1.81	96.38
3	28	0.4	2.89	1.03	1.97	96.06
3	**28**	**0.5**	**2.12**	**1.22**	**1.67**	**96.65**
3	28	0.6	2.09	1.27	1.68	96.64
3	28	0.7	1.87	1.56	1.72	96.56
3	28	0.8	1.61	1.81	1.71	96.58
3	30	0.5	2.2	1.41	1.81	96.38
3	32	0.5	2.32	1.4	1.86	96.28
4	12	0.5	5.93	50.43	28	43.8
4	14	0.5	4.77	32.36	18.45	63.01
4	16	0.5	3.95	28.55	16.15	67.64
4	18	0.5	4.28	10.61	7.42	85.15
4	20	0.5	4.28	4.39	4.34	91.33
4	22	0.5	3.91	2.79	3.36	93.29
4	24	0.5	8.78	2.32	5.58	88.85
4	26	0.5	2.95	1.03	2	96.01
4	28	0.5	2.95	1.03	2	96.01
4	30	0.5	2.71	1.05	1.89	96.22
4	32	0.5	2.71	1.07	1.9	96.2
5	12	0.5	6.91	50.1	28.33	43.14
5	14	0.5	5.69	29.48	17.49	64.95
5	16	0.5	6.57	27.75	17.08	65.79
5	18	0.5	4.34	9.49	6.89	86.21
5	20	0.5	3.91	3.63	3.77	92.46
5	22	0.5	4.16	2.72	3.45	93.11
5	24	0.5	8.94	2.25	5.62	88.76
5	26	0.5	3	1.09	2.05	95.9
5	28	0.5	3	1.09	2.05	95.9
5	30	0.5	3.02	1.09	2.06	95.88
5	32	0.5	3.02	1.09	2.06	95.88
6	12	0.5	8.71	45.71	27.06	45.71
6	14	0.5	6.05	26.52	16.2	67.54
6	16	0.5	6.53	27.01	16.69	66.57
6	18	0.5	4.64	8.96	6.78	86.43
6	20	0.5	4.19	3.94	4.07	91.87
6	22	0.5	4.69	2.96	3.83	92.34
6	24	0.5	9.25	1.61	5.46	89.08
6	26	0.5	3.43	1.07	2.26	95.48
6	28	0.5	3.43	1.07	2.26	95.48
6	30	0.5	3.43	1.07	2.26	95.48
6	32	0.5	3.45	1.07	2.27	95.47

Tabla A.13: **Sample42**: Resultado del ajuste de parámetros (ver gráfico).

C_S	C	δ_h	TIe	TIIe	Te	K
3	12	0.5	5.18	5.81	5.63	86.76
3	14	0.5	2.41	3.94	3.49	91.74
3	16	0.5	1.75	4.07	3.39	92
3	18	0.5	1.86	2.83	2.55	93.94
3	20	0.5	1.39	2.61	2.25	94.64
3	22	0.5	1.12	2.92	2.39	94.33
3	24	0.5	1.05	2.37	1.98	95.28
3	26	0.5	1.05	4.45	3.45	91.89
3	28	0.5	1.01	2.11	1.79	95.73
3	30	0.5	0.95	0.92	0.93	97.77
3	32	0.5	0.95	0.95	0.95	97.72
4	12	0.5	3.51	6.25	5.45	87.28
4	14	0.5	3.62	3.51	3.54	91.57
4	16	0.5	2.36	3.76	3.35	92.07
4	18	0.5	3.22	2.33	2.59	93.79
4	20	0.5	1.61	2.42	2.19	94.79
4	22	0.5	1.5	2.78	2.4	94.28
4	24	0.5	1.49	2.26	2.03	95.15
4	26	0.5	1.19	3.77	3.02	92.88
4	28	0.5	1.05	1.74	1.54	96.32
4	30	0.4	1.84	0.51	0.9	97.83
4	**30**	**0.5**	**1.1**	**0.69**	**0.81**	**98.05**
4	30	0.6	0.96	0.77	0.82	98.02
4	30	0.7	0.64	0.93	0.85	97.96
4	30	0.8	1.04	0.88	0.93	97.77
4	32	0.5	1.1	0.73	0.84	97.99
5	12	0.5	3.67	5.76	5.15	87.94
5	14	0.5	4.1	3.18	3.45	91.77
5	16	0.5	3.59	3.72	3.68	91.25
5	18	0.5	4.85	2.25	3.01	92.74
5	20	0.5	2.39	2.31	2.34	94.41
5	22	0.5	2.17	2.52	2.42	94.23
5	24	0.5	2.03	2.24	2.18	94.79
5	26	0.5	2.31	2.85	2.69	93.59
5	28	0.5	1.76	1.86	1.83	95.62
5	30	0.5	1.87	0.62	0.99	97.61
5	32	0.5	1.85	0.65	1	97.58
6	12	0.5	4.76	5.06	4.97	88.25
6	14	0.5	5.29	3.55	4.06	90.29
6	16	0.5	4.21	3.34	3.59	91.42
6	18	0.5	6.57	2.07	3.39	91.78
6	20	0.5	2.76	2.27	2.41	94.22
6	22	0.5	3.41	2.18	2.54	93.9
6	24	0.5	2.56	2.03	2.19	94.76
6	26	0.5	2.44	2.17	2.25	94.61
6	28	0.5	2.33	1.84	1.99	95.24
6	30	0.5	2.89	0.53	1.22	97.03
6	32	0.5	2.89	0.54	1.23	97.01

Tabla A.14: **Sample51**: Resultado del ajuste de parámetros (ver gráfico).

C_S	C	δ_h	TIe	TIIe	Te	K
3	06	0.5	0.12	26.57	5.9	80.93
3	08	0.5	0.16	23.88	5.34	82.92
3	10	0.5	0.13	30.4	6.74	77.87
3	12	0.5	0.11	34.87	7.7	74.24
3	14	0.5	0.05	39.49	8.66	70.44
3	16	0.5	0.06	39.33	8.64	70.54
3	18	0.5	0.09	42.11	9.26	68.05
3	20	0.5	0.08	43.44	9.54	66.88
3	22	0.5	0.14	44.54	9.83	65.75
3	24	0.5	0.04	46.55	10.19	64.15
3	26	0.5	0	49.68	10.84	61.3
4	06	0.5	0.29	16.15	3.75	88.36
4	08	0.5	0.39	11.78	2.88	91.23
4	10	0.5	0.34	14.61	3.45	89.37
4	12	0.5	0.23	16.3	3.74	88.4
4	14	0.5	0.16	17.77	4	87.5
4	16	0.5	0.17	17.64	3.98	87.56
4	18	0.5	0.2	18.59	4.21	86.8
4	20	0.5	0.18	18.95	4.28	86.59
4	22	0.5	0.16	19.69	4.42	86.08
4	24	0.5	0.19	20.08	4.53	85.73
4	26	0.5	0.08	21.72	4.8	84.75
5	06	0.5	0.46	11.4	2.85	91.35
5	08	0.5	0.55	7.88	2.15	93.56
5	10	0.5	0.53	8.47	2.26	93.2
5	12	0.5	0.47	8.88	2.3	93.07
5	14	0.5	0.4	9.32	2.35	92.92
5	16	0.5	0.52	9.17	2.4	92.76
5	18	0.5	0.47	9.42	2.43	92.69
5	20	0.5	0.42	9.68	2.44	92.64
5	22	0.5	0.52	9.83	2.55	92.31
5	24	0.5	0.43	9.94	2.5	92.43
5	26	0.5	0.35	10.42	2.55	92.27
6	06	0.5	0.65	9.11	2.5	92.49
6	08	0.5	0.72	6.01	1.88	94.43
6	10	0.5	0.44	6.8	1.83	94.53
6	12	0.5	0.65	6.24	1.87	94.44
6	14	0.5	0.6	6.16	1.82	94.6
6	16	0.5	0.44	6.93	1.85	94.46
6	18	0.5	0.6	6.16	1.82	94.6
6	20	0.5	0.61	6.16	1.82	94.59
6	22	0.5	0.42	7.11	1.88	94.37
6	24	0.5	0.56	6.26	1.8	94.63
6	26	0.4	0.8	5.55	1.84	94.56
6	**26**	**0.5**	**0.47**	**6.42**	**1.77**	**94.72**
6	26	0.6	0.32	7.65	1.92	94.25
6	26	0.7	0.2	8.14	1.93	94.18
6	26	0.8	0.17	8.86	2.07	93.76

Tabla A.15: **Sample52**: Resultado del ajuste de parámetros (ver gráfico).

C_S	C	δ_h	TIe	TIIe	Te	K
3	6	0.5	1.7	38.31	5.55	67.04
3	8	0.5	2.12	33.23	5.39	69.29
3	10	0.5	1.93	36.11	5.52	67.85
3	12	0.5	1.9	40.69	5.98	64.36
3	14	0.5	1.06	43.95	5.57	65.02
3	16	0.5	2.25	43.23	6.56	60.99
3	18	0.5	1.5	44.28	6	62.97
3	20	0.5	1.28	45.43	5.92	62.88
3	22	0.5	1	50.85	6.24	59.2
3	24	0.5	2.13	45.55	6.7	59.51
3	26	0.5	1.79	49.96	6.86	56.96
4	6	0.5	2.85	27.6	5.45	70.59
4	8	0.5	3.21	22.52	5.24	72.73
4	10	0.5	3.08	21.72	5.04	73.74
4	12	0.5	2.92	23.41	5.07	73.2
4	14	0.5	2.14	24.39	4.48	75.52
4	16	0.5	3.01	22.99	5.11	73.14
4	18	0.5	2.46	21.42	4.45	76.27
4	20	0.5	2.01	21.3	4.04	78.12
4	22	0.5	2.01	24.09	4.33	76.23
4	24	0.5	2.94	18.71	4.6	76.23
4	26	0.5	2.77	20.91	4.68	75.41
5	6	0.5	3.73	21.59	5.61	71.47
5	8	0.5	4.13	17.95	5.58	72.43
5	10	0.5	4.17	17.19	5.54	72.75
5	12	0.5	3.91	17.78	5.37	73.3
5	14	0.5	3.27	18.08	4.82	75.41
5	16	0.5	4.45	16.05	5.66	72.53
5	18	0.5	3.64	14.52	4.79	76.28
5	20	0.5	3.37	13.76	4.46	77.76
5	22	0.5	3.16	15.03	4.41	77.75
5	24	0.5	4.12	10.29	4.77	77.16
5	26	0.4	4.59	8.98	5.05	76.3
5	**26**	**0.5**	**3.68**	**11.01**	**4.45**	**78.27**
5	26	0.6	2.92	12.66	3.94	80.11
5	26	0.7	2.37	14.27	3.62	81.24
5	26	0.8	1.89	16.26	3.4	81.89
6	6	0.5	4.35	20.24	6.02	70.22
6	8	0.5	4.62	16.72	5.89	71.52
6	10	0.5	4.92	16.6	6.14	70.61
6	12	0.5	4.77	16.85	6.04	70.95
6	14	0.5	4.03	16.72	5.36	73.55
6	16	0.5	5.21	14.82	6.22	70.76
6	18	0.5	4.53	12.87	5.41	74.17
6	20	0.5	4.35	12.62	5.22	74.95
6	22	0.5	3.97	13.55	4.98	75.7
6	24	0.5	4.99	8.64	5.38	75.14
6	26	0.5	4.5	9.19	4.99	76.48

Tabla A.16: **Sample53**: Resultado del ajuste de parámetros (ver gráfico).

$\mathbf{C}_S$	**C**	δ_h	**TIe**	**TIIe**	**Te**	**K**
3	06	0.5	4.22	16.99	4.74	56.33
3	08	0.5	4.6	16.34	5.07	54.72
3	10	0.5	3.82	24.77	4.67	54.26
3	12	0.5	3.03	32.54	4.23	54.17
3	14	0.5	2.83	38.08	4.26	51.84
3	16	0.5	2.56	44.06	4.24	49.39
3	18	0.5	2.34	50.68	4.3	45.88
3	20	0.5	2.12	57.24	4.35	42.02
3	22	0.5	1.76	62.2	4.2	39.93
3	24	0.5	2.03	60.26	4.38	40.03
3	26	0.5	1.75	68.39	4.44	34.25
4	06	0.5	5.73	8.35	5.84	53.3
4	08	0.5	6.13	6.77	6.15	52.33
4	10	0.5	5.55	8.14	5.66	54.19
4	12	0.4	5.88	8.71	5.99	52.5
4	**12**	**0.5**	**4.86**	**10.08**	**5.07**	**56.52**
4	12	0.6	4.05	12.74	4.4	59.43
4	12	0.7	3.43	16.13	3.95	61.24
4	12	0.8	2.89	20.59	3.61	62.17
4	14	0.5	4.81	11.74	5.09	55.96
4	16	0.5	4.6	12.89	4.94	56.43
4	18	0.5	4.4	14.9	4.82	56.49
4	20	0.5	4.17	17.64	4.72	56.24
4	22	0.5	3.95	19.73	4.58	56.35
4	24	0.5	4.31	19.01	4.9	54.82
4	26	0.5	3.81	23.04	4.59	55.27
5	06	0.5	6.89	6.48	6.87	49.43
5	08	0.5	7.64	5.33	7.54	47.22
5	10	0.5	7.04	5.4	6.98	49.32
5	12	0.5	6.48	6.26	6.47	51.11
5	14	0.5	6.85	6.48	6.84	49.56
5	16	0.5	6.79	7.13	6.8	49.53
5	18	0.5	6.67	7.63	6.71	49.77
5	20	0.5	6.35	7.7	6.41	50.98
5	22	0.5	6.01	8.35	6.1	52.12
5	24	0.5	6.53	7.34	6.57	50.43
5	26	0.5	6.06	9.5	6.2	51.37
6	06	0.5	7.83	5.04	7.72	46.67
6	08	0.5	8.41	4.61	8.25	44.98
6	10	0.5	7.86	4.75	7.74	46.69
6	12	0.5	7.41	5.4	7.32	48
6	14	0.5	7.92	5.18	7.81	46.33
6	16	0.5	7.98	5.62	7.89	45.92
6	18	0.5	7.71	5.69	7.63	46.82
6	20	0.5	7.36	5.83	7.3	47.99
6	22	0.5	7.27	5.98	7.22	48.23
6	24	0.5	7.65	4.68	7.53	47.44
6	26	0.5	7.25	6.19	7.21	48.22

Tabla A.17: **Sample54**: Resultado del ajuste de parámetros (ver gráfico).

$\mathbf{C}_S$	**C**	δ_h	**TIe**	**TIIe**	**Te**	**K**
3	06	0.5	0.58	28.27	15.45	69.61
3	08	0.5	0.63	12.88	7.21	85.65
3	10	0.5	0.93	6.56	3.95	92.09
3	12	0.5	1.03	4.76	3.03	93.92
3	14	0.5	1.15	5.02	3.23	93.52
3	16	0.5	1.03	6.13	3.77	92.46
3	18	0.5	0.95	7.45	4.44	91.12
3	20	0.5	1.63	9.24	5.72	88.57
3	22	0.5	1.26	10.63	6.29	87.45
3	24	0.5	0.88	11.62	6.65	86.74
3	26	0.5	1.98	14.03	8.45	83.17
4	06	0.5	1.58	20.5	11.74	76.75
4	08	0.5	1.33	8.48	5.17	89.66
4	10	0.5	1.71	4	2.94	94.1
4	12	0.4	2.76	2.16	2.44	95.09
4	**12**	**0.5**	**1.93**	**2.79**	**2.39**	**95.19**
4	12	0.6	1.56	3.16	2.42	95.14
4	12	0.7	1.26	3.7	2.57	94.84
4	12	0.8	0.93	4.29	2.73	94.52
4	14	0.5	2.06	2.86	2.49	95
4	16	0.5	1.71	3.05	2.43	95.12
4	18	0.5	1.61	3.51	2.63	94.73
4	20	0.5	1.73	4.59	3.27	93.45
4	22	0.5	1.76	5.32	3.67	92.64
4	24	0.5	1.26	5.58	3.58	92.83
4	26	0.5	2.81	6.95	5.03	89.91
5	06	0.5	2.64	13.92	8.69	82.68
5	08	0.5	2.26	6.06	4.3	91.38
5	10	0.5	2.46	3.31	2.92	94.14
5	12	0.5	2.99	2.53	2.74	94.48
5	14	0.5	2.86	2.45	2.64	94.69
5	16	0.5	2.69	2.6	2.64	94.69
5	18	0.5	2.79	2.68	2.73	94.51
5	20	0.5	2.69	3.03	2.87	94.23
5	22	0.5	2.71	3.12	2.93	94.11
5	24	0.5	2.51	3.53	3.06	93.86
5	26	0.5	3.84	4.24	4.06	91.85
6	06	0.5	3.34	11.1	7.51	85
6	08	0.5	3.01	4.76	3.95	92.07
6	10	0.5	3.26	2.99	3.12	93.74
6	12	0.5	3.69	2.29	2.94	94.08
6	14	0.5	3.49	2.34	2.87	94.22
6	16	0.5	3.64	2.38	2.96	94.04
6	18	0.5	3.57	2.34	2.91	94.15
6	20	0.5	3.49	2.47	2.94	94.08
6	22	0.5	3.39	2.68	3.01	93.94
6	24	0.5	3.01	2.88	2.94	94.09
6	26	0.5	5.1	3.03	3.99	91.97

Tabla A.18: **Sample61**: Resultado del ajuste de parámetros (ver gráfico).

C_S	C	δ_h	TIe	TIIe	Te	K
3	06	0.4	1.42	7.79	1.64	78.62
3	**06**	**0.5**	**1.07**	**7.96**	**1.31**	**82.19**
3	06	0.6	0.86	8.71	1.13	84.17
3	06	0.7	0.77	9.87	1.08	84.63
3	06	0.8	0.62	11.77	1.01	85.25
3	08	0.5	2.58	4.39	2.65	70.01
3	10	0.5	3.86	5.39	3.91	60.66
3	12	0.5	3.24	7.79	3.4	63.48
3	14	0.5	3.42	9.29	3.63	61.53
3	16	0.5	3.33	9.29	3.53	62.18
3	18	0.5	3.13	11.53	3.42	62.39
3	20	0.5	2.65	15.84	3.1	63.59
3	22	0.5	2.61	16.58	3.09	63.47
3	24	0.5	2.51	18.49	3.06	63.16
3	26	0.5	2.4	21.48	3.06	62.3
4	06	0.5	1.36	4.64	1.47	80.93
4	08	0.5	3.88	1.91	3.82	62.12
4	10	0.5	4.68	0.75	4.54	58.05
4	12	0.5	4.2	1.41	4.11	60.42
4	14	0.5	3.99	1.49	3.9	61.67
4	16	0.5	3.92	1.58	3.84	62.07
4	18	0.5	3.32	2.4	3.29	65.55
4	20	0.5	3.03	2.9	3.03	67.37
4	22	0.5	3.08	3.23	3.08	66.87
4	24	0.5	2.89	3.81	2.93	67.93
4	26	0.5	2.75	4.81	2.82	68.5
5	06	0.5	1.75	2.9	1.79	78.01
5	08	0.5	4.57	0.83	4.44	58.58
5	10	0.5	5.05	0.41	4.89	56.2
5	12	0.5	4.7	0.83	4.56	57.9
5	14	0.5	4.98	0.5	4.83	56.53
5	16	0.5	4.63	1	4.5	58.19
5	18	0.5	4.08	1.08	3.97	61.33
5	20	0.5	3.78	1.58	3.7	62.96
5	22	0.5	3.57	2.57	3.54	63.79
5	24	0.5	3.33	3.07	3.32	65.21
5	26	0.5	3.16	1.99	3.12	66.88
6	06	0.5	2.07	2.07	2.07	75.46
6	08	0.5	4.79	0.75	4.65	57.46
6	10	0.5	5.13	0.5	4.97	55.76
6	12	0.5	4.87	0.5	4.72	57.11
6	14	0.5	5.19	0.5	5.03	55.47
6	16	0.5	4.89	0.58	4.74	56.98
6	18	0.5	4.55	0.75	4.42	58.73
6	20	0.5	4.24	1.08	4.14	60.33
6	22	0.5	3.96	1.16	3.86	62.03
6	24	0.5	3.91	2.24	3.85	61.82
6	26	0.5	3.32	2.07	3.27	65.75

Tabla A.19: **Sample71**: Resultado del ajuste de parámetros variables(ver gráfico).

C_S	C	δ_h	TIe	TIIe	Te	K
3	6	0.5	0.76	46.67	5.96	63.91
3	8	0.5	0.83	32.15	4.37	75.47
3	10	0.5	1.02	28.53	4.14	77.37
3	12	0.5	1.01	31.3	4.44	75.38
3	14	0.5	0.91	31.36	4.35	75.74
3	16	0.5	1	21.92	3.37	82.12
3	18	0.5	1.03	17.8	2.93	84.77
3	20	0.5	1.04	16.44	2.78	85.62
3	22	0.5	1.28	16.5	3	84.63
3	24	0.5	1.7	13.33	3.02	84.97
3	26	0.5	1.41	14.8	2.92	85.2
4	6	0.5	1.09	37.74	5.23	70.1
4	8	0.5	1.1	23.39	3.62	80.7
4	10	0.5	1.27	21.07	3.51	81.62
4	12	0.5	1.14	21.86	3.48	81.6
4	14	0.5	1.12	21.07	3.38	82.2
4	16	0.5	1.19	11.92	2.4	87.89
4	18	0.5	1.12	8.81	1.99	90.06
4	20	0.5	1.23	6.84	1.87	90.81
4	22	0.5	1.56	6.5	2.12	89.71
4	24	0.5	2.08	6.05	2.52	87.96
4	26	0.5	2.03	5.76	2.45	88.32
5	6	0.5	1.48	30.11	4.72	74.43
5	8	0.5	1.84	18.42	3.71	81.16
5	10	0.5	1.6	17.12	3.36	82.94
5	12	0.5	1.54	16.67	3.25	83.46
5	14	0.5	1.44	15.93	3.08	84.33
5	16	0.5	1.43	8.08	2.19	89.25
5	18	0.5	1.47	6.16	2	90.26
5	20	0.4	3.1	3.5	3.14	85.63
5	**20**	**0.5**	**1.55**	**4.07**	**1.83**	**91.17**
5	20	0.6	1.15	5.03	1.59	92.21
5	20	0.7	0.81	6.16	1.41	92.97
5	20	0.8	0.59	7.18	1.34	93.27
5	22	0.5	2.13	3.73	2.31	89.12
5	24	0.5	2.91	3.28	2.95	86.44
5	26	0.5	2.98	3.5	3.04	86.07
6	6	0.5	1.93	25.48	4.6	76.02
6	8	0.5	2.13	14.92	3.57	82.33
6	10	0.5	1.94	13.9	3.29	83.69
6	12	0.5	1.85	14.01	3.22	83.98
6	14	0.5	1.9	13.39	3.2	84.18
6	16	0.5	1.86	6.44	2.38	88.56
6	18	0.5	1.92	4.92	2.26	89.23
6	20	0.5	2.07	3.33	2.21	89.57
6	22	0.5	2.58	2.99	2.63	87.82
6	24	0.5	3.68	2.37	3.53	84.24
6	26	0.5	3.61	2.6	3.5	84.33

A.4 Efectividad del proceso de depurado y selección de puntos semilla.

Las siguientes gráficas representan cuantitativamente la efectividad del proceso de depurado para cada muestra, indicando el número original de puntos y los resultantes tras las dos fases del depurado, en función de si los puntos son terreno (P_g) o no (P_{ng}) y del valor del parámetro variable C. Adicionalmente se calculó el error total y el coeficiente Kappa para cada caso. En todos los casos $\delta_h = 0.5$ m.

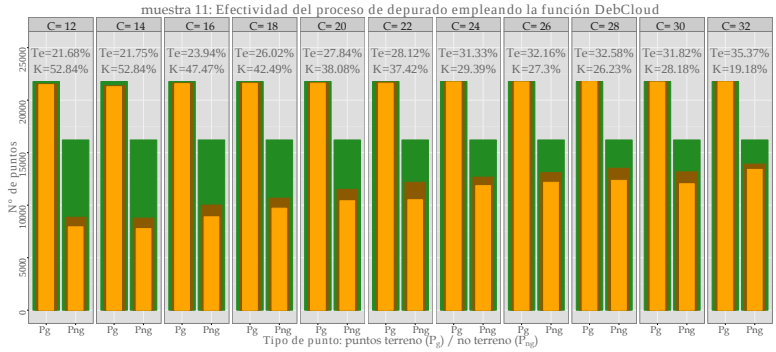

(a)

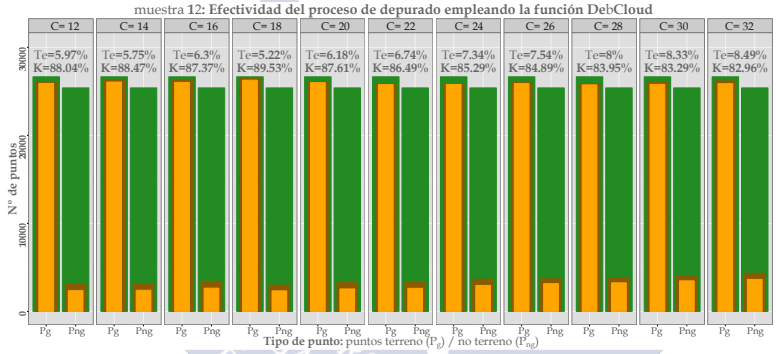

(b)

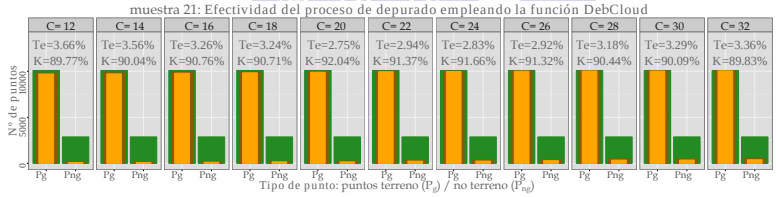

(c)

Figura A.7: Efectividad del proceso de depurado (parte 1). Resultados para las muestras a) 11, vegetación y edificios en pendiente elevada; b) 12, edificios y coches; c) 21, vegetación y edificios en pendiente elevada. Leyenda: la barra verde señala el número de puntos originales; la barra marrón, el número de puntos tras la primera fase del depurado; y la barra amarilla, el número de puntos tras la segunda fase del depurado.

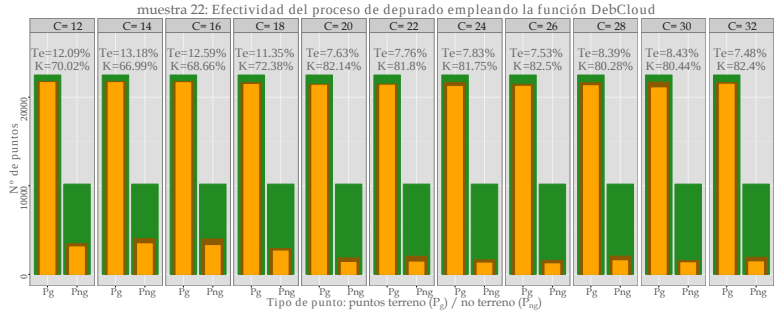

(a)

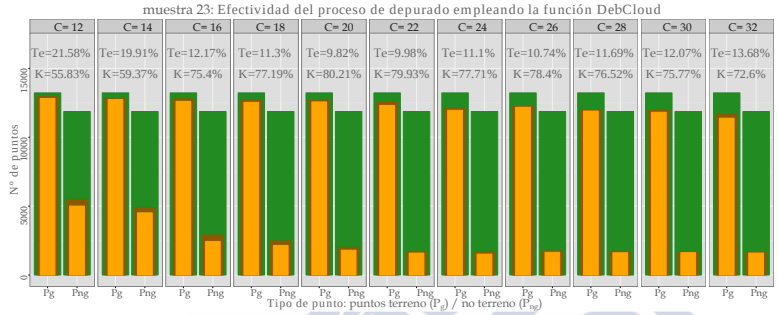

(b)

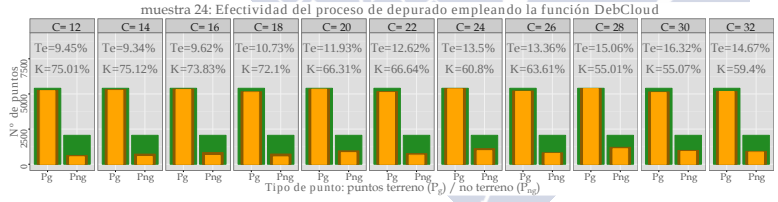

(c)

Figura A.8: Efectividad del proceso de depurado (parte 2). Resultados para las muestras a) 22, puente y pasarela; b) 23, grandes edificios y discontinuidades en el terreno; c) 24, rampa. Leyenda: la barra verde señala el número de puntos originales; la barra marrón, el número de puntos tras la primera fase del depurado; y la barra amarilla, el número de puntos tras la segunda fase del depurado.

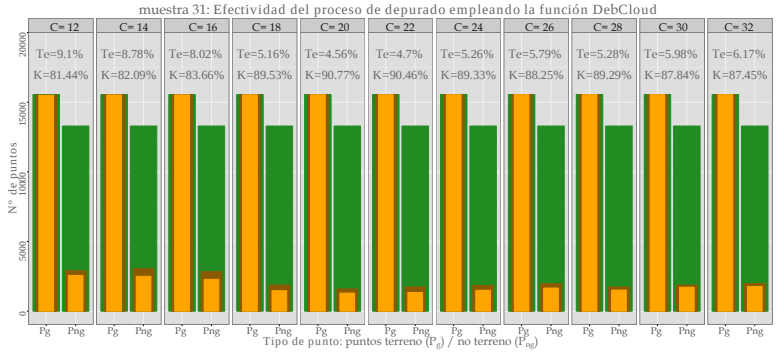

(a)

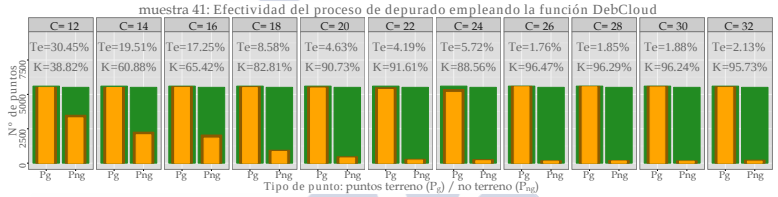

(b)

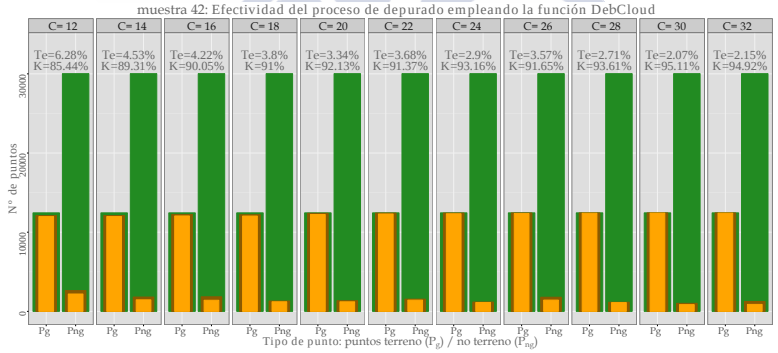

(c)

Figura A.9: Efectividad del proceso de depurado (parte 3). Resultados para las muestras a) 31, discontinuidades en el terreno e influencia de outliers; b) 41, presencia de outliers (efecto multi-path); c) 42, objetos alargados y de pequeño tamaño y relieve heterogéneo. Leyenda: la barra verde señala el número de puntos originales; la barra marrón, el número de puntos tras la primera fase del depurado; y la barra amarilla, el número de puntos tras la segunda fase del depurado.

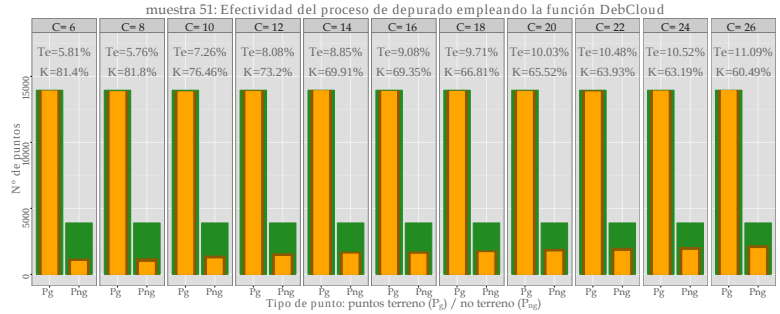

(a)

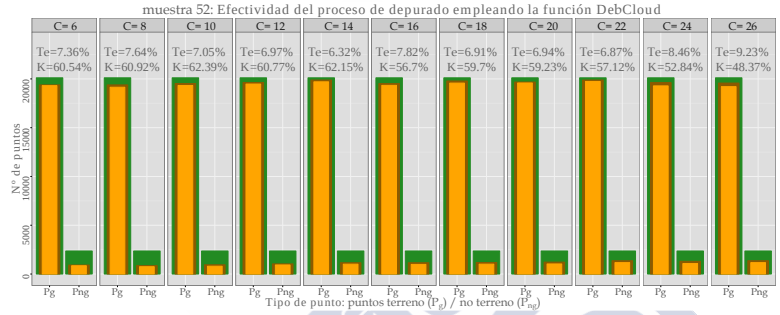

(b)

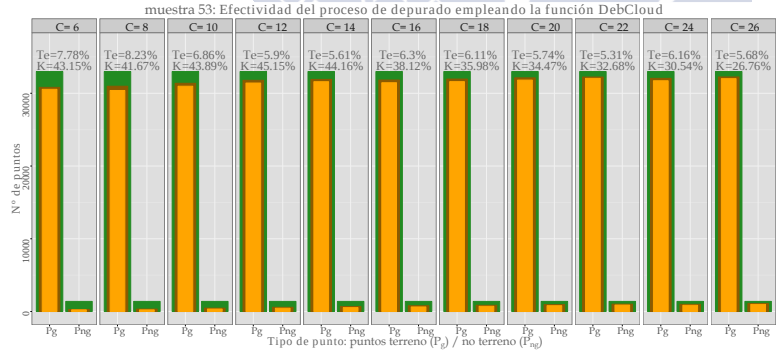

(c)

Figura A.10: Efectividad del proceso de depurado (parte 4). Resultados para las muestras a) 51, vegetación en pendiente elevada; b) 52, vegetación baja y discontinuidad por acantilado; c) 53, terreno discontinuo. Leyenda: la barra verde señala el número de puntos originales; la barra marrón, el número de puntos tras la primera fase del depurado; y la barra amarilla, el número de puntos tras la segunda fase del depurado.

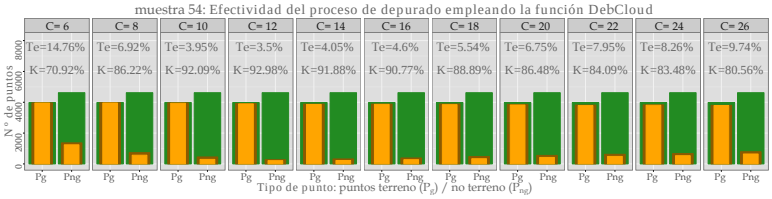

(a)

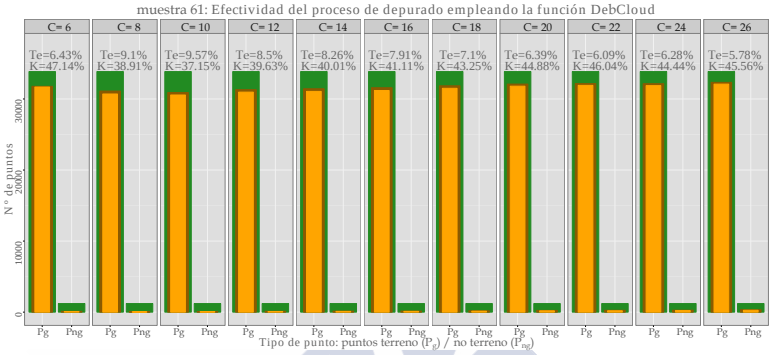

(b)

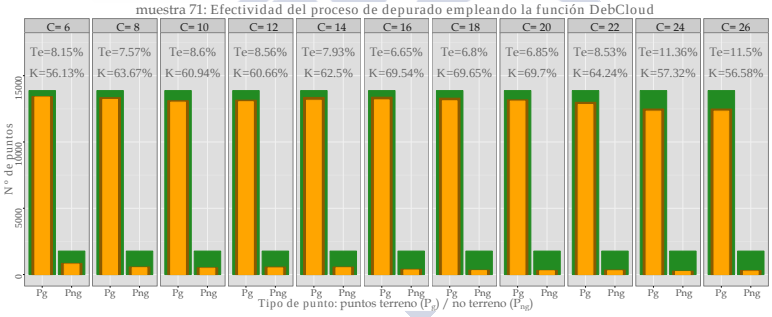

(c)

Figura A.11: Efectividad del proceso de depurado (parte 5). Resultados para las muestras a) 54, edificios bajos; b) 61, discontinuidades: acantilados y zanjas; c) 71, puente y terreno discontinuo. Leyenda: la barra verde señala el número de puntos originales; la barra marrón, el número de puntos tras la primera fase del depurado; y la barra amarilla, el número de puntos tras la segunda fase del depurado.

La Tabla A.20 contiene los resultados cuantitativos del proceso de depurado. Para su elaboración se tomó para cada muestra el resultado del depurado y de la selección de los puntos semilla obtenido a partir del empleo de los parámetros óptimos para cada caso. Las columnas que hacen referencia a la nube de puntos depurada indican el número de puntos terreno (P_g) y no terreno (P_{ng}) tras la fase 2 y el porcentaje de reducción de puntos con respecto al total.

Tabla A.20: Efectividad del proceso de depurado.

Muestras		**P**	**P_D**		**P_S**	**Estadísticos**	
		NºPtos	NºPtos	% reducción		Te (%)	K (%)
Muestra11	P_g	21777	21358	1.92	8818	22.28	51.54
	P_{ng}	16211	8046	50.37	449		
Muestra12	P_g	26654	26269	1.44	11246	5.22	89.53
	P_{ng}	25393	2334	90.81	95		
Muestra21	P_g	10085	10002	0.82	3647	2.92	91.32
	P_{ng}	2875	295	89.74	3		
Muestra22	P_g	22498	21237	5.60	8048	7.52	82.49
	P_{ng}	10185	1198	88.24	76		
Muestra23	P_g	13223	12192	7.80	5806	10.25	79.39
	P_{ng}	11871	1542	87.01	159		
Muestra24	P_g	5404	5337	1.24	2465	11.93	66.31
	P_{ng}	2058	823	60.01	82		
Muestra31	P_g	15554	15540	0.09	2852	4.62	90.63
	P_{ng}	13292	1319	90.08	5		
Muestra41	P_g	5602	5551	0.91	2250	1.85	96.29
	P_{ng}	5513	155	97.19	7		
Muestra42	P_g	12443	12418	0.20	3243	2.07	95.11
	P_{ng}	30025	853	97.16	23		
Muestra51	P_g	13950	13920	0.22	9281	11.09	60.49
	P_{ng}	3895	1949	49.96	145		
Muestra52	P_g	20112	19300	4.04	15213	8.84	49.58
	P_{ng}	2362	1175	50.25	99		
Muestra53	P_g	32989	31530	4.42	28048	5.62	45.87
	P_{ng}	1389	474	65.87	103		
Muestra54	P_g	3983	3894	2.23	3403	3.5	92.98
	P_{ng}	4620	212	95.41	42		
Muestra61	P_g	33854	32068	5.28	32018	5.36	51.85
	P_{ng}	1206	94	92.21	94		
Muestra71	P_g	13875	13182	4.99	8731	6.3	71.45
	P_{ng}	1770	292	83.5	50		

Las gráficas que se incluyen a continuación representan cualitativamente la efectividad del proceso de depurado y el resultado de la selección de los puntos semilla. Así, para cada una de las muestras se muestran tres figuras: la nube de puntos original clasificada en puntos terreno (P_g - en verde) y puntos no terreno (P_{ng} - en amarillo); la nube de puntos resultante del proceso de depurado; y finalmente los puntos seleccionados como semilla.

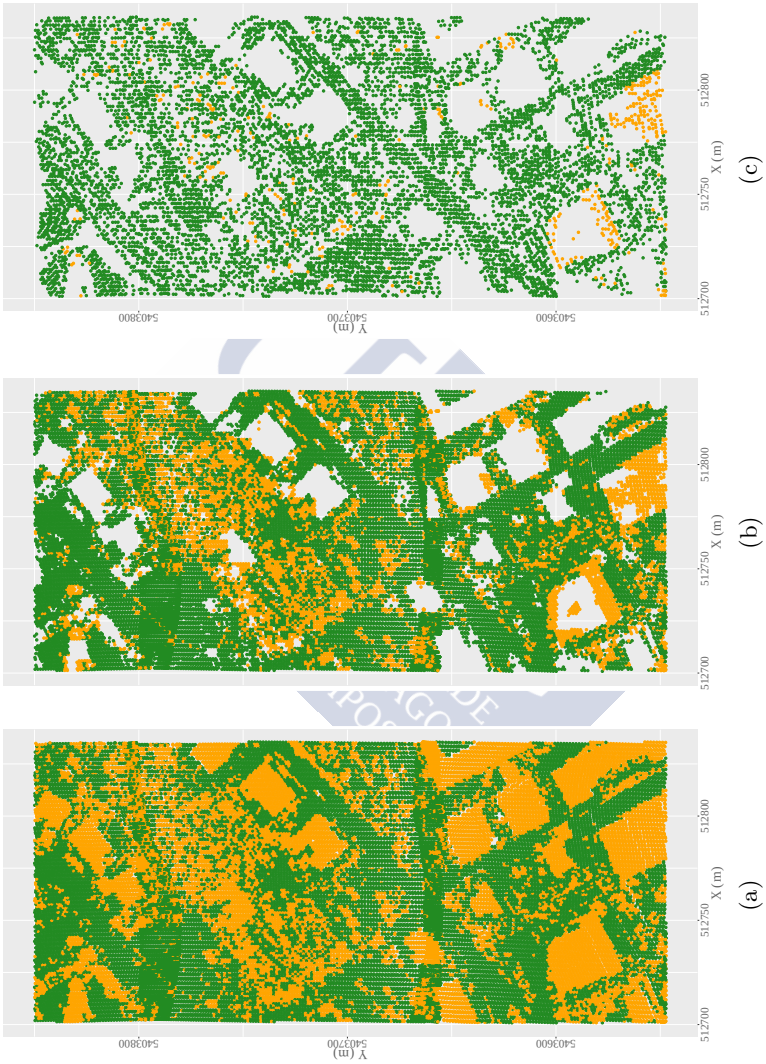

Figura A.12: Muestra 11: Efectividad del proceso de depurado. Donde: a) nube de puntos original clasificada en P_g (verde) y P_{ng} (amarillo); b) nube de puntos resultante del proceso de depurado y c) nube de puntos semilla.

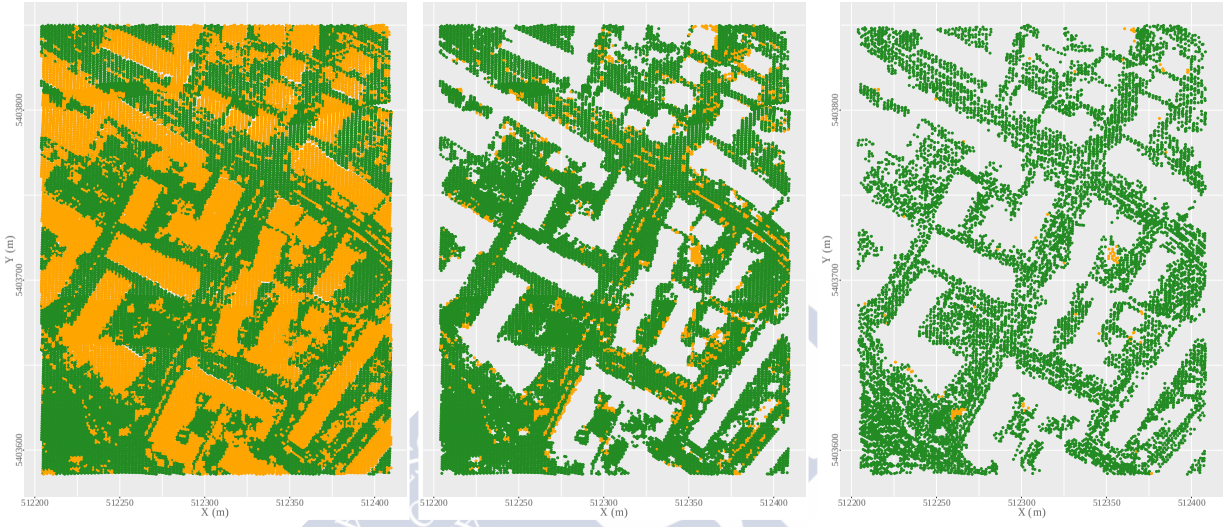

(a) (b) (c)

Figura A.13: Muestra 12: Efectividad del proceso de depurado. Donde: a) nube de puntos original clasificada en P_g (verde) y P_{ng} (amarillo); b) nube de puntos resultante del proceso de depurado y c) nube de puntos semilla.

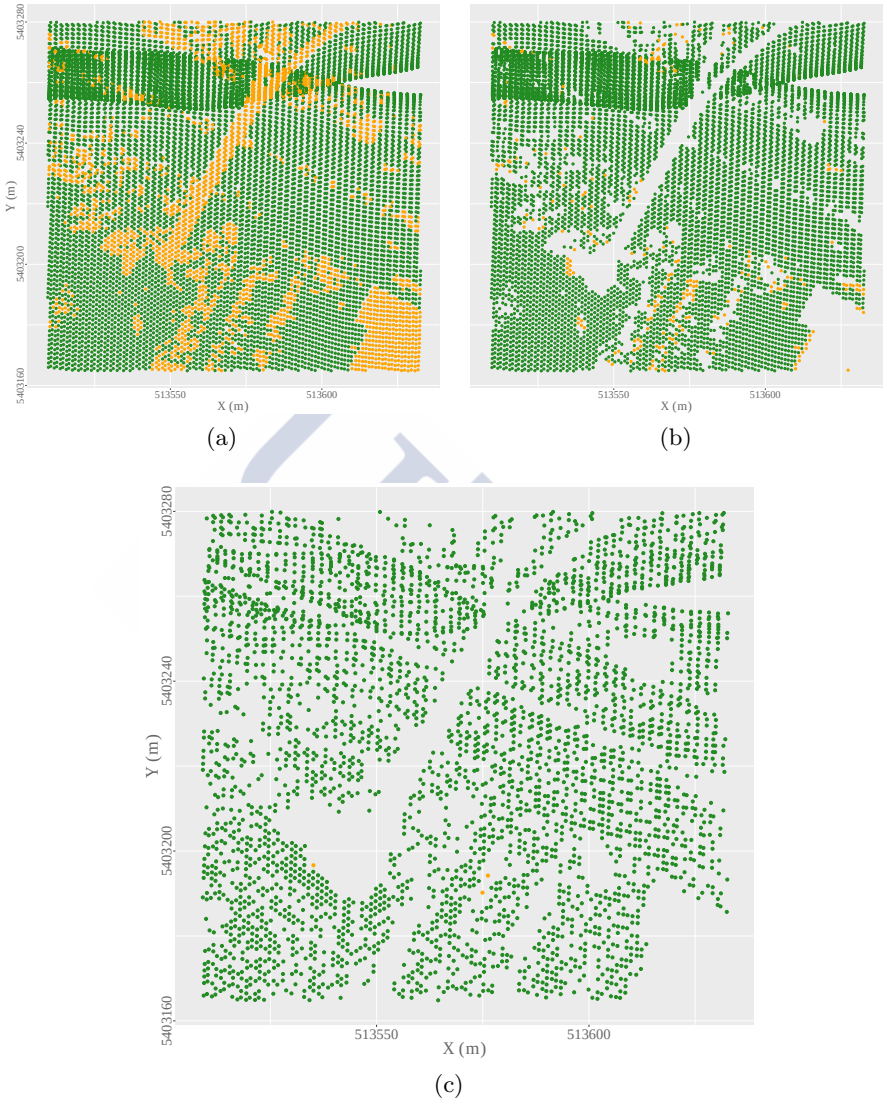

Figura A.14: Muestra 21: Efectividad del proceso de depurado. Donde: a) nube de puntos original clasificada en P_g (verde) y P_{ng} (amarillo); b) nube de puntos resultante del proceso de depurado y c) nube de puntos semilla.

Figura A.15: Muestra 22: Efectividad del proceso de depurado. Donde: a) nube de puntos original clasificada en P_g (verde) y P_{ng} (amarillo); b) nube de puntos resultante del proceso de depurado y c) nube de puntos semilla.

Figura A.16: Muestra 23: Efectividad del proceso de depurado. Donde: a) nube de puntos original clasificada en P_g (verde) y P_{ng} (amarillo); b) nube de puntos resultante del proceso de depurado y c) nube de puntos semilla.

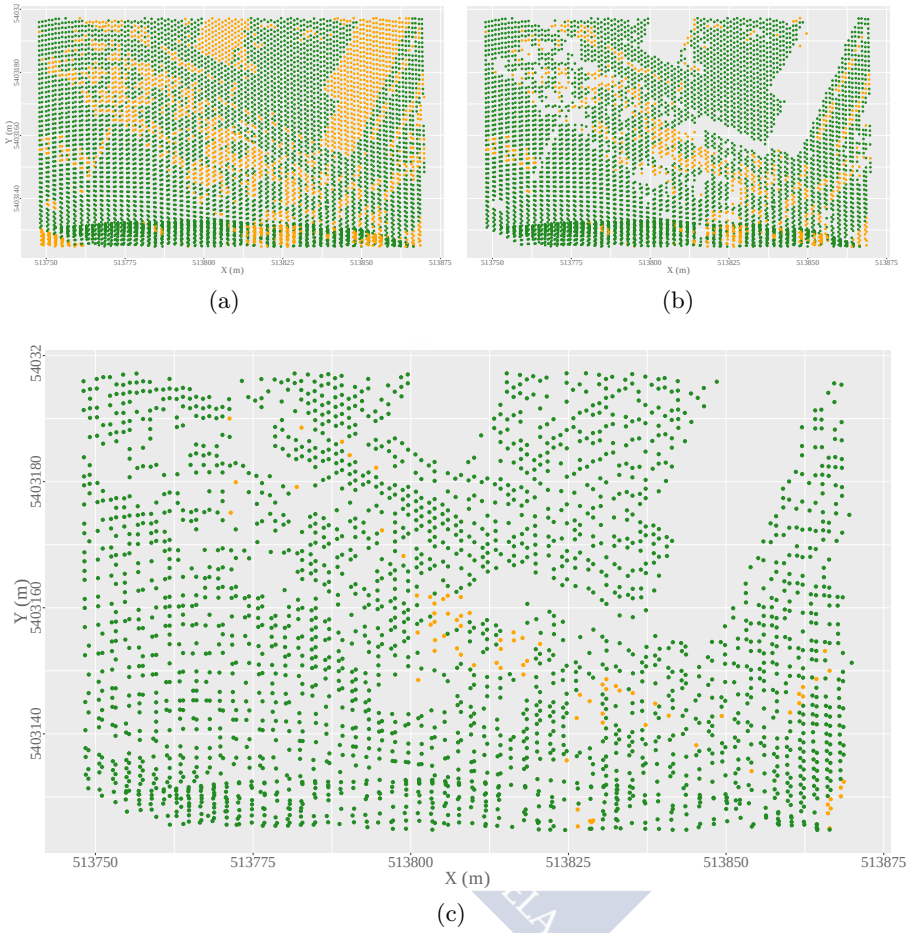

Figura A.17: Muestra 24: Efectividad del proceso de depurado. Donde: a) nube de puntos original clasificada en P_g (verde) y P_{ng} (amarillo); b) nube de puntos resultante del proceso de depurado y c) nube de puntos semilla.

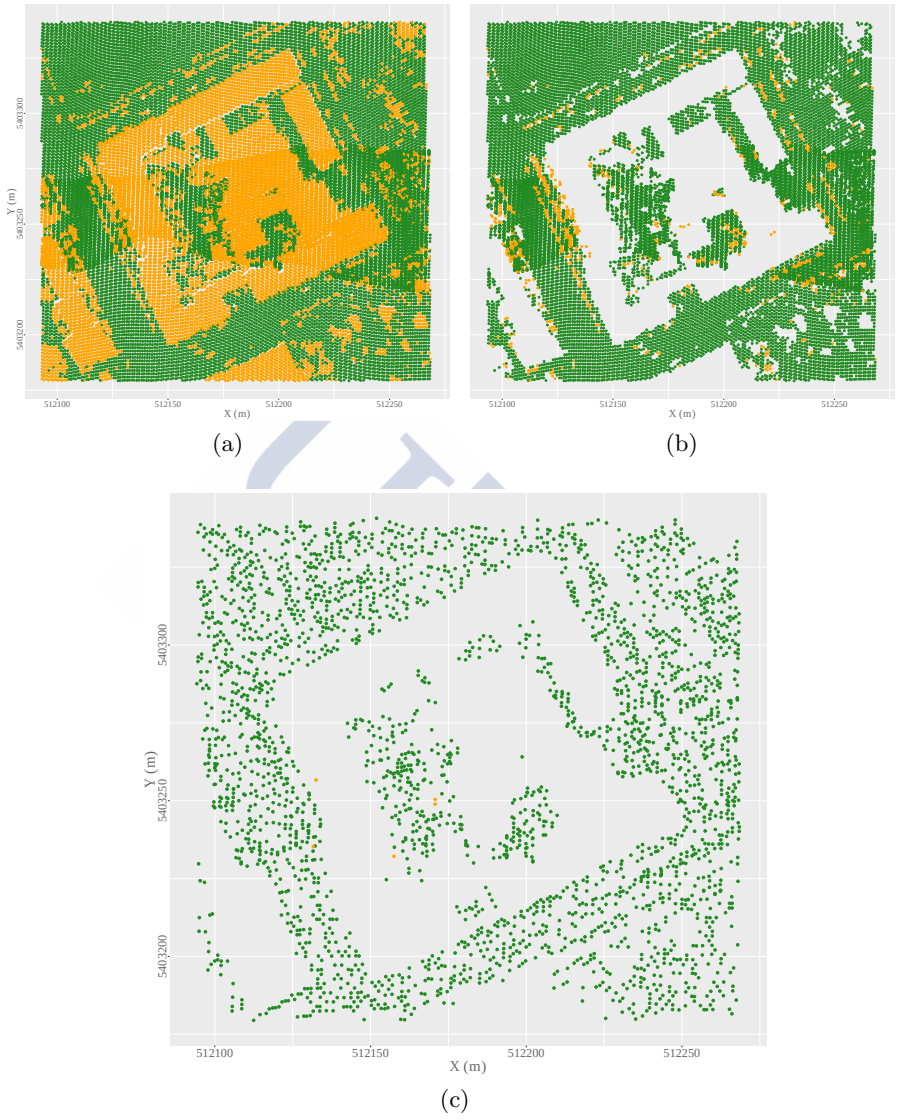

Figura A.18: Muestra 31: Efectividad del proceso de depurado. Donde: a) nube de puntos original clasificada en P_g (verde) y P_{ng} (amarillo); b) nube de puntos resultante del proceso de depurado y c) nube de puntos semilla.

Figura A.19: Muestra 41: Efectividad del proceso de depurado. Donde: a) nube de puntos original clasificada en P_g (verde) y P_{ng} (amarillo); b) nube de puntos resultante del proceso de depurado y c) nube de puntos semilla.

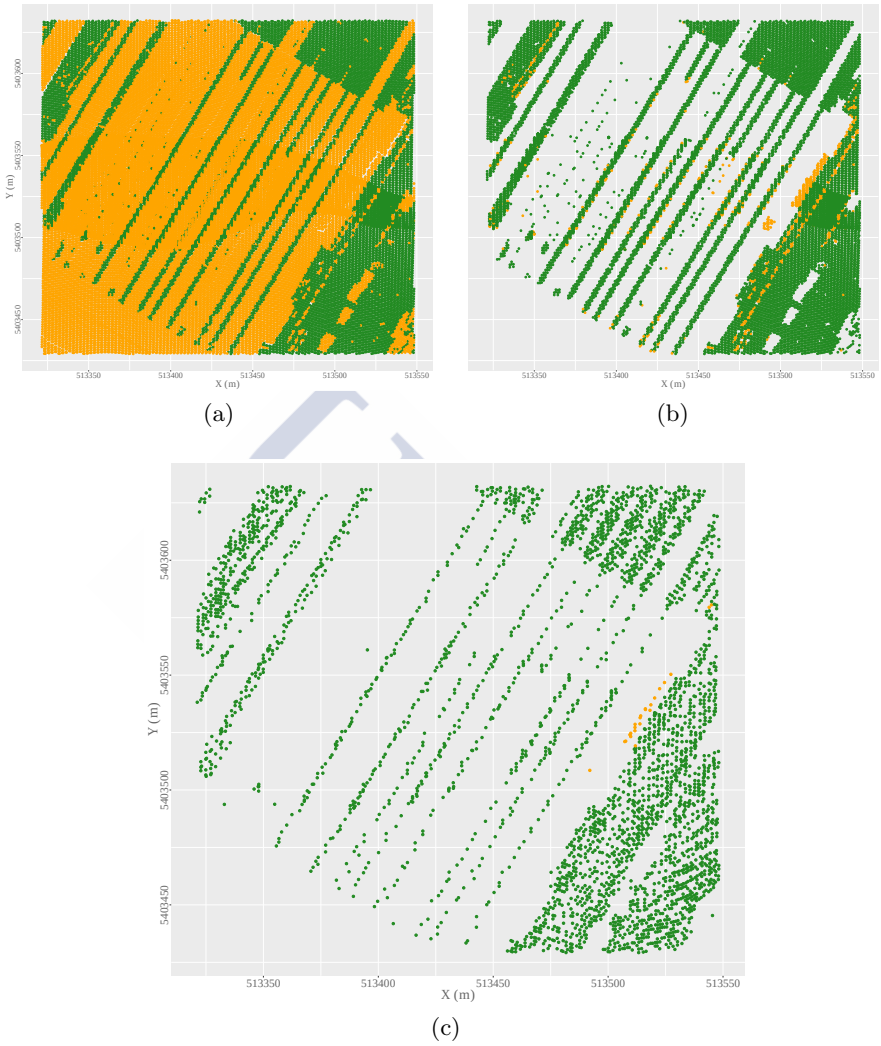

Figura A.20: Muestra 42: Efectividad del proceso de depurado. Donde: a) nube de puntos original clasificada en P_g (verde) y P_{ng} (amarillo); b) nube de puntos resultante del proceso de depurado y c) nube de puntos semilla.

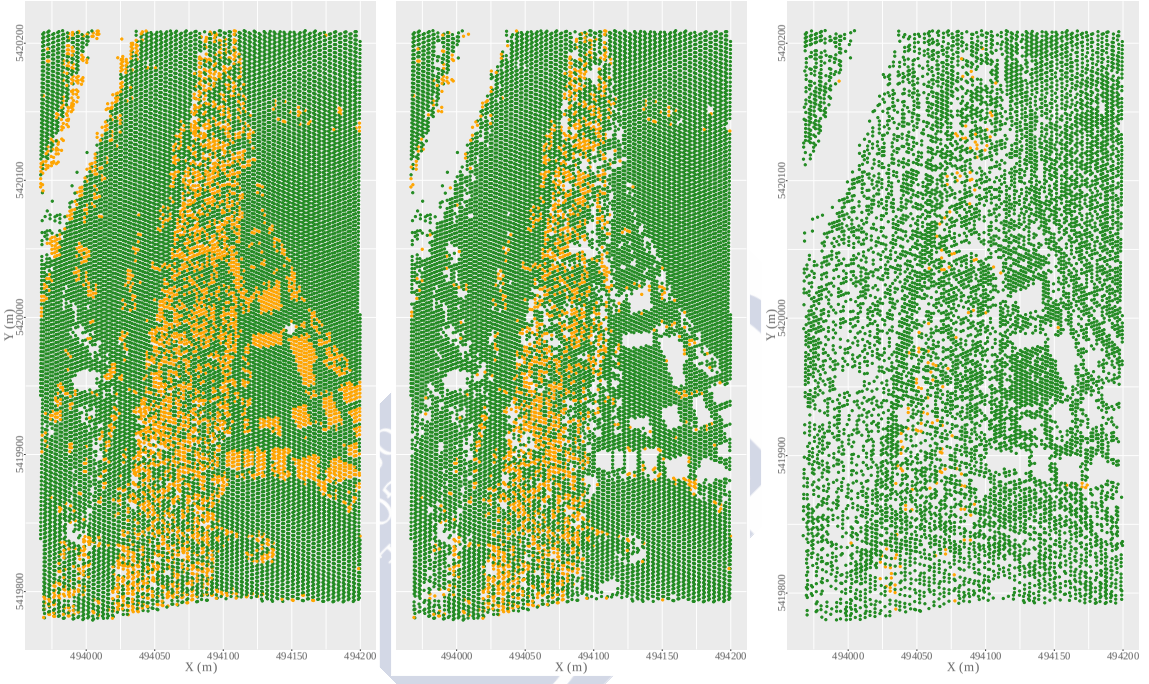

Figura A.21: Muestra 51: Efectividad del proceso de depurado. Donde: a) nube de puntos original clasificada en P_g (verde) y P_{ng} (amarillo); b) nube de puntos resultante del proceso de depurado y c) nube de puntos semilla.

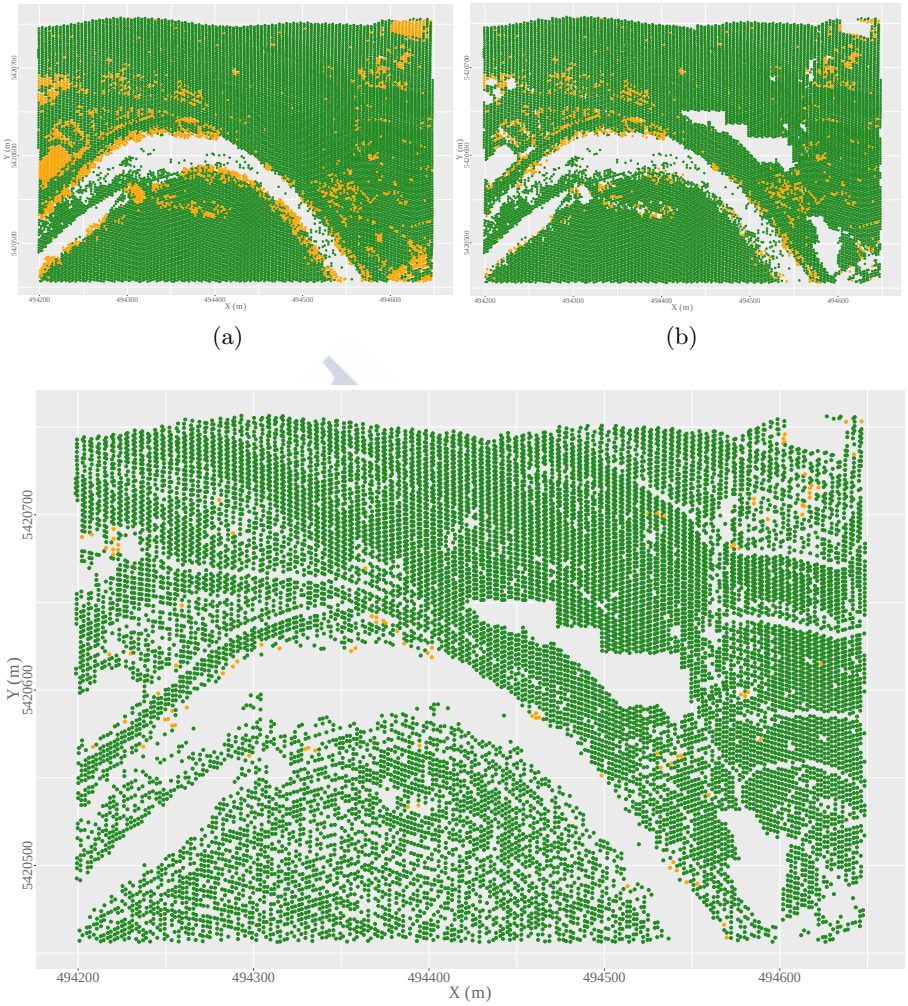

Figura A.22: Muestra 52: Efectividad del proceso de depurado. Donde: a) nube de puntos original clasificada en P_g (verde) y P_{ng} (amarillo); b) nube de puntos resultante del proceso de depurado y c) nube de puntos semilla.

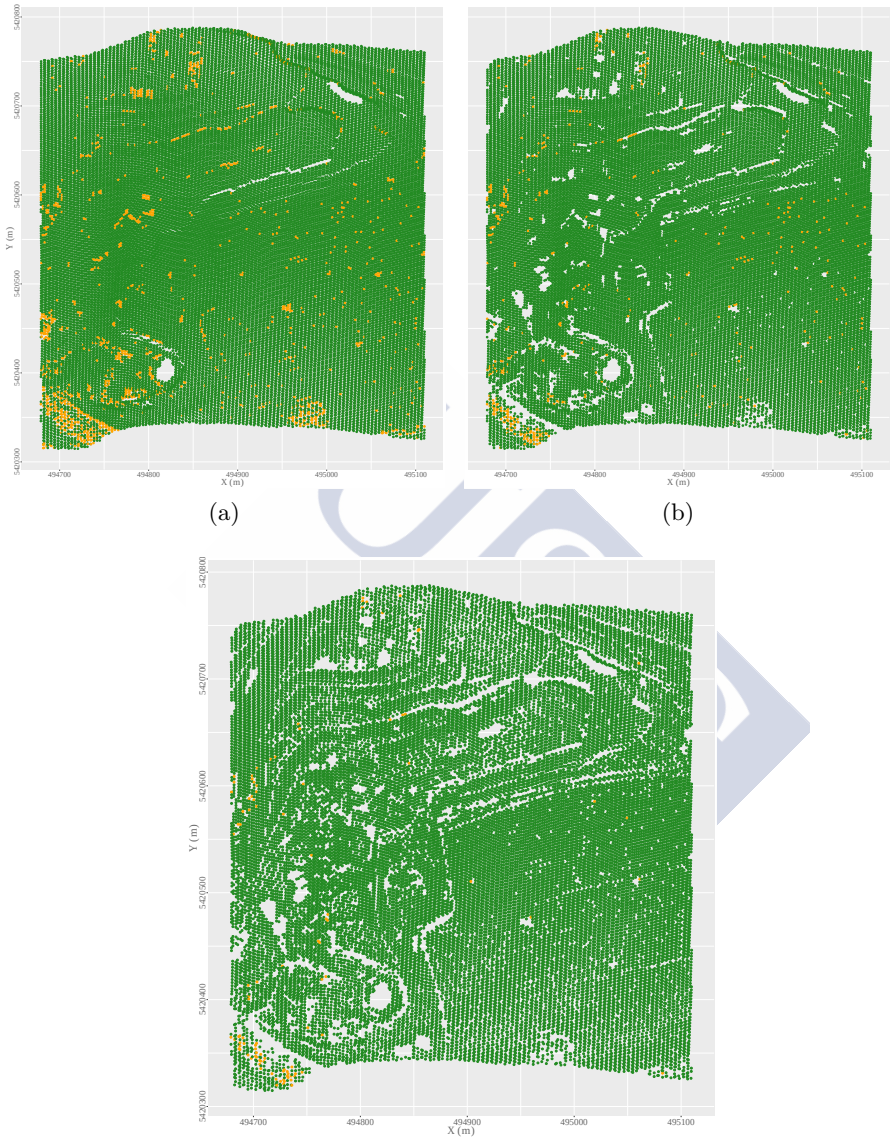

Figura A.23: Muestra 53: Efectividad del proceso de depurado. Donde: a) nube de puntos original clasificada en P_g (verde) y P_{ng} (amarillo); b) nube de puntos resultante del proceso de depurado y c) nube de puntos semilla.

Figura A.24: Muestra 54: Efectividad del proceso de depurado. Donde: a) nube de puntos original clasificada en P_g (verde) y P_{ng} (amarillo); b) nube de puntos resultante del proceso de depurado y c) nube de puntos semilla.

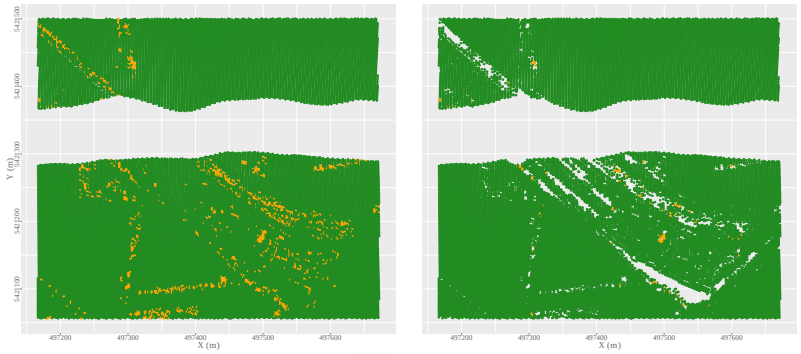

(a) (b)

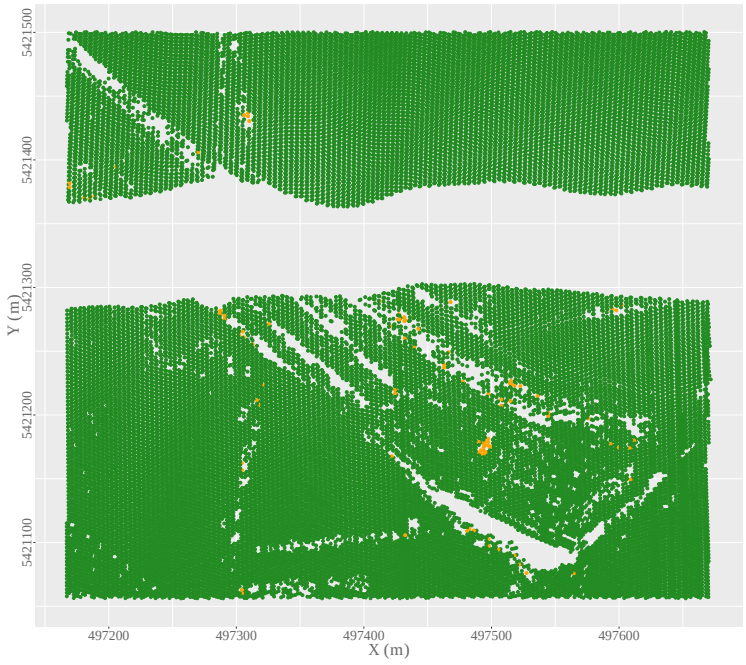

(c)

Figura A.25: Muestra 61: Efectividad del proceso de depurado. Donde: a) nube de puntos original clasificada en P_g (verde) y P_{ng} (amarillo); b) nube de puntos resultante del proceso de depurado y c) nube de puntos semilla.

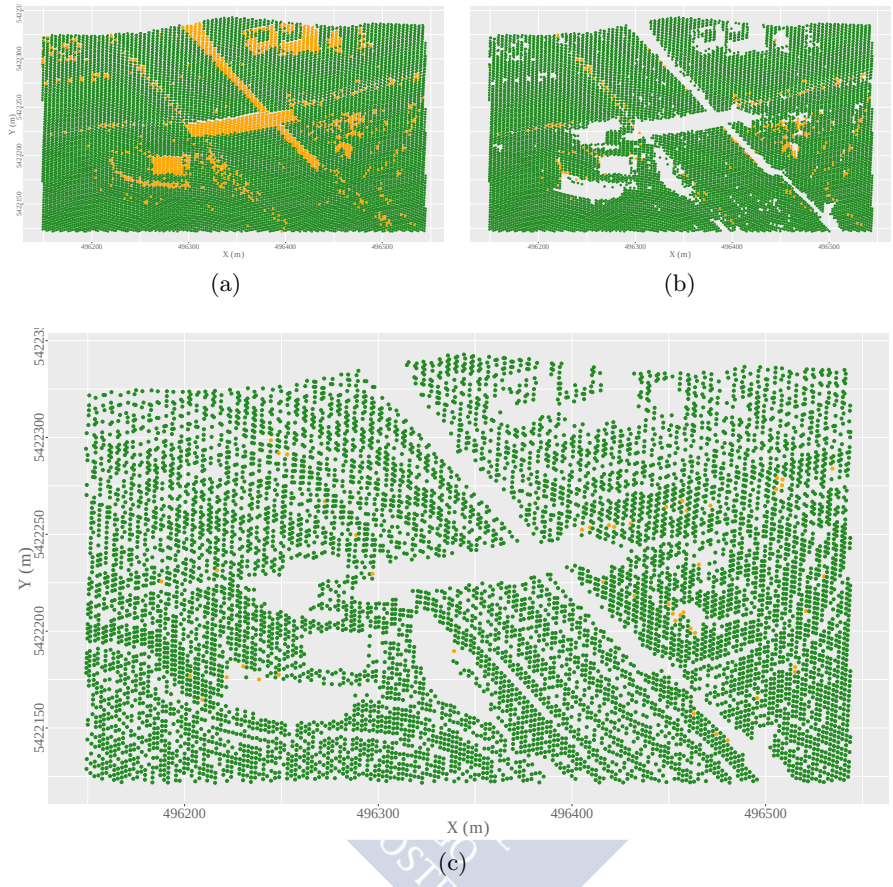

Figura A.26: Muestra 71: Efectividad del proceso de depurado. Donde: a) nube de puntos original clasificada en P_g (verde) y P_{ng} (amarillo); b) nube de puntos resultante del proceso de depurado y c) nube de puntos semilla.

USC
UNIVERSIDADE
DE SANTIAGO
DE COMPOSTELA

A.5 Comportamiento de *TIe*,*TIIe* y *Te* ante variaciones de los parámetros variables.

En las siguientes gráficas se representa para cada una de las muestras el comportamiento de los errores tipo I, II y total ante variaciones de los parámetros variables C, C_S y δ_h. En las figuras de la izquierda, sombreado en rosado se muestran los resultados que se obtuvieron a partir de los valores óptimos de los parámetros C y C_S (fase 1 del ajuste de parámetros), variando el parámetro δ_h y mientras que sombreado en azul se indica la combinación de parámetros óptima. En las figuras de la derecha se representa la influencia de los parámetros variables sobre el error total. De esta forma se observa gráficamente cómo variaciones de los diferentes parámetros afectan a la calidad del filtrado.

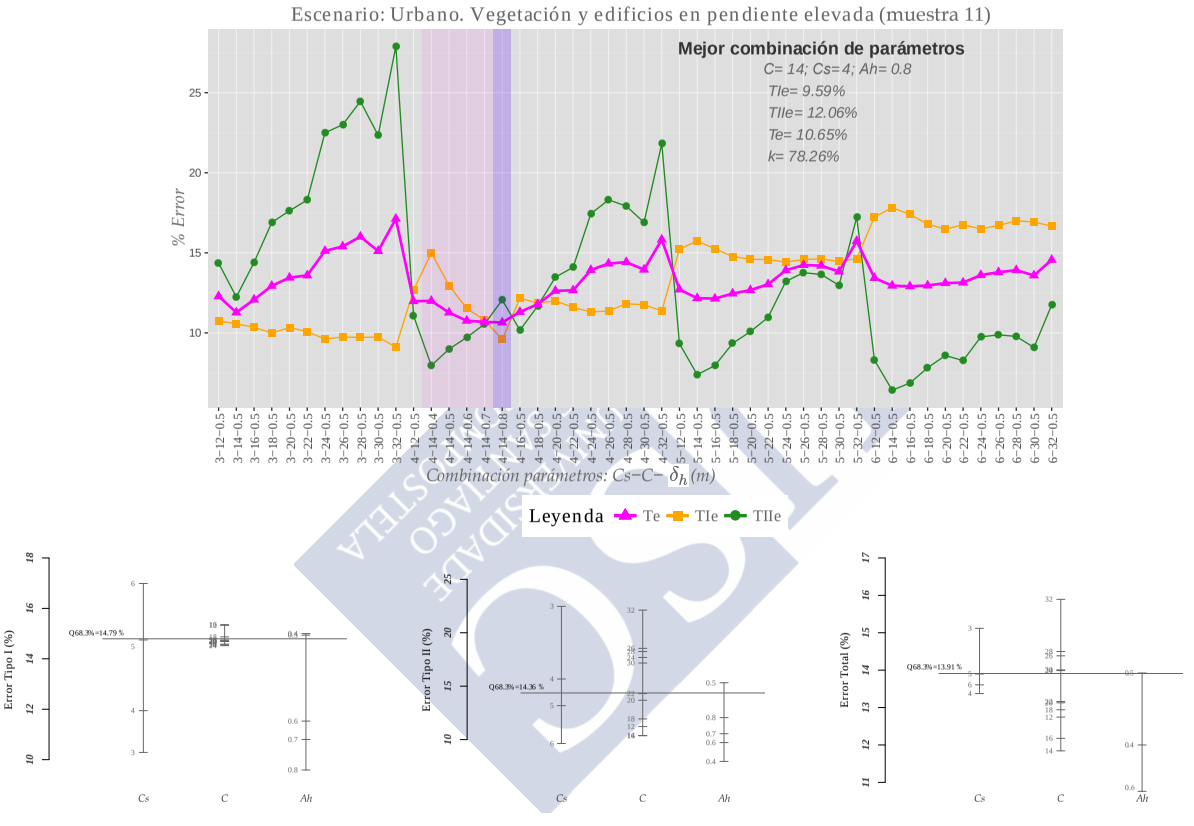

Figura A.27: Muestra 11: Vegetación y edificios en pendiente elevada. Influencia de la variación de los parámetros variables en los errores Tipo I, Tipo II y Total (ver gráfico).

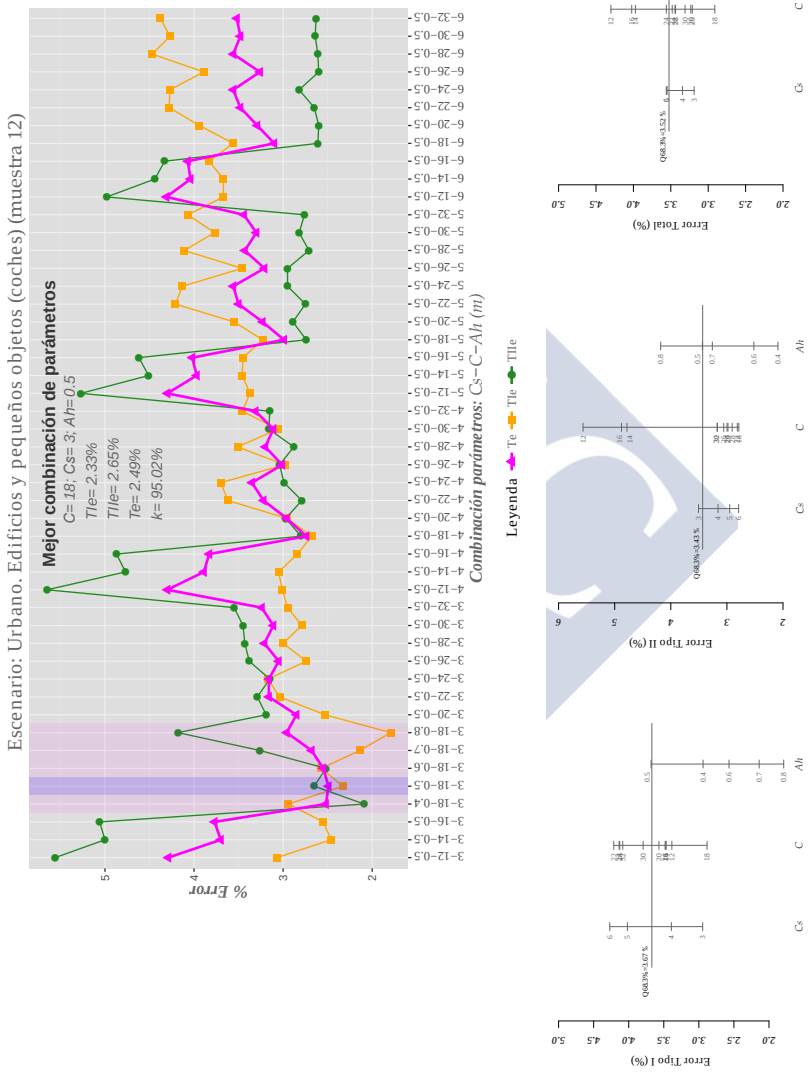

Figura A.28: Muestra 12: Edificios y coches. Influencia de la variación de los parámetros variables en los errores Tipo I, Tipo II y Total (ver gráfico).

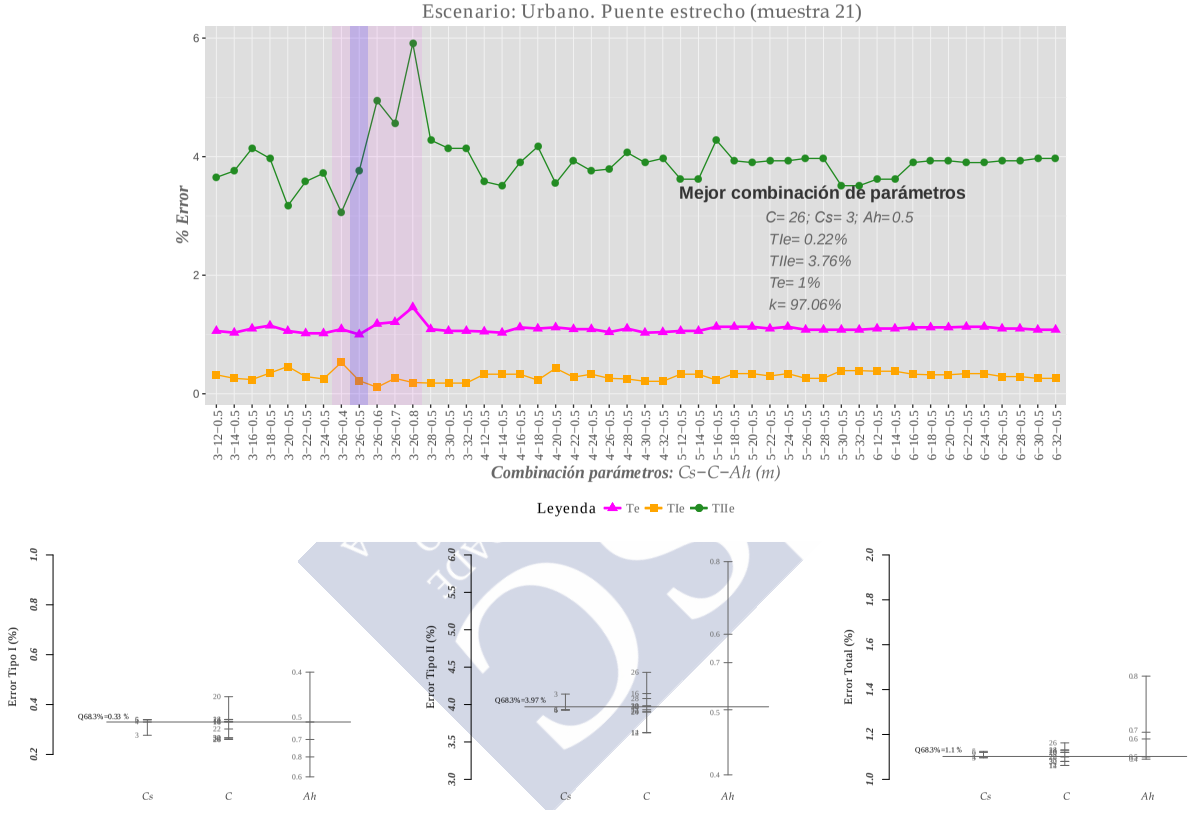

Figura A.29: Muestra 21: Vegetación y edificios en pendiente elevada. Influencia de la variación de los parámetros variables en los errores Tipo I, Tipo II y Total (ver gráfico).

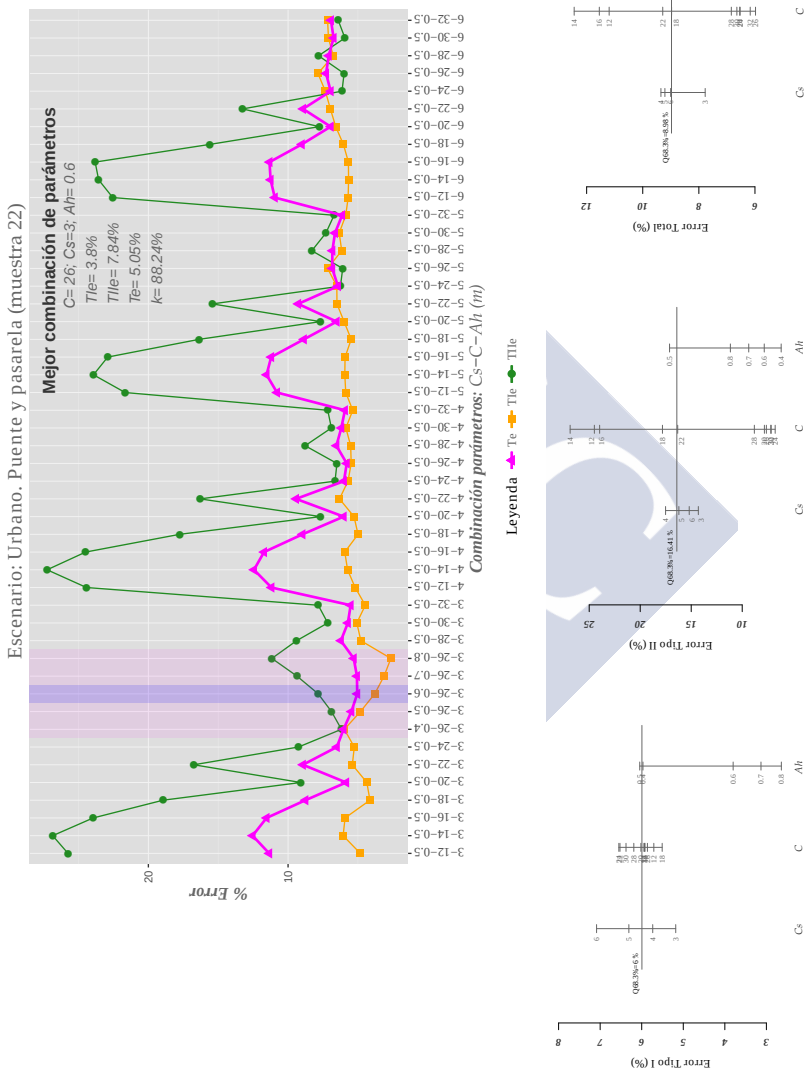

Figura A.30: Muestra 22: Puentes y pasarela. Influencia de la variación de los parámetros variables en los errores Tipo I, Tipo II y Total (ver gráfico).

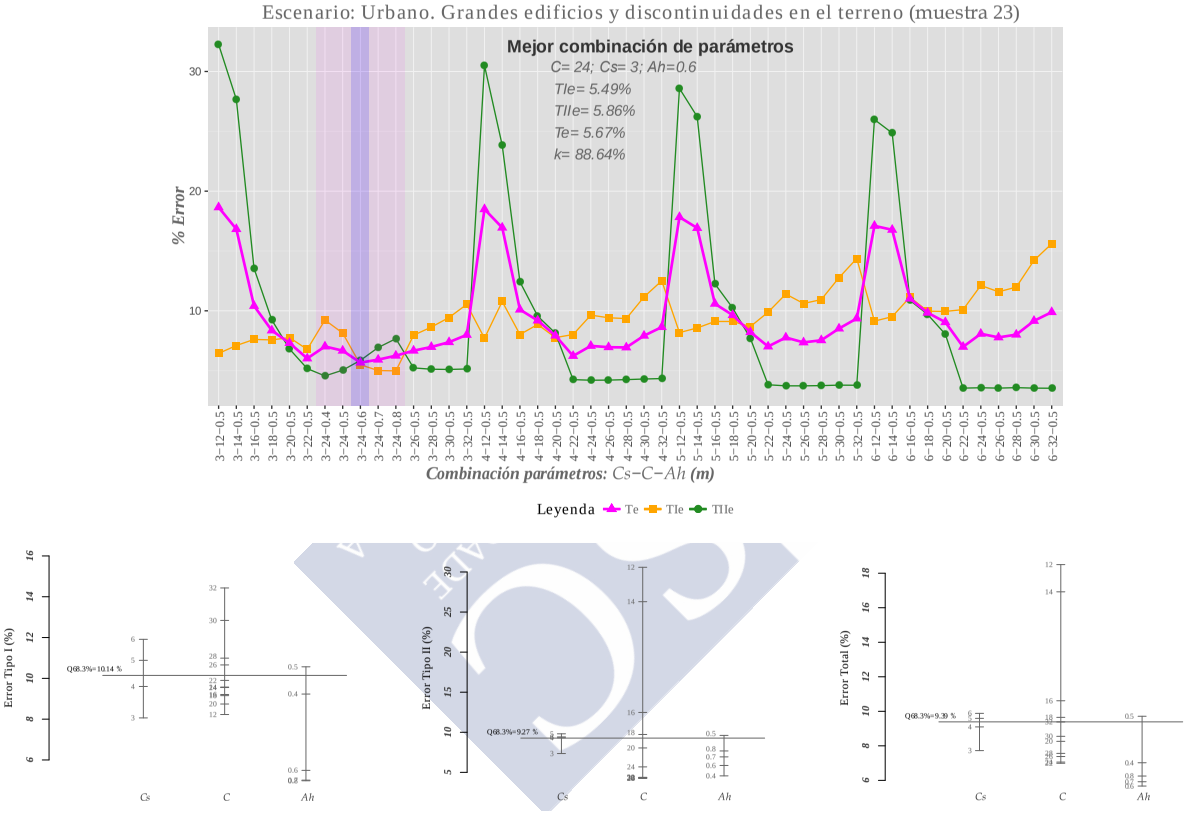

Figura A.31: Muestra 23: Grandes edificios y discontinuidades en el terreno. Influencia de la variación de los parámetros variables en los errores Tipo I, Tipo II y Total (ver gráfico).

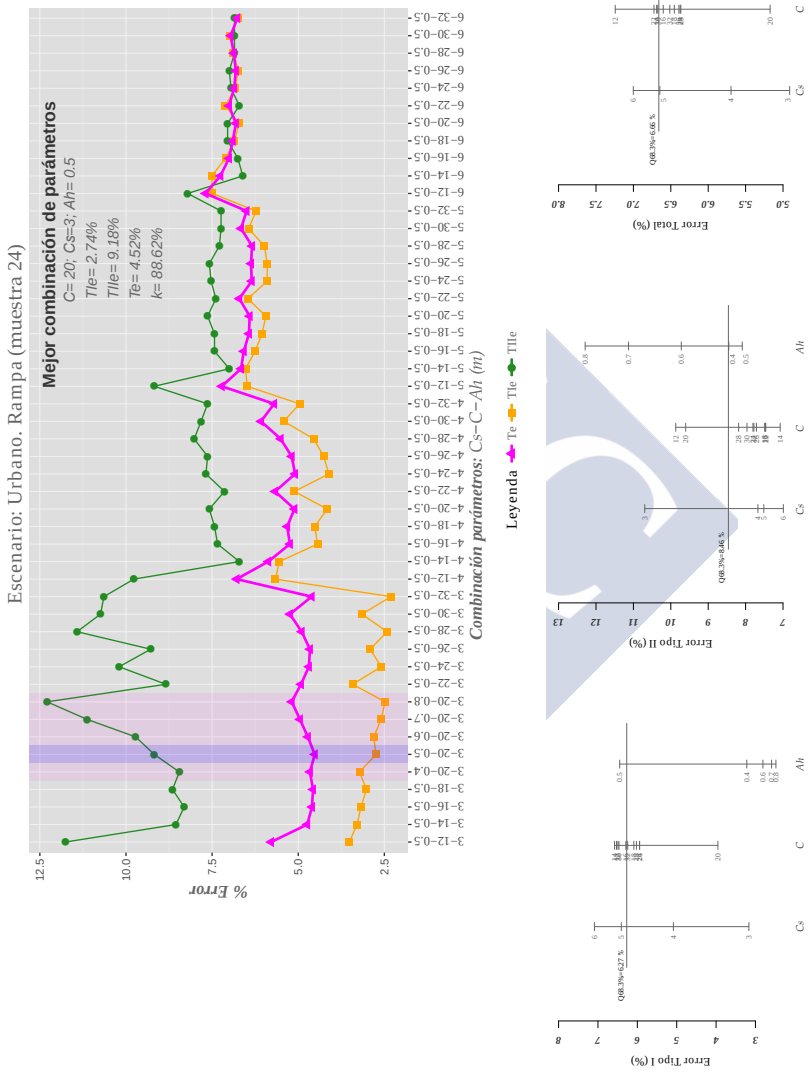

Figura A.32: Muestra 24: Presencia de rampas. Influencia de la variación de los parámetros variables en los errores Tipo I, Tipo II y Total (ver gráfico).

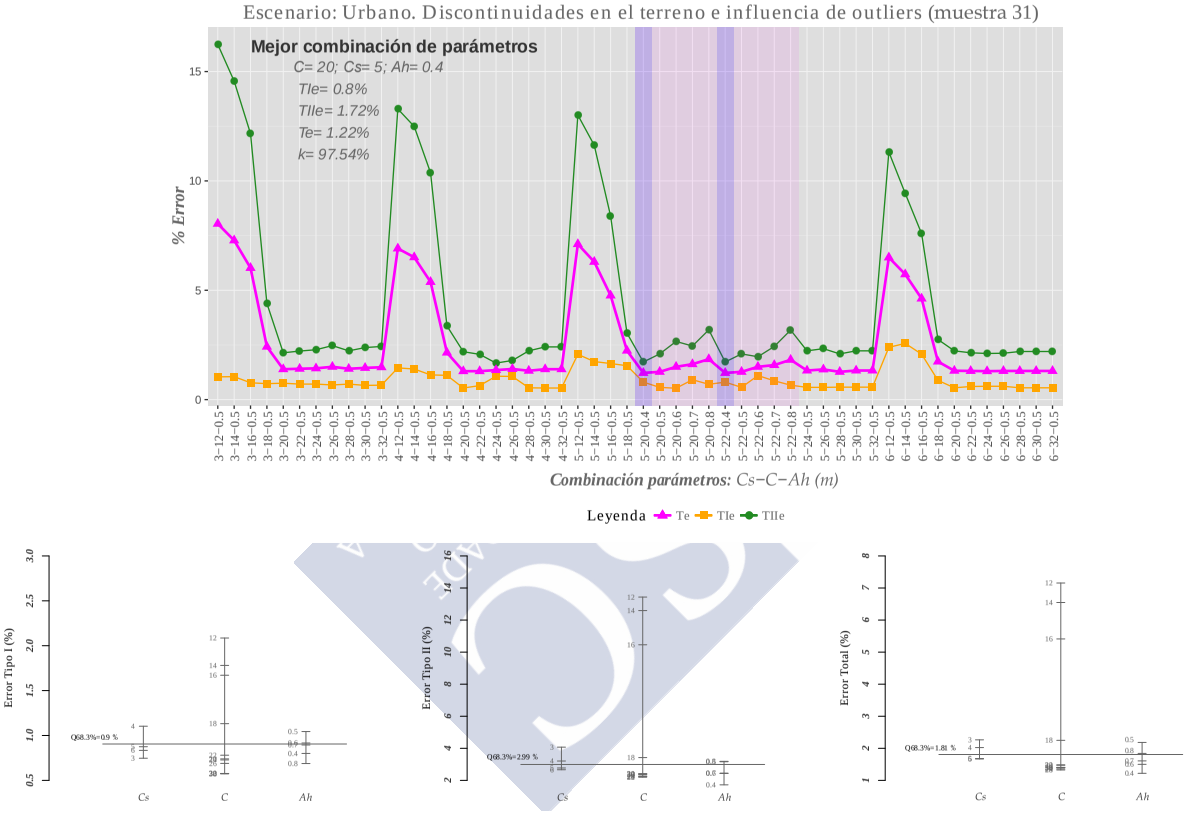

Figura A.33: Muestra 31: Grandes edificios. Influencia de la variación de los parámetros variables en los errores Tipo I, Tipo II y Total (ver gráfico).

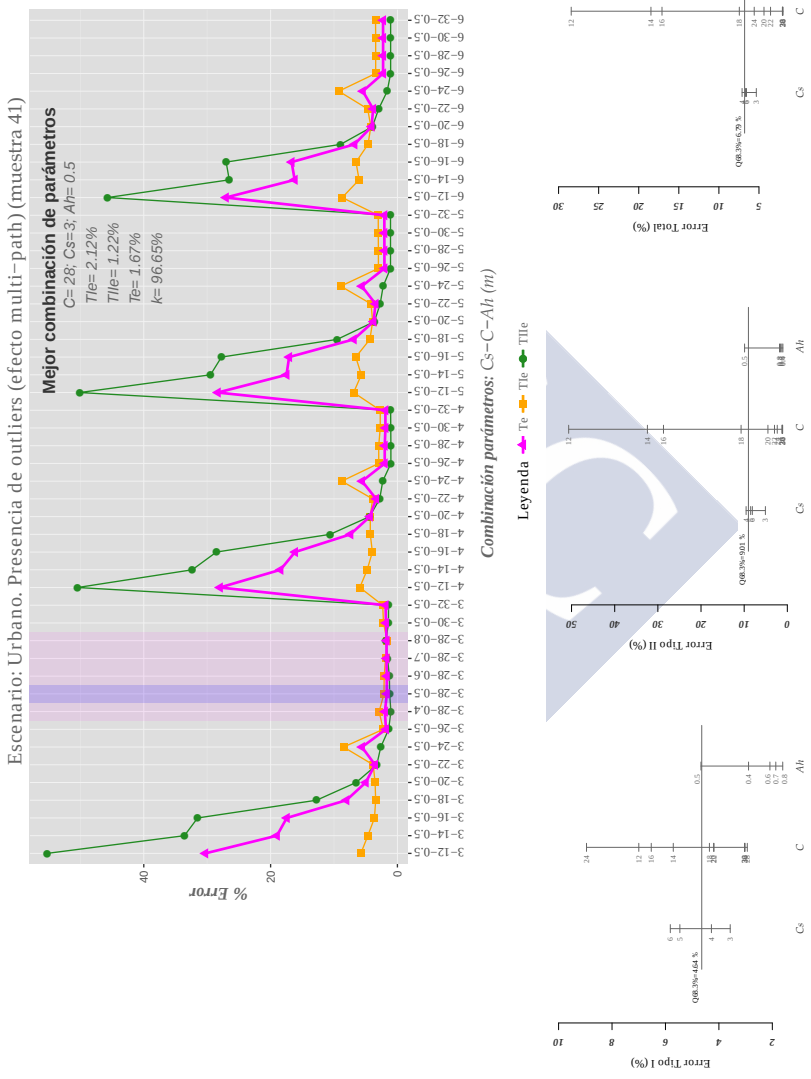

Figura A.34: Muestra 41: Presencia de *outliers*. Influencia de la variación de los parámetros variables en los errores Tipo I, Tipo II y Total (ver gráfico).

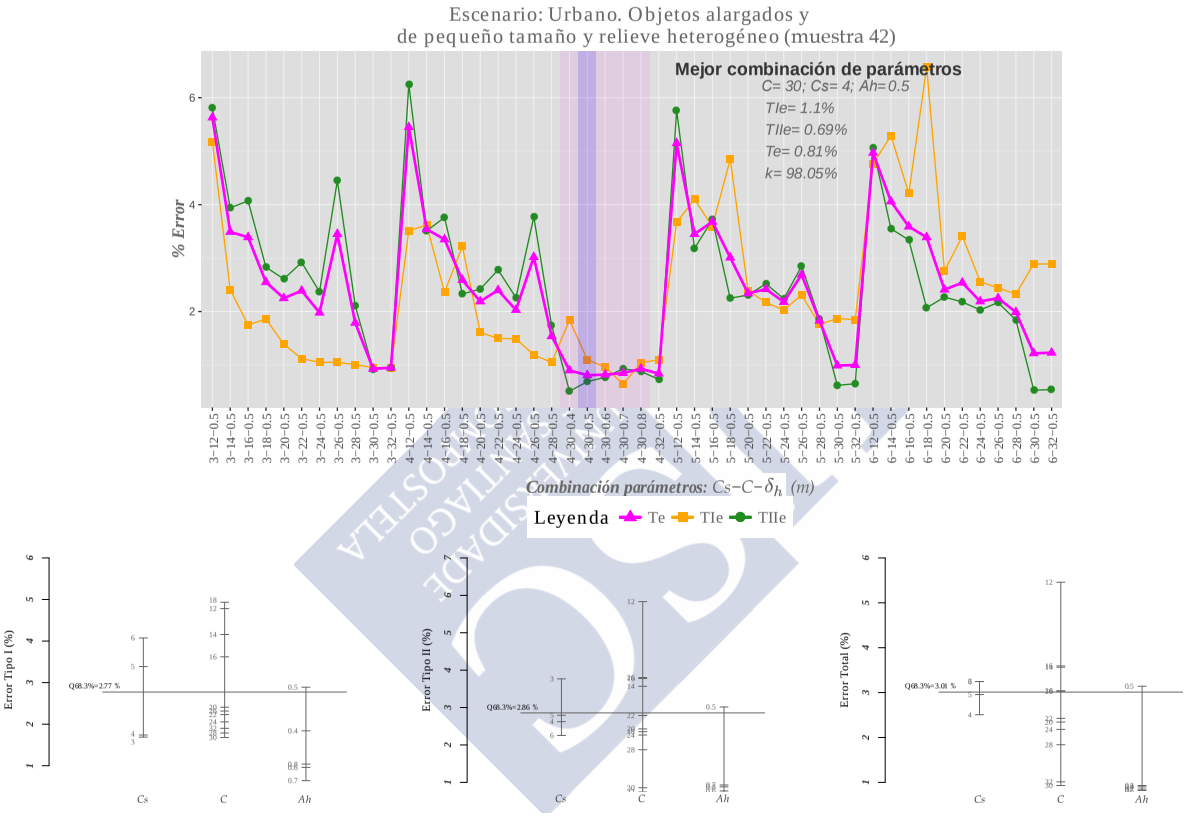

Figura A.35: Muestra 42: Presencia de rampas. Influencia de la variación de los parámetros variables en los errores Tipo I, Tipo II y Total (ver gráfico).

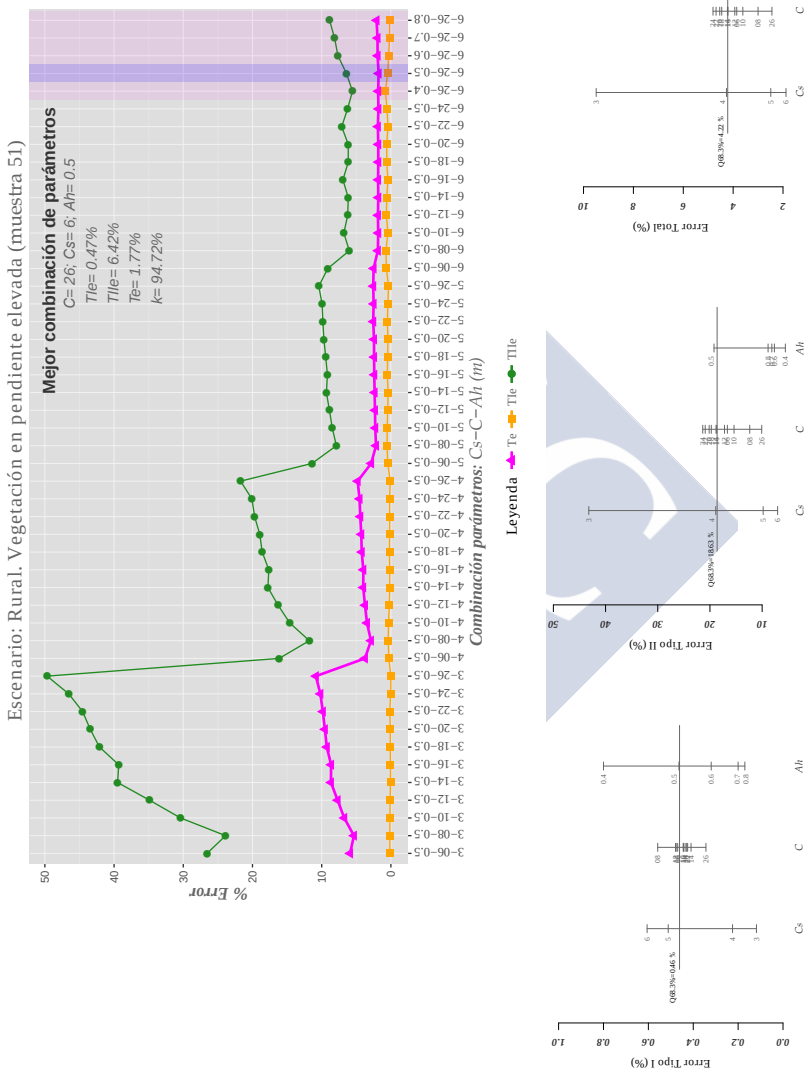

Figura A.36: Muestra 51: Vegetación en pendiente. Influencia de la variación de los parámetros variables en los errores Tipo I, Tipo II y Total (ver gráfico).

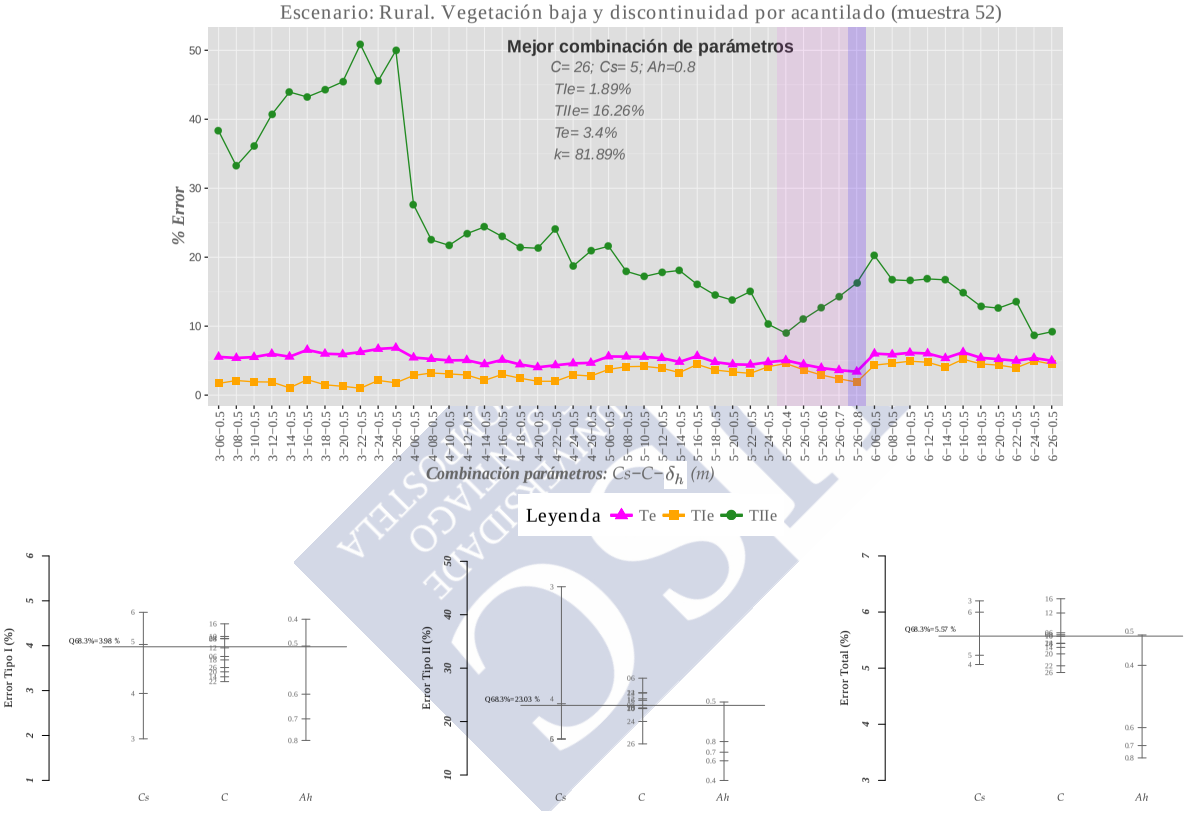

Figura A.37: Muestra 52: Pendiente. Influencia de la variación de los parámetros variables en los errores Tipo I, Tipo II y Total (ver gráfico).

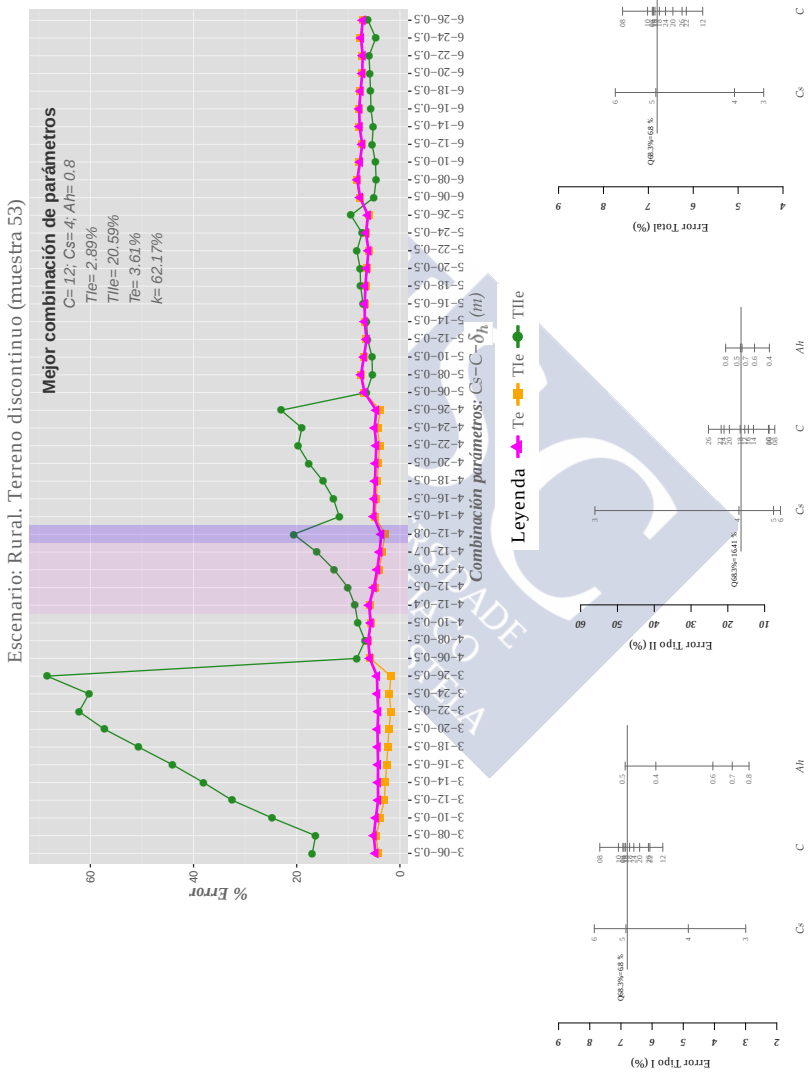

Figura A.38: Muestra 53: Terreno discontinuo. Influencia de la variación de los parámetros variables en los errores Tipo I, Tipo II y Total (ver gráfico).

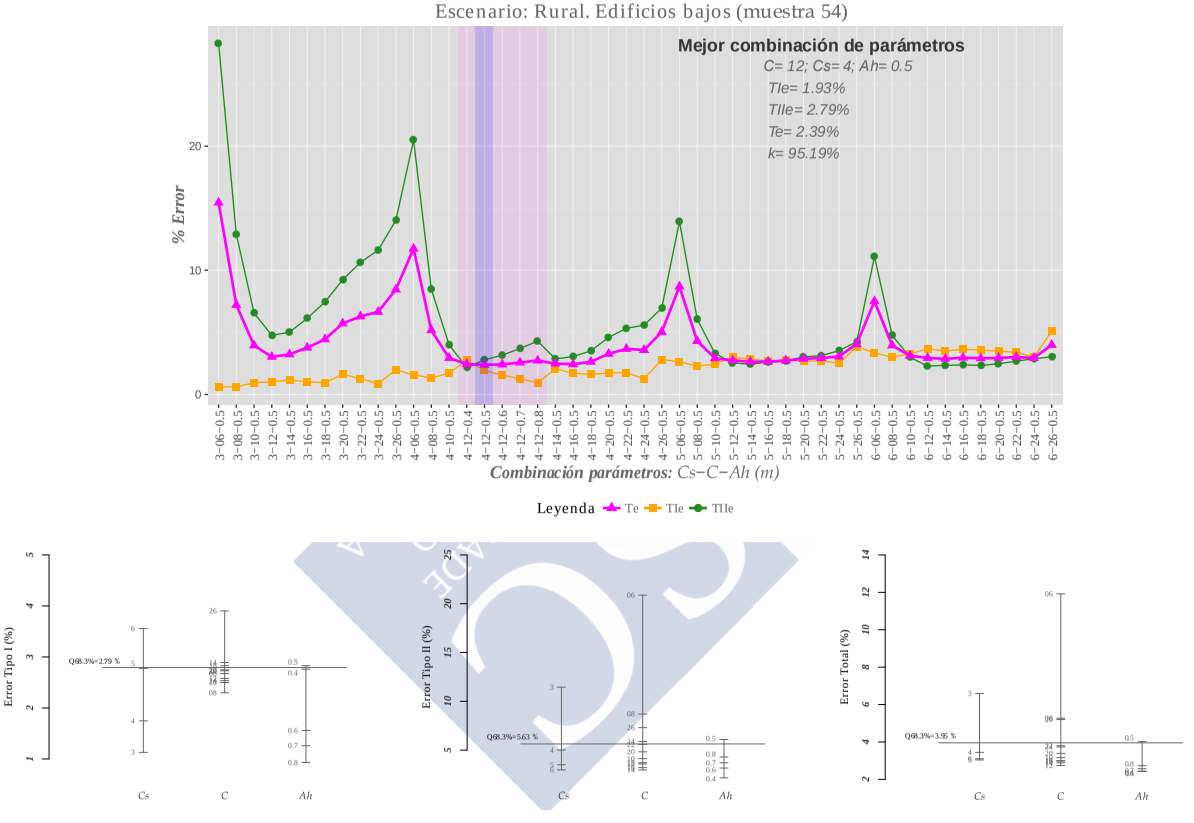

Figura A.39: Muestra 54: Edificios de baja resolución. Influencia de la variación de los parámetros variables en los errores Tipo I, Tipo II y Total (ver gráfico).

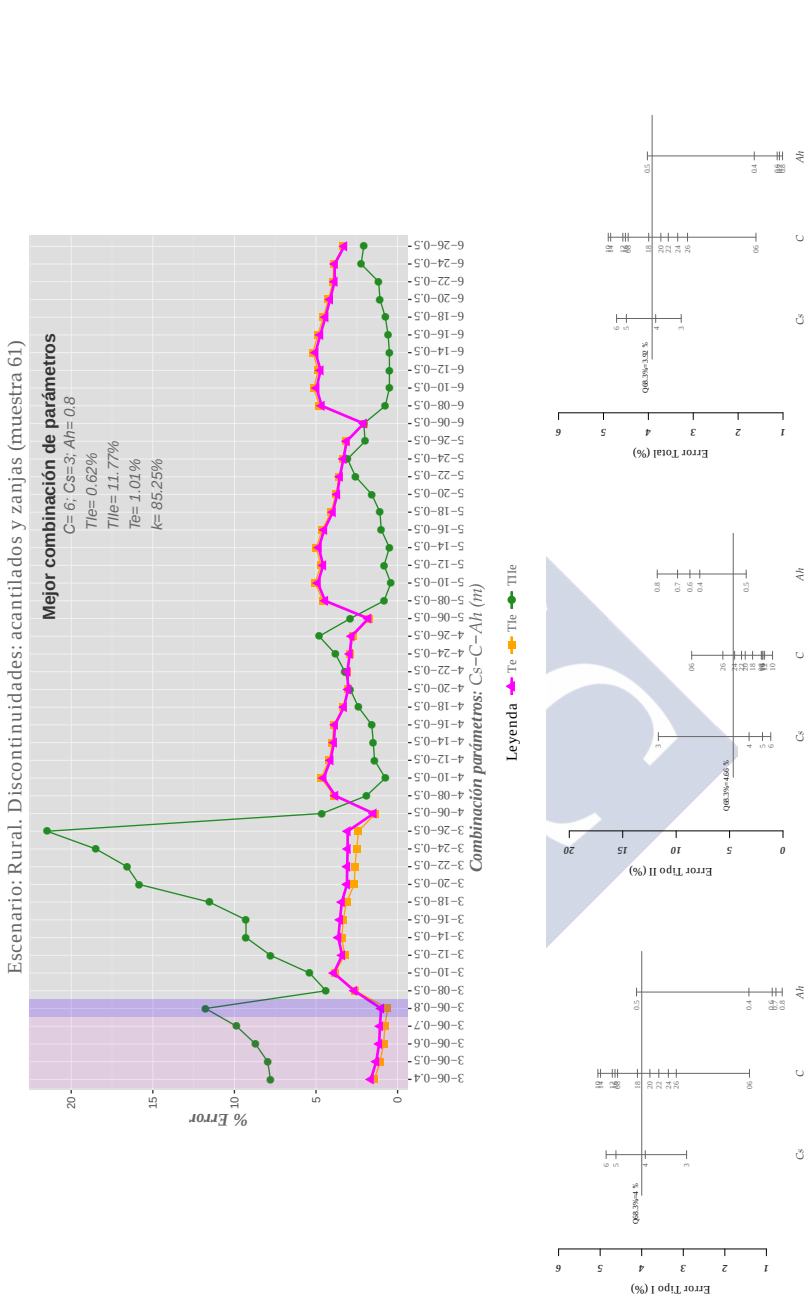

Figura A.40: Muestra 61: Bordes agudos y zanjas. Influencia de la variación de los parámetros variables en los errores Tipo I, Tipo II y Total (ver gráfico).

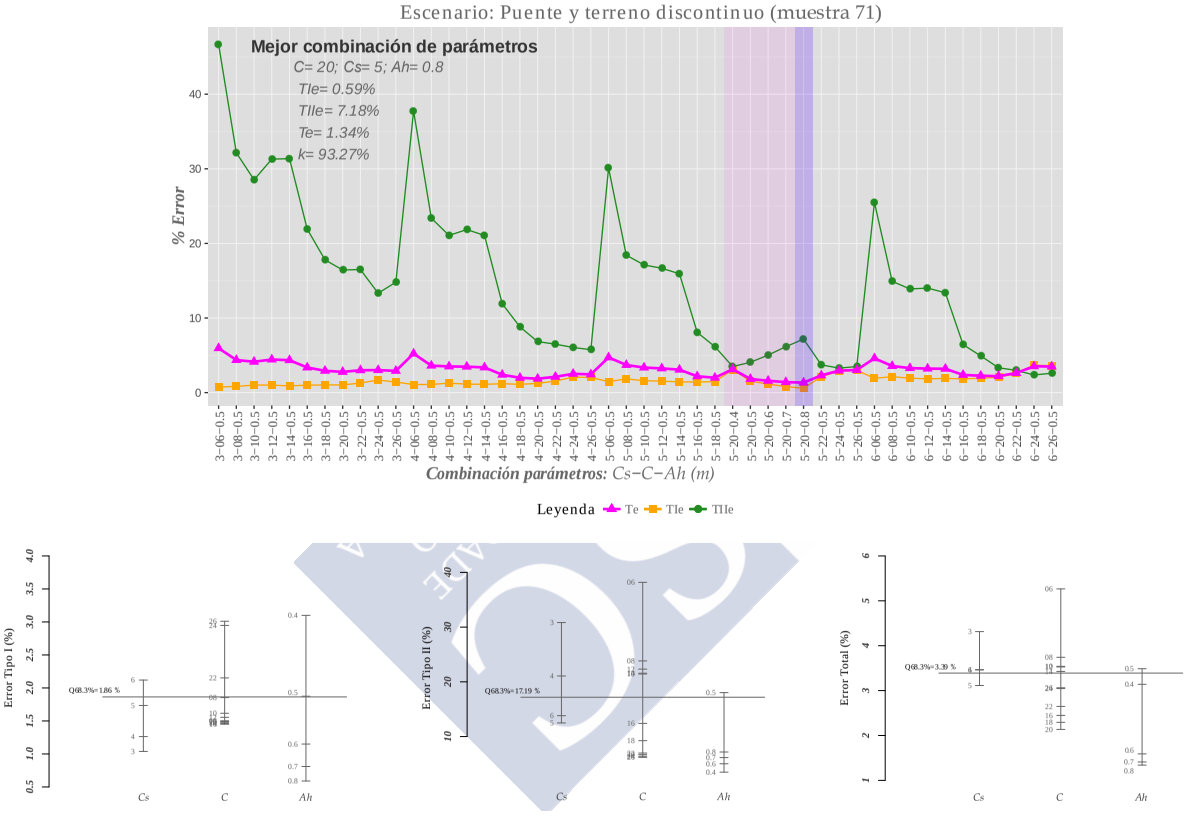

Figura A.41: Muestra 71: Puente y terreno discontinuo. Influencia de la variación de los parámetros variables en los errores Tipo I, Tipo II y Total (ver gráfico 3D).

A.6 Evaluación cualitativa y cuantitativa. Comparativa con otros métodos.

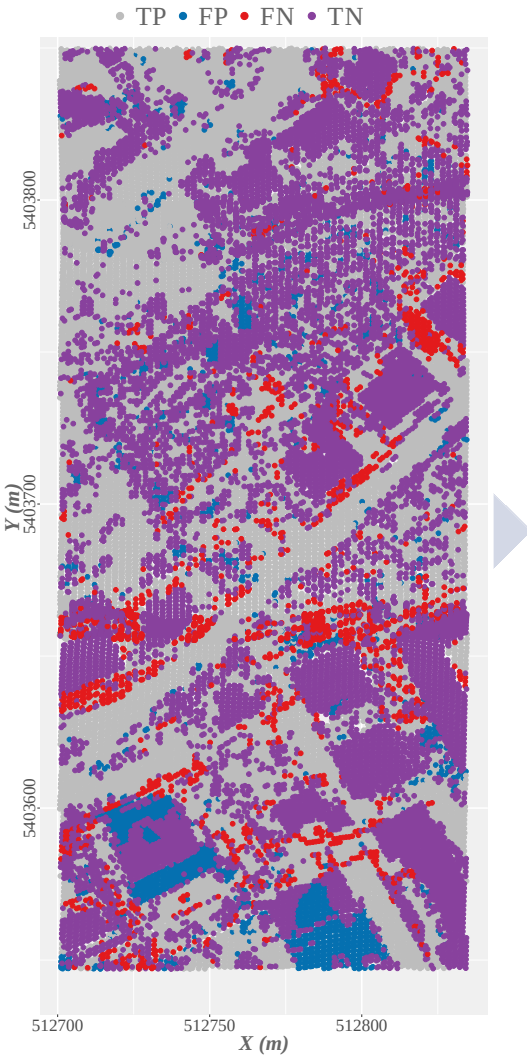

Figura A.42: Muestra 11: Resultados cualitativos del proceso de filtrado (ver gráfico 3D).

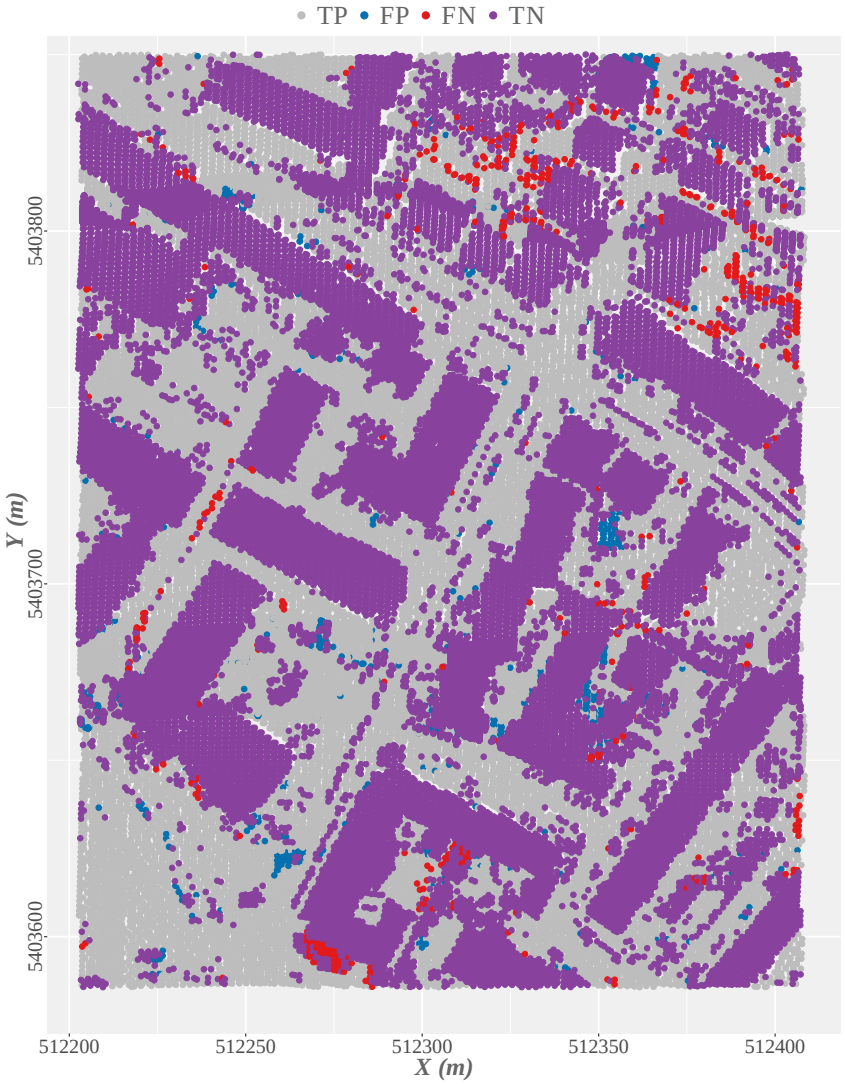

Figura A.43: Muestra 12: Resultados cualitativos del proceso de filtrado (ver gráfico 3D).

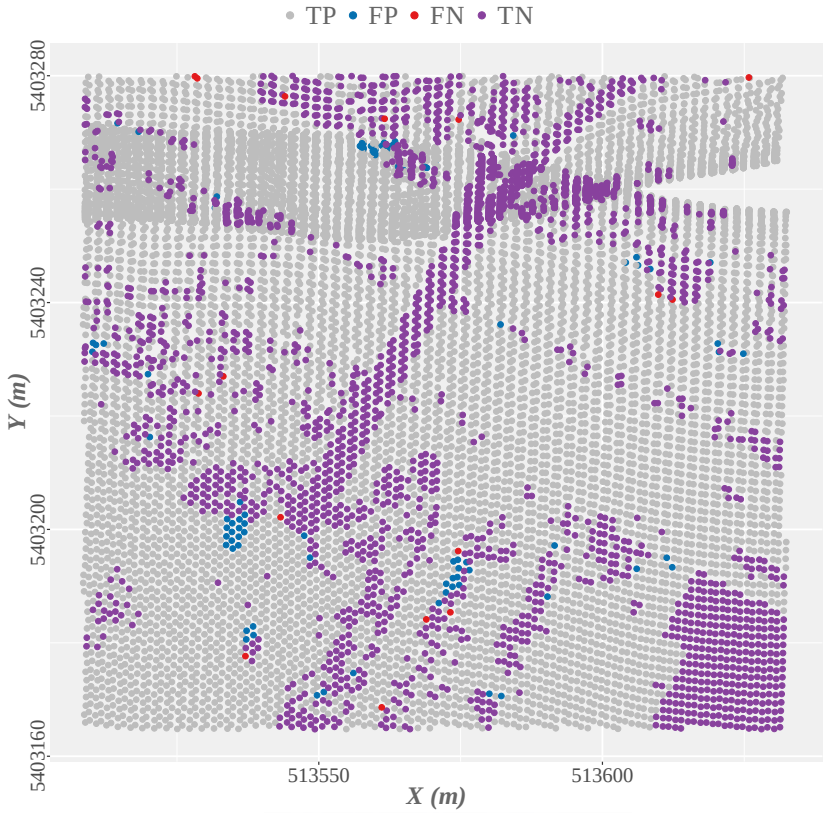

Figura A.44: Muestra 21: Resultados cualitativos del proceso de filtrado (ver gráfico 3D).

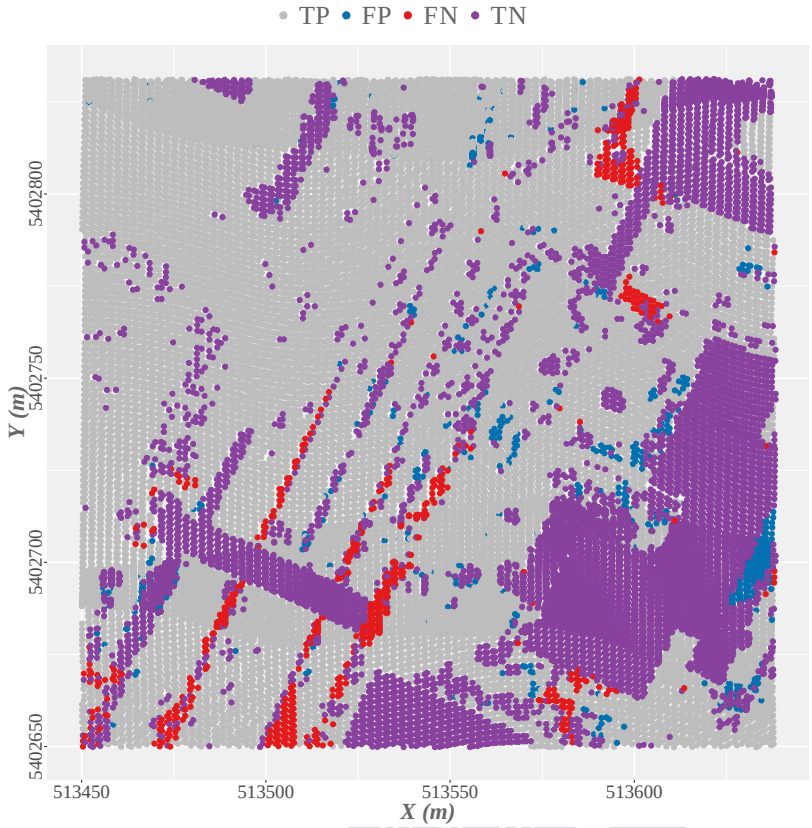

Figura A.45: Muestra 22: Resultados cualitativos del proceso de filtrado (ver gráfico 3D).

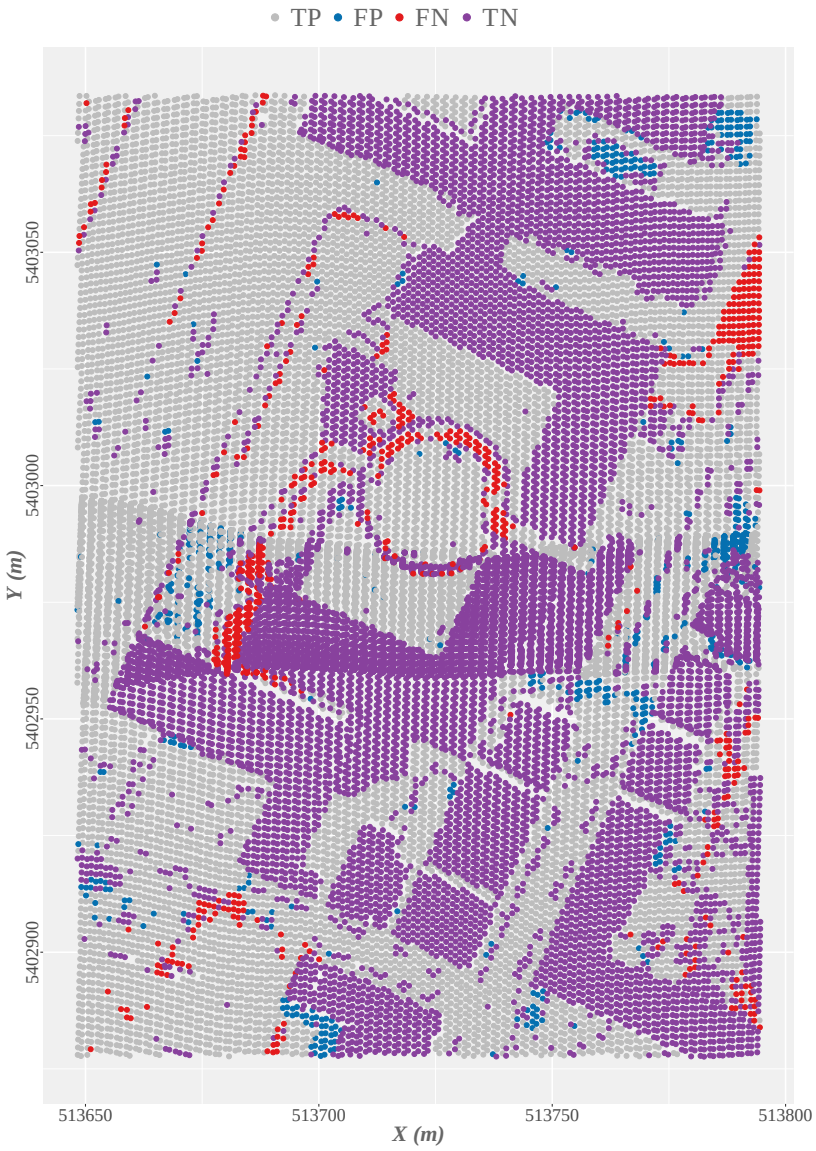

Figura A.46: Muestra 23: Resultados cualitativos del proceso de filtrado(ver gráfico 3D).

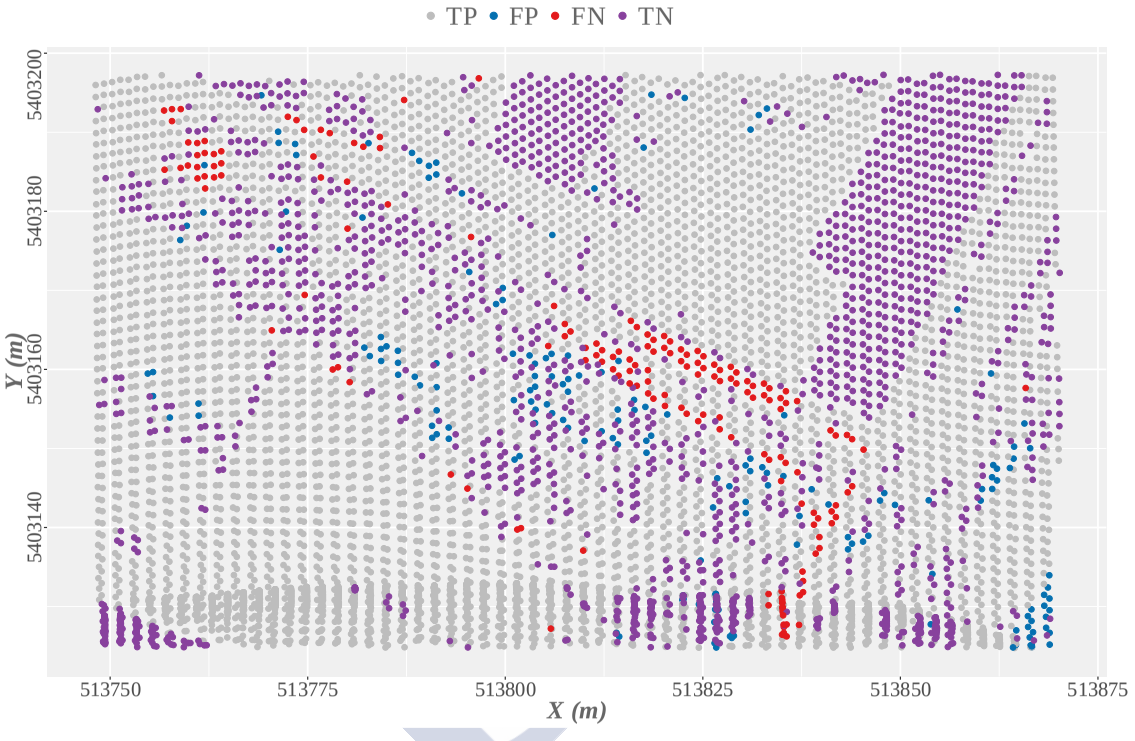

Figura A.47: Muestra 24: Resultados cualitativos del proceso de filtrado (ver gráfico 3D).

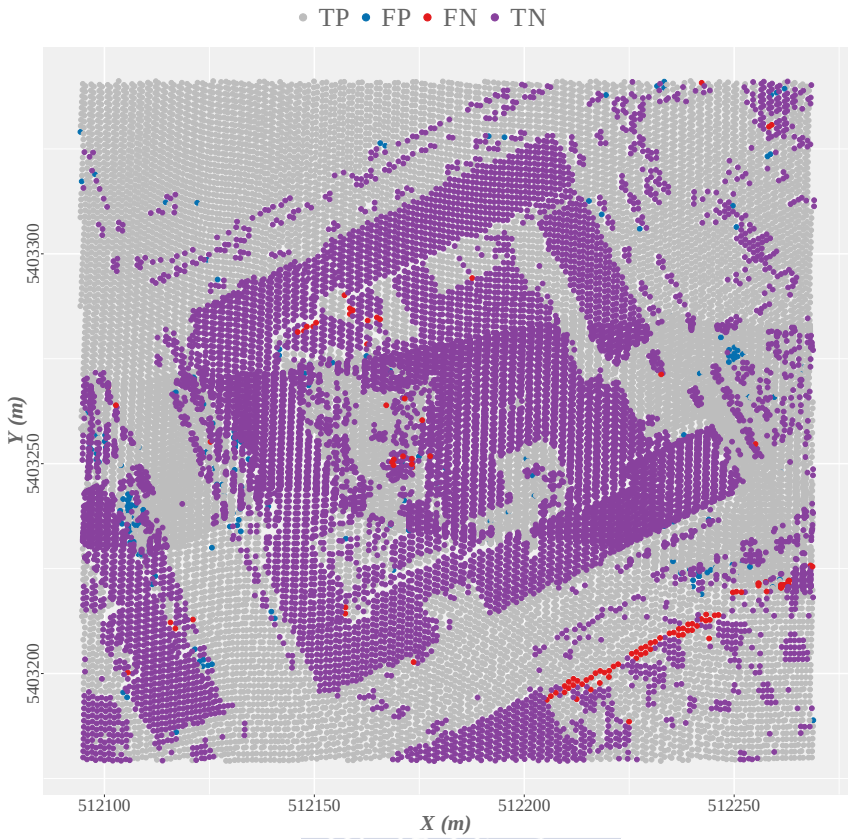

Figura A.48: Muestra 31: Resultados cualitativos del proceso de filtrado (ver gráfico 3D).

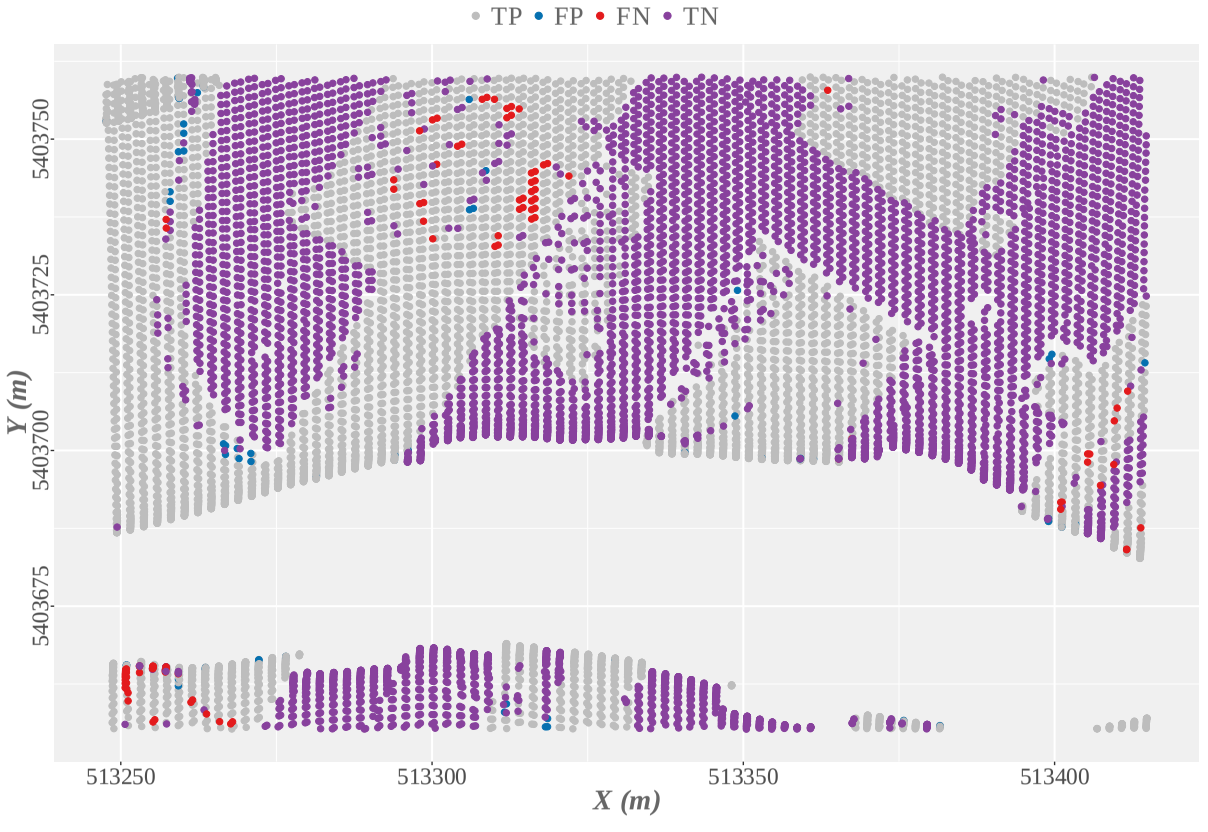

Figura A.49: Muestra 41: Resultados cualitativos del proceso de filtrado (ver gráfico 3D).

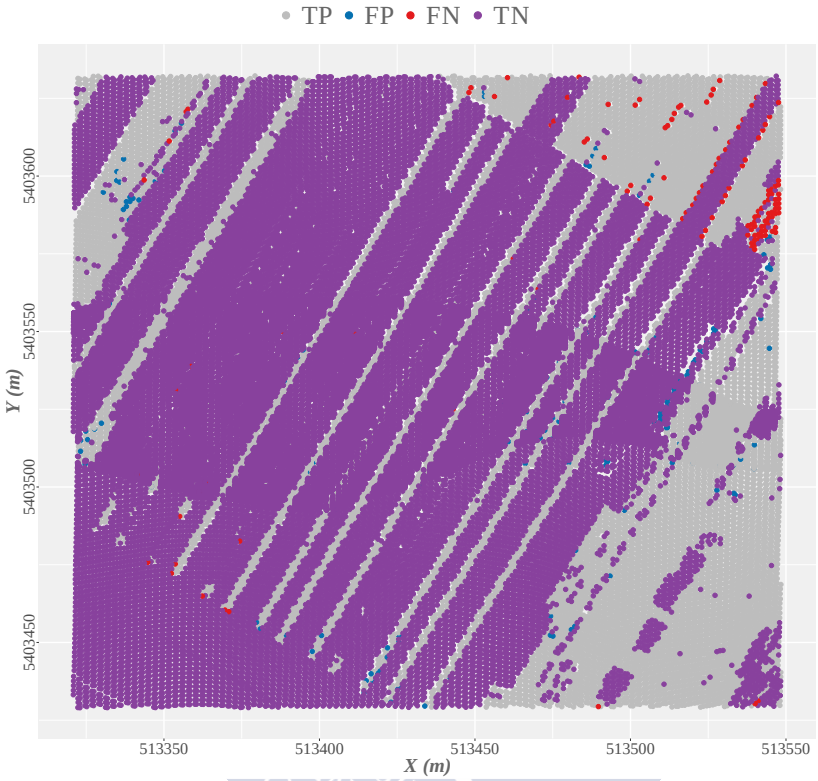

Figura A.50: Muestra 42: Resultados cualitativos del proceso de filtrado (ver gráfico 3D).

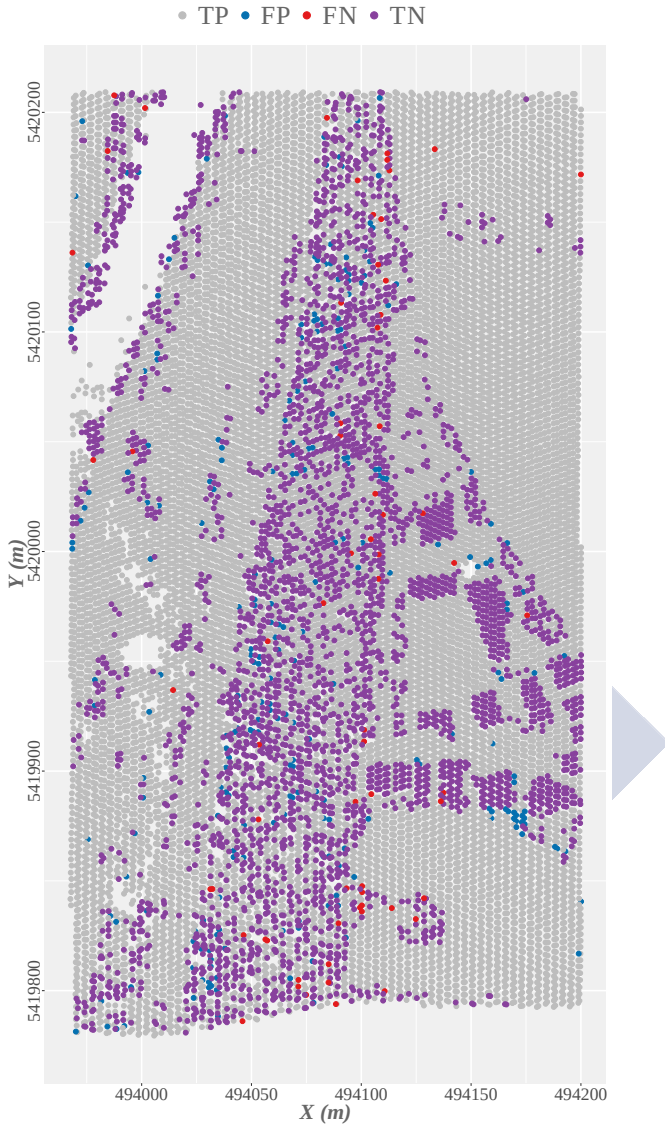

Figura A.51: Muestra 51: Resultados cualitativos del proceso de filtrado (ver gráfico 3D).

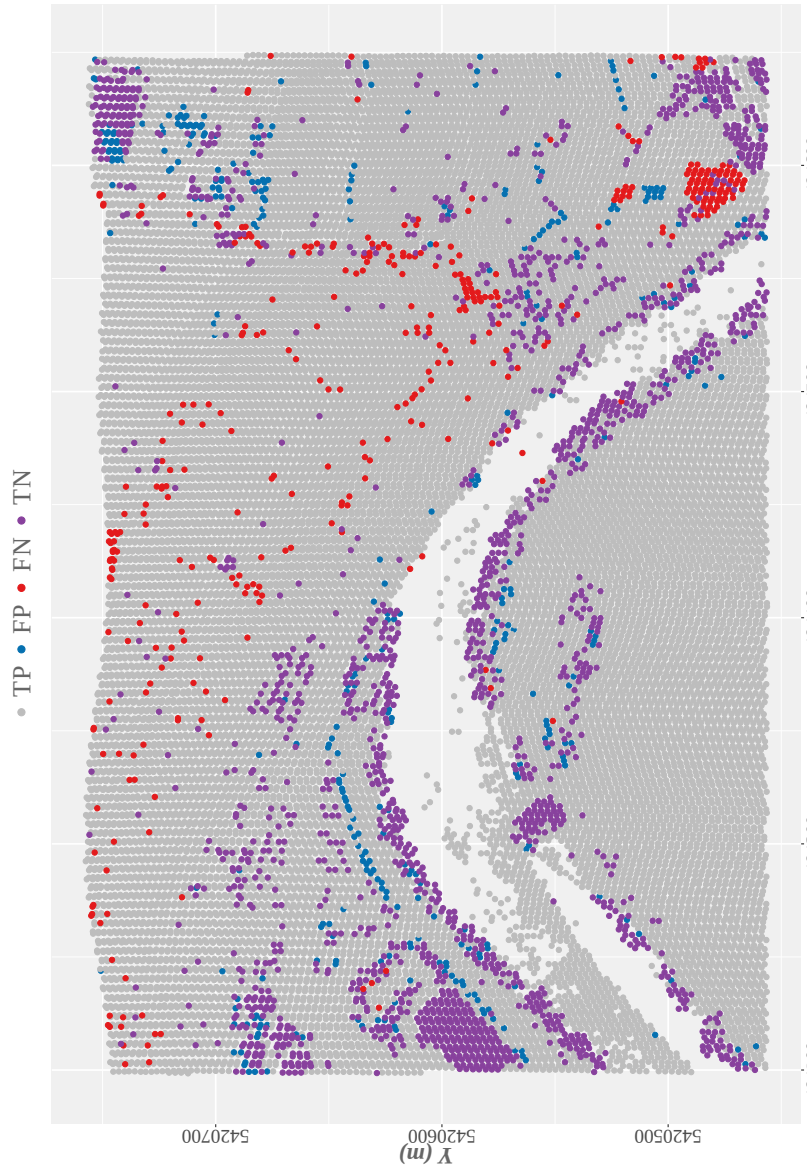

Figura A.52: Muestra 52: Resultados cualitativos del proceso de filtrado (ver gráfico 3D).

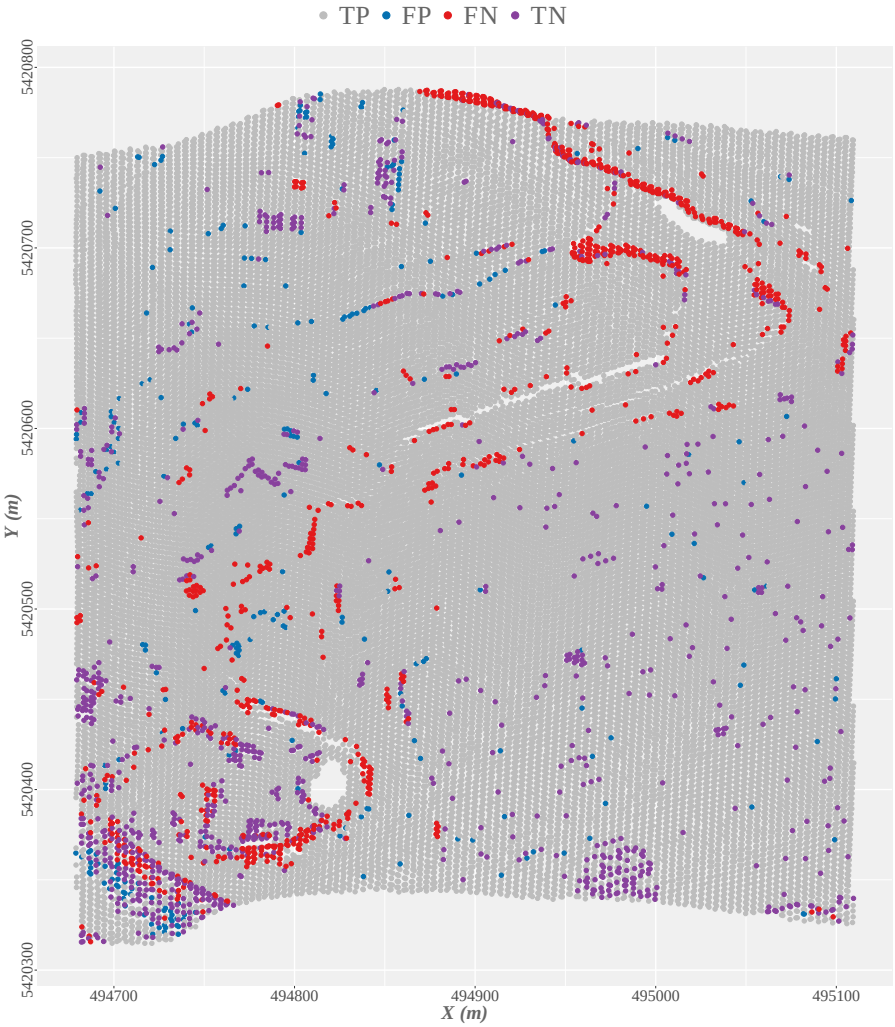

Figura A.53: Muestra 53: Resultados cualitativos del proceso de filtrado (ver gráfico 3D).

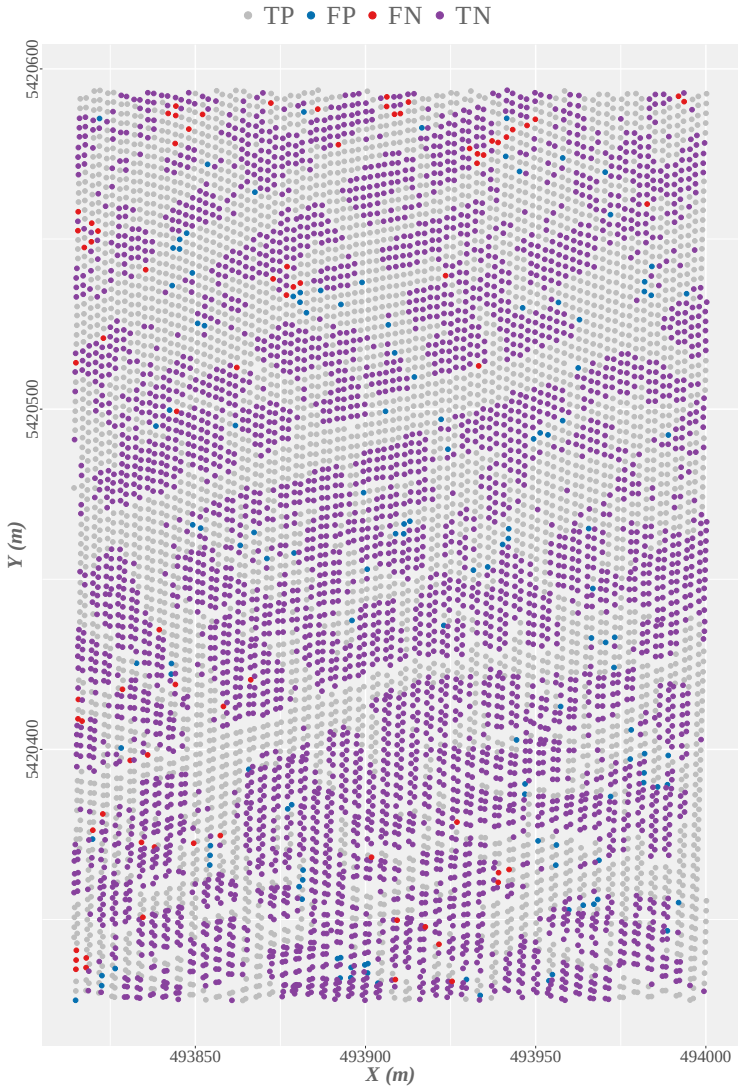

Figura A.54: Muestra 54: Resultados cualitativos del proceso de filtrado (ver gráfico 3D).

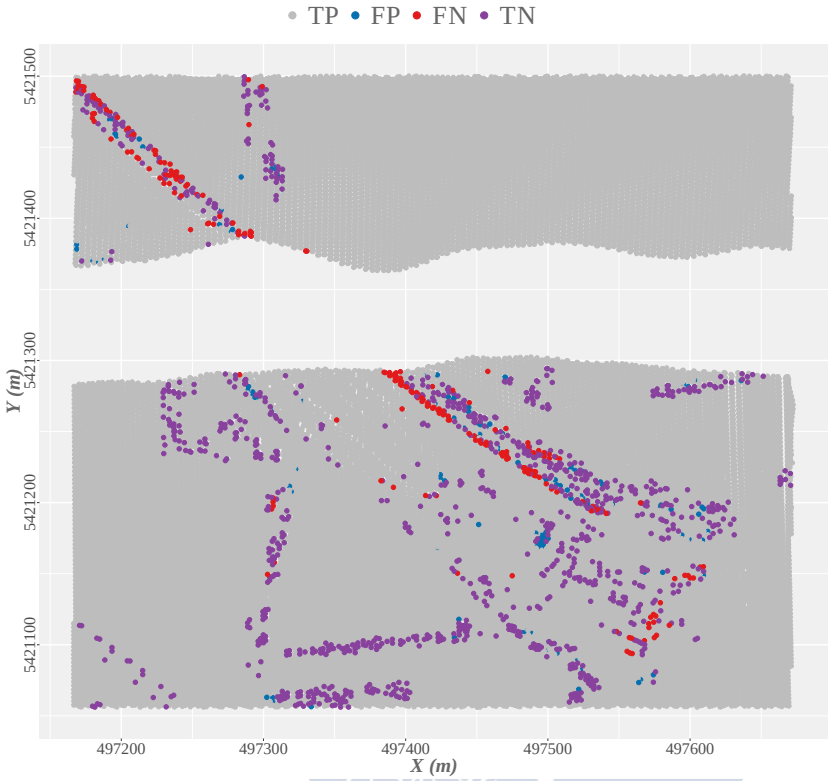

Figura A.55: Muestra 61: Resultados cualitativos del proceso de filtrado (ver gráfico 3D).

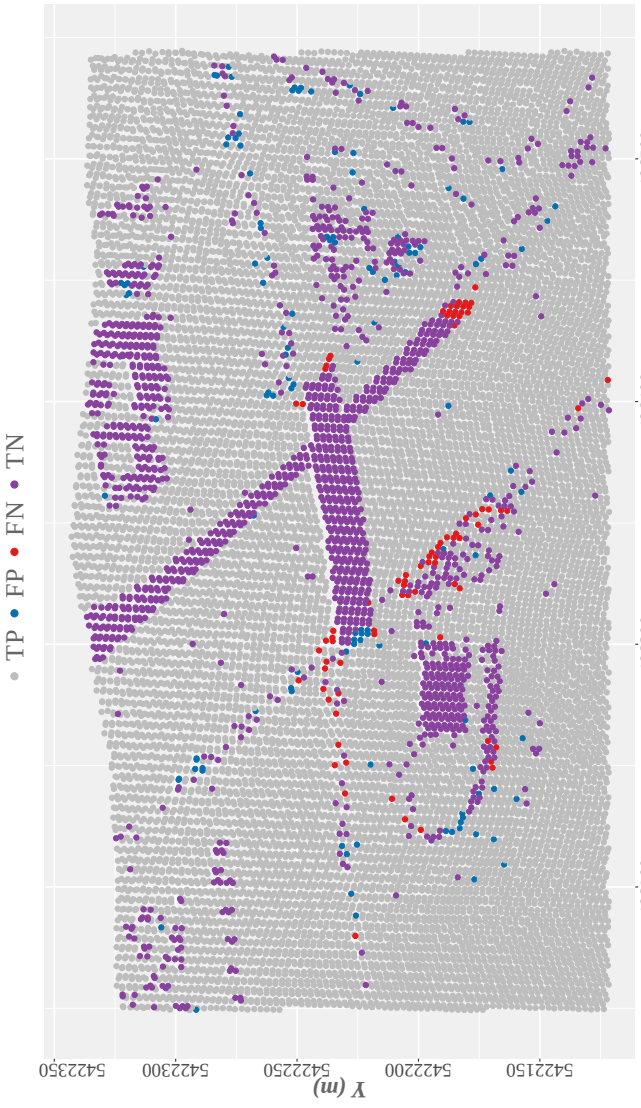

Figura A.56: Muestra 71: Resultados cualitativos del proceso de filtrado (ver gráfico 3D).

USC
UNIVERSIDADE
DE SANTIAGO
DE COMPOSTELA

Tabla A.21: Comparación de resultados para cada muestra de referencia con 23 trabajos previos desde 1998 hasta 2016 (Parte 1).

		Pfeifer et al. (1998)	Axelsson (1999)	Elmqvist et al. (2001)	Roggero (2001)	Sithole (2001)	Brovelli et al. (2002)	Sohn y Dowman (2002)	Wack y Wimmer (2002)	Lu et al. (2008)	Shao y Chen (2008)	Chang (2010) (SMSM)	Chang (2010) (SSA)
M11	TIe	28.3	16.0	33.6	33.2	37.7	62.0	26.6	39.1	51.8	13.0	5.3	11.4
	TIIe	2.4	3.7	4.4	3.9	3.5	2.5	12.2	3.4	1.3	10.4	24.1	10.0
	Te	17.4	10.8	22.4	20.8	23.3	37.0	20.5	24.0	21.5	11.9	13.3	10.8
	K	66.3	78.6	58.9	59.9	55.5	32.2	59.5	54.1	43.2	76.0	72.2	78.1
M12	TIe	7.3	4.9	12.4	11.9	19.2	29.6	8.9	11.9	16.7	5.0	2.1	3.2
	TIIe	1.5	1.5	3.3	0.9	0.6	2.0	7.9	0.9	2.5	3.0	5.0	2.5
	Te	4.5	3.3	8.2	6.6	10.2	16.3	8.4	6.6	8.2	4.0	3.5	2.9
	K	91.1	93.6	84.2	86.9	79.9	67.9	83.2	86.9	80.5	92.0	93.0	94.3
M21	TIe	2.8	0.5	25.9	12.5	9.6	11.4	8.4	5.2	12.7	5.3	0.2	1.5
	TIIe	1.6	18.5	1.8	0.0	0.7	1.6	10.4	2.3	9.6	2.3	4.7	2.7
	Te	2.6	4.3	8.5	9.8	7.8	9.3	8.8	4.6	11.7	4.7	1.2	1.8
	K	92.8	86.2	54.9	75.7	80.2	76.6	76.1	87.6	69.1	87.2	96.4	95.0
M22	TIe	8.3	2.7	20.6	33.4	29.3	31.2	5.7	9.7	13.5	7.1	1.2	2.3
	TIIe	3.1	5.9	1.9	1.0	1.0	1.8	11.9	2.4	2.4	9.5	1.9	5.6
	Te	6.7	3.6	8.9	23.8	20.9	22.3	7.5	7.5	12.0	5.5	2.6	3.4
	K	85.2	91.4	69.3	54.7	59.4	56.6	82.3	83.5	72.9	87.6	93.9	92.2
M23	TIe	12.1	3.7	18.7	41.9	40.9	50.3	7.3	18.4	16.5	5.3	2.3	4.7
	TIIe	3.8	4.3	4.0	1.9	2.1	2.4	12.8	2.6	4.1	4.2	6.0	4.7
	Te	8.2	4.0	12.3	23.2	22.7	27.8	9.8	11.0	9.4	4.8	4.0	4.7
	K	83.7	92.0	76.6	54.9	55.8	46.1	80.2	78.3	78.7	90.4	91.9	90.6
M24	TIe	8.5	3.4	31.8	30.4	32.8	47.6	13.2	14.4	20.6	4.2	5.1	2.9
	TIIe	9.0	7.5	3.0	1.7	3.5	2.9	13.8	3.3	4.9	7.0	9.6	11.4
	Te	8.6	4.4	13.8	23.3	25.3	36.1	13.3	11.5	14.1	5.0	6.4	5.2
	K	79.2	88.8	52.1	54.5	50.7	35.8	68.6	74.3	64.6	87.7	84.3	86.7
M31	TIe	1.6	7.9	8.5	3.0	4.9	21.8	4.8	3.2	7.5	1.1	0.6	0.4
	TIIe	2.0	1.0	2.3	1.1	1.1	2.4	8.3	1.1	2.3	1.3	1.9	1.8
	Te	1.8	4.8	5.3	2.1	3.2	12.9	6.4	2.2	4.6	1.2	1.2	1.0
	K	96.4	90.5	88.7	95.7	93.7	74.6	87.1	95.6	89.8	97.6	97.5	97.9
M41	TIe	19.9	25.8	14.4	21.6	47.1	32.4	19.3	17.6	23.4	8.2	3.3	2.7
	TIIe	1.6	1.9	0.9	2.7	1.7	0.5	3.2	0.5	2.7	1.8	10.8	3.5
	Te	10.8	13.9	8.8	12.2	23.7	17.0	11.3	9.0	11.7	4.9	7.1	3.1
	K	78.6	72.4	84.8	75.8	51.3	67.2	77.6	81.9	73.9	90.1	85.9	93.9
M42	TIe	8.0	4.7	4.3	13.4	12.2	20.4	1.0	10.7	9.1	5.2	0.9	3.1
	TIIe	0.2	0.3	2.0	0.3	0.2	0.3	2.1	0.4	3.1	0.9	1.5	0.7
	Te	2.6	1.6	3.7	4.3	3.9	6.4	1.8	3.5	4.4	2.1	1.3	1.4
	K	93.8	96.2	93.6	89.7	90.8	84.2	95.7	91.6	88.3	94.8	96.8	96.6
M51	TIe	4.2	0.1	49.3	1.9	7.0	28.2	10.3	14.0	5.8	0.4	0.6	0.4
	TIIe	1.9	12.0	1.6	7.0	7.0	3.6	5.7	2.2	7.3	15.0	12.3	14.7
	Te	3.7	2.7	21.3	3.0	7.0	22.8	9.3	11.5	6.4	3.6	3.1	3.5
	K	89.6	91.7	30.1	91.2	80.7	50.4	75.5	71.4	82.8	88.9	90.5	89.3
M52	TIe	21.3	1.8	85.1	9.8	30.4	50.4	12.3	26.5	7.6	2.0	0.8	1.0
	TIIe	5.7	14.2	1.3	9.7	3.6	3.8	9.5	1.0	25.3	9.5	26.8	17.4
	Te	19.6	3.1	58.0	9.8	27.5	45.6	12.0	23.8	11.0	2.8	3.5	2.7
	K	41.2	83.7	3.3	60.8	31.1	15.9	55.0	36.4	57.2	85.6	79.6	84.9
M53	TIe	12.5	8.6	92.5	17.8	38.4	54.9	20.5	28.3	20.1	5.0	2.0	1.2
	TIIe	14.2	16.8	0.2	4.7	4.8	1.6	13.2	1.0	23.1	12.1	33.5	29.2
	Te	12.6	8.9	48.5	17.3	37.1	52.8	20.2	27.2	20.4	5.3	3.2	2.4
	K	31.1	39.4	0.6	25.8	10.6	6.0	20.3	16.8	17.9	55.0	60.8	69.5
M54	TIe	1.0	27.9	10.7	49.5	15.9	12.4	1.3	6.7	6.9	1.4	2.0	3.8
	TIIe	8.4	2.6	1.0	2.0	0.5	1.1	4.9	4.8	6.2	3.9	3.5	4.8
	Te	5.0	21.3	5.5	23.9	7.6	6.3	3.2	5.7	6.4	2.7	2.8	4.3
	K	90.1	70.7	88.9	50.1	84.5	87.2	93.5	88.5	86.9	94.5	94.4	91.4
M61	TIe	7.2	1.9	91.3	19.6	22.4	22.5	3.0	13.9	6.6	1.0	0.5	0.2
	TIIe	0.2	6.2	0.1	0.6	0.3	0.0	3.7	0.3	7.4	12.8	19.4	28.1
	Te	6.9	2.1	35.9	19.0	21.6	21.7	3.0	13.5	6.7	1.4	1.1	1.1
	K	47.1	74.5	0.7	21.8	19.2	19.2	67.5	29.7	46.2	80.7	82.9	81.0
M71	TIe	9.8	0.1	75.2	5.4	24.6	39.4	1.3	18.9	1.5	2.0	0.6	0.6
	TIIe	1.6	13.3	0.2	2.8	0.3	0.8	9.5	2.0	44.8	11.9	13.8	15.5
	Te	8.9	1.6	34.2	5.1	21.8	35.0	2.2	17.0	9.6	3.1	2.1	2.2
	K	66.8	91.5	6.9	78.3	40.8	25.5	89.1	48.3	62.9	84.7	89.3	88.2

Tabla A.22: Comparación de resultados para cada muestra de referencia con 23 trabajos previos desde 1998 hasta 2016 (Parte 2).

		Mongus y Žalik (2012)	TerraScan in Mongus y Žalik (2012)	Yan et al. (2012)	Chen et al. (2013)	Li (2013)	Pingel et al. (2013)	Zhang y Lin (2013)	Hu et al. (2014)	Mongus y Žalik (2014)	Hui et al. (2016)	Zhang et al. (2016)	DTMofLabTe
M11	TIe	7.3	26.7	28.9	19.3	17.3	7.9	25.7	6.3	6.5	13.6	7.2	9.6
	TIIe	16.0	2.0	5.7	4.6	6.9	8.8	8.8	11.0	15.2	13.0	18.4	12.1
	Te	11.0	16.1	20.6	13.0	12.9	8.3	18.5	8.3	10.2	13.3	12.0	10.6
	K	77.3	68.4	62.8	74.1	74.3	83.1	63.4	83.0	79.0	72.9	75.2	78.3
M12	TIe	4.2	21.5	11.4	4.0	4.0	2.6	8.1	1.8	2.2	4.9	1.2	2.3
	TIIe	6.2	1.1	1.6	2.8	3.5	3.3	3.6	3.5	4.5	2.1	4.9	2.7
	Te	5.2	11.6	7.1	3.4	3.7	2.9	5.9	2.6	3.3	3.5	3.0	2.5
	K	89.7	77.0	86.7	93.2	92.5	94.1	88.2	94.8	93.4	93.0	94.0	95.0
M21	TIe	0.0	14.3	7.1	0.8	2.4	0.3	1.2	0.4	0.8	0.0	3.9	0.2
	TIIe	8.9	2.0	5.0	3.4	3.1	4.1	18.2	3.0	3.4	10.0	1.8	3.8
	Te	2.0	11.6	6.8	1.3	2.6	1.1	5.0	1.0	1.4	2.2	3.4	1.0
	K	94.1	71.4	82.0	96.1	92.8	96.8	84.9	97.2	96.0	93.4	90.5	97.1
M22	TIe	5.0	14.5	15.8	2.7	3.7	2.6	19.1	1.7	2.7	5.3	1.3	3.8
	TIIe	10.1	2.6	2.1	9.1	4.8	5.1	3.4	6.7	7.8	5.7	25.9	7.8
	Te	6.6	10.8	12.0	4.7	4.1	3.4	14.2	3.2	4.3	5.4	9.0	5.1
	K	84.7	76.8	75.4	89.0	90.6	92.2	70.1	92.4	90.1	87.6	77.7	88.2
M23	TIe	4.4	12.9	27.9	4.5	7.7	3.2	19.3	4.7	6.1	4.0	3.5	5.5
	TIIe	7.5	2.5	2.3	6.1	4.4	6.2	4.1	4.1	6.2	6.4	6.2	5.9
	Te	5.8	8.0	16.6	5.2	6.2	4.6	12.1	4.4	6.2	5.1	4.8	5.7
	K	88.3	84.0	68.8	89.5	87.7	90.7	76.0	91.2	87.6	89.7	90.4	88.6
M24	TIe	5.7	16.4	28.4	5.5	5.4	2.3	22.9	2.2	3.5	7.5	1.0	2.7
	TIIe	14.0	4.0	3.4	8.3	6.3	6.9	13.4	8.1	7.2	7.5	7.7	9.2
	Te	8.0	13.0	22.5	6.3	5.7	3.5	20.3	3.8	4.5	7.5	2.9	4.5
	K	80.0	71.0	55.7	84.5	86.1	91.1	55.6	90.4	88.8	81.9	92.7	88.6
M31	TIe	0.2	8.4	5.6	0.6	0.3	0.4	2.1	0.5	0.2	0.9	1.0	0.8
	TIIe	7.0	9.0	1.9	1.8	5.0	1.5	2.6	1.4	7.4	1.9	2.4	1.7
	Te	3.3	8.6	4.0	1.1	2.5	0.9	2.3	0.9	3.5	1.3	1.6	1.2
	K	93.3	82.6	92.3	97.8	95.0	98.2	95.3	98.2	92.9	97.3	96.8	97.5
M41	TIe	3.4	25.1	27.3	9.1	10.3	3.6	39.5	3.0	3.6	18.2	1.5	2.1
	TIIe	4.0	0.7	0.9	2.1	3.1	8.2	1.4	8.9	4.5	3.1	8.8	1.2
	Te	3.7	13.2	14.0	5.6	6.7	5.9	20.4	5.9	4.1	10.6	5.1	1.7
	K	92.6	74.2	71.9	88.8	86.6	88.2	59.1	88.2	91.9	78.8	89.7	96.7
M42	TIe	0.1	8.0	9.4	4.7	1.2	0.3	9.7	0.4	5.4	3.0	3.3	1.1
	TIIe	8.1	1.4	3.2	0.5	3.8	2.0	1.6	0.9	1.7	1.5	0.9	0.7
	Te	5.7	3.3	5.2	1.7	3.1	1.5	3.9	0.7	2.8	1.9	1.6	0.8
	K	87.0	91.9	87.8	95.8	92.8	96.5	90.3	98.3	93.2	95.4	96.2	98.1
M51	TIe	0.4	0.4	6.8	0.7	2.5	0.6	2.1	0.5	0.1	1.4	2.7	0.5
	TIIe	10.6	0.3	6.4	4.9	8.9	4.4	17.0	7.5	28.0	17.3	4.6	6.4
	Te	2.6	1.3	6.7	1.6	3.9	1.4	5.3	2.0	6.1	4.9	3.1	1.8
	K	92.2	98.9	81.6	95.2	88.5	95.8	83.9	93.9	80.1	85.1	91.1	94.7
M52	TIe	6.6	4.7	11.6	3.1	16.0	3.1	12.5	1.1	2.2	5.6	1.0	1.9
	TIIe	11.4	4.5	7.7	13.8	10.9	10.1	16.8	14.9	24.1	14.9	28.8	16.3
	Te	7.1	5.4	11.2	4.2	15.4	3.8	13.0	2.5	4.5	6.6	3.9	3.4
	K	68.4	78.4	57.5	78.9	47.1	81.0	50.6	86.2	75.6	69.5	77.1	81.9
M53	TIe	8.4	3.6	19.1	7.2	11.6	1.2	4.3	1.6	3.0	6.8	3.9	2.9
	TIIe	11.6	11.0	4.1	10.5	13.6	32.0	37.2	38.8	30.9	23.9	37.1	20.6
	Te	8.5	4.0	18.5	7.3	11.7	2.4	5.6	2.7	4.1	7.5	5.2	3.6
	K	42.1	62.8	24.4	46.7	33.1	68.2	44.8	59.6	55.6	41.8	46.9	62.2
M54	TIe	1.2	2.5	14.7	3.4	2.0	2.5	3.6	2.3	0.8	4.9	3.8	1.9
	TIIe	11.5	13.7	2.0	2.8	5.6	2.1	8.8	2.4	7.9	3.5	2.6	2.8
	Te	6.7	8.5	7.9	3.1	3.9	2.3	6.4	2.4	4.6	4.2	3.2	2.4
	K	86.6	83.1	84.1	93.8	92.1	95.4	87.2	95.3	90.8	91.6	93.6	95.2
M61	TIe	3.2	1.6	11.7	1.7	5.8	0.5	16.6	0.3	3.0	1.5	0.9	0.6
	TIIe	4.9	4.8	0.8	5.0	6.6	10.7	2.5	16.8	17.9	24.5	18.9	11.8
	Te	4.9	1.7	11.4	1.8	5.8	0.9	16.1	0.8	3.5	2.3	1.5	1.0
	K	65.1	78.4	33.9	77.4	50.0	87.3	25.0	86.8	60.1	67.8	78.1	85.3
M71	TIe	2.4	1.7	16.1	0.4	4.1	1.0	10.1	0.9	0.4	1.0	1.6	0.6
	TIIe	9.2	3.6	3.1	9.0	8.8	6.8	13.4	5.9	25.3	25.4	37.9	7.2
	Te	3.1	1.9	14.6	1.3	4.6	1.7	10.4	1.5	3.2	3.7	5.7	1.3
	K	85.0	90.9	52.7	93.2	79.2	91.8	59.5	92.6	82.5	79.9	68.0	93.3

Tabla A.23: Comparación de resultados para cada muestra de referencia con 23 trabajos previos desde 1998 hasta 2016. Parámetros únicos

		Shao y Chen (2008)	Chang (2010) (SMSM)	Hu et al. (2014)	DTMofLabTe
M11	TIe	13.1	6.3	6.4	11.8
	TIIe	10.4	26.4	11.1	16.9
	Te	11.9	14.9	8.4	14.0
	K	75.9	68.9	82.8	71.4
M12	TIe	5.0	1.5	1.2	3.1
	TIIe	3.0	7.5	4.9	3.2
	Te	4.0	4.4	3.0	3.1
	K	92.0	91.2	94.0	93.8
M21	TIe	5.3	0.0	0.0	0.2
	TIIe	2.3	7.0	8.6	3.9
	Te	4.7	1.6	1.9	1.0
	K	87.2	95.3	94.3	97.0
M22	TIe	8.3	0.9	1.7	5.9
	TIIe	2.1	10.2	7.5	6.9
	Te	6.3	3.8	3.5	6.2
	K	85.9	90.9	91.8	85.8
M23	TIe	5.3	2.3	4.6	11.2
	TIIe	4.2	5.9	5.0	4.3
	Te	4.8	4.0	4.8	7.9
	K	90.4	91.9	90.5	84.2
M24	TIe	4.2	5.0	2.1	5.4
	TIIe	7.0	10.3	9.5	7.8
	Te	5.0	6.5	4.1	6.1
	K	87.7	83.9	89.5	85.0
M31	TIe	1.1	0.2	0.1	0.5
	TIIe	1.4	6.9	7	2.4
	Te	1.2	3.3	3.3	1.4
	K	97.5	93.4	93.4	97.2
M41	TIe	8.2	3.5	3.0	2.7
	TIIe	1.8	11.5	9.5	1.1
	Te	4.9	7.5	6.3	1.9
	K	90.1	85.0	87.5	96.2
M42	TIe	5.2	0.5	0.5	1.1
	TIIe	0.9	2.8	1.5	0.7
	Te	2.1	2.1	1.2	0.8
	K	94.8	95.0	97.1	98.1
M51	TIe	0.4	0.3	0.1	0.2
	TIIe	15.6	16.6	12.3	19.0
	Te	3.7	3.8	2.8	4.3
	K	88.4	88.2	91.5	86.6
M52	TIe	2.0	2.2	2.3	2.0
	TIIe	9.5	21.4	11.1	21.3
	Te	2.8	4.2	3.2	4.0
	K	85.6	77.5	83.7	78.1
M53	TIe	5.0	5.6	5.4	4.2
	TIIe	12.1	12.4	12.0	17.6
	Te	5.3	5.8	5.7	4.7
	K	55.0	52.2	53.1	56.3
M54	TIe	1.4	2.3	1.5	1.7
	TIIe	4.5	4.0	3.7	4.6
	Te	3.1	3.2	2.7	3.3
	K	93.8	93.5	94.6	93.5
M61	TIe	1.0	1.5	2.2	3.0
	TIIe	12.8	17.8	8.6	2.9
	Te	1.4	2.0	2.4	3.0
	K	80.7	72.4	71.1	67.4
M71	TIe	2.0	0.7	0.8	1.2
	TIIe	15.4	15.5	10.6	6.8
	Te	3.5	2.4	1.9	1.9
	K	82.6	87.7	90.5	90.8

A.7 Resumen resultados (gráficas *online*).

En las siguientes tablas se incluyen los enlaces a las gráficas *online* con los resultados cuantitativos y cualitativos de este estudio.

Tabla A.24: Muestras urbanas: Resultados cualitativos y cuantitativos (*online*).

Resultados [a]	**M11**	**M12**	**M21**	**M22**	**M23**	**M24**	**M31**	**M41**	**M42**
Influencia parámetros variables									
Resultados cuantitativos									
Resultados cualitativos	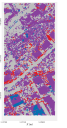								

[a] Activar WebGl si no se pueden visualizar los gráficos: instrucciones para Google Chrome aquí y para Firefox aquí.

Tabla A.25: Muestras rurales: Resultados cualitativos y cuantitativos (*online*).

Resultados [a]	**M51**	**M52**	**M53**	**M54**	**M61**	**M71**
Influencia parámetros variables						
Resultados cuantitativos						
Resultados cualitativos	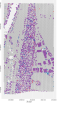					

[a] Activar WebGl si no se pueden visualizar los gráficos: instrucciones para Google Chrome aquí y para Firefox aquí.

ANEXO B

Anexos del Capítulo 2. Factores que afectan a la precisión de los MDT

B.1 Características de las muestras.

En las siguientes figuras se muestra para cada área de referencia la distribución espacial de los puntos empleando una paleta de colores para representar la elevación de cada uno, mientras que el tipo de punto (P_g o P_{ng}) se representa mediante simbología. Se incluye también el MDT_O obtenido a partir de la interpolación de los puntos originales codificados como 0 (P_g) y la imagen de pendiente del MDT_O. Como complemento a estos dos modelos se incluye el histograma de frecuencias de cada uno y se señalan el percentil del 68.3% (flecha naranja) y del 95% (flecha azul).

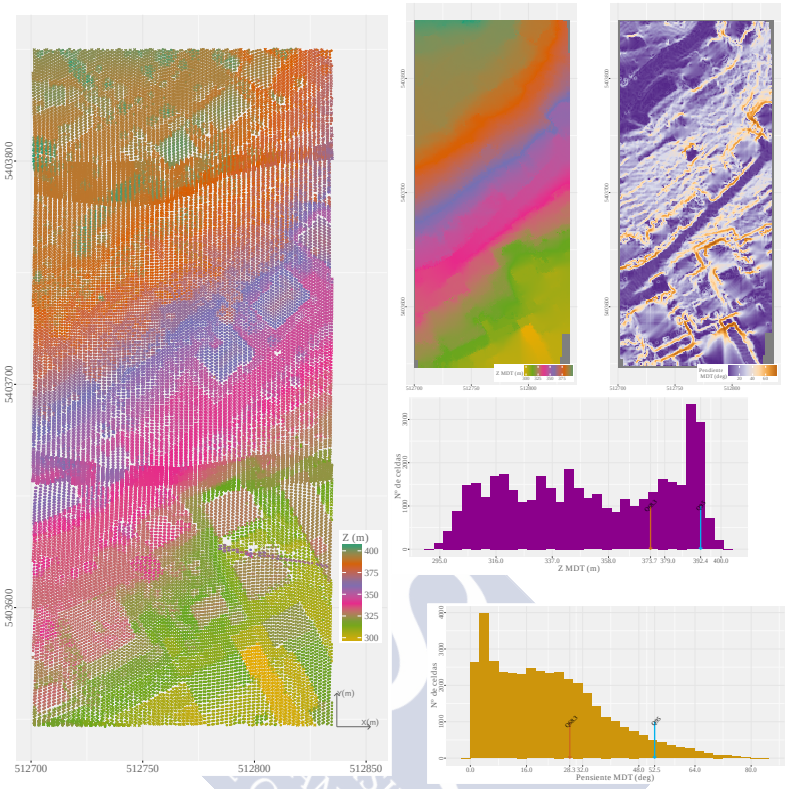

(a) Distribución de los puntos originales en función de la elevación y tipo de punto (la x representa los P_g y el • los P_{ng}).

(b) MDT e imagen de pendientes y sus correspondientes histogramas de frecuencia (las flechas naranja y azul marcan el valor del percentil del 68.3% y el 95%, respectivamente).

Figura B.1: Características de la muestra 11.

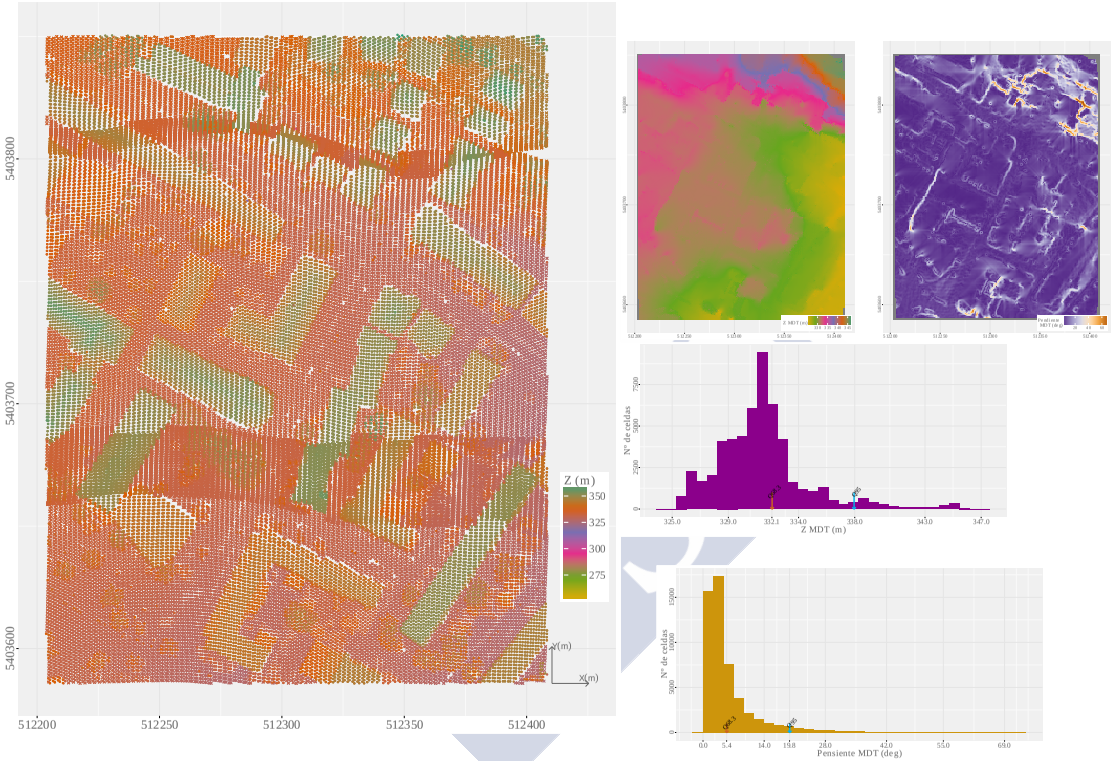

(a) Distribución de los puntos originales en función de la elevación y tipo de punto (la x representa los P_g y el • los P_{ng}).

(b) MDT, imagen de pendiente y sus histogramas de frecuencia (flechas naranja y azul marcan el percentil del 68.3% y el 95%, respectivamente).

Figura B.2: Características de la muestra 12.

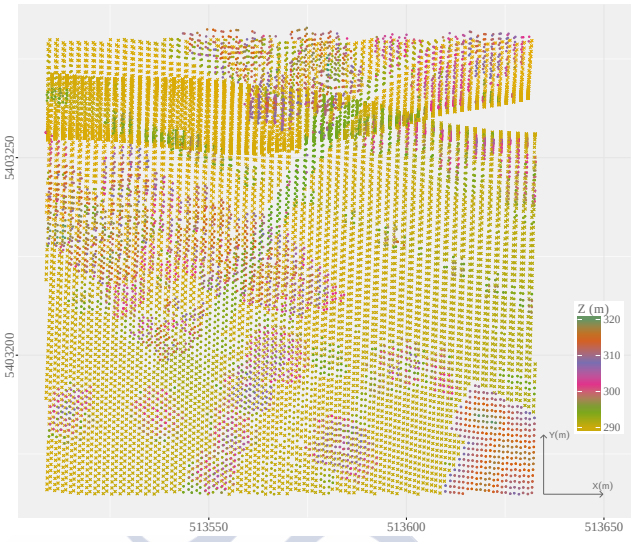

(a) Distribución de los puntos originales en función de la elevación y tipo de punto (la x representa los P_g y el • los P_{ng}).

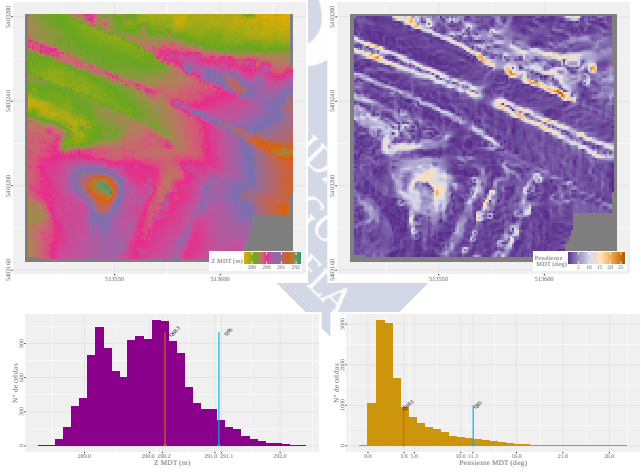

(b) MDT e imagen de pendientes y sus correspondientes histogramas de frecuencia (las flechas naranja y azul marcan el valor del percentil del 68.3% y el 95%, respectivamente).

Figura B.3: Características de la muestra 21.

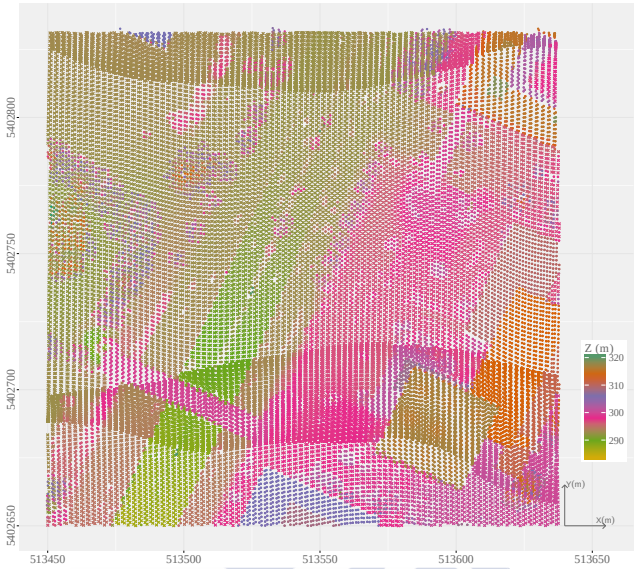

(a) Distribución de los puntos originales en función de la elevación y tipo de punto (la x representa los P_g y el • los P_{ng}).

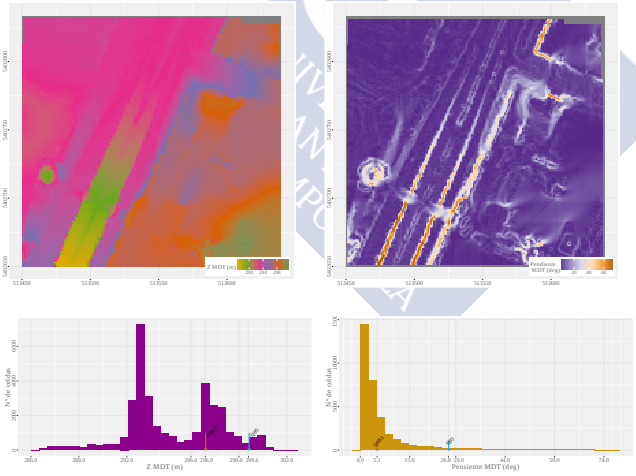

(b) MDT e imagen de pendientes y sus correspondientes histogramas de frecuencia (las flechas naranja y azul marcan el valor del percentil del 68.3% y el 95%, respectivamente).

Figura B.4: Características de la muestra 22.

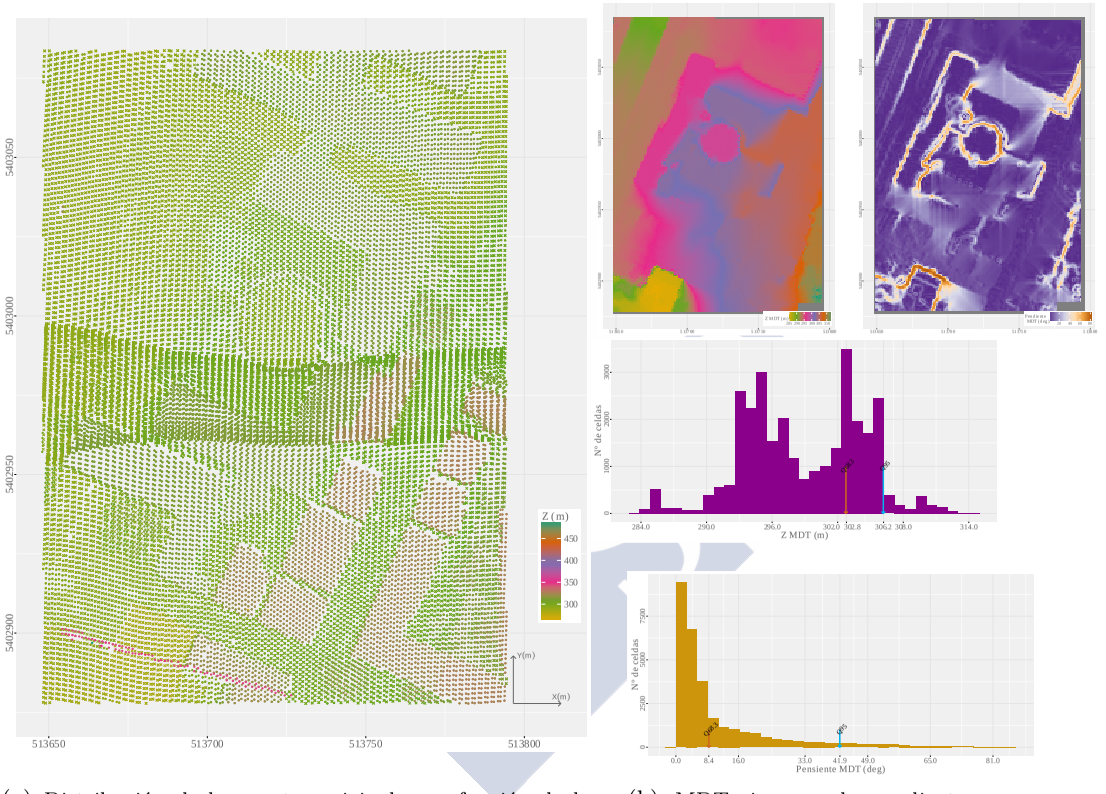

(a) Distribución de los puntos originales en función de la elevación y tipo de punto (la x representa los P_g y el • los P_{ng}).

(b) MDT, imagen de pendiente y sus histogramas de frecuencia (flechas naranja y azul marcan el percentil del 68.3% y el 95%, respectivamente).

Figura B.5: Características de la muestra 23.

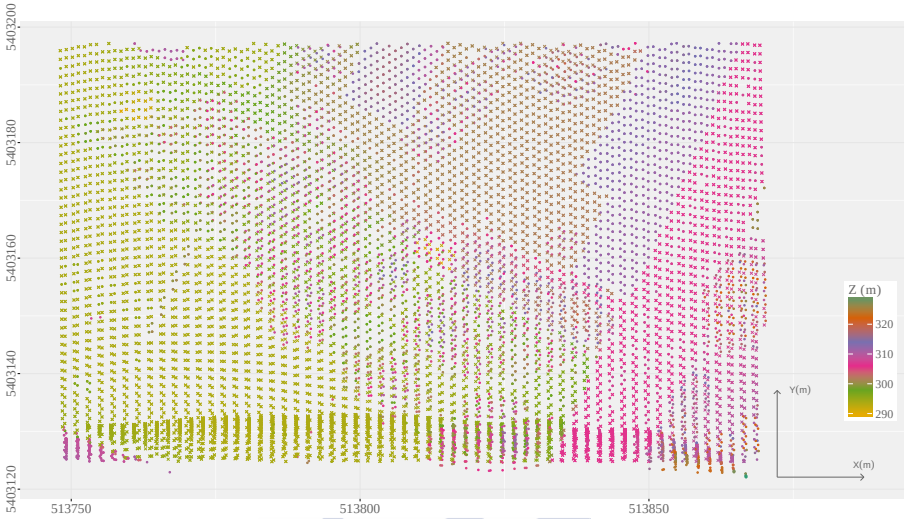

(a) Distribución de los puntos originales en función de la elevación y tipo de punto (la x representa los P_g y el • los P_{ng}).

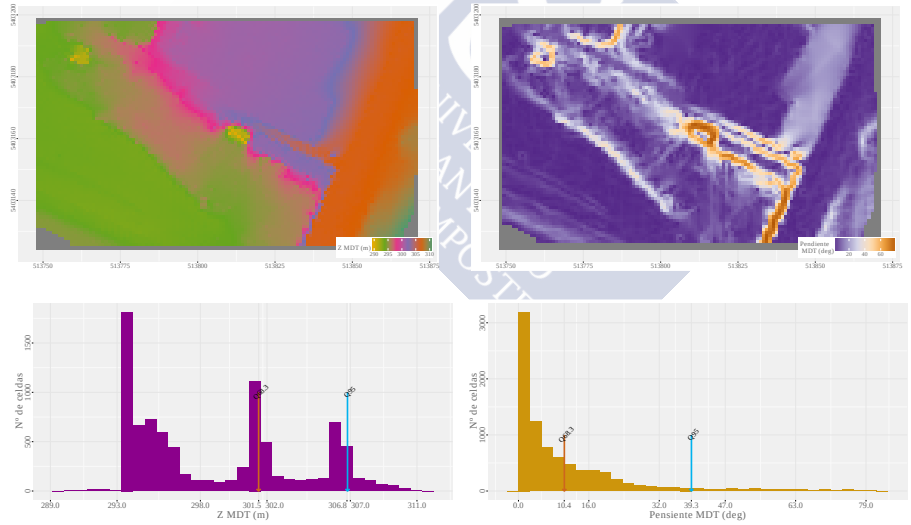

(b) MDT e imagen de pendientes y sus correspondientes histogramas de frecuencia (las flechas naranja y azul marcan el valor del percentil del 68.3% y el 95%, respectivamente).

Figura B.6: Características de la muestra 24.

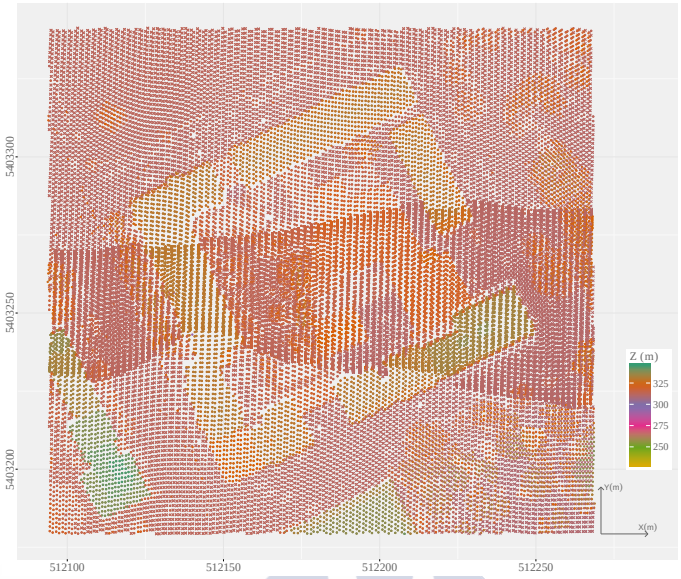

(a) Distribución de los puntos originales en función de la elevación y tipo de punto (la x representa los P_g y el • los P_{ng}).

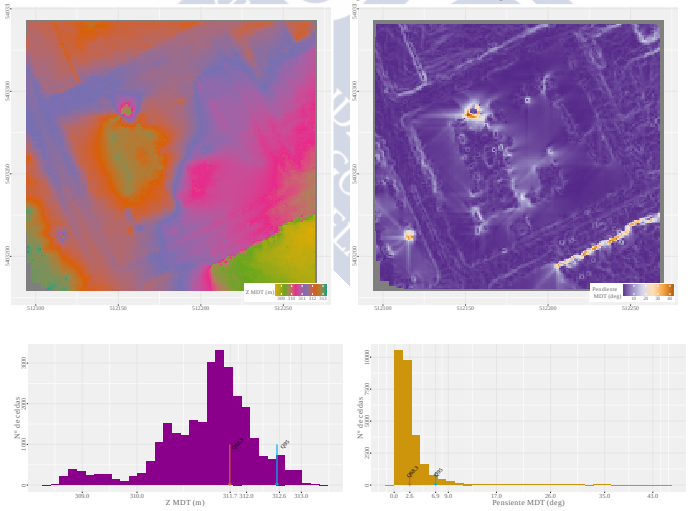

(b) MDT e imagen de pendientes y sus correspondientes histogramas de frecuencia (las flechas naranja y azul marcan el valor del percentil del 68.3% y el 95%, respectivamente).

Figura B.7: Características de la muestra 31.

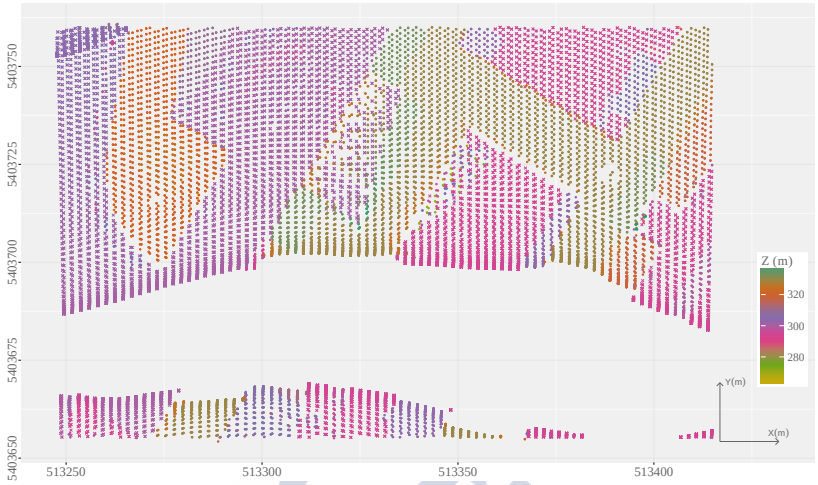

(a) Distribución de los puntos originales en función de la elevación y tipo de punto (la x representa los P_g y el • los P_{ng}).

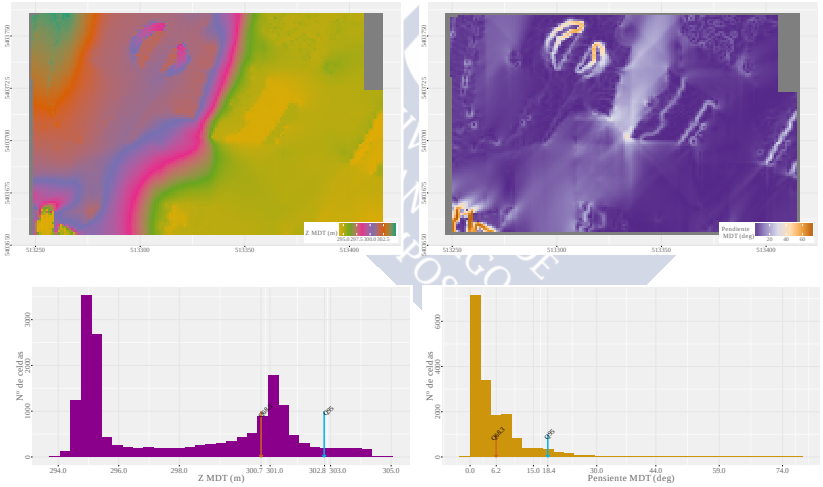

(b) MDT e imagen de pendientes y sus correspondientes histogramas de frecuencia (las flechas naranja y azul marcan el valor del percentil del 68.3% y el 95%, respectivamente).

Figura B.8: Características de la muestra 41.

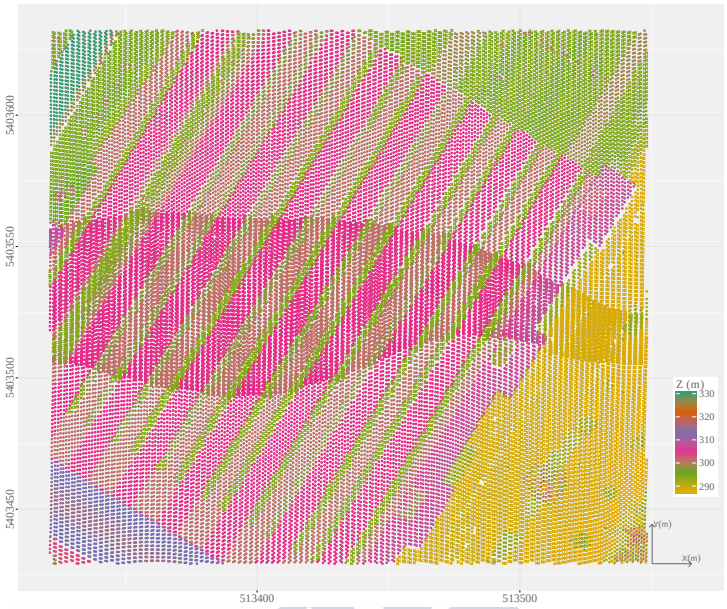

(a) Distribución de los puntos originales en función de la elevación y tipo de punto (la x representa los P_g y el • los P_{ng}).

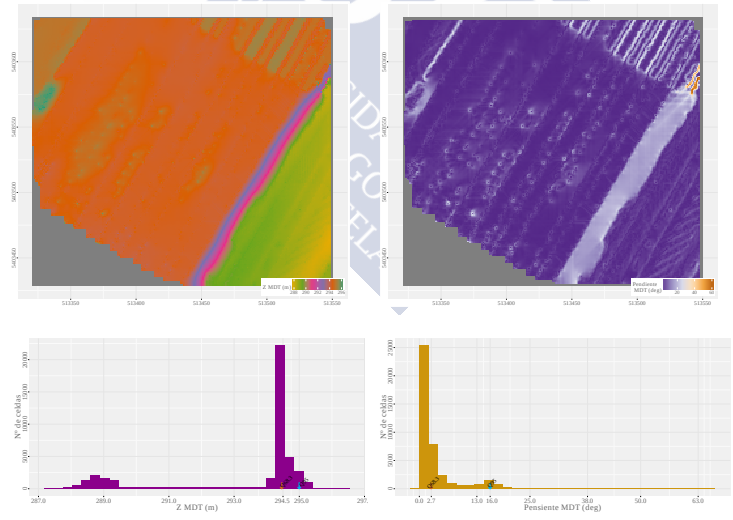

(b) MDT e imagen de pendientes y sus correspondientes histogramas de frecuencia (las flechas naranja y azul marcan el valor del percentil del 68.3% y el 95%, respectivamente).

Figura B.9: Características de la muestra 42.

B.2 Código fuente de la función DecimaTe.

Función 1 *DecimaTe*. Reducción de la densidad de puntos LiDAR

Inputs: *Pointcloud*={S} s_i=(x_i, y_i, z_i, I_i, *retorno*$_i$), *densidad reducida* D_D, *metodo* ∈ {*RpA, SRpC, PpC*}

Cálculo automático de variables

Calcular la densidad media ponderada a partir de {S} → $\overline{D}$

- **if** *metodo=RpA* **then**
  - Calcular el número de puntos a partir de {S} → N
  - Calcular el % de selección → $R = D_D / \overline{D}$
  - Calcular el número de puntos a seleccionar → $n = R \cdot N$
- **else if** *metodo=SRpC* **then**
  - Fijar el número de puntos a seleccionar → $n = 8$
  - Calcular el tamaño de celda → $c = \sqrt{n / D_D}$
- **else if** *metodo=PpC* **then**
  - Fijar el número teórico de puntos a seleccionar → $n_T = 4$
  - Calcular el tamaño de celda → $c = \sqrt{n_T / D_D}$
  - Calcular el % de selección → $R = D_D / \overline{D}$
- **end if**

Selección de puntos

- **if** *metodo=RpA* **then**
  - Obtener la nube de puntos reducida {S_{D_D}} ← *sample* (S, n)
  - **Return** {S_{D_D}}
- **else if** *metodo=SRpC* **then**
  - Fijar el ámbito geográfico a partir de {S} y c → $TRC=(x_{topright}, y_{topright})$ y $LLC=(x_{bottomleft}, y_{bottomleft})$
  - Dividir el área en celdas c x c → Lista de celdas {P}
  - **for all** {P} **do**
    - Puntos disponibles en la celda ij {S_{ij}}; Número de puntos en la celda ij → n_{ij}
    - Número de primeros retornos en la celda ij → FR_{ij}
    - Número de últimos retornos en la celda ij → LR_{ij}
    - **if** n_{ij} ≥ n **and** FR_{ij} ≥ n/2 **and** LR_{ij} ≥ n/2 **then**
      - {S_{FR}} ← *sample* (S_{ij}[*which*(*return*$_i$=1),], n/2); {S_{FR}} $\xrightarrow{include}$ {S_{D_D}}
      - {S_{LR}} ← *sample* (S_{ij}[*which*(*return*$_i$!=1),], n/2); {S_{LR}} $\xrightarrow{include}$ {S_{D_D}}
      - {S_{FR}} ← Ø ; {S_{LR}} ← Ø; {S_{ij}} ← Ø
    - **else if** n_{ij} ≥ n **and** FR_{ij} < n/2 **and** LR_{ij} ≥ n- FR_{ij} **then**
      - {S_{FR}} ← S_{ij}[*which*(*return*$_i$=1),]; {S_{FR}} $\xrightarrow{include}$ {S_{D_D}}
      - {S_{LR}} ← *sample* (S_{ij}[*which*(*return*$_i$!=1),], n- FR_{ij}); {S_{LR}} $\xrightarrow{include}$ {S_{D_D}}
      - {S_{FR}} ← Ø ; {S_{LR}} ← Ø; {S_{ij}} ← Ø
    - **else if** n_{ij} ≥ n **and** LR_{ij} < n/2 **and** FR_{ij} ≥ n- LR_{ij} **then**
      - {S_{LR}} ← S_{ij}[*which*(*return*$_i$!=1),]; {S_{LR}} $\xrightarrow{include}$ {S_{D_D}}
      - {S_{FR}} ← *sample* (S_{ij}[*which*(*return*$_i$=1),], n- LR_{ij}); {S_{FR}} $\xrightarrow{include}$ {S_{D_D}}
      - {S_{FR}} ← Ø ; {S_{LR}} ← Ø; {S_{ij}} ← Ø
    - **else if** 0 < n_{ij} < n **then**
      - {S_{ij}} $\xrightarrow{include}$ {S_{D_D}}; {S_{ij}} ← Ø
    - **end if**
  - **end for**
  - **Return** {S_{D_D}}
- **else if** *metodo=PpC* **then**
  - Fijar ámbito geográfico a partir de {S} y c → $TRC=(x_{topright}, y_{topright})$ y $LLC=(x_{bottomleft}, y_{bottomleft})$
  - Dividir el área en celdas c x c → Lista de celdas {P}
  - **for all** {P} **do**
    - Puntos disponibles en la celda ij {S_{ij}}; Número de puntos en la celda ij → n_{ij}
    - Número de primeros retornos en la celda ij → FR_{ij}
    - Número de últimos retornos en la celda ij → LR_{ij}
    - Calcular el número de puntos a seleccionar en la celda ij → n=$R \cdot n_{ij}$
    - Calcular el % de selección de primeros retornos → RFR_{ij}= FR_{ij} / n_{ij}
    - Calcular el número de primeros retornos a seleccionar en la celda ij → nFR_{ij}= $RFR_{ij} \cdot n$
    - Calcular el número de puntos a seleccionar en la celda ij → nLR_{ij}= n - nFR_{ij}
    - {S_{FR}} ← *sample* (S_{ij}[*which*(*return*$_i$=1),], nFR_{ij}); {S_{FR}} $\xrightarrow{include}$ {S_{D_D}}
    - {S_{LR}} ← *sample* (S_{ij}[*which*(*return*$_i$!=1),], nLR_{ij}); {S_{LR}} $\xrightarrow{include}$ {S_{D_D}}
    - {S_{FR}} ← Ø ; {S_{LR}} ← Ø; {S_{ij}} ← Ø
  - **end for**
  - **Return** {S_{D_D}}
- **end if**

Figura B.10: Pseudo-código de DecimaTe

B.3 Indicadores de la evaluación del método. Resultados cualitativos y cuantitativos.

Resultados cualitativos

En las siguientes figuras se incluyen los resultados cualitativos de la evaluación a nivel método referentes al *indicador 1* (*distribución de los puntos*). Las diferentes figuras muestran en formato ráster la distribución de la densidad de puntos para cada muestra considerando cada método de reducción y densidad de puntos reducida.

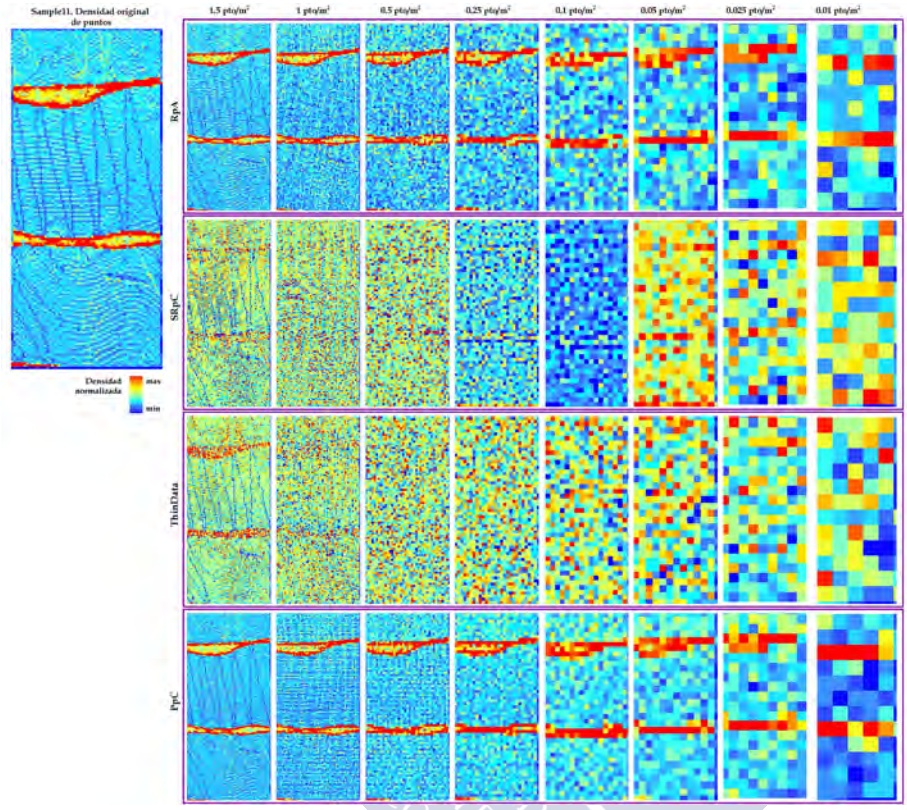

Figura B.11: Muestra 11: Resultados cualitativos del Indicador 1. Comparación de la distribución espacial de la densidad de la nube de puntos original con las nubes de puntos con densidad reducida.

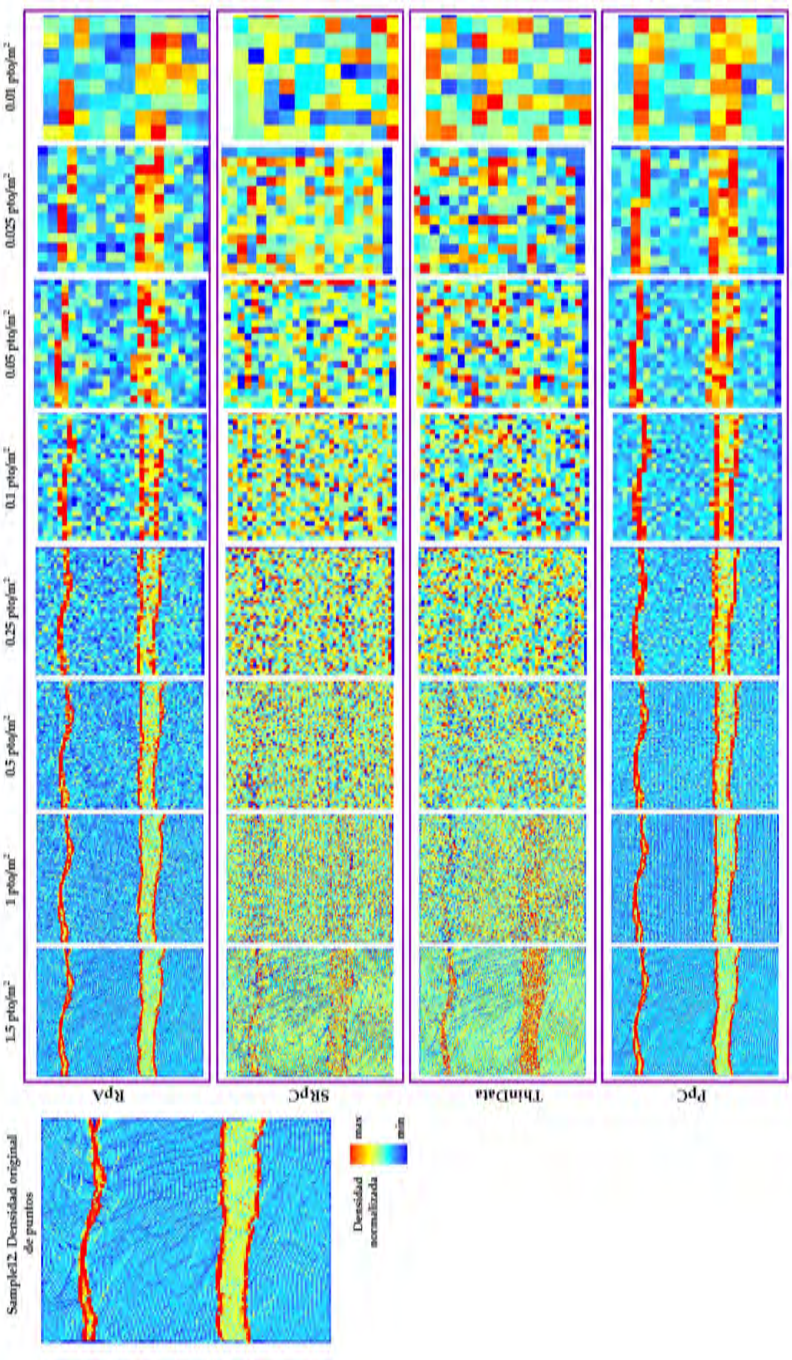

Figura B.12: Muestra 12: Resultados cualitativos del Indicador 1. Comparación de la distribución espacial de la densidad de la nube de puntos original con las nubes de puntos con densidad reducida.

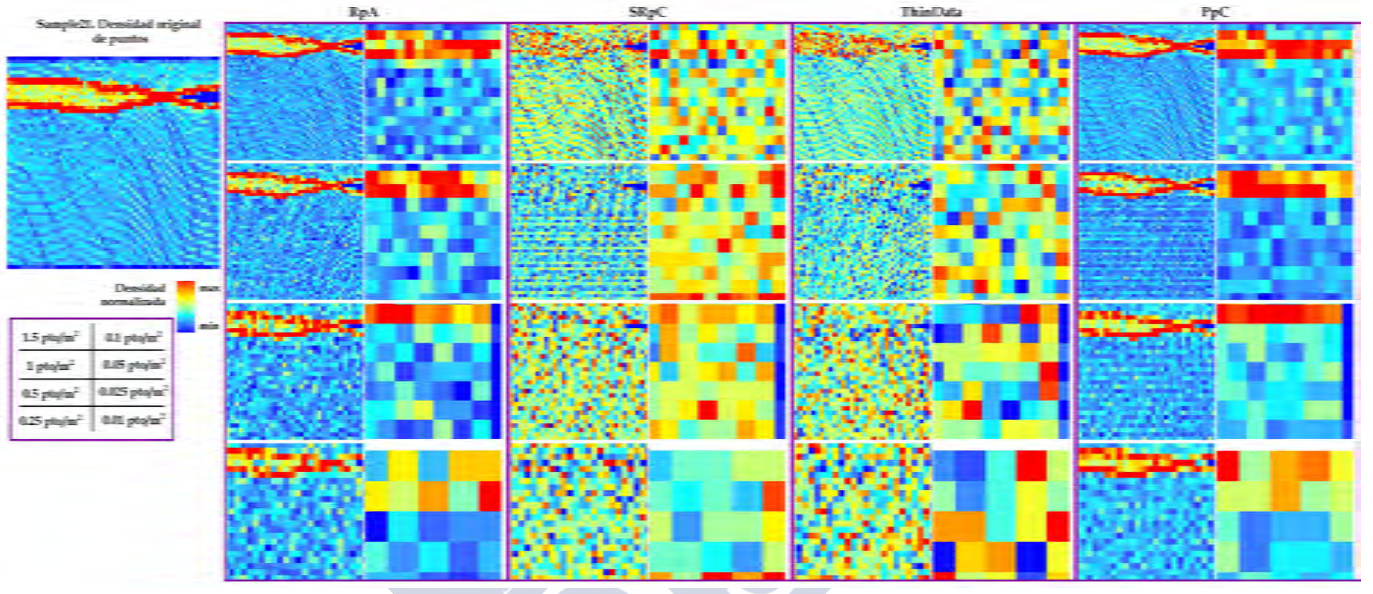

Figura B.13: Muestra 21: Resultados cualitativos del Indicador 1. Comparación de la distribución espacial de la densidad de la nube de puntos original con las nubes de puntos con densidad reducida.

Figura B.14: Muestra 22: Resultados cualitativos del Indicador 1. Comparación de la distribución espacial de la densidad de la nube de puntos original con las nubes de puntos con densidad reducida.

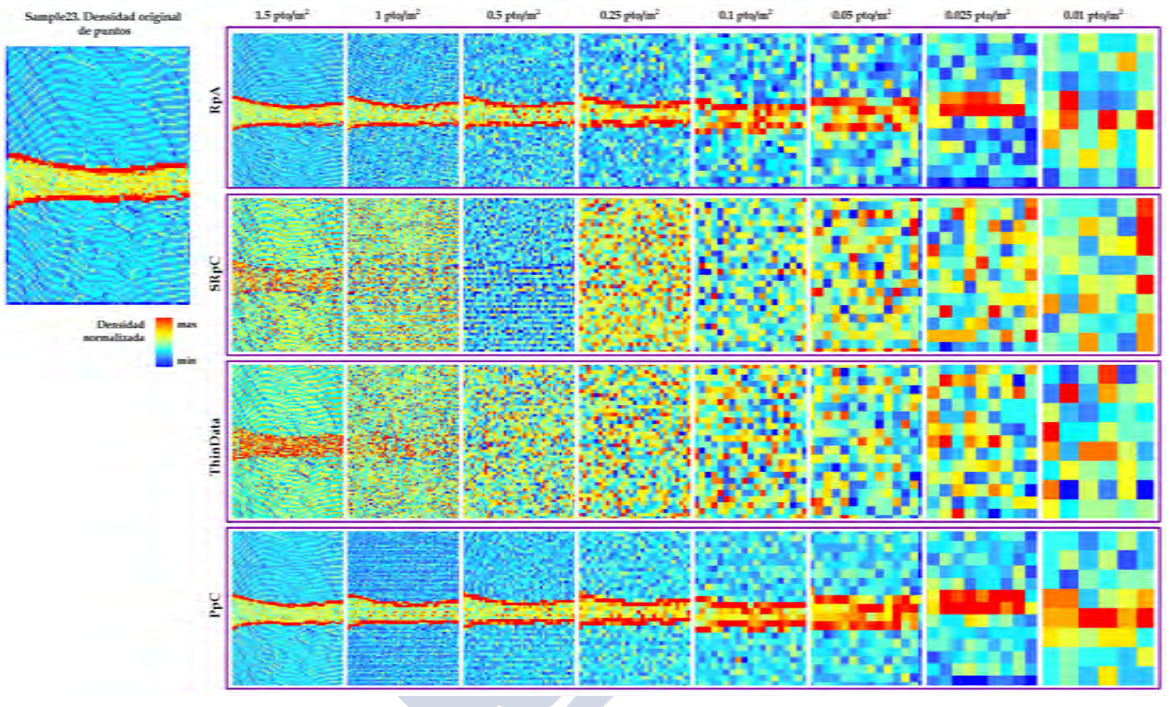

Figura B.15: Muestra 23: Resultados cualitativos del Indicador 1. Comparación de la distribución espacial de la densidad de la nube de puntos original con las nubes de puntos con densidad reducida.

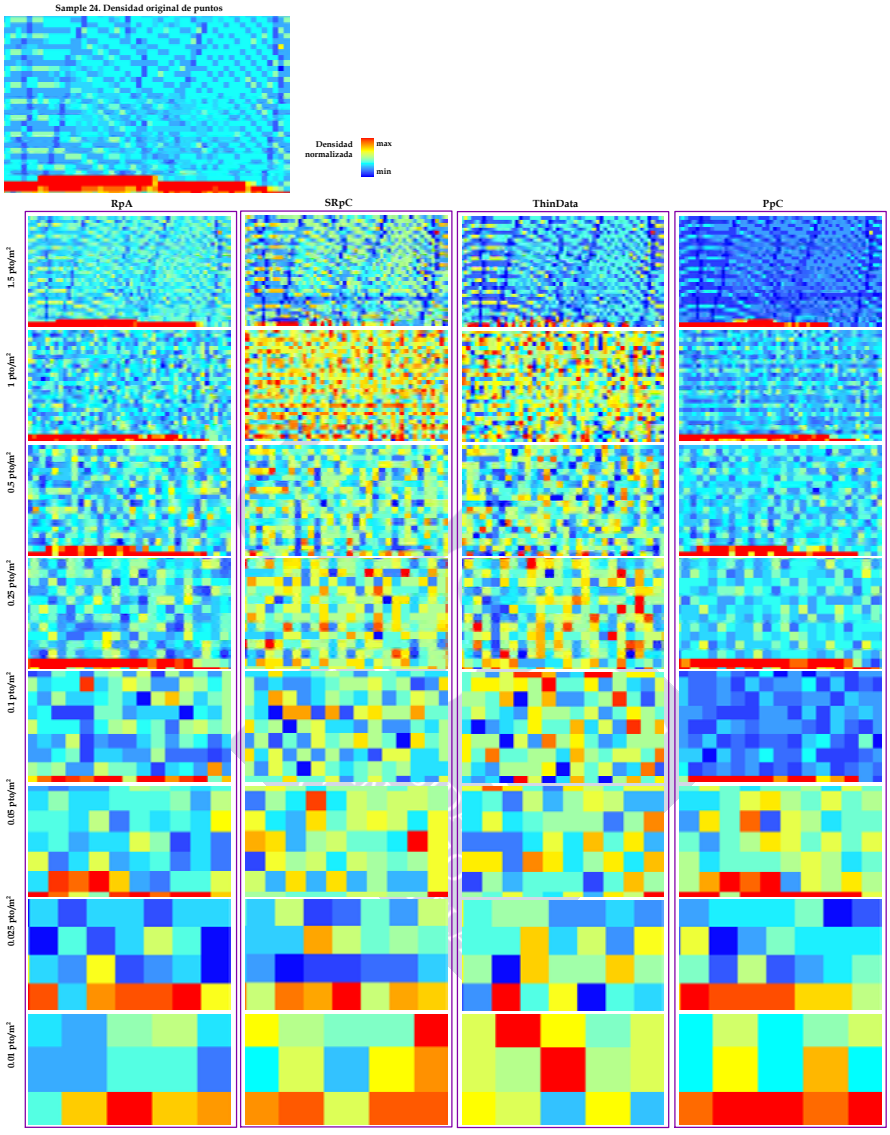

Figura B.16: Muestra 24: Resultados cualitativos del Indicador 1. Comparación de la distribución espacial de la densidad de la nube de puntos original con las nubes de puntos con densidad reducida.

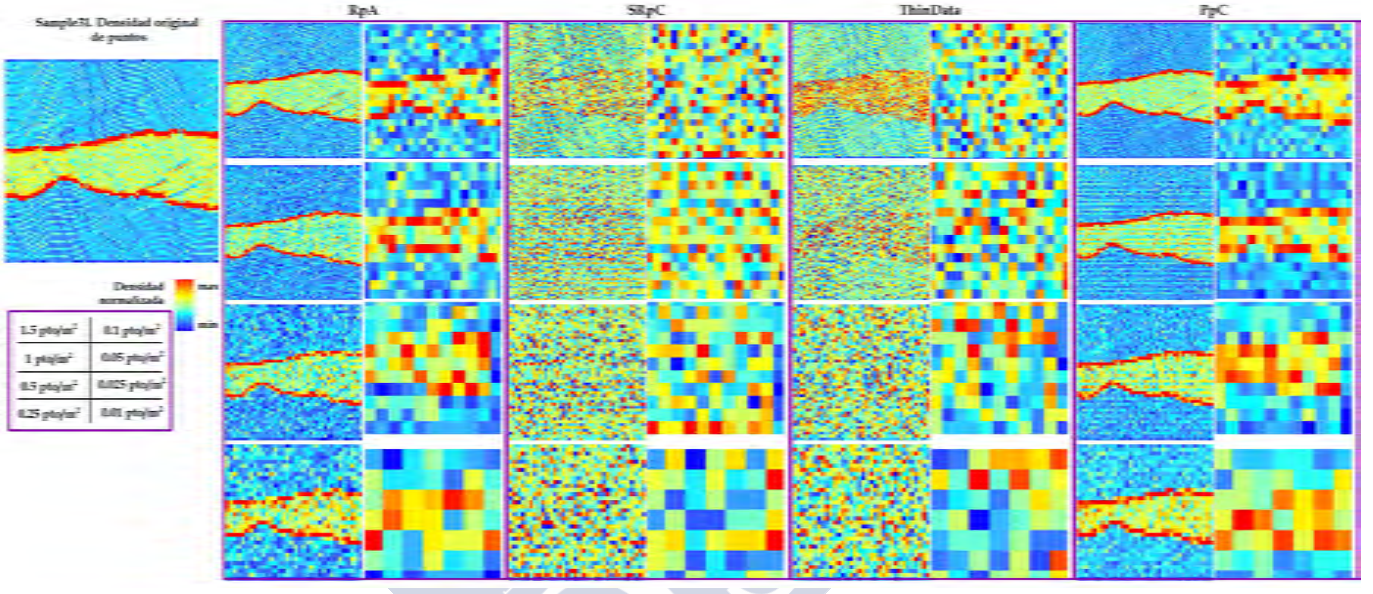

Figura B.17: Muestra 31: Resultados cualitativos del Indicador 1. Comparación de la distribución espacial de la densidad de la nube de puntos original con las nubes de puntos con densidad reducida.

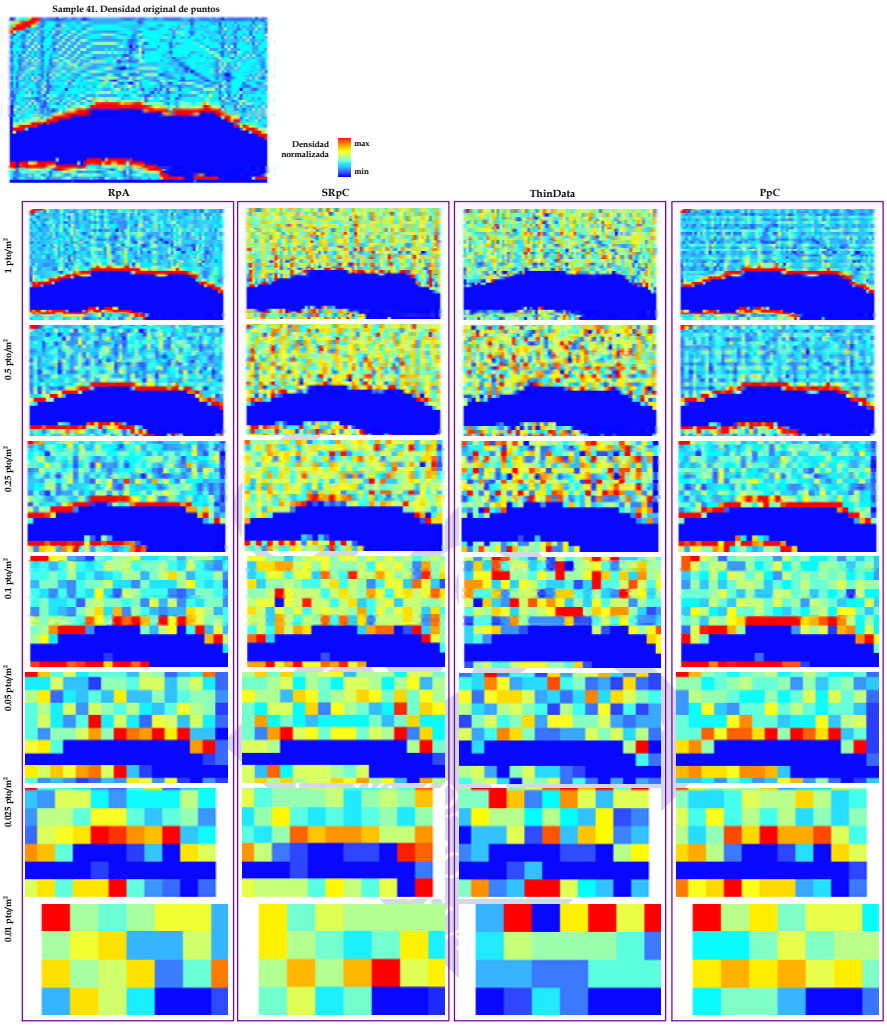

Figura B.18: Muestra 41: Resultados cualitativos del Indicador 1. Comparación de la distribución espacial de la densidad de la nube de puntos original con las nubes de puntos con densidad reducida.

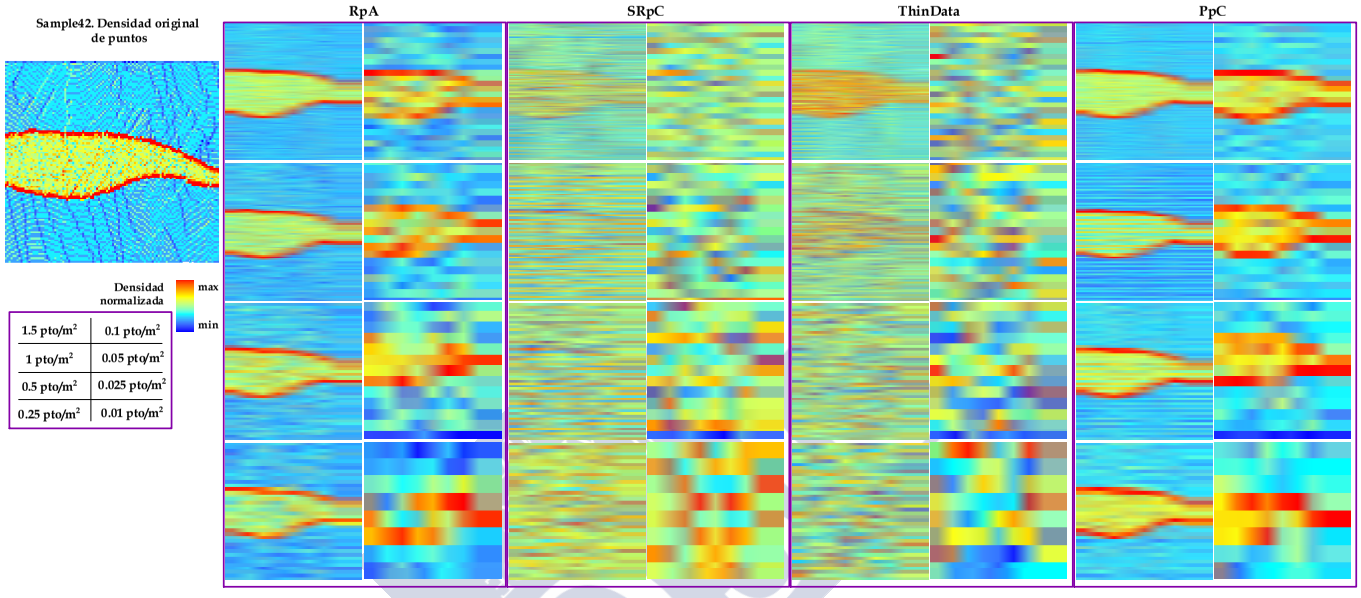

Figura B.19: Muestra 42: Resultados cualitativos del Indicador 1. Comparación de la distribución espacial de la densidad de la nube de puntos original con las nubes de puntos con densidad reducida.

Resultados cuantitativos

A continuación, las siguientes figuras muestran los resultados cuantitativos de la evaluación a nivel método referentes al *Indicador 1* (*distribución de los puntos*). Para cada muestra la figura a) representa la distribución de frecuencias de la densidad de puntos empleando los diferentes métodos de reducción en comparación con los datos originales (linea de color negro); mientras que la figura b) muestra el ajuste lineal entre los píxeles del ráster de densidad original y cada uno de los ráster con densidad reducida diferenciando entre los 4 métodos de reducción (los colores naranja, rosa, verde y azul representan los resultados de los métodos *RpA*, *PpC*, *ThinData* y *SPpC*, respectivamente).

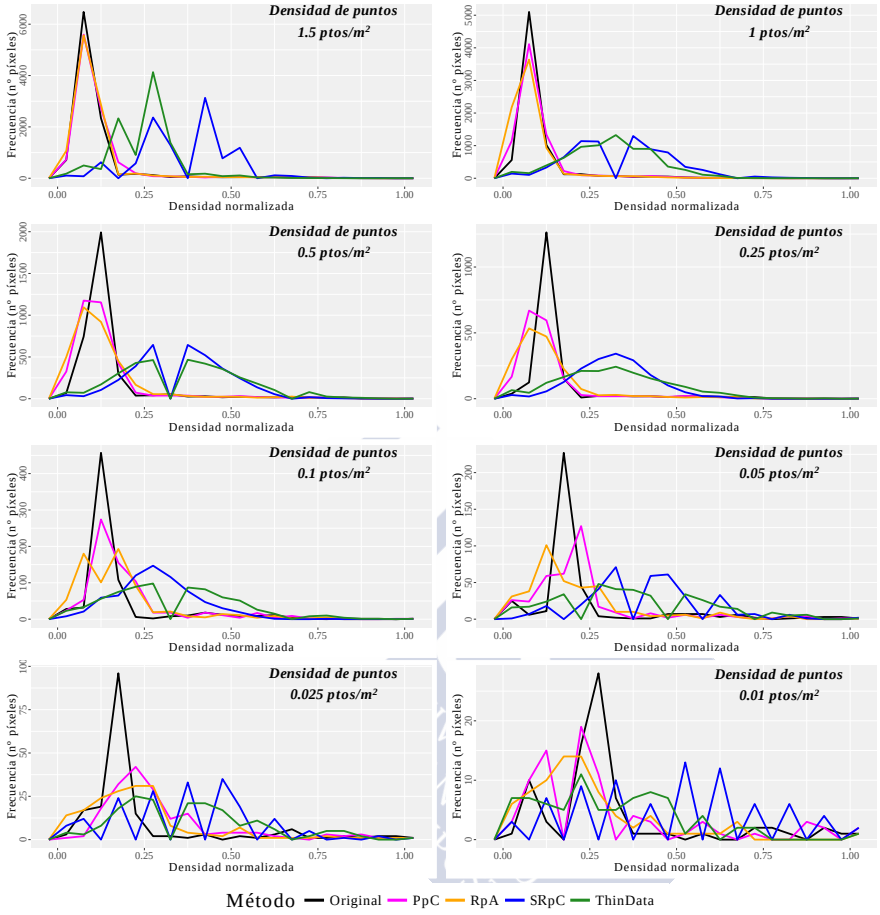

Figura B.20: Muestra 11: Resultados cuantitativos a nivel método del I1. Distribución de frecuencias.

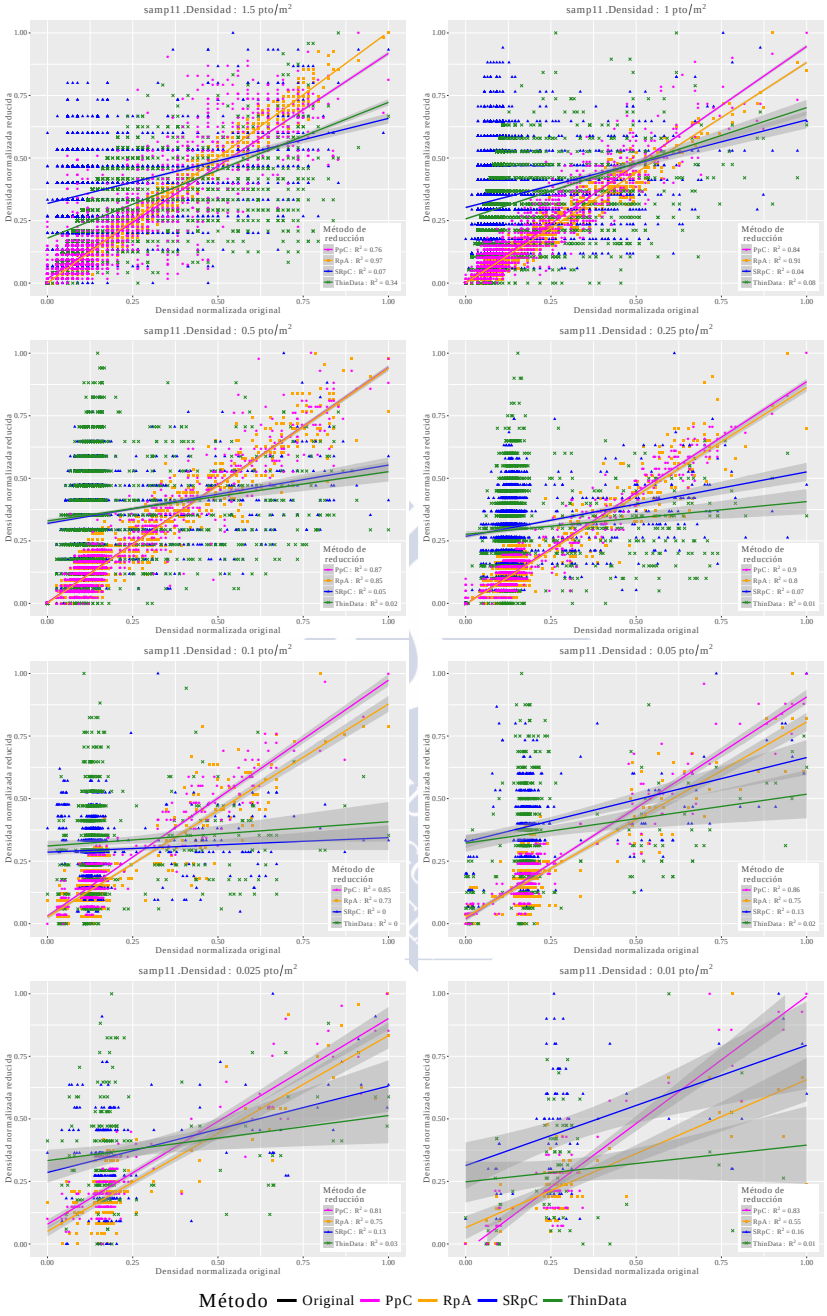

Figura B.21: Muestra 11: Resultados cuantitativos a nivel método del I1. Ajuste lineal.

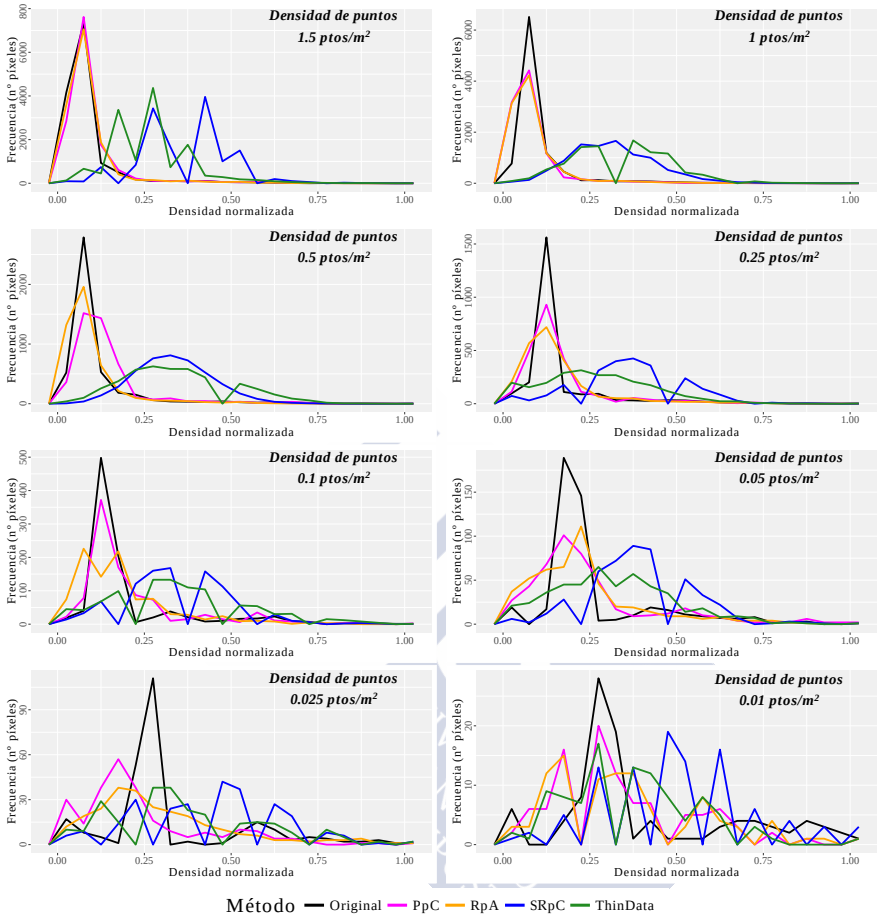

Figura B.22: Muestra 12: Resultados cuantitativos a nivel método del I1. Distribución de frecuencias.

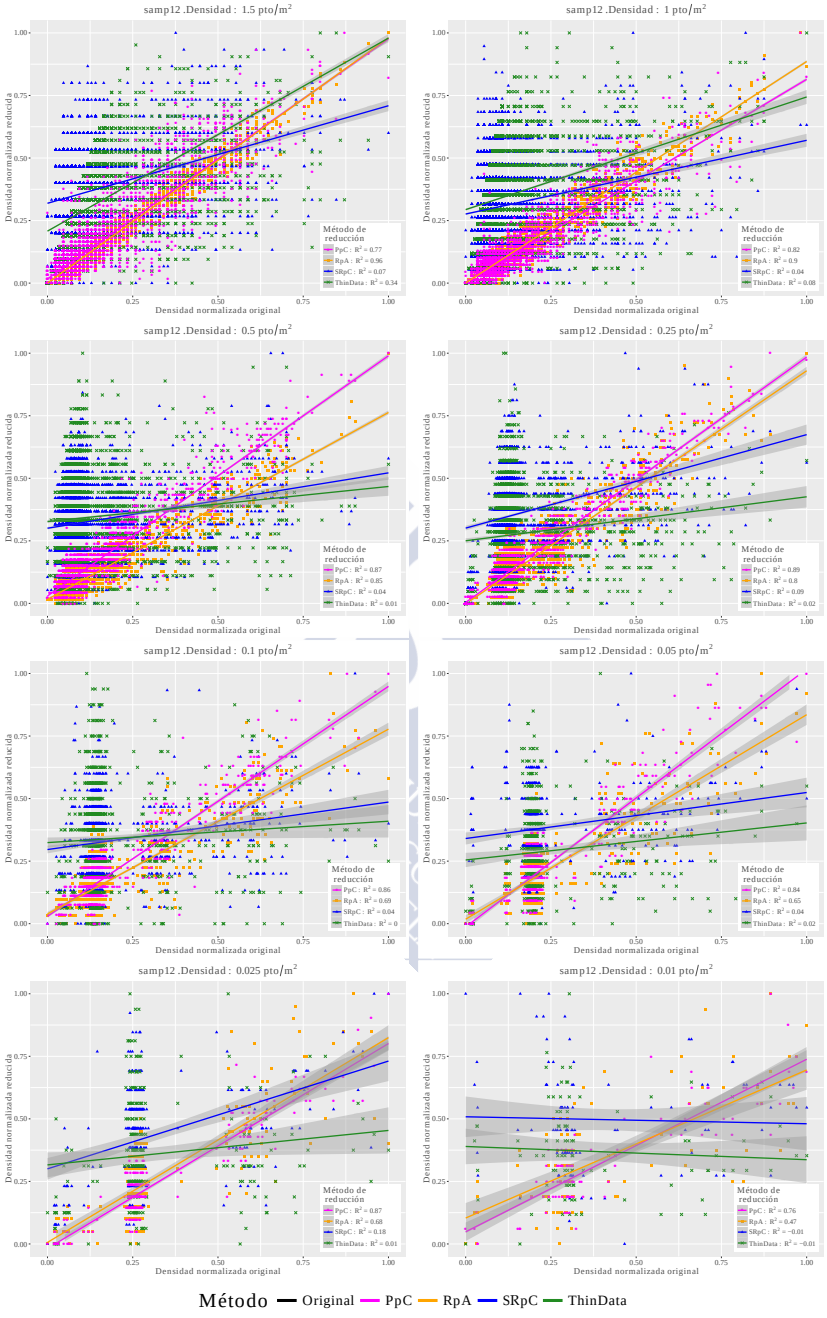

Figura B.23: Muestra 12: Resultados cuantitativos a nivel método del I1. Ajuste lineal.

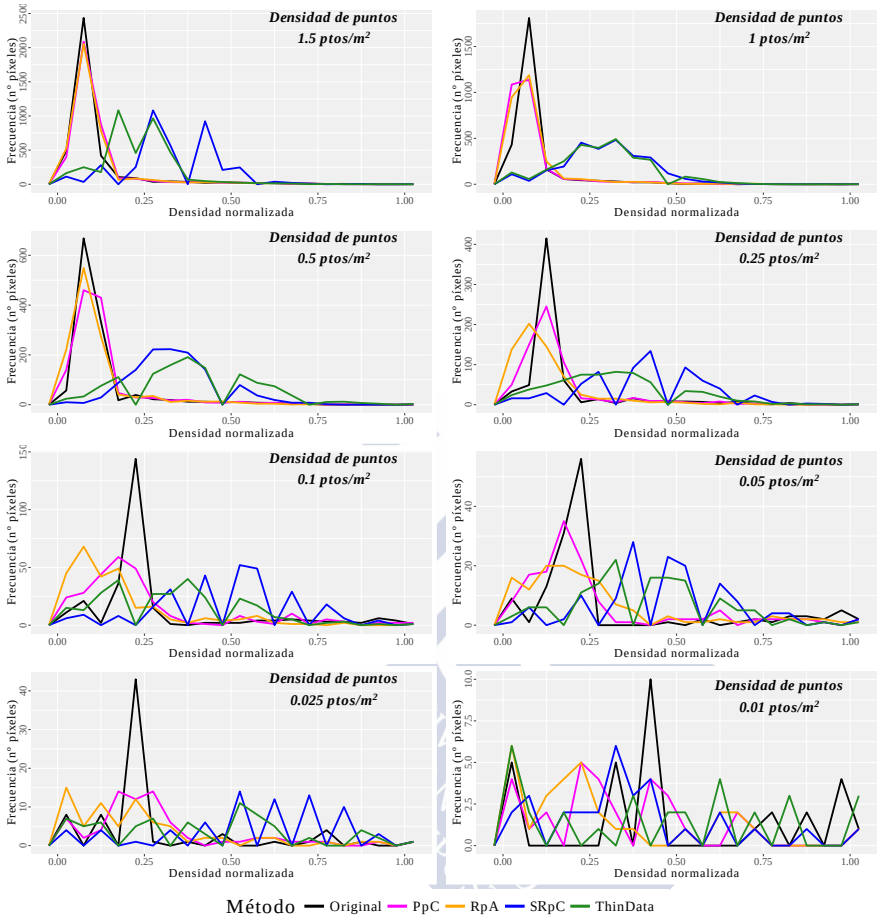

Figura B.24: Muestra 21: Resultados cuantitativos a nivel método del I1. Distribución de frecuencias.

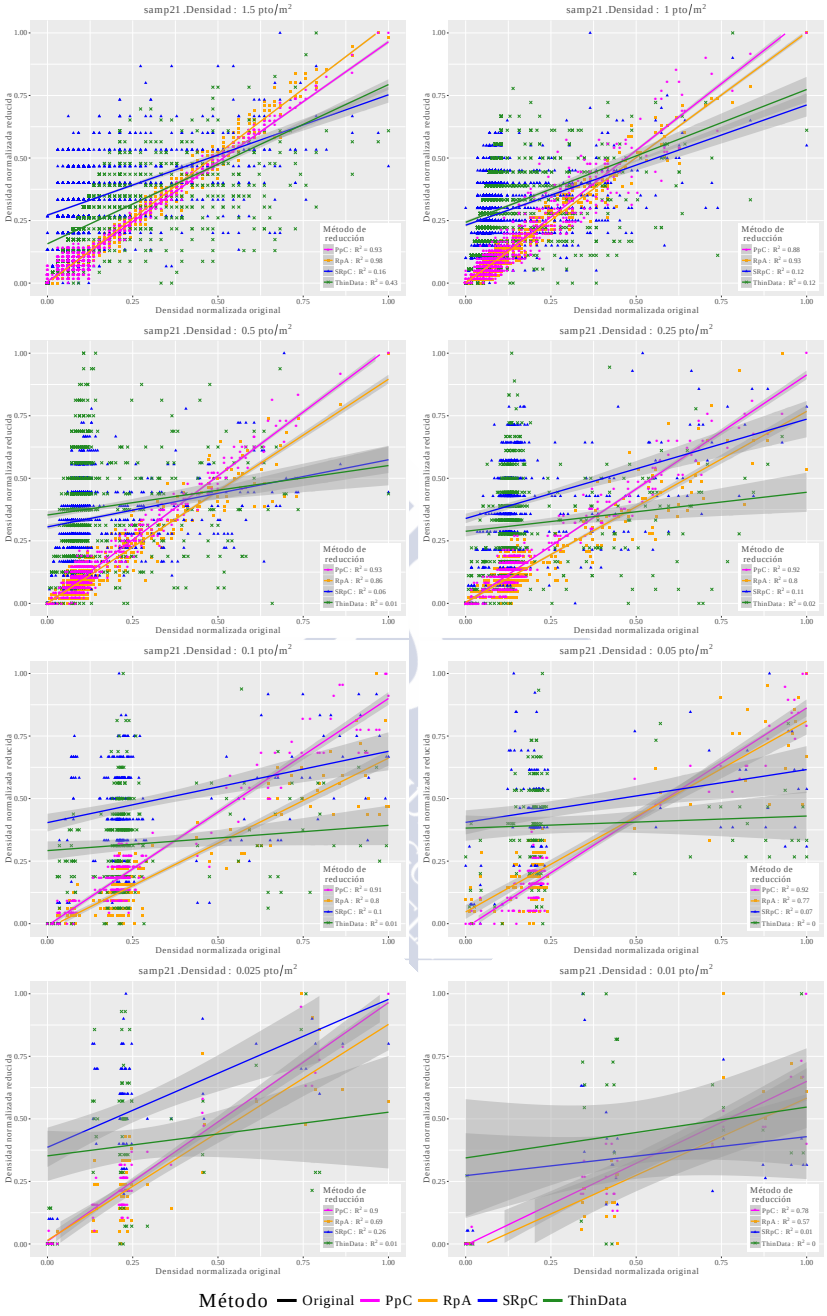

Figura B.25: Muestra 21: Resultados cuantitativos a nivel método del I1. Ajuste lineal.

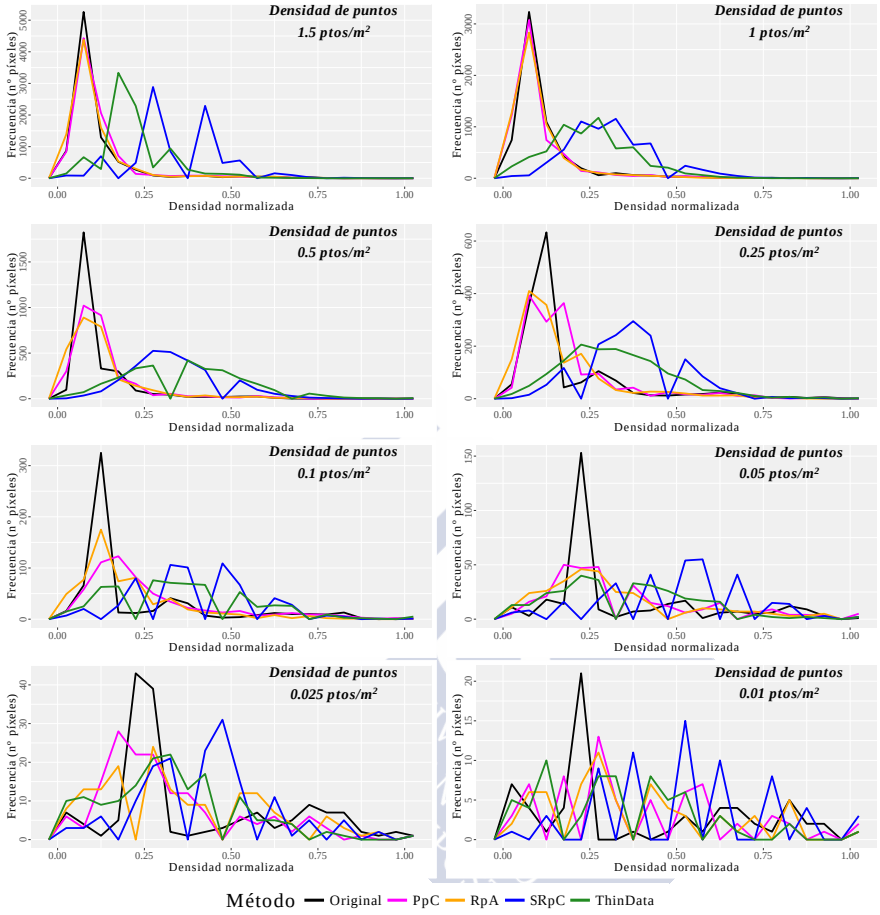

Figura B.26: Muestra 22: Resultados cuantitativos a nivel método del I1. Distribución de frecuencias.

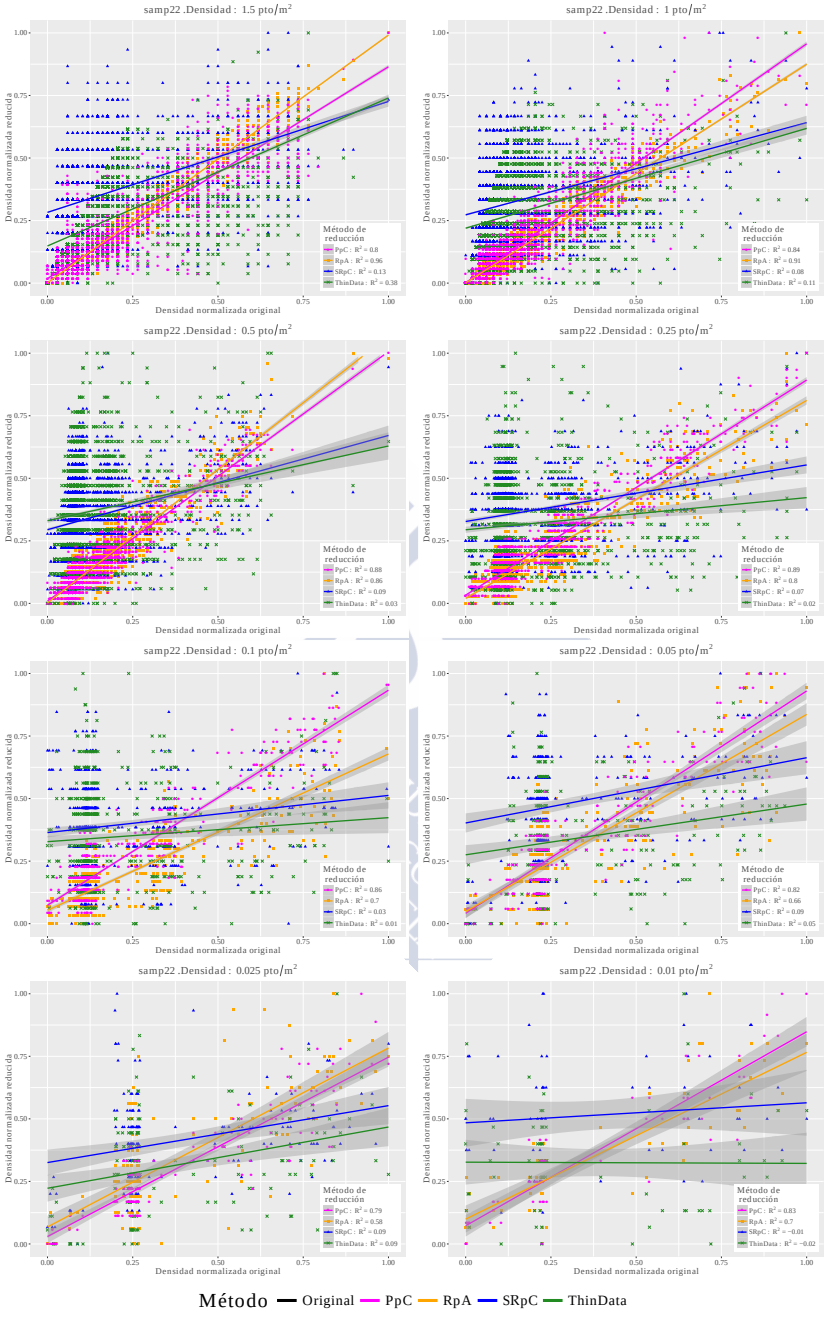

Figura B.27: Muestra 22: Resultados cuantitativos a nivel método del I1. Ajuste lineal.

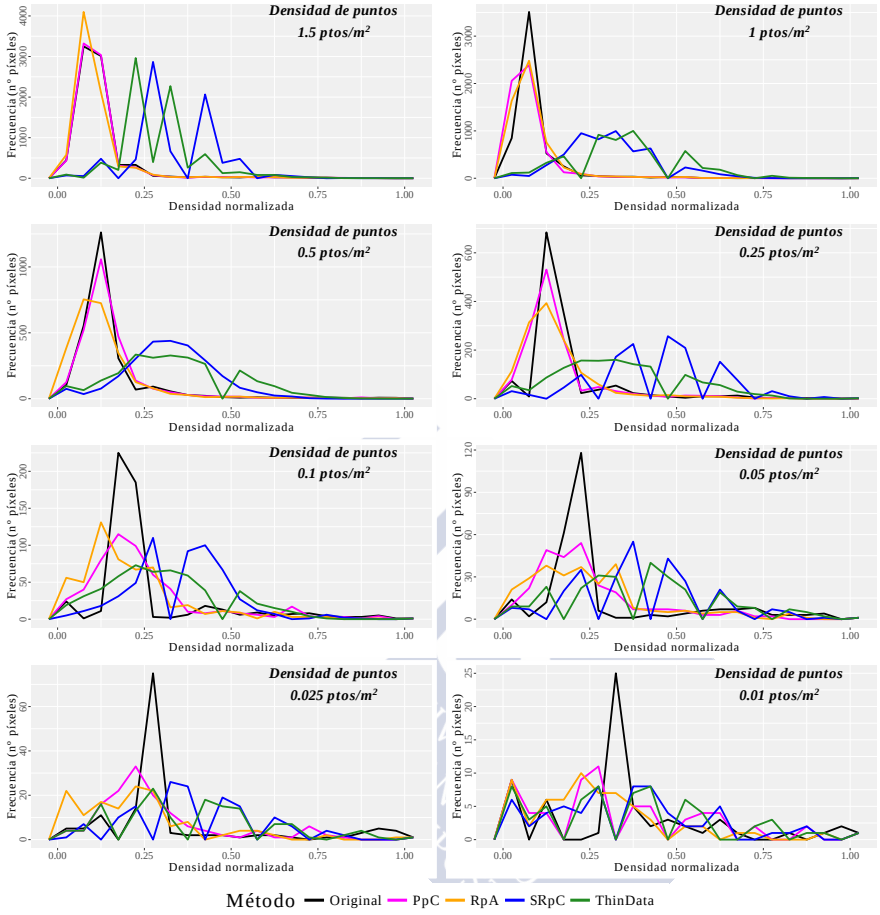

Figura B.28: Muestra 23: Resultados cuantitativos a nivel método del I1. Distribución de frecuencias.

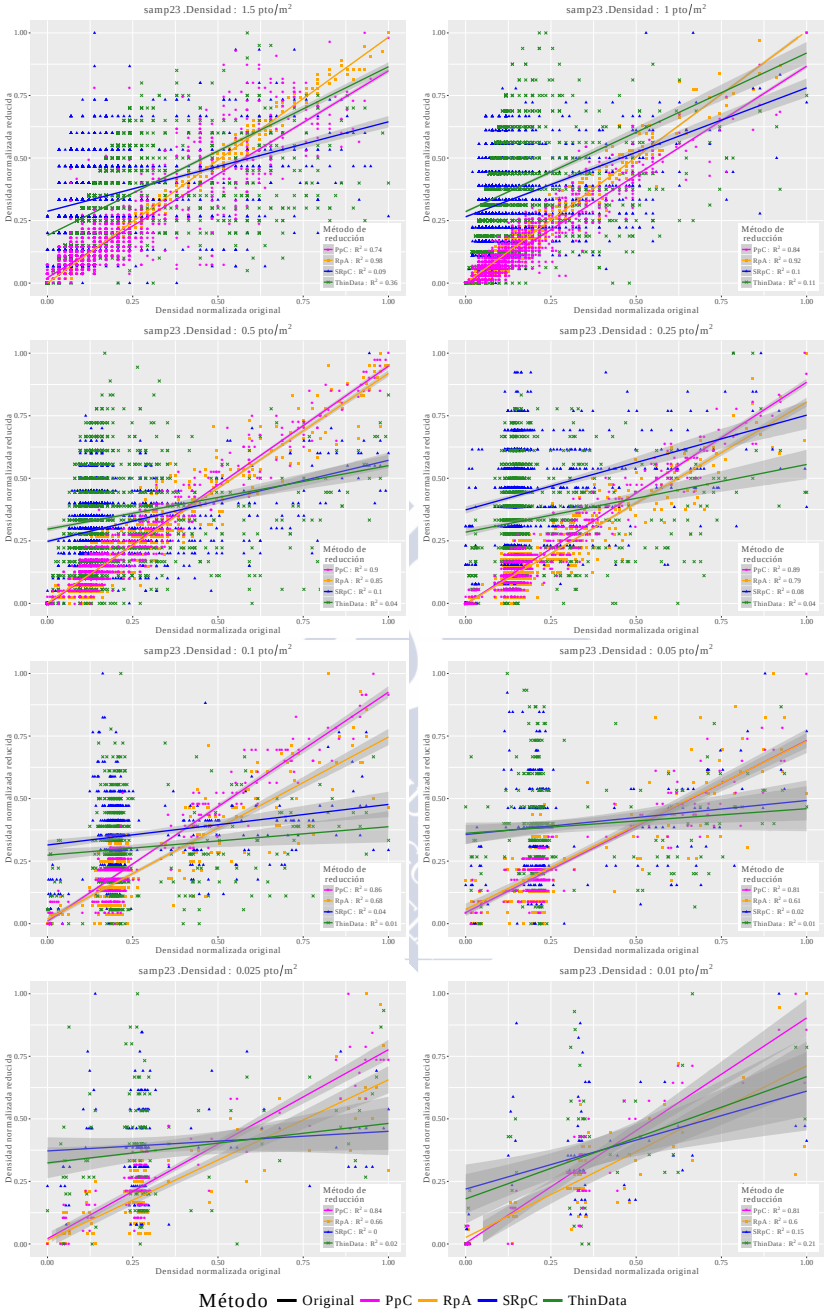

Figura B.29: Muestra 23: Resultados cuantitativos a nivel método del I1. Ajuste lineal.

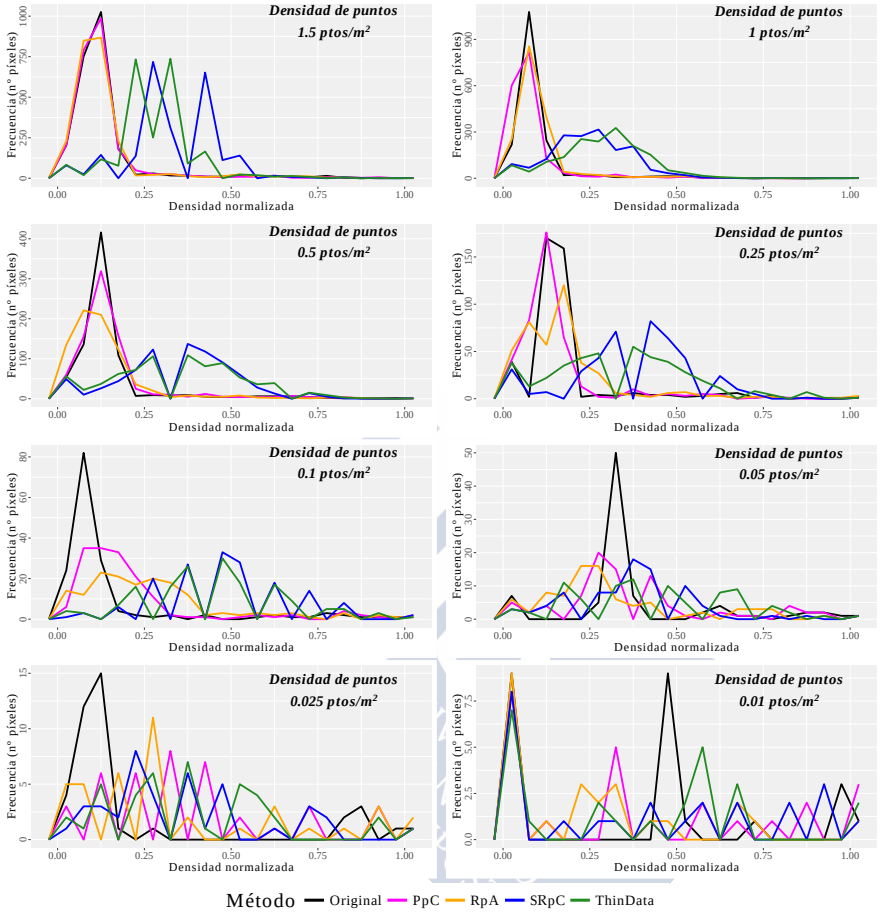

Figura B.30: Muestra 24: Resultados cuantitativos a nivel método del I1. Distribución de frecuencias.

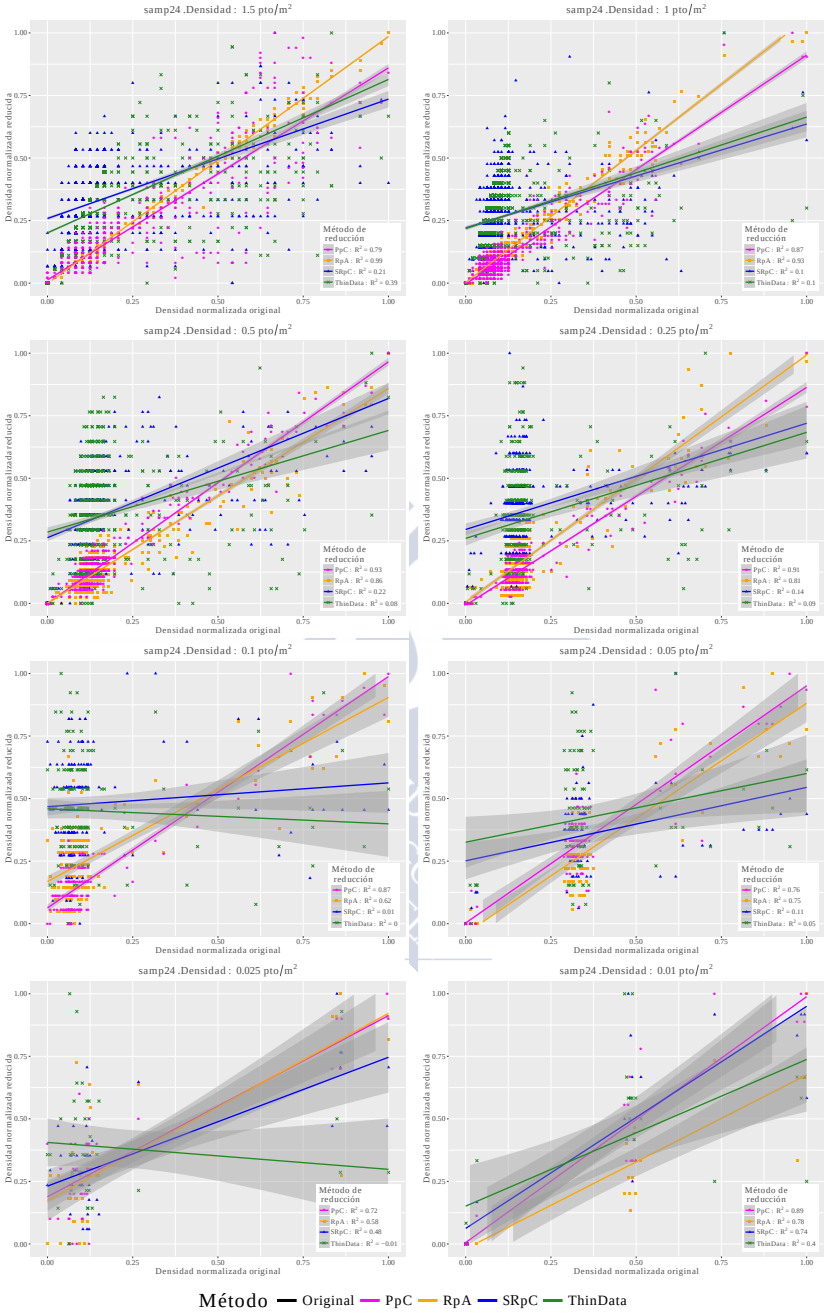

Figura B.31: Muestra 24: Resultados cuantitativos a nivel método del I1. Ajuste lineal.

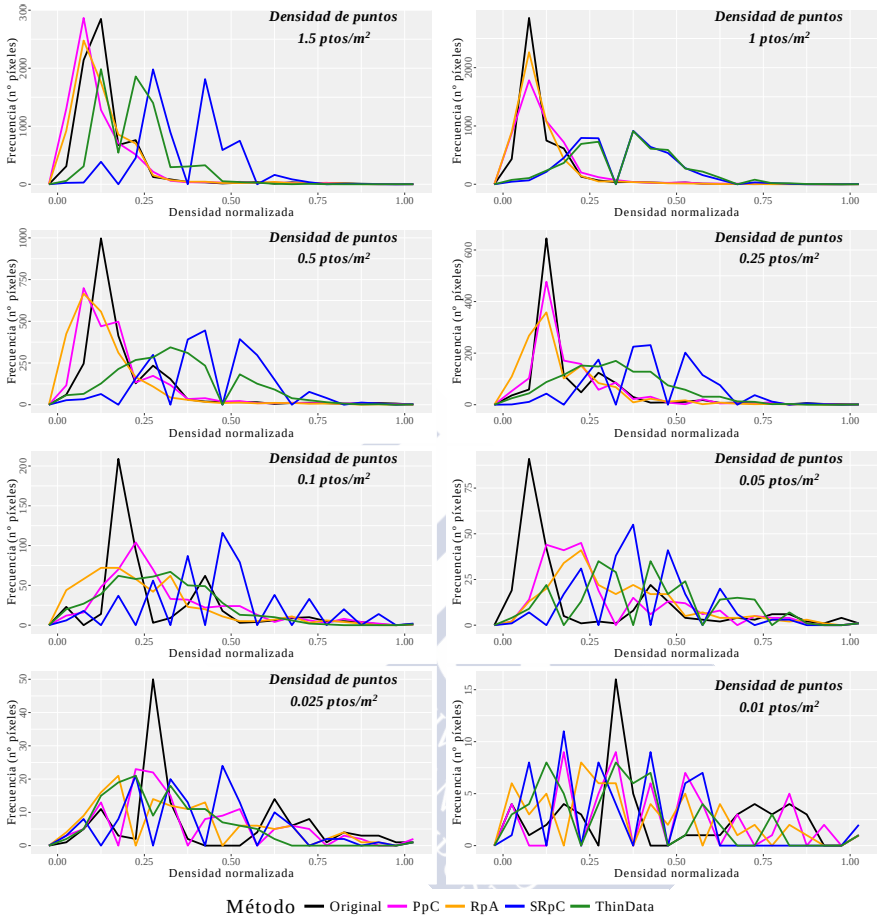

Figura B.32: Muestra 31: Resultados cuantitativos a nivel método del I1. Distribución de frecuencias.

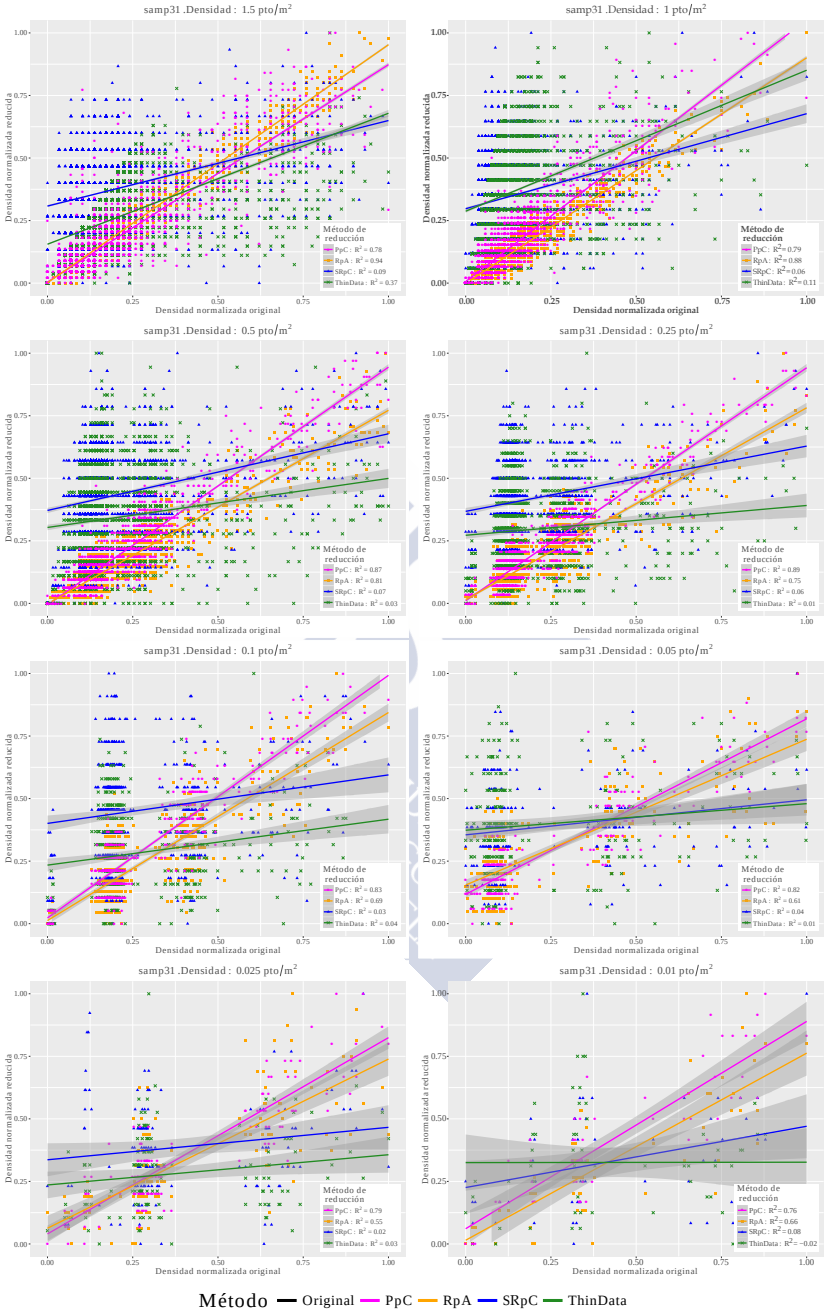

Figura B.33: Muestra 31: Resultados cuantitativos a nivel método del I1. Ajuste lineal.

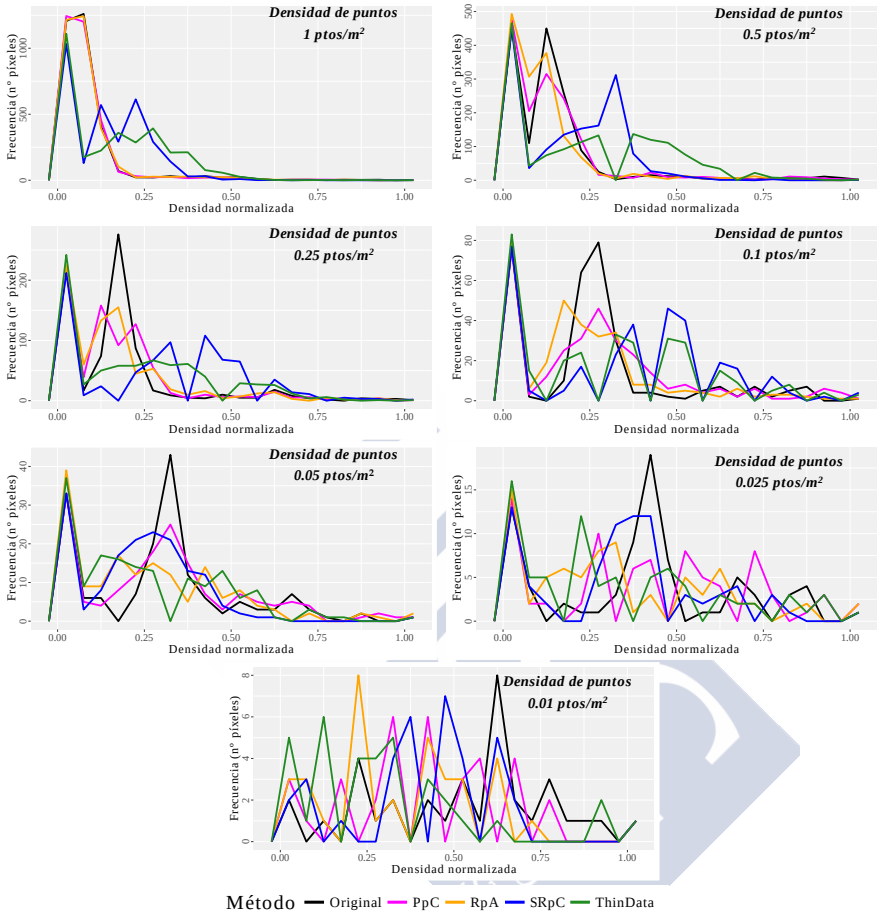

Figura B.34: Muestra 41: Resultados cuantitativos a nivel método del I1. Distribución de frecuencias.

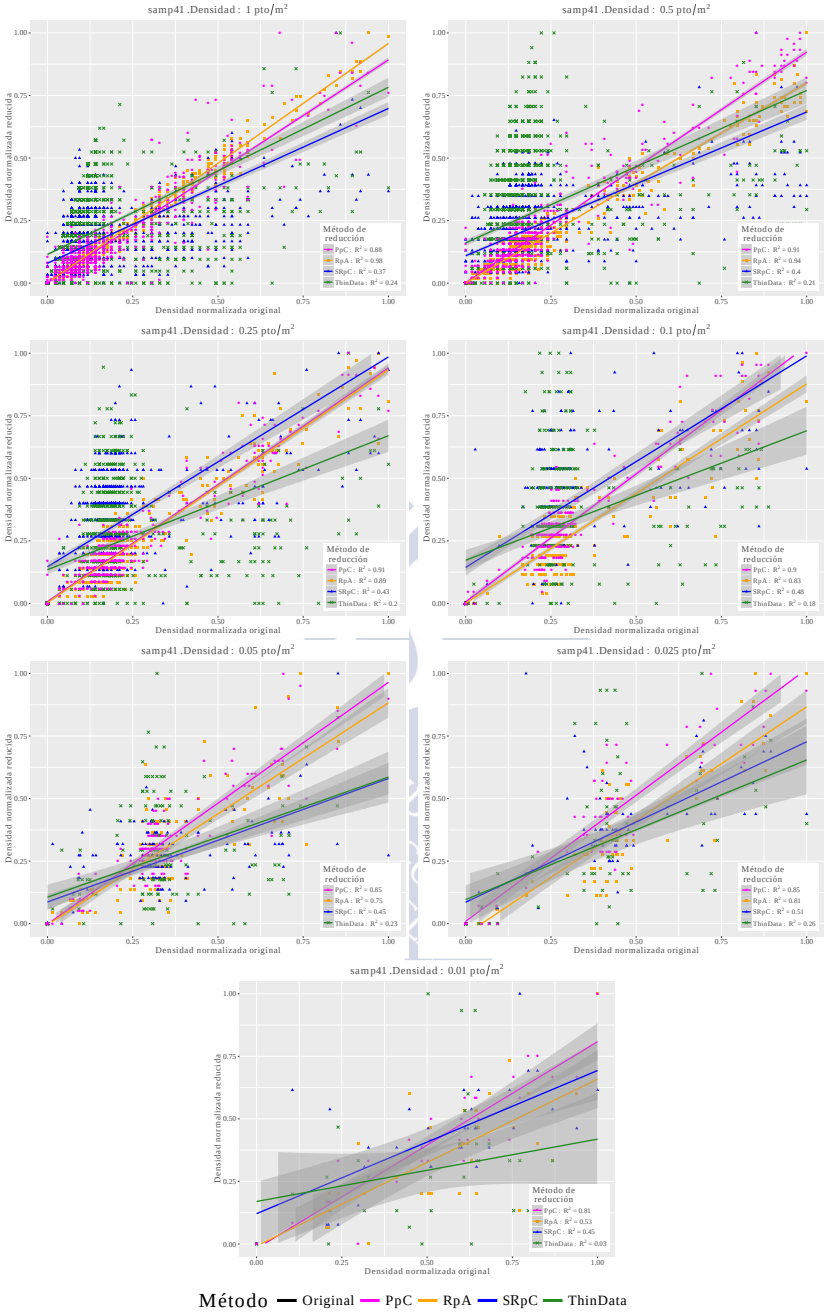

Figura B.35: Muestra 41: Resultados cuantitativos a nivel método del I1. Ajuste lineal.

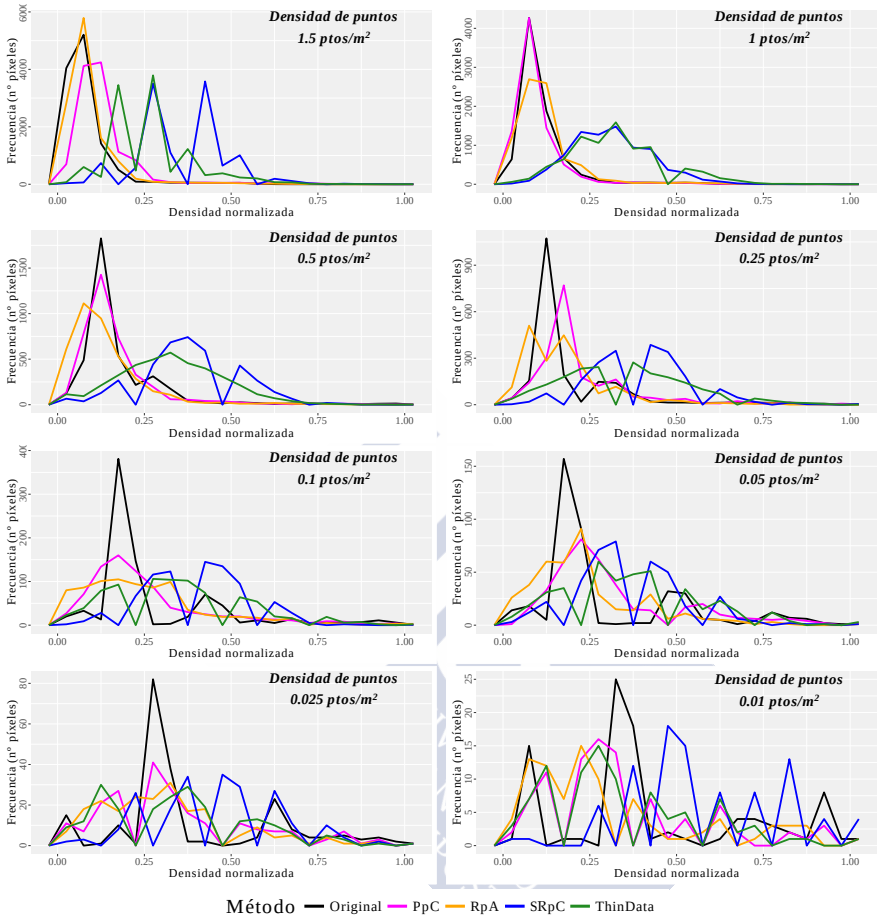

Figura B.36: Muestra 42: Resultados cuantitativos a nivel método del I1. Distribución de frecuencias.

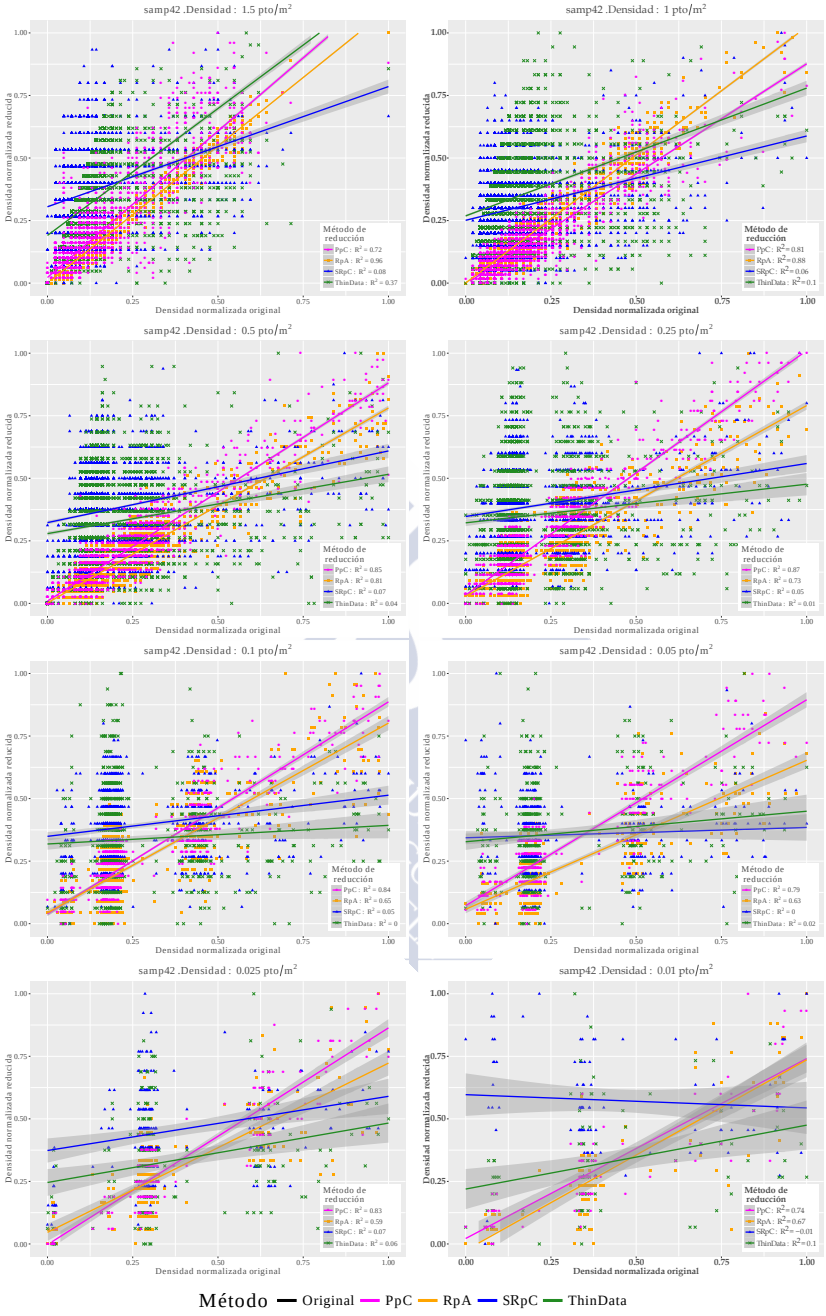

Figura B.37: Muestra 42: Resultados cuantitativos a nivel método del I1. Ajuste lineal.

Tabla B.1: Resultados del Indicador 1 en la evaluación cuantitativa a nivel método. Las celdas de esta tabla incluyen el valor del coeficiente de determinación (R^2) para cada caso.

Indicador 1: Distribución de puntos.

Indicador (I)	Descripción	Grado de cumplimiento
Distribución de los puntos	Análisis de la dependencia lineal entre las celdas del ráster de distribución original de puntos y el obtenido tras la reducción y cálculo del coeficiente de determinación (R^2).	Good $\leftarrow R^2 \in [0.8, 1]$ Regular $\leftarrow R^2 \in [0.6, 0.8]$ Poor $\leftarrow R^2 \in [0, 0.6)$

Método	**RpA**				**SRpC**				**ThinData**				**PpC**			
Densidad (ptos m^2)	**1.5**	**1**	**0.5**	**0.25**	**1.5**	**1**	**0.5**	**0.25**	**1.5**	**1**	**0.5**	**0.25**	**1.5**	**1**	**0.5**	**0.25**
M11	0.97	0.91	0.85	0.80	0.07	0.04	0.05	0.07	0.34	0.08	0.02	0.01	0.76	0.84	0.87	0.90
M12	0.96	0.90	0.85	0.80	0.07	0.04	0.04	0.09	0.34	0.08	0.01	0.02	0.77	0.82	0.87	0.89
M21	0.98	0.93	0.86	0.80	0.16	0.12	0.06	0.11	0.43	0.12	0.01	0.02	0.93	0.88	0.93	0.92
M22	0.96	0.91	0.86	0.80	0.13	0.08	0.09	0.07	0.38	0.11	0.03	0.02	0.80	0.84	0.88	0.89
M23	0.98	0.92	0.85	0.79	0.09	0.1	0.1	0.08	0.36	0.11	0.04	0.04	0.74	0.84	0.90	0.89
M24	0.99	0.93	0.86	0.81	0.21	0.10	0.22	0.14	0.39	0.1	0.08	0.09	0.79	0.87	0.93	0.91
M31	0.94	0.88	0.81	0.75	0.09	0.06	0.07	0.06	0.37	0.11	0.03	0.01	0.78	0.79	0.87	0.89
M41		0.98	0.94	0.89		0.37	0.4	0.43		0.24	0.21	0.20		0.88	0.91	0.91
M42	0.96	0.88	0.81	0.73	0.08	0.06	0.07	0.05	0.37	0.10	0.04	0.01	0.72	0.81	0.85	0.87
Densidad (ptos m^2)	**0.1**	**0.05**	**0.025**	**0.01**	**0.1**	**0.05**	**0.025**	**0.01**	**0.1**	**0.05**	**0.025**	**0.01**	**0.1**	**0.05**	**0.025**	**0.01**
M11	0.73	0.75	0.75	0.55	0	0.13	0.13	0.16	0	0.02	0.03	0.01	0.85	0.86	0.81	0.83
M12	0.69	0.65	0.68	0.47	0.04	0.04	0.18	-0.01	0	0.02	0.01	-0.01	0.86	0.84	0.87	0.76
M21	0.80	0.77	0.69	0.57	0.1	0.07	0.26	0.01	0.01	0	0.01	0	0.91	0.92	0.90	0.78
M22	0.70	0.66	0.58	0.70	0.03	0.09	0.09	-0.01	0.01	0.05	0.09	-0.02	0.86	0.82	0.79	0.83
M23	0.68	0.61	0.66	0.60	0.04	0.02	0	0.15	0.01	0.01	0.02	0.21	0.86	0.81	0.84	0.81
M24	0.62	0.75	0.58	0.78	0.01	0.11	0.48	0.74	0	0.05	-0.01	0.4	0.87	0.76	0.72	0.89
M31	0.69	0.61	0.55	0.66	0.03	0.04	0.02	0.08	0.04	0.01	0.03	-0.02	0.83	0.82	0.79	0.76
M41	0.83	0.75	0.81	0.53	0.48	0.45	0.51	0.45	0.18	0.23	0.26	0.03	0.90	0.85	0.85	0.81
M42	0.65	0.63	0.59	0.67	0.05	0	0.07	-0.01	0	0.02	0.06	0.1	0.84	0.79	0.83	0.74

Tabla B.2: Resultados del Indicador 2 en la evaluación cuantitativa a nivel método. En las celdas de esta tabla se incluyeron los valores del ratio FR_R:LR_R obtenido tras el proceso de reducción. Los valores en cursiva indican donde $D^O_{RFR:LR}$ toma valores negativos.

Indicador 2: Proporción entre retornos.

Indicador (I)	Descripción	Grado de cumplimiento
Proporción entre retornos	Diferencia absoluta entre el ratio FP:LP obtenido a partir de los datos originales y tras la reducción ($D^O_{RFP:LP}$).	Good $\leftarrow D^O_{RFP:LP} \in [0, 5\%*FP_O : LP_O]$ Regular $\leftarrow D^O_{RFP:LP} \in [5\%*\frac{FP_O}{LP_O}, 10\%*\frac{FP_O}{LP_O}]$ Poor $\leftarrow D^O_{RFP:LP} \in (10\%*FP_O : LP_O, +\infty]$

	FR_O:LR_O		Método →	RpA				SRpC				ThinData				PpC			
Org.	**5% Org.**	**10% Org.**	**Densidad (ptos/m^2) →**	**1.5**	**1**	**0.5**	**0.25**	**1.5**	**1**	**0.5**	**0.25**	**1.5**	**1**	**0.5**	**0.25**	**1.5**	**1**	**0.5**	**0.25**
1	±0.05	±0.1	M11	1	0.99	0.99	1	1	1	1	1	*1.01*	*1.04*	*1.03*	*1.02*	0.99	0.99	0.99	*1.01*
1	±0.05	±0.1	M12	1	1	1	*1.01*	1	1	1	1	1	*1.03*	*1.03*	*1.01*	0.99	0.99	*1.01*	1
1	±0.05	±0.1	M21	1	1	*1.01*	0.94	1	0.99	*1.01*	1	*1.01*	*1.03*	*1.03*	*1.02*	0.98	0.98	*1.01*	1
1	±0.05	±0.1	M22	*1.01*	1	0.98	0.99	1	1	1	1	*1.01*	*1.03*	*1.02*	1	0.99	0.99	1	*1.01*
1	±0.05	±0.1	M23	1	1	1	0.97	1	1	1	1	*1.01*	*1.03*	*1.03*	*1.01*	1	1	1	1
1	±0.05	±0.1	M24	*1.01*	0.98	*1.01*	0.98	*1.01*	1	1	*1.02*	1	*1.03*	*1.03*	*1.01*	1	1	1	*1.01*
1	±0.05	±0.1	M31	*1.01*	1	0.99	*1.01*	1	1	1	1	*1.01*	*1.03*	*1.02*	1	0.99	0.99	1	1
1	±0.05	±0.1	M41		1	*1.04*	*1.01*		1	1	1		*1.03*	1	0.97		1	1	*1.02*
1	±0.05	±0.1	M42	1	*1.01*	1	*1.02*	1	1	1	1	*1.01*	*1.03*	*1.02*	1	1	0.99	1	1
Org.	**5% Org.**	**10% Org.**	**Densidad (ptos/m^2) →**	**0.1**	**0.05**	**0.025**	**0.01**	**0.1**	**0.05**	**0.025**	**0.01**	**0.1**	**0.05**	**0.025**	**0.01**	**0.1**	**0.05**	**0.025**	**0.01**
1	±0.05	±0.1	M11	0.97	*1.02*	0.97	0.90	1	1	1	1	*1.01*	*1.01*	*1.02*	1	*1.01*	0.98	1	0.99
1	±0.05	±0.1	M12	*1.02*	*1.02*	*1.06*	*1.01*	1	1	1	1	1	*1.01*	*1.01*	*1.01*	0.99	1	0.99	0.97
1	±0.05	±0.1	M21	0.99	0.97	0.89	*1.18*	*1.01*	1	1	1	*1.05*	*1.03*	*1.07*	*1.13*	0.98	*1.03*	*1.01*	0.96
1	±0.05	±0.1	M22	*1.04*	0.96	0.96	*1.02*	1	1	1	1	0.98	0.97	0.94	0.96	0.99	0.98	1	*1.07*
1	±0.05	±0.1	M23	*1.01*	0.99	*1.11*	0.94	1	1	1	1	*1.02*	*1.02*	*1.04*	0.96	1	*1.01*	0.99	0.95
1	±0.05	±0.1	M24	0.99	*1.08*	*1.32*	*1.07*	1	*1.03*	1	1	0.97	*1.01*	0.98	0.88	*1.02*	0.97	0.96	*1.05*
1	±0.05	±0.1	M31	1	*1.01*	*1.14*	0.94	1	1	1	1	0.97	0.96	0.97	0.95	*1.01*	*1.01*	0.96	0.97
1	±0.05	±0.1	M41	0.94	*1.17*	0.94	*1.07*	1	0.98	1	1	0.98	1	0.98	*1.14*	*1.01*	*1.01*	*1.04*	*1.08*
1	±0.05	±0.1	M42	1	0.94	*1.02*	0.93	1	1	1	1	1	0.99	0.99	1	*1.01*	1	*1.01*	0.99

Tabla B.3: Resultados del Indicador 3 en la evaluación cuantitativa a nivel método. En las celdas de esta tabla se incluyeron los valores del ratio P_{gR}:P_{ngR} obtenido tras el proceso de reducción. Los valores en cursiva indican donde $D^{O}_{RP_g:P_{ng}}$ toma valores negativos.

Indicador 3: Proporción entre P_g y P_{ng}

Indicador (I)	Descripción	Grado de cumplimiento
Proporción entre GP y nGP	Diferencia absoluta entre el ratio GP:nGP obtenido a partir de los datos originales y tras la reducción ($D^{O}_{RGP:nGP}$).	Good $\leftarrow D^{O}_{RGP:nGP} \in [0, 5\% * GP_O : nGP_O)$ Improvable $\leftarrow D^{O}_{RGP:nGP} \in [5\% * \frac{GP_O}{nGP_O} : 10\% * \frac{GP_R}{nGP_R}]$ Poor $\leftarrow D^{O}_{RGP:nGP} \leq [10\% * GP_R : nGP_O, +\infty]$

	P_{gO}:P_{ngO}		Método →	RpA				SRpC				ThinData				PpC			
Org.	5% **Org.**	10% **Org.**	**Densidad (ptos/m^2)** →	**1.5**	**1**	**0.5**	**0.25**	**1.5**	**1**	**0.5**	**0.25**	**1.5**	**1**	**0.5**	**0.25**	**1.5**	**1**	**0.5**	**0.25**
1	±0.05	±0.1	M11	1	1	0.99	0.98	0.97	0.98	0.98	0.96	0.98	0.98	0.98	0.97	1.00	0.99	*1.01*	*1.01*
0.83	±0.04	±0.08	M12	0.83	0.83	0.81	0.83	*0.87*	*0.89*	*0.88*	*0.87*	*0.87*	*0.88*	*0.87*	*0.85*	*0.84*	0.83	*0.84*	*0.84*
1.86	±0.09	±0.19	M21	1.84	1.85	*1.87*	*1.94*	1.76	1.79	1.77	1.77	1.80	1.77	1.79	1.80	1.84	*1.87*	*1.89*	1.85
1.82	±0.09	±0.18	M22	1.82	1.80	*1.85*	1.76	*1.93*	*1.98*	*1.96*	*1.93*	*1.89*	*1.94*	*2.00*	*2.01*	1.85	1.82	1.85	1.85
0.99	±0.05	±0.1	M23	0.98	0.98	*1.02*	*1.01*	*1.08*	*1.10*	*1.11*	*1.13*	*1.05*	*1.08*	*1.09*	*1.07*	0.99	0.96	0.99	0.98
1.72	±0.09	±0.17	M24	*1.73*	*1.76*	1.71	1.63	1.55	1.55	1.52	1.63	1.60	1.50	1.57	1.53	1.72	1.71	1.71	*1.78*
0.91	±0.05	±0.09	M31	0.91	0.91	0.90	*0.92*	*1.07*	*1.10*	*1.08*	*1.08*	*1.03*	*1.06*	*1.07*	*1.04*	0.90	*0.93*	0.89	*0.92*
0.95	±0.05	±0.1	M41		*0.96*	*0.96*	0.95		0.91	0.94	0.89		0.86	0.91	0.94		0.94	*0.97*	*0.96*
0.39	±0.02	±0.04	M42	0.39	*0.40*	0.39	*0.40*	*0.45*	*0.46*	*0.47*	*0.46*	*0.42*	*0.45*	*0.47*	*0.45*	*0.40*	*0.40*	*0.40*	0.39

Org.	5% **Org.**	10% **Org.**	**Densidad (ptos/m^2)** →	**0.1**	**0.05**	**0.025**	**0.01**	**0.1**	**0.05**	**0.025**	**0.01**	**0.1**	**0.05**	**0.025**	**0.01**	**0.1**	**0.05**	**0.025**	**0.01**
1	±0.05	±0.1	M11	*1.03*	*1.02*	1	*1.08*	0.96	0.94	0.97	0.98	0.95	0.92	0.85	0.84	0.97	*1.02*	0.94	0.87
0.83	±0.04	±0.08	M12	*0.88*	0.81	0.77	0.76	*0.89*	*0.91*	*0.88*	0.82	*0.85*	*0.88*	*0.89*	*1.08*	0.82	*0.84*	0.82	*0.98*
1.86	±0.09	±0.19	M21	*2.06*	1.82	*2.07*	1.64	1.77	1.75	*1.93*	*2.08*	1.77	1.81	1.66	1.45	*1.90*	1.76	1.80	*2.15*
1.82	±0.09	±0.18	M22	*1.87*	1.75	1.81	1.82	*1.87*	*2.12*	*1.90*	*2.19*	*2.12*	*2.11*	*2.34*	*2.27*	*1.87*	1.74	1.78	*2.00*
0.99	±0.05	±0.1	M23	*1.02*	*1.09*	*1.03*	*1.00*	*1.08*	*1.11*	*1.04*	*1.04*	*1.14*	*1.21*	*1.16*	*1.38*	0.99	*1.02*	0.93	*1.36*
1.72	±0.09	±0.17	M24	*1.74*	*1.85*	1.52	1.27	1.56	1.48	1.57	1.45	1.43	1.33	1.41	1.41	1.70	*1.73*	1.60	*2.19*
0.91	±0.05	±0.09	M31	0.87	0.90	*0.92*	0.88	*1.13*	*1.11*	*1.06*	*1.14*	*1.03*	*1.05*	*1.07*	*1.12*	0.86	*0.95*	*0.93*	0.82
0.95	±0.05	±0.1	M41	*1.00*	0.87	0.86	0.88	0.91	*0.96*	*1.01*	0.88	0.85	*0.96*	0.88	0.80	*0.93*	0.91	0.87	*0.94*
0.39	±0.02	±0.04	M42	0.39	0.38	*0.44*	0.39	*0.47*	*0.46*	*0.49*	*0.55*	*0.49*	*0.47*	*0.42*	*0.48*	0.39	0.39	0.39	*0.40*

Tabla B.4: Resultados del Indicador 4 en la evaluación cuantitativa a nivel método. En las celdas de esta tabla se incluyeron los valores de la densidad de las muestras con densidad reducida (D_R). Los valores en cursiva indican donde $D^{D}_{R\,D}$ toma valores negativos.

Indicador 4: Acuerdo entre la densidad fijada y la calculada.

Indicador (I)	Descripción	Grado de cumplimiento
Acuerdo entre la densidad fijada y la calculada	Diferencia absoluta entre la densidad fijada y la calculada (D^{D}_{RDens}).	Good $\leftarrow D^{D}_{RDens} \in [0, 5\% * Dens_F)$ Improvable $\leftarrow D^{D}_{RDens} \in [5\% * Dens_F, 10\% * Dens_F)$ Poor $\leftarrow D^{D}_{RDens} \in [10\% * Dens_F, +\infty]$

Método →	RpA				SRpC				ThinData				PpC			
$\mathbf{D}_D$ →	**1.5**	**1**	**0.5**	**0.25**	**1.5**	**1**	**0.5**	**0.25**	**1.5**	**1**	**0.5**	**0.25**	**1.5**	**1**	**0.5**	**0.25**
5% $\mathbf{D}_D$ →	±0.08	±0.05	±0.03	±0.01	±0.08	±0.05	±0.03	±0.01	±0.08	±0.05	±0.03	±0.01	±0.08	±0.05	±0.03	±0.01
10% $\mathbf{D}_D$ →	±0.15	±0.1	±0.05	±0.03	±0.15	±0.1	±0.05	±0.03	±0.15	±0.1	±0.05	±0.03	±0.15	±0.1	±0.05	±0.03
M11	1.5	1.0	0.5	0.25	1.35	*1.01*	0.5	*0.252*	1.443	*1.006*	*0.508*	*0.254*	*1.534*	0.96	0.5	0.246
M12	1.5	1.0	0.5	0.25	1.33	*1.01*	*0.51*	0.248	1.454	1.0	*0.505*	*0.252*	*1.569*	0.98	*0.511*	*0.253*
M21	1.5	1.0	0.5	0.25	1.23	0.97	0.5	0.248	1.306	0.925	0.497	0.247	*1.537*	0.96	0.499	0.25
M22	1.5	1.0	0.5	*0.251*	1.26	0.99	*0.51*	*0.253*	1.403	0.973	*0.515*	*0.259*	*1.577*	0.97	*0.518*	*0.255*
M23	1.5	*1.01*	*0.504*	0.25	1.23	0.99	0.5	0.25	1.34	0.968	*0.51*	*0.261*	*1.582*	0.93	0.487	0.246
M24	1.5	1.0	0.5	0.25	1.22	0.97	0.5	0.248	1.28	0.927	*0.501*	*0.254*	*1.575*	0.93	0.48	0.243
M31	1.5	1.0	*0.503*	0.25	1.34	*1.01*	0.5	*0.251*	*1.547*	*1.042*	*0.513*	*0.254*	1.372	0.98	0.47	0.243
M41		1.0	0.5	*0.252*		0.69	0.36	0.186		0.629	0.352	0.177		1.01	0.49	0.25
M42	1.5	1.0	0.5	0.25	1.3	1.0	0.5	0.248	1.464	*1.019*	*0.51*	*0.254*	*1.554*	0.94	*0.504*	0.249

$\mathbf{D}_D$ →	**0.1**	**0.05**	**0.025**	**0.01**	**0.1**	**0.05**	**0.025**	**0.01**	**0.1**	**0.05**	**0.025**	**0.01**	**0.1**	**0.05**	**0.025**	**0.01**
5% $\mathbf{D}_D$ →	±0.005	±0.003	±0.001	±0	±0.005	±0.003	±0.001	±0	±0.005	±0.003	±0.001	±0	±0.005	±0.003	±0.001	±0
10% $\mathbf{D}_D$ →	±0.01	±0.005	±0.003	±0.001	±0.01	±0.005	±0.003	±0.001	±0.01	±0.005	±0.003	±0.001	±0.01	±0.005	±0.003	±0.001
M11	*0.101*	0.05	0.025	0.01	*0.109*	*0.053*	*0.026*	*0.011*	0.098	*0.052*	*0.028*	*0.011*	0.098	0.048	0.024	0.01
M12	0.1	0.05	0.025	0.01	*0.104*	*0.054*	*0.026*	*0.012*	0.094	*0.051*	*0.027*	*0.011*	0.1	0.049	0.024	0.01
M21	*0.101*	*0.052*	*0.026*	*0.011*	*0.106*	*0.054*	*0.026*	*0.013*	0.094	*0.053*	*0.027*	0.01	0.098	0.049	0.024	0.01
M22	0.1	0.05	0.025	0.01	*0.107*	*0.052*	*0.028*	*0.011*	0.097	*0.052*	*0.026*	*0.011*	*0.101*	*0.051*	0.025	0.01
M23	0.1	*0.051*	0.025	0.01	*0.107*	*0.053*	*0.028*	*0.013*	0.097	*0.051*	*0.026*	0.01	0.098	0.048	0.024	0.009
M24	*0.101*	0.05	*0.026*	*0.011*	*0.108*	*0.052*	*0.03*	*0.013*	0.1	0.05	*0.028*	*0.012*	0.096	0.049	0.024	0.009
M31	*0.101*	0.05	0.025	0.01	*0.106*	*0.051*	*0.028*	*0.012*	0.096	*0.051*	0.025	0.01	0.099	0.05	0.025	0.01
M41	*0.102*	*0.051*	*0.026*	0.01	0.08	0.045	0.024	*0.011*	0.069	0.038	0.021	0.009	0.1	0.05	0.025	0.01
M42	0.1	0.05	0.025	0.01	*0.103*	*0.054*	*0.027*	*0.012*	0.094	0.05	0.024	0.01	0.099	0.049	0.024	0.01

B.4 Evaluación de los modelos. Resultados cualitativos y cuantitativos.

Tabla B.5: Precisión ($Q68.3_{|\Delta h|}$ - m) de los modelos diferenciando entre los 4 métodos de reducción y las diferentes densidades de puntos, en función de la resolución, la cobertura, la penetrabilidad, la pendiente y el coeficiente de variación. Los modelos empleados para la elaboración de esta tabla fueron aquellos cuya resolución es óptima en función de la densidad de puntos, salvo en el caso del factor resolución.

	Método	*RpA*								*SRpC*								*ThinData*								*PpC*							
	Densidad	*1.5*	*1*	*0.5*	*0.25*	*0.1*	*0.05*	*0.025*	*0.01*	*1.5*	*1*	*0.5*	*0.25*	*0.1*	*0.05*	*0.025*	*0.01*	*1.5*	*1*	*0.5*	*0.25*	*0.1*	*0.05*	*0.025*	*0.01*	*1.5*	*1*	*0.5*	*0.25*	*0.1*	*0.05*	*0.025*	*0.01*
	Método	0.26	0.27	0.29	0.33	0.40	0.46	0.58	0.77	0.27	0.27	0.28	0.32	0.38	0.46	0.57	0.73	0.26	0.27	0.29	0.34	0.42	0.51	0.64	0.89	0.26	0.26	0.29	0.32	0.39	0.47	0.56	0.71
Resolución	***1***	0.01	0.03	0.08	0.15	0.28	0.43	0.59	0.96	0.01	0.02	0.07	0.14	0.28	0.43	0.57	0.85	0.00	0.03	0.09	0.18	0.36	0.52	0.75	1.02	0.01	0.03	0.07	0.14	0.27	0.43	0.59	0.84
	2	0.08	0.08	0.09	0.13	0.22	0.33	0.50	0.81	0.07	0.08	0.09	0.12	0.21	0.34	0.48	0.72	0.07	0.08	0.09	0.14	0.28	0.42	0.63	0.94	0.07	0.07	0.09	0.12	0.20	0.33	0.48	0.71
	5	0.19	0.19	0.19	0.20	0.24	0.29	0.40	0.65	0.19	0.19	0.19	0.20	0.22	0.28	0.40	0.59	0.19	0.19	0.19	0.20	0.27	0.35	0.51	0.77	0.19	0.19	0.19	0.19	0.23	0.29	0.39	0.57
	10	0.38	0.37	0.37	0.36	0.39	0.39	0.46	0.62	0.38	0.37	0.38	0.37	0.38	0.41	0.45	0.58	0.38	0.38	0.38	0.38	0.39	0.42	0.51	0.76	0.38	0.37	0.38	0.37	0.39	0.40	0.45	0.58
	15	0.54	0.52	0.53	0.53	0.54	0.53	0.58	0.68	0.54	0.53	0.53	0.52	0.52	0.52	0.60	0.70	0.54	0.53	0.54	0.54	0.55	0.54	0.62	0.84	0.54	0.52	0.53	0.52	0.52	0.53	0.56	0.67
	30	0.98	0.96	0.95	0.96	0.98	0.95	0.99	1.00	0.96	0.95	0.95	0.95	0.96	0.98	0.98	1.01	0.96	0.94	0.94	0.93	0.93	0.91	0.93	1.17	0.97	0.96	0.95	0.95	0.95	0.95	0.98	0.96
Cobertura	***Sd***	0.01	0.02	0.04	0.09	0.17	0.25	0.35	0.60	0.00	0.01	0.03	0.08	0.15	0.23	0.32	0.53	0.00	0.01	0.04	0.10	0.21	0.28	0.43	0.68	0.00	0.02	0.04	0.09	0.15	0.24	0.33	0.55
	V_{nd}	0.01	0.05	0.14	0.24	0.35	0.45	0.58	0.84	0.01	0.05	0.14	0.23	0.37	0.48	0.58	0.92	0.01	0.06	0.17	0.25	0.40	0.51	0.65	1.08	0.01	0.05	0.14	0.23	0.33	0.47	0.61	0.81
	V_{gl}	0.01	0.04	0.10	0.18	0.28	0.38	0.49	0.77	0.00	0.02	0.08	0.17	0.27	0.38	0.49	0.75	0.00	0.03	0.11	0.19	0.35	0.44	0.59	0.87	0.01	0.04	0.10	0.17	0.27	0.39	0.49	0.71
	V_{md}	0.01	0.03	0.08	0.15	0.25	0.34	0.44	0.72	0.00	0.02	0.06	0.15	0.23	0.33	0.45	0.67	0.00	0.02	0.08	0.16	0.30	0.41	0.56	0.82	0.00	0.03	0.07	0.15	0.23	0.35	0.45	0.66
	V_{pd}	0.01	0.02	0.05	0.13	0.21	0.28	0.38	0.62	0.01	0.03	0.07	0.13	0.22	0.30	0.39	0.66	0.01	0.03	0.08	0.15	0.27	0.33	0.51	0.76	0.01	0.02	0.05	0.12	0.18	0.29	0.37	0.57
	Ed	0.01	0.03	0.09	0.13	0.23	0.27	0.37	0.55	0.01	0.03	0.09	0.13	0.22	0.26	0.39	0.52	0.01	0.04	0.11	0.15	0.29	0.35	0.52	0.72	0.01	0.03	0.09	0.12	0.21	0.26	0.38	0.53
Pendiente	***Low***	0.01	0.02	0.04	0.07	0.12	0.16	0.22	0.35	0.00	0.01	0.04	0.06	0.11	0.15	0.21	0.31	0.00	0.02	0.05	0.07	0.15	0.18	0.30	0.42	0.01	0.02	0.04	0.06	0.11	0.15	0.22	0.32
	Medium	0.01	0.04	0.10	0.16	0.26	0.33	0.48	0.74	0.01	0.03	0.09	0.16	0.26	0.35	0.49	0.68	0.01	0.04	0.12	0.17	0.33	0.44	0.61	0.86	0.01	0.04	0.09	0.15	0.24	0.36	0.45	0.65
	High	0.02	0.09	0.25	0.45	0.67	0.91	1.10	1.66	0.01	0.05	0.20	0.42	0.62	0.86	1.09	1.58	0.00	0.08	0.26	0.48	0.72	0.97	1.23	1.84	0.01	0.08	0.24	0.44	0.65	0.90	1.13	1.69
CV	***Low***	0.01	0.02	0.05	0.08	0.13	0.18	0.25	0.40	0.01	0.02	0.05	0.07	0.13	0.17	0.24	0.36	0.00	0.02	0.06	0.08	0.17	0.22	0.34	0.48	0.01	0.02	0.05	0.07	0.13	0.17	0.25	0.37
	Medium	0.02	0.07	0.20	0.33	0.51	0.69	0.88	1.43	0.01	0.04	0.16	0.30	0.46	0.67	0.86	1.30	0.00	0.06	0.21	0.35	0.58	0.77	1.03	1.57	0.01	0.07	0.19	0.31	0.50	0.72	0.89	1.37
	High	0.02	0.15	0.43	0.83	1.06	1.48	1.68	2.16	0.01	0.08	0.35	0.79	1.04	1.37	1.64	2.14	0.00	0.13	0.47	0.86	1.12	1.50	1.71	2.47	0.01	0.14	0.41	0.80	1.04	1.37	1.66	2.38

Tabla B.6: Precisión ($Q95_{|\Delta h|}$ - metros) de los modelos diferenciando entre los 4 métodos de reducción y las diferentes densidades de puntos, en función de la resolución, la cobertura, la penetrabilidad, la pendiente y el coeficiente de variación. Los modelos empleados para la elaboración de esta tabla fueron aquellos cuya resolución es óptima en función de la densidad de puntos, salvo en el caso del factor resolución.

	Método	***RpA***								***SRpC***								***ThinData***								***PpC***							
	Densidad	***1.5***	***1***	***0.5***	***0.25***	***0.1***	***0.05***	***0.025***	***0.01***	***1.5***	***1***	***0.5***	***0.25***	***0.1***	***0.05***	***0.025***	***0.01***	***1.5***	***1***	***0.5***	***0.25***	***0.1***	***0.05***	***0.025***	***0.01***	***1.5***	***1***	***0.5***	***0.25***	***0.1***	***0.05***	***0.025***	***0.01***
	Método	2.08	2.02	2.04	2.06	2.27	2.40	2.80	3.40	2.03	2.03	2.05	2.10	2.21	2.36	2.68	3.23	2.04	2.02	2.03	2.14	2.26	2.55	3.00	3.97	2.06	1.99	2.06	2.09	2.25	2.35	2.74	3.42
Resolución	***1***	0.06	0.19	0.44	0.74	1.23	1.57	2.30	3.19	0.07	0.15	0.37	0.69	1.20	1.67	2.30	3.28	0.05	0.19	0.47	0.81	1.37	2.01	2.92	3.94	0.05	0.18	0.42	0.72	1.18	1.60	2.36	3.10
	2	0.44	0.46	0.52	0.71	1.10	1.37	1.98	2.89	0.44	0.43	0.50	0.66	1.05	1.39	1.90	2.83	0.43	0.46	0.55	0.75	1.16	1.62	2.48	3.55	0.44	0.45	0.53	0.67	1.04	1.39	1.86	2.86
	5	1.04	1.06	1.07	1.12	1.32	1.49	1.89	2.50	1.04	1.02	1.06	1.09	1.20	1.34	1.84	2.40	1.04	1.03	1.08	1.16	1.25	1.59	2.03	3.08	1.04	1.03	1.07	1.12	1.25	1.42	1.91	2.50
	10	1.85	1.83	1.83	1.83	2.00	2.02	2.34	2.62	1.85	1.81	1.83	1.90	1.87	2.00	2.19	2.56	1.86	1.89	1.91	1.95	1.96	2.04	2.26	3.13	1.86	1.84	1.89	1.87	1.99	1.95	2.36	2.70
	15	2.42	2.39	2.42	2.40	2.55	2.45	2.89	3.18	2.40	2.35	2.40	2.41	2.47	2.50	2.62	2.86	2.40	2.37	2.38	2.42	2.49	2.73	2.81	3.46	2.42	2.37	2.42	2.40	2.46	2.47	2.72	3.35
	30	3.90	3.85	3.91	3.86	4.13	3.87	4.27	4.46	3.93	3.91	3.89	3.91	3.93	3.93	4.26	4.32	3.93	3.87	3.92	4.00	3.95	4.06	4.39	4.73	3.91	3.87	3.88	3.83	3.82	3.72	4.27	4.58
Cobertura	***Sd***	0.03	0.11	0.37	0.69	1.04	1.54	1.83	2.75	0.03	0.07	0.27	0.63	0.98	1.49	1.90	2.58	0.02	0.11	0.39	0.74	1.14	1.62	2.07	3.38	0.03	0.10	0.32	0.66	1.01	1.49	1.89	2.84
	V_{sd}	0.12	0.36	0.66	0.91	1.33	1.76	2.16	3.06	0.16	0.31	0.60	0.88	1.32	1.65	2.15	3.00	0.12	0.37	0.70	0.98	1.33	1.78	2.19	3.23	0.11	0.36	0.64	0.89	1.25	1.77	2.39	3.30
	V_{d}	0.09	0.28	0.58	0.91	1.36	1.82	2.20	2.85	0.08	0.21	0.51	0.87	1.26	1.69	2.08	2.97	0.05	0.25	0.60	0.94	1.37	1.90	2.23	3.18	0.07	0.28	0.57	0.92	1.25	1.65	2.21	3.12
	V_{rnd}	0.06	0.24	0.55	0.96	1.37	1.90	2.24	2.97	0.06	0.17	0.45	0.91	1.26	1.74	2.15	2.87	0.04	0.23	0.62	1.05	1.47	2.08	2.52	3.43	0.04	0.22	0.51	0.90	1.29	1.69	2.30	2.94
	V_{pd}	0.05	0.19	0.44	0.91	1.26	1.87	2.03	3.15	0.14	0.24	0.54	0.95	1.32	1.83	2.33	2.69	0.10	0.33	0.69	1.10	1.44	2.26	2.56	3.70	0.04	0.17	0.45	0.89	1.16	1.75	1.99	3.05
	Ed	0.06	0.18	0.38	0.53	0.92	1.11	1.59	2.20	0.08	0.15	0.32	0.49	0.86	0.96	1.56	2.15	0.06	0.18	0.41	0.60	0.96	1.28	1.76	2.81	0.06	0.17	0.37	0.50	0.85	1.09	1.56	2.26
Pendiente	***Low***	0.03	0.07	0.17	0.24	0.45	0.57	0.86	1.43	0.05	0.07	0.17	0.23	0.43	0.51	0.89	1.34	0.03	0.09	0.21	0.27	0.59	0.74	1.21	1.94	0.03	0.07	0.17	0.21	0.40	0.54	0.85	1.29
	Medium	0.05	0.17	0.35	0.51	0.86	1.22	1.71	2.52	0.09	0.15	0.32	0.45	0.84	1.10	1.72	2.46	0.06	0.18	0.39	0.55	1.00	1.48	1.95	3.40	0.06	0.16	0.34	0.46	0.81	1.24	1.78	2.39
	High	0.15	0.48	1.00	1.45	2.06	2.72	3.37	4.00	0.16	0.37	0.86	1.42	1.90	2.46	3.11	3.95	0.11	0.48	1.10	1.56	2.11	2.88	3.42	5.43	0.13	0.46	0.94	1.42	2.11	2.49	3.28	4.20
CV	***Low***	0.03	0.09	0.19	0.27	0.50	0.64	0.99	1.63	0.05	0.09	0.19	0.26	0.48	0.60	1.01	1.51	0.04	0.10	0.23	0.31	0.64	0.85	1.32	2.11	0.03	0.08	0.19	0.25	0.44	0.65	0.96	1.47
	Medium	0.12	0.32	0.64	0.87	1.47	1.90	2.53	3.37	0.12	0.25	0.53	0.81	1.40	1.71	2.31	3.16	0.09	0.32	0.68	0.97	1.55	2.08	2.64	4.31	0.10	0.30	0.62	0.84	1.46	1.81	2.59	3.43
	High	0.24	0.90	1.57	2.30	2.79	3.80	4.45	4.91	0.29	0.70	1.49	2.27	2.78	3.53	4.31	5.05	0.19	0.89	1.76	2.37	2.84	3.98	4.63	7.86	0.19	0.86	1.58	2.29	2.95	3.57	4.36	5.26

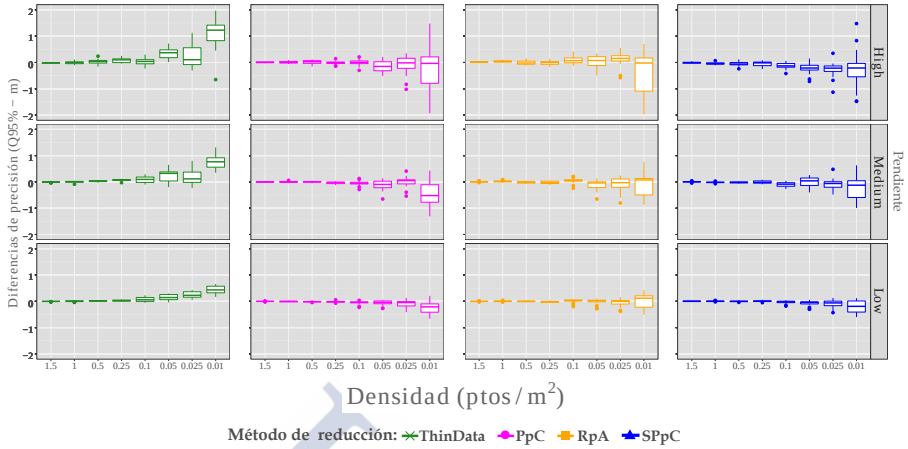

Figura B.38: Diferencias de precisión entre modelos ($Q95_{|\Delta h|}$-m) generados con nubes reducidas por diferentes métodos.

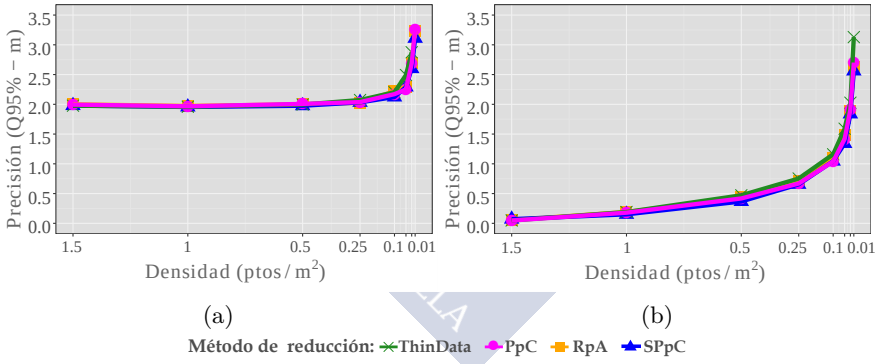

Figura B.39: Precisión de los modelos ($Q95_{|\Delta h|}$-metros) en función de la densidad y métodos de reducción: a) considerando todas las resoluciones y b) las resoluciones óptimas en función de la densidad.

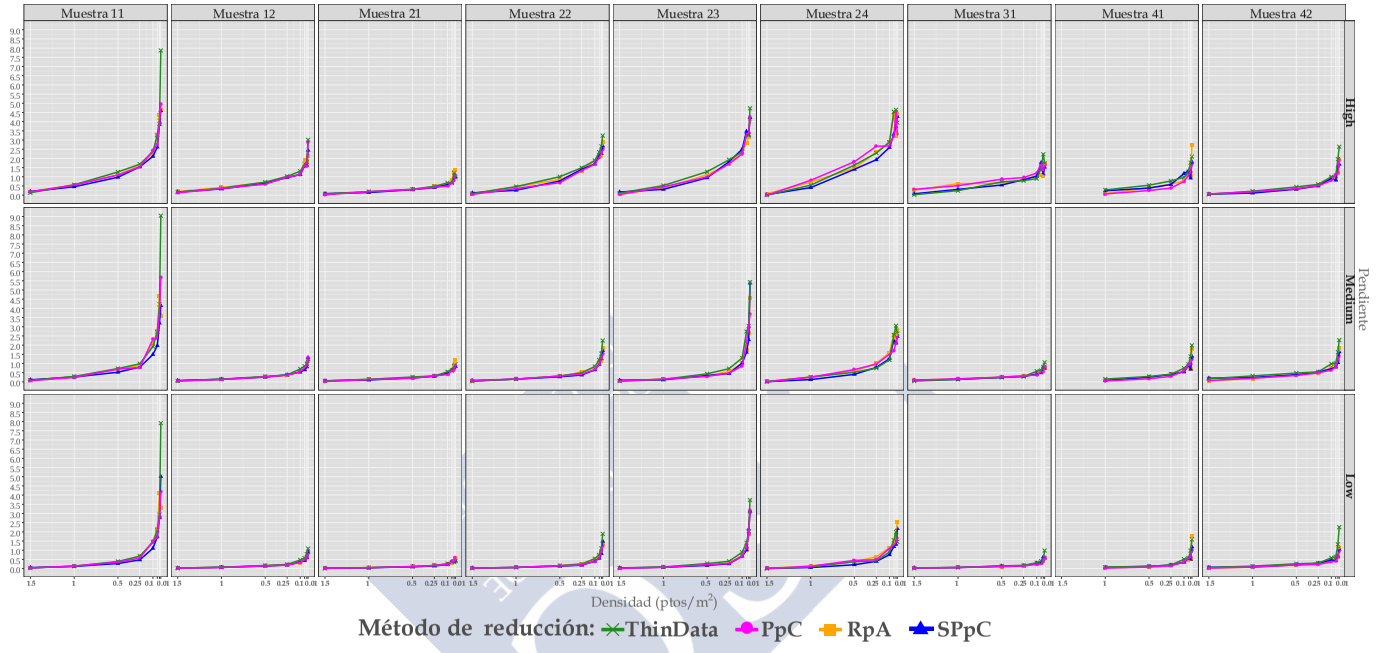

Figura B.40: Precisión general de los MDT ($Q95_{|\Delta h|}$ - m) para cada muestra en función de la densidad de puntos, el método de reducción y la pendiente de los modelos (para cada combinación de método de reducción y densidad se emplearon los modelos con la resolución óptima en relación a la densidad).

Tabla B.7: Precisión (Q68.3$_{|\Delta h|}$ - m) de los modelos diferenciando entre los 4 métodos de reducción y las diferentes densidades de puntos, en función de la pendiente y la muestra de referencia. Los modelos empleados para la elaboración de esta tabla fueron aquellos cuya resolución es óptima en función de la densidad de puntos.

Método		*RpA*								*SRpC*								*ThinData*								*PpC*							
Densidad⟶	Pendiente↓	*1.5*	*1*	*0.5*	*0.25*	*0.1*	*0.05*	*0.025*	*0.01*	*1.5*	*1*	*0.5*	*0.25*	*0.1*	*0.05*	*0.025*	*0.01*	*1.5*	*1*	*0.5*	*0.25*	*0.1*	*0.05*	*0.025*	*0.01*	*1.5*	*1*	*0.5*	*0.25*	*0.1*	*0.05*	*0.025*	*0.01*
M11	*Low*	0.01	0.02	0.07	0.12	0.30	0.49	0.71	1.08	0.00	0.02	0.05	0.12	0.29	0.44	0.62	1.14	0.00	0.02	0.08	0.14	0.45	0.56	0.95	1.42	0.01	0.03	0.07	0.13	0.30	0.42	0.67	1.23
	Medium	0.01	0.06	0.16	0.25	0.53	0.77	1.12	1.51	0.01	0.04	0.14	0.24	0.53	0.77	0.95	1.54	0.00	0.05	0.20	0.30	0.61	0.80	1.15	2.04	0.01	0.05	0.15	0.26	0.54	0.76	1.06	1.96
	High	0.03	0.12	0.32	0.56	0.81	1.13	1.48	2.07	0.01	0.07	0.25	0.49	0.76	1.05	1.31	2.05	0.00	0.09	0.31	0.57	0.82	1.14	1.41	2.31	0.02	0.11	0.31	0.52	0.81	1.12	1.47	2.28
M12	*Low*	0.01	0.02	0.05	0.07	0.11	0.16	0.20	0.32	0.00	0.02	0.04	0.06	0.10	0.14	0.18	0.27	0.00	0.02	0.05	0.07	0.13	0.16	0.24	0.33	0.01	0.02	0.04	0.06	0.11	0.15	0.19	0.30
	Medium	0.01	0.03	0.08	0.14	0.19	0.29	0.35	0.48	0.01	0.03	0.09	0.14	0.19	0.28	0.34	0.50	0.01	0.04	0.10	0.14	0.24	0.32	0.41	0.48	0.01	0.03	0.08	0.12	0.19	0.30	0.34	0.47
	High	0.02	0.07	0.20	0.32	0.43	0.64	0.83	0.87	0.01	0.06	0.17	0.37	0.42	0.59	0.64	0.97	0.01	0.08	0.21	0.37	0.53	0.67	0.73	0.98	0.01	0.07	0.17	0.35	0.44	0.62	0.65	0.93
M21	*Low*	0.00	0.02	0.04	0.06	0.08	0.11	0.18	0.16	0.00	0.01	0.03	0.05	0.07	0.12	0.13	0.17	0.00	0.01	0.03	0.05	0.09	0.12	0.13	0.19	0.00	0.01	0.03	0.05	0.08	0.12	0.16	0.20
	Medium	0.01	0.03	0.07	0.15	0.19	0.25	0.33	0.47	0.00	0.01	0.06	0.13	0.19	0.31	0.31	0.40	0.00	0.02	0.08	0.15	0.21	0.28	0.37	0.46	0.00	0.03	0.07	0.14	0.19	0.30	0.30	0.43
	High	0.01	0.03	0.11	0.22	0.26	0.42	0.45	0.65	0.00	0.02	0.09	0.17	0.26	0.39	0.47	0.56	0.00	0.03	0.10	0.19	0.29	0.37	0.50	0.52	0.00	0.04	0.09	0.19	0.22	0.37	0.38	0.59
M22	*Low*	0.01	0.02	0.04	0.07	0.13	0.17	0.23	0.39	0.00	0.01	0.03	0.06	0.11	0.15	0.19	0.33	0.00	0.01	0.04	0.07	0.16	0.20	0.25	0.47	0.00	0.02	0.04	0.06	0.10	0.15	0.22	0.43
	Medium	0.01	0.03	0.09	0.16	0.26	0.32	0.40	0.58	0.01	0.03	0.07	0.15	0.23	0.27	0.35	0.46	0.00	0.03	0.10	0.15	0.26	0.36	0.41	0.66	0.01	0.04	0.09	0.14	0.21	0.30	0.34	0.59
	High	0.01	0.06	0.22	0.40	0.57	0.74	0.81	1.09	0.00	0.03	0.15	0.38	0.48	0.71	0.84	1.00	0.00	0.05	0.22	0.38	0.60	0.84	0.96	1.28	0.01	0.05	0.17	0.39	0.52	0.67	0.82	0.97
M23	*Low*	0.00	0.02	0.05	0.08	0.18	0.23	0.60	1.07	0.00	0.01	0.04	0.06	0.15	0.24	0.68	0.82	0.00	0.02	0.06	0.09	0.31	0.45	0.85	1.22	0.00	0.02	0.05	0.07	0.18	0.28	0.54	1.03
	Medium	0.01	0.04	0.10	0.17	0.30	0.32	0.80	1.62	0.01	0.03	0.09	0.15	0.28	0.43	0.99	1.39	0.01	0.04	0.12	0.21	0.45	0.84	1.26	2.00	0.00	0.04	0.09	0.15	0.26	0.48	0.70	1.17
	High	0.01	0.07	0.23	0.47	0.76	1.02	1.25	1.91	0.01	0.05	0.19	0.49	0.73	0.99	1.42	1.62	0.00	0.08	0.31	0.60	0.90	1.16	1.47	1.95	0.00	0.08	0.25	0.48	0.73	0.96	1.45	1.85
M24	*Low*	0.00	0.02	0.06	0.10	0.33	0.37	0.54	1.23	0.00	0.01	0.04	0.07	0.17	0.28	0.48	0.70	0.00	0.01	0.07	0.11	0.28	0.36	0.48	0.83	0.00	0.02	0.06	0.10	0.24	0.32	0.65	0.53
	Medium	0.00	0.05	0.19	0.24	0.64	0.90	1.01	1.43	0.00	0.02	0.12	0.24	0.59	0.66	0.62	1.40	0.00	0.04	0.17	0.27	0.48	0.71	0.71	0.89	0.00	0.05	0.21	0.28	0.48	0.71	1.16	0.92
	High	0.00	0.11	0.34	0.67	0.99	1.32	1.36	2.15	0.00	0.04	0.25	0.57	0.87	1.17	1.33	1.83	0.00	0.07	0.33	0.68	0.94	1.60	1.87	1.86	0.00	0.10	0.35	0.70	0.82	1.13	1.47	1.56
M31	*Low*	0.01	0.02	0.04	0.05	0.08	0.11	0.13	0.20	0.01	0.02	0.04	0.05	0.08	0.10	0.13	0.14	0.00	0.02	0.04	0.06	0.10	0.11	0.15	0.21	0.01	0.02	0.04	0.05	0.08	0.09	0.13	0.17
	Medium	0.02	0.04	0.09	0.12	0.20	0.25	0.29	0.36	0.02	0.04	0.09	0.14	0.22	0.24	0.33	0.37	0.01	0.04	0.10	0.15	0.25	0.25	0.38	0.54	0.02	0.05	0.08	0.14	0.19	0.25	0.26	0.44
	High	0.03	0.15	0.24	0.32	0.41	0.48	0.47	0.69	0.01	0.05	0.17	0.30	0.37	0.63	0.51	0.67	0.00	0.06	0.22	0.29	0.37	0.56	0.83	0.80	0.05	0.13	0.29	0.39	0.47	0.67	0.51	0.70
M41	*Low*	-	0.01	0.03	0.05	0.09	0.14	0.19	0.26	-	0.01	0.03	0.05	0.09	0.12	0.15	0.23	-	0.02	0.03	0.06	0.11	0.13	0.28	0.39	-	0.01	0.03	0.04	0.07	0.12	0.14	0.33
	Medium	-	0.02	0.10	0.19	0.22	0.37	0.40	0.54	-	0.02	0.10	0.14	0.25	0.40	0.38	0.63	-	0.04	0.11	0.19	0.35	0.33	0.76	0.79	-	0.02	0.06	0.13	0.27	0.30	0.45	0.61
	High	-	0.03	0.14	0.24	0.34	0.69	0.68	1.41	-	0.05	0.14	0.19	0.36	0.68	0.52	0.98	-	0.06	0.16	0.30	0.41	0.58	1.00	1.04	-	0.01	0.10	0.16	0.39	0.67	0.65	0.94
M42	*Low*	0.01	0.02	0.05	0.07	0.13	0.14	0.18	0.30	0.01	0.02	0.06	0.07	0.13	0.14	0.20	0.29	0.01	0.03	0.07	0.08	0.16	0.18	0.36	0.43	0.01	0.02	0.05	0.07	0.12	0.12	0.23	0.23
	Medium	0.01	0.03	0.15	0.19	0.32	0.37	0.39	0.52	0.03	0.05	0.15	0.24	0.34	0.38	0.47	0.52	0.02	0.08	0.19	0.26	0.39	0.46	0.56	0.61	0.01	0.04	0.14	0.23	0.29	0.35	0.44	0.46
	High	0.01	0.06	0.16	0.24	0.42	0.41	0.58	1.10	0.01	0.03	0.14	0.23	0.39	0.43	0.67	0.81	0.01	0.06	0.19	0.29	0.52	0.52	0.94	1.23	0.01	0.06	0.16	0.23	0.40	0.54	0.51	0.99

Tabla B.8: Precisión ($Q95_{|\Delta h|}$ - metros) de los modelos diferenciando entre los 4 métodos de reducción y las diferentes densidades de puntos, en función de la pendiente y la muestra de referencia. Los modelos empleados para la elaboración de esta tabla fueron aquellos cuya resolución es óptima en función de la densidad de puntos.

Método		*RpA*								*SRpC*								*ThinData*								*PpC*							
Densidad⟶	Pendiente↓	*1.5*	*1*	*0.5*	*0.25*	*0.1*	*0.05*	*0.025*	*0.01*	*1.5*	*1*	*0.5*	*0.25*	*0.1*	*0.05*	*0.025*	*0.01*	*1.5*	*1*	*0.5*	*0.25*	*0.1*	*0.05*	*0.025*	*0.01*	*1.5*	*1*	*0.5*	*0.25*	*0.1*	*0.05*	*0.025*	*0.01*
M11	*Low*	0.04	0.14	0.35	0.66	1.45	2.17	4.10	3.30	0.06	0.12	0.28	0.48	1.11	1.73	2.77	5.02	0.04	0.13	0.39	0.68	1.43	2.10	2.94	7.92	0.04	0.14	0.35	0.57	1.49	1.71	2.79	4.18
	Medium	0.08	0.29	0.69	0.89	2.05	2.76	4.69	3.56	0.11	0.26	0.53	0.81	1.49	1.97	3.20	4.15	0.09	0.29	0.73	0.98	1.92	2.72	4.22	9.04	0.06	0.24	0.69	0.78	2.32	2.38	3.69	5.69
	High	0.20	0.57	1.11	1.61	2.26	3.22	4.35	4.63	0.19	0.46	0.98	1.54	2.11	2.62	3.85	4.59	0.13	0.56	1.26	1.69	2.36	3.28	4.05	7.87	0.18	0.54	1.10	1.54	2.43	2.74	3.91	4.96
M12	*Low*	0.03	0.08	0.15	0.20	0.33	0.48	0.68	0.89	0.03	0.07	0.14	0.20	0.36	0.43	0.59	0.91	0.03	0.08	0.17	0.23	0.47	0.57	0.79	1.09	0.03	0.06	0.15	0.19	0.34	0.47	0.61	0.82
	Medium	0.05	0.14	0.27	0.35	0.54	0.71	1.03	1.15	0.08	0.14	0.26	0.38	0.54	0.66	0.82	1.31	0.05	0.15	0.30	0.38	0.70	0.85	0.98	1.24	0.05	0.13	0.27	0.36	0.55	0.76	0.89	1.31
	High	0.20	0.42	0.69	0.98	1.13	1.89	1.85	2.12	0.17	0.34	0.65	0.96	1.12	1.58	1.65	2.44	0.16	0.38	0.71	1.02	1.30	1.70	1.81	3.01	0.13	0.36	0.60	0.98	1.11	1.62	1.58	2.86
M21	*Low*	0.03	0.06	0.12	0.17	0.25	0.31	0.40	0.57	0.02	0.04	0.10	0.15	0.22	0.38	0.37	0.43	0.01	0.05	0.11	0.17	0.27	0.36	0.36	0.42	0.02	0.05	0.11	0.17	0.23	0.37	0.38	0.58
	Medium	0.05	0.14	0.23	0.33	0.44	0.63	0.93	1.17	0.06	0.10	0.22	0.30	0.49	0.65	0.76	0.84	0.05	0.14	0.27	0.33	0.55	0.62	0.86	0.96	0.02	0.13	0.20	0.32	0.40	0.61	0.65	0.92
	High	0.06	0.18	0.31	0.49	0.59	0.81	1.28	1.35	0.08	0.14	0.30	0.41	0.57	0.70	0.98	1.01	0.07	0.19	0.32	0.48	0.67	0.65	1.21	0.97	0.02	0.19	0.30	0.43	0.50	0.67	0.79	1.12
M22	*Low*	0.03	0.06	0.16	0.28	0.54	0.69	0.85	1.38	0.03	0.06	0.14	0.19	0.40	0.56	0.82	1.49	0.02	0.06	0.16	0.24	0.54	0.74	1.10	1.89	0.03	0.07	0.15	0.20	0.40	0.58	0.92	1.25
	Medium	0.05	0.15	0.32	0.53	0.79	1.06	1.16	1.86	0.06	0.15	0.27	0.37	0.66	0.95	1.27	1.71	0.04	0.15	0.32	0.49	0.84	1.19	1.54	2.25	0.09	0.15	0.32	0.41	0.67	0.94	1.28	1.52
	High	0.09	0.46	0.85	1.34	1.87	2.08	2.16	2.89	0.12	0.27	0.77	1.41	1.69	2.15	2.27	2.67	0.09	0.46	1.01	1.49	1.89	2.34	2.66	3.24	0.04	0.36	0.68	1.34	1.68	2.05	2.30	2.48
M23	*Low*	0.02	0.08	0.21	0.30	0.71	1.07	1.86	3.10	0.04	0.07	0.18	0.26	0.68	1.01	2.15	3.13	0.03	0.09	0.28	0.40	0.89	1.41	2.04	3.73	0.01	0.07	0.21	0.28	0.65	1.15	1.87	3.16
	Medium	0.03	0.16	0.33	0.56	1.01	1.71	2.67	4.55	0.09	0.11	0.35	0.45	1.02	1.61	2.29	5.38	0.04	0.14	0.44	0.72	1.30	2.74	3.04	5.43	0.05	0.15	0.30	0.48	0.86	2.18	2.98	3.69
	High	0.05	0.39	1.11	1.70	2.33	2.84	3.19	4.12	0.17	0.32	0.94	1.82	2.50	3.47	3.24	4.23	0.11	0.52	1.28	1.92	2.36	3.26	3.26	4.73	0.03	0.45	1.00	1.70	2.23	3.36	3.38	4.25
M24	*Low*	0.02	0.14	0.38	0.64	1.14	1.32	1.83	2.53	0.01	0.06	0.21	0.39	0.76	1.20	1.32	2.18	0.00	0.09	0.37	0.42	0.90	1.55	1.99	1.46	0.00	0.13	0.45	0.48	1.10	1.27	1.44	1.66
	Medium	0.03	0.27	0.59	1.01	1.59	2.55	2.11	2.83	0.01	0.13	0.41	0.79	1.26	2.28	2.12	2.48	0.01	0.26	0.52	0.75	1.20	2.55	3.06	2.63	0.00	0.26	0.67	0.97	1.50	1.70	2.13	2.49
	High	0.08	0.71	1.47	2.33	2.88	4.41	3.21	4.44	0.03	0.41	1.41	1.93	2.60	3.32	3.74	4.28	0.01	0.54	1.63	2.29	2.88	4.54	4.64	3.95	0.00	0.81	1.82	2.66	2.68	3.23	4.56	3.31
M31	*Low*	0.04	0.06	0.11	0.16	0.27	0.32	0.44	0.60	0.04	0.06	0.14	0.16	0.29	0.31	0.63	0.58	0.02	0.07	0.15	0.18	0.32	0.41	0.53	0.98	0.04	0.06	0.11	0.15	0.23	0.27	0.38	0.60
	Medium	0.10	0.16	0.26	0.35	0.44	0.58	0.62	0.79	0.09	0.14	0.24	0.30	0.42	0.49	0.81	0.74	0.04	0.14	0.25	0.29	0.58	0.62	0.80	1.06	0.09	0.17	0.26	0.33	0.38	0.54	0.55	0.83
	High	0.26	0.63	0.64	0.86	1.05	1.12	1.06	1.71	0.07	0.32	0.55	0.84	1.03	1.77	1.15	1.52	0.02	0.25	0.73	0.79	0.90	1.45	2.23	1.73	0.32	0.52	0.87	0.96	1.20	1.71	1.32	1.66
M41	*Low*	-	0.03	0.11	0.18	0.39	0.45	0.50	1.79	-	0.07	0.12	0.19	0.35	0.55	0.51	1.18	-	0.08	0.13	0.19	0.51	0.57	0.98	1.59	-	0.03	0.08	0.15	0.36	0.56	0.61	0.99
	Medium	-	0.09	0.24	0.43	0.56	0.83	0.71	1.81	-	0.08	0.26	0.40	0.55	0.90	0.69	1.39	-	0.16	0.29	0.42	0.74	0.96	1.39	1.99	-	0.05	0.17	0.30	0.59	0.90	0.97	1.25
	High	-	0.09	0.39	0.60	0.78	1.11	1.07	2.73	-	0.24	0.39	0.58	1.18	1.31	0.93	1.81	-	0.28	0.54	0.77	0.97	1.27	1.76	2.10	-	0.07	0.25	0.39	0.75	1.07	1.25	1.71
M42	*Low*	0.03	0.08	0.20	0.25	0.45	0.46	0.64	1.14	0.07	0.10	0.21	0.29	0.47	0.43	0.67	1.05	0.06	0.14	0.26	0.30	0.58	0.64	1.32	2.25	0.03	0.09	0.20	0.23	0.37	0.41	0.65	0.94
	Medium	0.05	0.17	0.40	0.48	0.77	0.81	1.17	1.86	0.20	0.24	0.39	0.53	0.72	0.82	1.04	1.64	0.17	0.32	0.48	0.54	0.98	1.01	1.62	2.28	0.07	0.20	0.35	0.49	0.64	0.82	1.15	1.40
	High	0.07	0.16	0.36	0.56	0.93	0.88	1.23	1.92	0.05	0.12	0.32	0.50	0.91	0.82	1.58	1.68	0.05	0.22	0.45	0.59	1.00	1.06	1.96	2.64	0.07	0.19	0.35	0.51	0.80	1.11	1.22	1.91

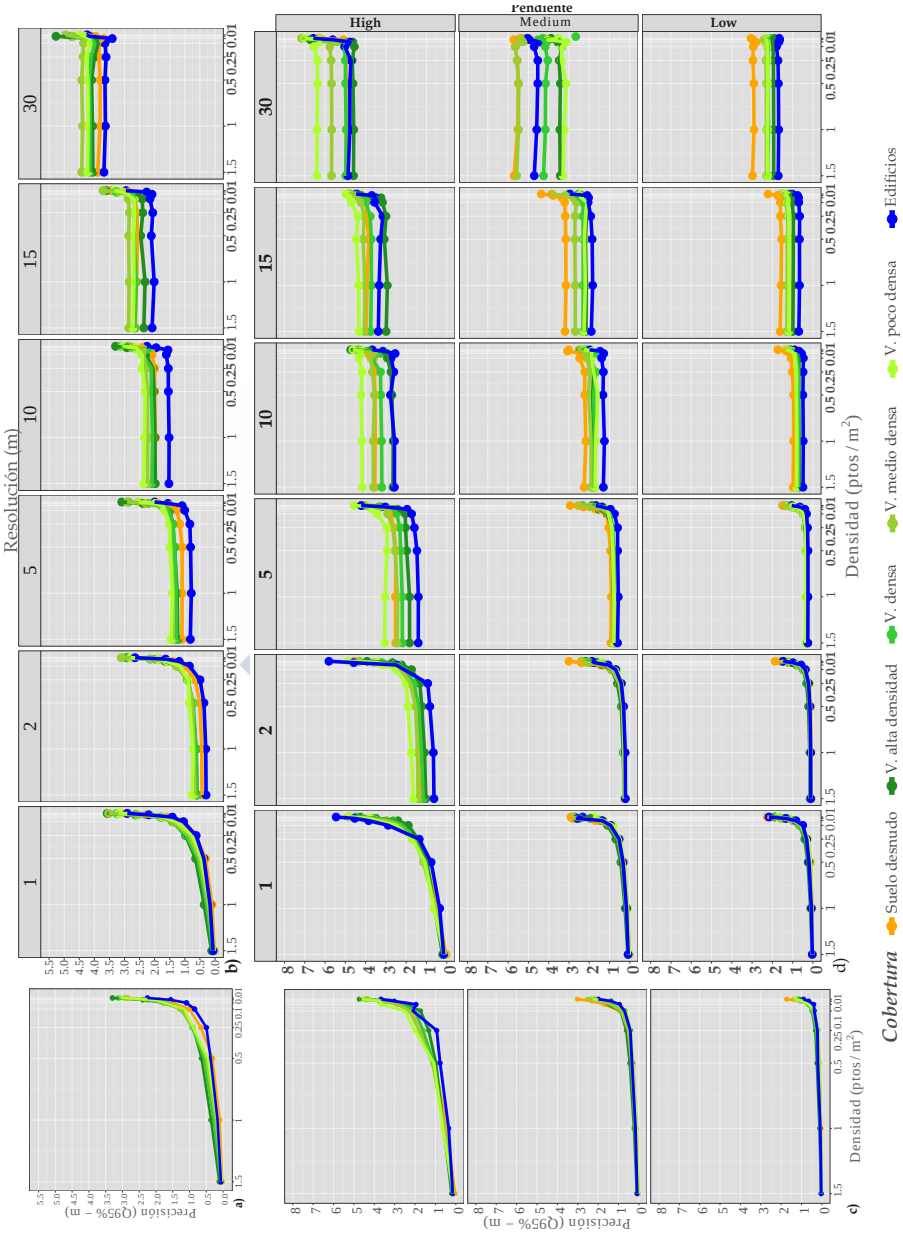

Figura B.41: Precisión de los MDT ($Q95_{|\Delta h|}$ - m) teniendo en cuenta la densidad y la cobertura (fig.sup.izq.)(resoluciones óptimas), la resolución, cobertura y la densidad (fig. sup. drch.), la pendiente, densidad y cobertura (fig.inf.izq.)(resoluciones óptimas) y adicionalmente la resolución (fig. inf. drch.).

ANEXO C

Anexos del Capítulo 3. Las coberturas del suelo

C.1 Coordenadas de los puntos de control terreno.

En la Tabla C.1 se incluyen las coordenadas de los puntos de control terreno capturados en campo por métodos topográficos. Estos datos se emplearon para validar la precisión de los MDT.

Tabla C.1: Coordenadas puntos control terreno (año 2004) (parte 1).

ID	X	Y	Z	Clase	ID	X	Y	Z	Clase	ID	X	Y	Z	Clase	ID	X	Y	Z	Clase
1	644731.93	4807900.63	310.13	Cm	2	644866.53	4807705.39	292.28	Pv	3	644598.9	4808337.59	340.7	Pv	4	644574.44	4808306.69	342.39	Pv
5	645027.61	4808524.3	459.56	Cm	6	644960.03	4808186.24	400.69	Cm	7	645055.12	4808568.64	466.56	Cm	8	644962.98	4808286.16	419.93	FO
9	644964	4808287.26	419.94	FO	10	644967.37	4808285.78	418.8	FO	11	644969.91	4808295.45	420.3	FO	12	644967.92	4808292.19	420.05	FO
13	644972.42	4808295.03	419.59	FO	14	644971.37	4808289.11	418.56	FO	15	644971.41	4808287.06	417.89	FO	16	644969.15	4808282.33	417.38	FO
17	644973.41	4808287.69	417.51	FO	18	644974.69	4808289.14	417.5	FO	19	644976.17	4808294.57	418.52	FO	20	644978.16	4808294.35	417.93	FO
21	644978.23	4808293.76	417.76	FO	22	644975.47	4808287.81	417.02	FO	23	644976.02	4808284.23	416.07	FO	24	644977.55	4808284.5	415.77	FO
25	644976.76	4808286.88	416.49	FO	26	644982.48	4808293.22	416.68	FO	27	645056.07	4808589.67	468.96	FO	28	645042.81	4808598.09	469.49	FO
29	645041.98	4808595.67	469.03	FO	30	645043.1	4808591.72	468.85	FO	31	645040.66	4808585.89	467.97	FO	32	645039.26	4808598.01	469.03	FO
33	645034.95	4808596.81	468.08	FO	34	645034.48	4808594.3	467.78	FO	35	645031.85	4808585.69	466.71	FO	36	645031.67	4808584.37	466.72	FO
37	645048.61	4808237.61	381.19	FO	38	645044.09	4808228.26	380.1	FO	39	645046.25	4808231.03	380.19	FO	40	645048.18	4808226.71	378.44	FO
41	645055.65	4808231.35	377.41	FO	42	645053.89	4808230.12	377.61	FO	43	645052.83	4808228.54	377.52	FO	44	645048.26	4808223.2	377.53	FO
45	645048.82	4808220.36	376.73	FO	46	645052.59	4808233.81	378.98	FO	47	645006.36	4808134.43	377.92	FO	48	645006.5	4808130.95	377.33	FO
49	645004.79	4808130.28	377.89	FO	50	645007.24	4808126.92	376.65	FO	51	645003.96	4808123.68	377.45	FO	52	645010.13	4808128.81	375.78	FO
53	645012.57	4808124.88	374.61	FO	54	645019.84	4808130.87	372.26	FO	55	645007.08	4808137.37	378.15	FO	56	645017.03	4808123.67	372.89	FO
57	645043.53	4808113.2	359.44	FO	58	645022.34	4808068.63	366.43	FO	59	645020.31	4808070.39	367.24	FO	60	645019.72	4808070.63	367.43	FO
61	645017.54	4808071.35	368.26	FO	62	645019.38	4808065.34	367.3	FO	63	645022.55	4808059.37	365.52	FO	64	645023.92	4808057.72	364.76	FO
65	645022.01	4808062.1	365.96	FO	66	645018.82	4808061.59	366.88	FO	67	645018.47	4808063.08	367.17	FO	68	645016.47	4808064.03	367.99	FO
69	645017.79	4808060.29	367.09	FO	70	645011.66	4808061.94	369.34	FO	71	645024.45	4808065.38	365.5	FO	72	645023.01	4808057.97	365.1	FO
73	645015.1	4808062.46	368.3	FO	74	644885.51	4807855.33	319.81	Cm	75	644913.26	4807796.66	317.14	Cm	76	644960.19	4807812.51	314.69	Cm
77	644952.08	4807799.52	311.68	FO	78	644956.82	4807787.42	307.82	FO	79	644959.56	4807788.01	307.67	FO	80	644959.86	4807791.93	308.57	FO
81	644957.97	4807795.55	309.76	FO	82	644962.84	4807792.02	308.38	FO	83	644965.65	4807801.66	310.75	FO	84	644967.45	4807794.49	308.58	FO
85	644968.38	4807790.45	307.51	FO	86	644957.66	4807799.13	310.83	FO	87	644966.74	4807802.56	310.96	FO	88	645127.79	4807910.06	309.32	FO
89	645125.4	4807914.49	311.32	Cm	90	645133.13	4807909.23	307.67	FO	91	645133.93	4807909.11	307.24	FO	92	645135.86	4807909.02	306.7	FO
93	645136.67	4807907.67	306.32	FO	94	645138.21	4807909.04	305.99	FO	95	645139.29	4807906.23	305.44	FO	96	645141.04	4807908.28	305.07	FO
97	645141.78	4807906.41	304.74	FO	98	645143.96	4807905.88	303.9	FO	99	645144.72	4807904.24	303.68	FO	100	645145.85	4807902.37	303.2	FO
101	645146.36	4807908.63	303.4	FO	102	645144.81	4807908.55	303.79	FO	103	645145.35	4807910.39	303.9	FO	104	645143.16	4807909.03	304.5	FO
105	645136.19	4807911.38	306.9	FO	106	645137.1	4807915.62	307.15	FO	107	645137.67	4807917.22	307.03	FO	108	645140.65	4807914.92	305.92	FO
109	645138.13	4807912.36	306.48	FO	110	645141.58	4807911.98	305.3	FO	111	645142.28	4807914.24	305.33	FO	112	645142.98	4807912.94	304.94	FO
113	645143.01	4807911.31	304.81	FO	114	645143.49	4807910.91	304.61	FO	115	645148.48	4807909.04	303	FO	116	645148.87	4807911.75	302.86	FO
117	645144.32	4807913.91	304.56	FO	118	645146.97	4807914.83	303.73	FO	119	645149.51	4807915.43	302.89	FO	120	645152.09	4807915.92	301.91	FO
121	645142.59	4807917.31	305.3	FO	122	645140.22	4807919.92	306.26	FO	123	645138.2	4807920.8	307.04	FO	124	645139.12	4807923.06	306.84	FO
125	645146.12	4807917.81	304.32	FO	126	645092.78	4807855.53	308.28	FO	127	645092.59	4807854.69	308.07	FO	128	645093.24	4807854.88	308.16	FO
129	645092.98	4807856.57	308.35	FO	130	645093.9	4807851.5	307.34	FO	131	645096.34	4807849.41	306.69	FO	132	645094.87	4807849.19	306.69	FO
133	645092.05	4807846.31	306.41	FO	134	645094.43	4807845.29	306.01	FO	135	645095.86	4807844.16	305.58	FO	136	645096.98	4807844.27	305.41	FO
137	645099.37	4807843.24	304.96	FO	138	645091.71	4807844.55	306.06	FO	139	645090.43	4807845.69	306.41	FO	140	645090.4	4807845.28	306.31	FO
141	645089.24	4807846.04	306.55	FO	142	645089.81	4807847.25	306.85	FO	143	645090.17	4807848.01	306.92	FO	144	645088.78	4807848.31	307.23	FO
145	645086.05	4807849.65	307.67	FO	146	645082.93	4807850.48	308.03	FO	147	645081.27	4807848.94	308.02	FO	148	645079.51	4807850.32	308.47	FO
149	645088.32	4807852.92	308.18	FO	150	645088.85	4807854.07	308.24	FO	151	645089.67	4807851.15	307.67	FO	152	645091.73	4807850.95	307.49	FO
153	645091.42	4807850.61	307.41	FO	154	645087.89	4807840.99	305.67	FO	155	645090.32	4807886.8	314.53	FO	156	645091.31	4807881.58	313.29	FO
157	645090.11	4807882.81	313.76	FO	158	645093.63	4807883.25	313.19	FO	159	645093.24	4807884.73	313.55	FO	160	645093.27	4807885.91	313.81	FO
161	645094.4	4807888.51	314.06	FO	162	645096.08	4807887.38	313.45	FO	163	645098.11	4807889.75	313.41	FO	164	645096.96	4807890.78	313.95	FO
165	645097.94	4807892.75	314.16	FO	166	645095.68	4807893.34	314.81	FO	167	645096.39	4807895.37	314.93	FO	168	645092.93	4807891.68	315.01	FO
169	645093.35	4807893.02	315.23	FO	170	645091.42	4807892.25	315.47	FO	171	645091.91	4807894.52	315.87	FO	172	645093.17	4807897.03	316.02	FO
173	645087.55	4807891.51	316.37	FO	174	645089.21	4807886.93	314.84	FO	175	645091.1	4807889.17	314.94	FO	176	645086.86	4807890.36	316.28	FO
177	645085.07	4807889.07	316.42	FO	178	645085.86	4807888.03	315.97	FO	179	645086.06	4807886.99	315.74	FO	180	645087.49	4807887.15	315.33	FO
181	645088.54	4807885.42	314.71	FO	182	645094.8	4807887.51	313.77	FO	183	645083.99	4807888.46	316.53	FO	184	645082.82	4807891.37	317.55	FO
185	645082.48	4807892.32	317.84	FO	186	645085.65	4807892.36	316.94	FO	187	645089.35	4807895.09	316.76	FO	188	645088.04	4807896.05	317.29	FO
189	645091.26	4807896.4	316.42	FO	190	645091.1	4807897.57	316.71	FO	191	645089.61	4807899.08	317.47	FO	192	645089.59	4807895.75	316.83	FO
193	645090.53	4807902.72	317.79	FO	194	645081.22	4807890.83	318.01	FO	195	645111.81	4807953.32	318.31	FO	196	645113.69	4807953.71	317.92	FO
197	645184.77	4808131.78	301.7	FO	198	645098.89	4807946.67	321.63	FO	199	645100.39	4807945.28	321.07	FO	200	645101.11	4807943.21	320.58	FO

Tabla C.2: Coordenadas puntos control terreno (año 2004) (parte 2).

ID	X	Y	Z	Clase	ID	X	Y	Z	Clase	ID	X	Y	Z	Clase	ID	X	Y	Z	Clase
201	645104.65	4807945.07	319.73	FO	202	645104.62	4807943.54	319.59	FO	203	645106.5	4807944.32	319.16	FO	204	645110.18	4807940.28	317.81	FO
205	645112.25	4807946.16	317.73	FO	206	645110.69	4807945.45	318.06	FO	207	645107.26	4807947.2	319.23	FO	208	645108.68	4807947.57	318.83	FO
209	645105.59	4807947.07	319.81	FO	210	645101.69	4807947.31	320.8	FO	211	645100.67	4807947.74	321.32	FO	212	645099.58	4807953.43	322.2	FO
213	645101.48	4807953.36	321.78	FO	214	645102.43	4807955.87	321.78	FO	215	645103.63	4807953.93	321.16	FO	216	645102.45	4807951.3	321.21	FO
217	645103.89	4807950.61	320.53	FO	218	645105.14	4807950.2	320.2	FO	219	645106.71	4807955.25	320.22	FO	220	645106.65	4807952.49	320.03	FO
221	645107.24	4807951.24	319.64	FO	222	645109.68	4807949.4	318.72	FO	223	645111.49	4807949.27	318.1	FO	224	644774.76	4807670.66	277.63	FO
225	644772.09	4807670.4	278.28	FO	226	644766.82	4807669.85	279.57	FO	227	644766.39	4807667.08	279.61	FO	228	644768.82	4807675.79	279.3	FO
229	644773.46	4807673.45	278.01	FO	230	644775.89	4807673.63	277.39	FO	231	644778.48	4807674.09	276.81	FO	232	644779.54	4807669.1	276.54	FO
233	644777	4807668.67	277.08	FO	234	644774.25	4807668.19	277.71	FO	235	644771.61	4807667.83	278.26	FO	236	644775.36	4807669.28	277.44	FO
237	644767.19	4807676.07	279.7	FO	238	644779.92	4807662.12	276.48	FO	239	644768.36	4807664.59	279.12	FO	240	644770.77	4807664.94	278.52	FO
241	644774.64	4807663.21	277.56	FO	242	644777.35	4807663.48	277.02	FO	243	644778.19	4807666.23	276.85	FO	244	644775.86	4807665.8	277.37	FO
245	644768.98	4807667.41	279.03	FO	246	644768.12	4807672.76	279.33	FO	247	644770.96	4807672.72	278.63	FO	248	644780.32	4807671.6	276.43	FO
249	644875.96	4807937.32	318.28	Cm	250	644889.21	4807862.09	319.48	Cm	251	644765.18	4807661.39	279.19	FO	252	644765.59	4807663.72	279.69	FO
253	644769.46	4807662.14	278.69	FO	254	644771.95	4807662.58	278.15	FO	255	644777.42	4807671.07	277.06	FO	256	644942.2	4808381.69	435.22	Mto
257	644949.73	4808281.11	420.25	FO	258	644971.27	4808375.85	437.14	Mto	259	644633.74	4808053.19	338.08	Pv	260	644966.11	4808291.64	420.4	FO
261	644969.44	4808290.88	419.28	FO	262	644971.53	4808294.22	419.69	FO	263	644972.23	4808296.23	419.91	FO	264	644974.63	4808294.52	418.94	FO
265	644972.85	4808292.21	418.77	FO	266	644971.46	4808289.87	418.65	FO	267	644970.39	4808283.52	417.31	FO	268	644967.72	4808283.25	418.08	FO
269	644974.53	4808284.46	416.56	FO	270	644980.07	4808293.17	417.06	FO	271	644981.43	4808291.77	416.44	FO	272	644976.76	4808288.64	416.97	FO
273	644974.96	4808279.34	415.3	FO	274	644976.56	4808282.94	415.6	FO	275	644975.44	4808278.44	415.13	FO	276	644970.51	4808292.75	419.5	FO
277	644965.26	4808285.06	419.15	FO	278	644965.97	4808288.58	419.57	FO	279	644975.12	4808286.24	416.57	FO	280	644979.71	4808289.87	416.37	FO
281	644968.78	4808296.29	420.66	FO	282	645044.13	4808588.46	468.63	FO	283	645040.98	4808589.08	468.36	FO	284	645040.15	4808587.19	468.04	FO
285	645035.22	4808587.64	467.4	FO	286	645037.08	4808593.33	468.2	FO	287	645038.72	4808599.68	469.07	FO	288	645044.13	4808586.09	468.41	FO
289	645036.14	4808599.33	468.57	FO	290	645034.26	4808594	467.76	FO	291	645032.53	4808597.47	467.79	FO	292	645033.06	4808599.5	467.99	FO
293	645029.86	4808599.16	467.52	FO	294	645049.02	4808236.49	380.71	FO	295	645042.46	4808225.62	380.13	FO	296	645047.24	4808228.36	379.12	FO
297	645048.84	4808227.94	378.66	FO	298	645051.65	4808230.17	378.3	FO	299	645054.34	4808233.3	378.26	FO	300	645047.05	4808221.74	377.68	FO
301	645050.45	4808219.01	375.98	FO	302	645051.47	4808222.06	376.26	FO	303	645055.86	4808226.23	375.87	FO	304	645045.86	4808228.97	379.77	FO
305	645052.94	4808232	378.31	FO	306	645059.6	4808230.85	375.91	FO	307	645049.04	4808238.1	381.15	FO	308	645051.89	4808236.58	379.91	FO
309	645051.85	4808235.42	379.62	FO	310	645006.97	4808135.17	377.78	FO	311	645007.36	4808135.85	377.8	FO	312	645006.81	4808129.56	377.12	FO
313	645006.01	4808129.01	377.41	FO	314	645004.36	4808128.99	377.97	FO	315	645006.17	4808125.78	376.96	FO	316	645003.04	4808123.43	377.72	FO
317	645009.57	4808134.36	376.54	FO	318	645010.45	4808130.91	375.82	FO	319	645013.28	4808131.47	374.86	FO	320	645014.74	4808129.92	374.19	FO
321	645018.86	4808127.85	372.34	FO	322	645009.21	4808126.3	375.8	FO	323	645012.16	4808124.63	374.7	FO	324	645009.27	4808125.03	375.69	FO
325	645012.92	4808121.8	373.98	FO	326	645014.09	4808123.83	373.86	FO	327	645015.07	4808123.26	373.44	FO	328	645017.62	4808123.91	372.72	FO
329	645017.36	4808124.15	372.65	FO	330	644718.8	4808011.78	320.35	Pv	331	644719.72	4808009.96	320.4	Pv	332	644535.72	4808201.44	347.92	Pv
333	644733.8	4807655.75	288.79	Mto	334	644531	4808427.97	377.88	Cm	335	645182.2	4807747.57	265.92	Pv	336	645023.03	4807716.32	278.96	Pv
337	644859.35	4807877.29	304.18	Pv	338	644840.5	4808032.93	313.91	Cm	339	644622.93	4808229.4	335.16	Pv	340	644515.95	4808508.9	405.23	FO
341	644954.39	4808290.87	421.82	Cm	342	644969.09	4808299.3	421.45	FO	343	644965.55	4808286.66	419.38	FO	344	644967.4	4808288.04	419.24	FO
345	644967.11	4808294.24	420.67	FO	346	644968.96	4808294.17	420.25	FO	347	644967.38	4808290.53	419.76	FO	348	644969.05	4808286.5	418.39	FO
349	644968.69	4808289.1	419.11	FO	350	644975.27	4808295.71	419.11	FO	351	644973.4	4808282.92	416.47	FO	352	644972.46	4808285.7	417.34	FO
353	644975.74	4808290.56	417.69	FO	354	644977.05	4808291.88	417.59	FO	355	644975.27	4808292.6	418.27	FO	356	644979.92	4808292.81	417.05	FO
357	644981.02	4808292.03	416.51	FO	358	644980.22	4808290.73	416.39	FO	359	644974.55	4808284.57	416.54	FO	360	644979.11	4808287.1	416.04	FO
361	644968.98	4808283.18	417.67	FO	362	644971.92	4808284.28	417.13	FO	363	644974.31	4808280.34	415.57	FO	364	644972.97	4808290.24	418.16	FO
365	644970.82	4808297.29	420.52	FO	366	644970.95	4808297.51	420.57	FO	367	644967.93	4808296.24	420.85	FO	368	644980.52	4808294.21	417.11	FO
369	644981.27	4808293.68	416.85	FO	370	644979.41	4808292.38	416.98	FO	371	645044.29	4808600.97	469.78	FO	372	645042.69	4808600.13	469.62	FO
373	645038.36	4808590.46	468.17	FO	374	645032.15	4808592.3	467.23	FO	375	645031.44	4808595	467.23	FO	376	645038.78	4808597.56	468.9	FO
377	645036.99	4808246.55	387.91	FO	378	645048.25	4808235.88	380.81	FO	379	645043.67	4808231.14	381.04	FO	380	645041.72	4808228.36	381.02	FO
381	645040.54	4808226.97	381.38	FO	382	645039.5	4808227.47	381.89	FO	383	645045.03	4808229.76	380.12	FO	384	645047.87	4808232.64	380.06	FO
385	645051.15	4808232.08	378.97	FO	386	645049.6	4808231.49	379.22	FO	387	645048.3	4808229.85	379.3	FO	388	645045.86	4808226.74	379.16	FO
389	645044.59	4808225.41	379.36	FO	390	645043.94	4808224.3	379.38	FO	391	645046.74	4808224.25	378.28	FO	392	645050.01	4808228.59	378.3	FO
393	645052.45	4808231.39	378.26	FO	394	645053.24	4808232.55	378.45	FO	395	645054.34	4808233.3	378.26	FO	396	645050.22	4808226.23	377.68	FO
397	645051.96	4808222.33	376.16	FO	398	645057.78	4808229.38	376.18	FO	399	645053.15	4808226.85	377	FO	400	645051.75	4808225.34	376.98	FO

Tabla C.3: Coordenadas puntos control terreno (año 2004) (parte 3).

ID	X	Y	Z	Clase	ID	X	Y	Z	Clase	ID	X	Y	Z	Clase	ID	X	Y	Z	Clase
401	645054.92	4808228.75	376.86	FO	402	645051.92	4808227.65	377.53	FO	403	645048.27	4808229.81	379.23	FO	404	645050.58	4808219.29	375.81	FO
405	645047.76	4808237.79	381.39	FO	406	645046.51	4808236.3	381.37	FO	407	645003.74	4808188.77	386.05	Mto	408	645048.49	4808239.32	381.75	FO
409	645003.26	4808140.35	379.8	FO	410	645006.97	4808135.17	377.78	FO	411	645007.52	4808132.96	377.33	FO	412	645005.51	4808132.21	377.95	FO
413	645005.3	4808127.92	377.54	FO	414	645007.66	4808125.17	376.32	FO	415	645007.26	4808123.89	376.37	FO	416	645008.48	4808123.07	375.78	FO
417	645006.76	4808122.21	376.32	FO	418	645002.18	4808123.03	378.05	FO	419	645015.12	4808131.47	374.04	FO	420	645016.43	4808130.31	373.53	FO
421	645017.44	4808129.49	373.12	FO	422	645018.52	4808131.28	372.81	FO	423	645017.46	4808131.64	373.24	FO	424	645016.65	4808132.36	373.63	FO
425	645015.36	4808127.8	373.76	FO	426	645013.1	4808126.74	374.55	FO	427	645007.77	4808128.3	376.58	FO	428	645010.79	4808121.8	374.7	FO
429	645015.15	4808122.94	373.62	FO	430	645015.69	4808121.41	373.08	FO	431	645015.09	4808120.98	373.21	FO	432	645016.76	4808120.05	372.55	FO
433	645027.16	4808065.36	364.5	FO	434	645025.66	4808067.25	365.29	FO	435	645024.44	4808068.33	365.67	FO	436	645016.71	4808070.59	368.53	FO
437	645017.46	4808066.95	368	FO	438	645025.84	4808063.55	364.89	FO	439	645021.18	4808054.05	364.99	FO	440	645022.04	4808053.33	364.73	FO
441	645022.97	4808055.6	364.68	FO	442	645020.13	4808055.65	365.68	FO	443	645019.78	4808056.34	365.9	FO	444	645020.48	4808057.2	365.87	FO
445	645020.8	4808057.52	365.84	FO	446	645019.68	4808058.03	366.18	FO	447	645020.19	4808059.08	366.16	FO	448	645019.66	4808060.34	366.49	FO
449	645018.16	4808060.83	367.03	FO	450	645017.15	4808060.89	367.29	FO	451	645015.56	4808064.54	368.33	FO	452	645011.74	4808062.81	369.35	FO
453	645012.43	4808062.7	369.05	FO	454	645012.16	4808062.59	369.29	FO	455	645012.44	4808060.84	368.93	FO	456	645017.08	4808059.15	367.14	FO
457	645017.92	4808058.03	366.73	FO	458	645020.82	4808056.05	365.51	FO	459	645021.17	4808055.79	365.56	FO	460	645010.59	4808061.9	369.59	FO
461	645017.76	4808057.46	366.67	FO	462	645017.39	4808056.88	366.72	FO	463	645016.12	4808073.22	368.94	FO	464	645028.96	4808066.53	363.95	FO
465	644880.97	4807807.62	320.86	FO	466	644954.09	4807798.75	311.19	FO	467	644954.53	4807795.16	310.07	FO	468	644953.89	4807791.93	309.26	FO
469	644962.96	4807788.07	307.36	FO	470	644957.17	4807791.59	308.77	FO	471	644961.43	4807795.27	309.43	FO	472	644960.92	4807799.28	310.62	FO
473	644966.94	4807797.86	309.61	FO	474	644969.34	4807788.29	307.04	FO	475	644954.76	4807785.34	307.38	FO	476	645059.37	4807845.84	310.85	Cm
477	645092.45	4807864.79	310.2	Cm	478	645137.34	4807909.13	306.34	FO	479	645137.67	4807907.01	305.92	FO	480	645140.88	4807907.48	305.03	FO
481	645142.65	4807905.69	304.3	FO	482	645143.54	4807904.2	303.93	FO	483	645146.5	4807905.67	303.1	FO	484	645145.68	4807906.82	303.41	FO
485	645142.5	4807908.96	304.75	FO	486	645141.09	4807909.73	305.15	FO	487	645136.77	4807913.57	306.95	FO	488	645136.22	4807915.03	307.4	FO
489	645137.98	4807919.26	307.02	FO	490	645139.82	4807917.64	306.26	FO	491	645139.95	4807915.57	306.2	FO	492	645147.23	4807911.08	303.39	FO
493	645146.64	4807912.51	303.65	FO	494	645143.31	4807915.55	305.15	FO	495	645144.49	4807916.1	304.61	FO	496	645149.39	4807913.5	302.74	FO
497	645151.21	4807914.68	302.15	FO	498	645144.76	4807918.17	304.64	FO	499	645093.09	4807853.81	307.88	FO	500	645093.75	4807852.4	307.55	FO
501	645095.22	4807851.93	307.28	FO	502	645094.92	4807850.19	306.94	FO	503	645093.68	4807847.95	306.7	FO	504	645095.04	4807846.52	306.12	FO
505	645093.64	4807844.79	306	FO	506	645097.72	4807844.97	305.46	FO	507	645098.77	4807844.13	305.18	FO	508	645099.04	4807843.63	305.04	FO
509	645095.47	4807842.02	305.09	FO	510	645093.29	4807842.35	305.31	FO	511	645091.03	4807840.87	305.38	FO	512	645090	4807842.61	305.81	FO
513	645087.62	4807848.2	307.27	FO	514	645087.62	4807847.67	307.17	FO	515	645085.3	4807845.92	307.01	FO	516	645084.93	4807846.88	307.21	FO
517	645087	4807848.86	307.47	FO	518	645085.35	4807850.45	307.83	FO	519	645084.19	4807852.23	308.39	FO	520	645083.22	4807850.82	308.15	FO
521	645082.56	4807850.89	308.21	FO	522	645087.68	4807838.24	305.15	FO	523	645089.2	4807852.77	308.03	FO	524	645091.36	4807853.88	308.08	FO
525	645091.17	4807853.07	307.97	FO	526	645089.39	4807854.99	308.41	FO	527	645089.68	4807840.38	305.39	FO	528	645091.16	4807880.2	312.95	FO
529	645090.59	4807880.94	313.26	FO	530	645089.26	4807882.61	313.82	FO	531	645094.18	4807884.6	313.29	FO	532	645094.33	4807886.48	313.67	FO
533	645092.02	4807884.96	313.87	FO	534	645092.13	4807885.97	314.13	FO	535	645090.7	4807884.55	313.98	FO	536	645092.99	4807887.4	314.1	FO
537	645092.5	4807888.81	314.4	FO	538	645093.18	4807889.42	314.5	FO	539	645097.31	4807888.38	313.45	FO	540	645099.95	4807890.88	313.4	FO
541	645096.96	4807890.78	313.95	FO	542	645095.7	4807892.37	314.55	FO	543	645094.5	4807891.39	314.61	FO	544	645094	4807890.99	314.6	FO
545	645091.33	4807893.76	315.83	FO	546	645092.69	4807896.08	315.95	FO	547	645089.68	4807893	316.2	FO	548	645089.25	4807893.4	316.32	FO
549	645089.01	4807893.97	316.51	FO	550	645088.26	4807893.13	316.49	FO	551	645088.33	4807889.99	315.69	FO	552	645088.54	4807888.66	315.34	FO
553	645089.35	4807888.04	315.13	FO	554	645090.87	4807890.61	315.26	FO	555	645087.24	4807886.18	315.18	FO	556	645083.66	4807889.55	316.92	FO
557	645084.71	4807890.96	317.03	FO	558	645085.97	4807894.14	317.28	FO	559	645084.19	4807894.25	317.78	FO	560	645085.3	4807895.5	317.81	FO
561	645087.34	4807896.98	317.66	FO	562	645087.23	4807898.41	317.88	FO	563	645089.07	4807897.42	317.31	FO	564	645090.53	4807895.7	316.51	FO
565	645090.98	4807898.02	316.93	FO	566	645090.35	4807900.83	317.64	FO	567	645092.13	4807899.26	316.84	FO	568	645092.11	4807899.71	316.88	FO
569	645093.91	4807898.28	316.11	FO	570	645100.85	4807891.23	313.34	FO	571	645111.51	4807950.85	318.2	FO	572	645111.55	4807952.49	318.34	FO
573	645099.98	4807957	322.46	FO	574	645128.79	4807985.17	312.24	FO	575	645110.54	4807939.04	317.5	FO	576	645097.28	4807942.59	321.74	FO
577	645098.17	4807942.7	321.43	FO	578	645099.07	4807945.37	321.46	FO	579	645102.19	4807945.3	320.59	FO	580	645104.3	4807945.37	319.83	FO
581	645105.72	4807943.25	319.34	FO	582	645108.25	4807944.4	318.62	FO	583	645109.11	4807943.97	318.34	FO	584	645110.41	4807941.68	317.73	FO
585	645106.95	4807941.31	318.8	FO	586	645111.03	4807947.51	318.11	FO	587	645108.32	4807946.07	318.57	FO	588	645107.88	4807946.91	319.03	FO
589	645105.3	4807946.62	319.77	FO	590	645107	4807948.6	319.2	FO	591	645103.71	4807947.53	320.45	FO	592	645103.21	4807947.39	320.59	FO
593	645100.71	4807947.73	321.31	FO	594	645100.52	4807949.29	321.49	FO	595	645099.91	4807950.99	322.06	FO	596	645102.08	4807955.32	321.76	FO
597	645100.61	4807956.06	322.15	FO	598	645103.65	4807955.87	321.13	FO	599	645103.95	4807952.56	320.92	FO	600	645103.51	4807949.37	320.68	FO

Tabla C.4: Coordenadas puntos control terreno (año 2004) (parte 4).

ID	X	Y	Z	Clase	ID	X	Y	Z	Clase	ID	X	Y	Z	Clase	ID	X	Y	Z	Clase
601	645105.46	4807952.62	320.57	FO	602	645105.53	4807955.01	320.56	FO	603	645105.8	4807953.86	320.46	FO	604	645106.58	4807949.92	319.88	FO
605	645108.06	4807951.85	319.47	FO	606	645107.85	4807954.03	319.71	FO	607	645108.87	4807954.3	319.33	FO	608	645110.24	4807953.28	318.93	FO
609	645109.06	4807951.3	319	FO	610	645110.24	4807949.4	318.68	FO	611	645046.76	4808234.01	380.79	FO	612	645045.94	4808222.83	378.24	FO
613	645159.05	4808159.28	318.1	FO	614	645158.39	4808157.72	317.69	FO	615	645157.4	4808158.45	318.3	FO	616	645161.57	4808157.72	316.68	FO
617	645160.76	4808157.47	316.79	FO	618	645159.43	4808156.46	317	FO	619	645160.06	4808156.23	316.58	FO	620	645161.22	4808156.36	316.35	FO
621	645161.99	4808156.18	316.02	FO	622	645162.38	4808155.41	315.73	FO	623	645163.58	4808155.66	315.42	FO	624	645162.41	4808154.14	315.34	FO
625	645164.57	4808154.47	314.8	FO	626	645163.67	4808152.81	314.42	FO	627	645164.66	4808152.79	314.1	FO	628	645165.53	4808152.15	313.81	FO
629	645166.42	4808153.04	313.79	FO	630	645166.78	4808153.7	314.01	FO	631	645168.57	4808152.64	313.28	FO	632	645168.98	4808152.83	313.34	FO
633	645168.88	4808151.99	313.03	FO	634	645166.85	4808150.63	312.92	FO	635	645166.67	4808150.54	312.98	FO	636	645165.98	4808149.34	312.65	FO
637	645166.88	4808148.12	312.18	FO	638	645166.78	4808148.42	312.22	FO	639	645164.92	4808147.46	312.39	FO	640	645164.69	4808148.37	312.69	FO
641	645164.87	4808150.04	313.24	FO	642	645163.91	4808150.52	313.75	FO	643	645163.28	4808149.72	313.52	FO	644	645163.28	4808148.43	313.17	FO
645	645161.73	4808152.49	314.78	FO	646	645160.91	4808151.3	314.84	FO	647	645160.7	4808151.56	314.93	FO	648	645159.27	4808152.33	315.62	FO
649	645160.43	4808153.39	315.45	FO	650	645161.57	4808154.23	315.47	FO	651	645158.81	4808155.11	316.71	FO	652	645157.95	4808156.18	317.35	FO
653	645157.52	4808155.6	317.31	FO	654	645158.43	4808154.77	316.75	FO	655	645154.52	4808153.21	317.92	FO	656	645154.71	4808151.1	317.26	FO
657	645153.45	4808149.18	317.3	FO	658	645153.5	4808148.43	317.2	FO	659	645153.67	4808147.46	316.74	FO	660	645152.25	4808147.74	317.4	FO
661	645150.89	4808146.9	317.87	FO	662	645150.61	4808146.82	317.98	FO	663	645155.3	4808146.76	315.86	FO	664	645156.86	4808150.81	316.19	FO
665	645158.32	4808151.18	315.69	FO	666	645156.52	4808148.41	315.63	FO	667	645157.22	4808148.66	315.47	FO	668	645158.55	4808147.54	314.56	FO
669	645160.81	4808148.59	314	FO	670	645159.54	4808146.57	314	FO	671	645159.41	4808145.61	313.8	FO	672	645158.33	4808144.3	313.69	FO
673	645158.2	4808143.18	313.5	FO	674	645161.13	4808146.7	313.39	FO	675	645162.34	4808147.35	313.06	FO	676	645162.81	4808146.31	312.66	FO
677	645161.75	4808144.77	312.52	FO	678	645161.64	4808143.25	312.17	FO	679	645161.27	4808142.15	312.03	FO	680	645163.82	4808143.27	311.42	FO
681	645163.31	4808144.13	311.84	FO	682	645164.82	4808144.46	311.46	FO	683	645162.07	4808140.02	311.18	FO	684	645158.43	4808160.18	318.44	FO
685	645141.92	4808153.86	323.9	Cm	686	645129.45	4808160.62	329.62	FO	687	645127.56	4808162.09	330.69	FO	688	645128.98	4808162.72	330.24	FO
689	645129.66	4808162.68	329.95	FO	690	645129.9	4808163.67	330.15	FO	691	645129.81	4808164.4	330.35	FO	692	645132.15	4808164.7	329.49	FO
693	645127.14	4808163.68	331.17	FO	694	645124.62	4808164.15	332.33	FO	695	645124.9	4808165.56	332.57	FO	696	645125.73	4808165.83	332.3	FO
697	645126.59	4808167.42	332.36	FO	698	645127.6	4808165.84	331.53	FO	699	645128.68	4808167.4	331.53	FO	700	645130	4808166.79	330.92	FO
701	645132.14	4808166.46	329.92	FO	702	645131.74	4808168.45	330.61	FO	703	645131.49	4808169.84	331.1	FO	704	645132.13	4808170.94	331.03	FO
705	645133.56	4808169.42	330.17	FO	706	645135.56	4808171.89	330.07	FO	707	645136.28	4808172.5	330.04	FO	708	645136.05	4808172.86	330.18	FO
709	645132.87	4808174.04	331.54	FO	710	645132.55	4808172.72	331.35	FO	711	645133.34	4808174.75	331.58	FO	712	645132.11	4808174.78	331.99	FO
713	645132	4808175.84	332.31	FO	714	645130.4	4808173.22	332.23	FO	715	645128.93	4808173.49	332.88	FO	716	645130.32	4808175.98	333.05	FO
717	645129.64	4808175.72	333.18	FO	718	645128.61	4808175.24	333.42	FO	719	645129.23	4808177.95	333.91	FO	720	645127.38	4808176.99	334.43	FO
721	645127.69	4808179.18	334.65	FO	722	645126.89	4808178.77	334.98	FO	723	645125.9	4808177.16	334.95	FO	724	645125.67	4808179.91	335.74	FO
725	645124.52	4808178.37	335.85	FO	726	645123.56	4808176.87	335.8	FO	727	645125.67	4808175.49	334.6	FO	728	645126.51	4808173.3	333.87	FO
729	645125.26	4808172.37	334.02	FO	730	645127.72	4808172.64	333.14	FO	731	645128.3	4808170.86	332.47	FO	732	645130.11	4808170.42	331.74	FO
733	645128.39	4808169.69	332.21	FO	734	645127.6	4808169.67	332.43	FO	735	645127.24	4808170.96	332.9	FO	736	645125.49	4808168.31	332.99	FO
737	645123.9	4808168.18	333.55	FO	738	645123.56	4808167.32	333.47	FO	739	645122.24	4808166.85	333.8	FO	740	645120.98	4808166.8	334.38	FO
741	645119.93	4808167.3	334.93	FO	742	645119.17	4808168.29	335.39	FO	743	645118.3	4808168.31	335.71	FO	744	645120.22	4808169.57	335.32	FO
745	645119.35	4808169.91	335.65	FO	746	645121.56	4808171.34	335.16	FO	747	645122.99	4808171.35	334.65	FO	748	645122.76	4808172.27	334.94	FO
749	645117.43	4808168.29	336.04	FO	750	645126.11	4808180.87	335.9	FO	751	645137.5	4808173.23	329.69	FO	752	645123.05	4808174.77	335.44	FO
753	645125.19	4808170.02	333.45	FO	754	644954	4807830.19	320.48	Mto	755	644954.51	4807831.96	321.02	Mto	756	644955.38	4807831.14	320.5	Mto
757	644956.43	4807832.29	320.66	Mto	758	644954.86	4807834.63	321.71	Mto	759	644952.47	4807834.35	321.97	Mto	760	644952.34	4807836.29	322.51	Mto
761	644954.2	4807836.9	322.49	Mto	762	644953.96	4807837.45	322.61	Mto	763	644951.05	4807838.78	323.62	Mto	764	644952.38	4807839.84	323.73	Mto
765	644954.84	4807839.69	323.11	Mto	766	644949.17	4807841.89	324.94	Mto	767	644948.36	4807843.24	325.52	Mto	768	644952.09	4807841.53	324.26	Mto
769	644953.9	4807844.99	324.86	Mto	770	644954.5	4807842.11	323.88	Mto	771	644956.77	4807842.72	323.73	Mto	772	644957.1	4807840.18	323.03	Mto
773	644956.8	4807838.15	322.53	Mto	774	644956.99	4807835.58	321.66	Mto	775	644958.33	4807836.55	321.64	Mto	776	644958.95	4807835.58	321.3	Mto
777	644960.84	4807836.26	321.28	Mto	778	644962.9	4807835.9	320.72	Mto	779	644962.89	4807836.58	320.99	Mto	780	644963.94	4807834.99	320.41	Mto
781	644962.28	4807834.15	320.3	Mto	782	644960.23	4807833.33	320.48	Mto	783	644958.64	4807832.54	320.5	Mto	784	644965.25	4807835.3	320.3	Mto
785	644964.52	4807837.64	321.12	Mto	786	644965.77	4807837.64	320.94	Mto	787	644963.23	4807839.84	321.85	Mto	788	644962.02	4807838.5	321.66	Mto
789	644964.5	4807840.77	321.92	Mto	790	644964.06	4807843.29	322.73	Mto	791	644961.31	4807841.42	322.62	Mto	792	644963.17	4807844.81	323.35	Mto
793	644960.02	4807841.97	322.92	Mto	794	644962.29	4807846.45	323.92	Mto	795	644960.17	4807846.38	324.32	Mto	796	644962.28	4807848.22	324.41	Mto
797	644957.99	4807845.95	324.53	Mto	798	644956.04	4807844.99	324.51	Mto	799	644958.81	4807841.1	323.02	Mto	800	644960.52	4807838.79	322.05	Mto

Tabla C.5: Coordenadas puntos control terreno (año 2004) (parte 5).

ID	X	Y	Z	Clase	ID	X	Y	Z	Clase	ID	X	Y	Z	Clase	ID	X	Y	Z	Clase
801	644959.01	4807837.9	321.97	Mto	802	644958.52	4807843.14	323.54	Mto	803	644968.21	4807834.29	319.75	Mto	804	644883.1	4807728.15	299.94	FO
805	644882.93	4807729.21	300.2	FO	806	644881.12	4807731.42	300.59	FO	807	644878.09	4807734.47	300.91	FO	808	644879.59	4807735.24	301.27	FO
809	644880.28	4807736.04	301.51	FO	810	644881.14	4807734.6	301.25	FO	811	644881.71	4807733.89	301.11	FO	812	644882.38	4807731.9	300.73	FO
813	644883.67	4807730.26	300.45	FO	814	644884.56	4807728.79	300.18	FO	815	644885.32	4807728.2	300.06	FO	816	644886.09	4807727.5	299.94	FO
817	644888.93	4807728.89	300.44	FO	818	644887.23	4807729.22	300.44	FO	819	644885.87	4807729.75	300.39	FO	820	644886.26	4807730.96	300.69	FO
821	644886.57	4807731.94	301.06	FO	822	644884.61	4807733.42	301.22	FO	823	644883.66	4807733.79	301.26	FO	824	644882.09	4807734.87	301.35	FO
825	644877.31	4807737.56	301.37	FO	826	644878.7	4807737.48	301.63	FO	827	644879.15	4807738.4	301.92	FO	828	644880.68	4807739.16	302.3	FO
829	644882.35	4807738.11	302.25	FO	830	644885.1	4807735.53	301.72	FO	831	644885.57	4807734.91	301.71	FO	832	644887.25	4807733.62	301.42	FO
833	644887.22	4807733.11	301.33	FO	834	644887.86	4807730.3	300.67	FO	835	644888.8	4807730.79	300.76	FO	836	644889.48	4807731.13	300.85	FO
837	644890.94	4807731.69	300.99	FO	838	644889.1	4807732.5	301.26	FO	839	644887.9	4807733.55	301.42	FO	840	644889.02	4807734.24	301.58	FO
841	644889.83	4807733.57	301.49	FO	842	644890.77	4807733.34	301.38	FO	843	644892.59	4807733.5	301.47	FO	844	644890.44	4807734.63	301.62	FO
845	644889.68	4807735.09	301.76	FO	846	644888.95	4807735.76	301.94	FO	847	644887.31	4807736.9	302.15	FO	848	644885.79	4807738.4	302.45	FO
849	644883.29	4807738.97	302.44	FO	850	644882.52	4807740.79	302.92	FO	851	644885.25	4807741.15	303.09	FO	852	644886.39	4807740.75	303.02	FO
853	644887.19	4807740.11	302.91	FO	854	644888.46	4807738.73	302.77	FO	855	644888.48	4807739.95	302.98	FO	856	644889.16	4807740.41	303.08	FO
857	644889.61	4807738.92	302.83	FO	858	644891.05	4807738.52	302.66	FO	859	644890.63	4807737.51	302.38	FO	860	644891.56	4807736.06	302.03	FO
861	644892.5	4807736.15	302.11	FO	862	644892.39	4807734.31	301.64	FO	863	644893.57	4807736.34	302.18	FO	864	644894.76	4807734.89	301.77	FO
865	644896	4807735.87	302.02	FO	866	644893.66	4807737.58	302.45	FO	867	644891.07	4807740.46	303.13	FO	868	644889.02	4807742.16	303.5	FO
869	644885.84	4807743.55	303.79	FO	870	644885.41	4807746.05	304.36	FO	871	644885.58	4807725.29	299.65	FO	872	644875.26	4807736.07	300.86	FO
873	644956.66	4807703.33	284.4	FO	874	644946.1	4807719.75	289.76	FO	875	644945.83	4807721.14	290.26	FO	876	644944.84	4807724.59	291.4	FO
877	644946.28	4807726.82	291.84	FO	878	644945.11	4807728.43	292.58	FO	879	644944.4	4807727.97	292.61	FO	880	644944.27	4807727.42	292.39	FO
881	644943.65	4807729.94	293.35	FO	882	644942.97	4807730.5	293.62	FO	883	644942.37	4807730.46	293.7	FO	884	644944.16	4807731.45	293.67	FO
885	644943.08	4807732.33	294.12	FO	886	644942.92	4807732.97	294.35	FO	887	644943.36	4807733.71	294.48	FO	888	644944.64	4807734.63	294.5	FO
889	644945.57	4807733.74	294.1	FO	890	644945.09	4807732.69	293.9	FO	891	644945.09	4807731.69	293.61	FO	892	644945.83	4807731.11	293.29	FO
893	644947.59	4807730.98	293.03	FO	894	644948.94	4807730.9	292.86	FO	895	644948.41	4807729.81	292.52	FO	896	644949.88	4807730.38	292.56	FO
897	644948.45	4807727.68	291.9	FO	898	644949.29	4807728.29	291.96	FO	899	644947.91	4807725.76	291.43	FO	900	644949.59	4807725.38	291.15	FO
901	644949.55	4807725.97	291.35	FO	902	644950.02	4807722.47	290.15	FO	903	644950.93	4807722.14	289.89	FO	904	644952.19	4807722.88	290.07	FO
905	644953.31	4807723.75	290.24	FO	906	644954.61	4807723.17	289.93	FO	907	644955.4	4807724.38	290.12	FO	908	644959.9	4807725.01	289.86	FO
909	644954.06	4807725.82	290.76	FO	910	644952.77	4807725.99	290.94	FO	911	644951.73	4807725.79	291.08	FO	912	644950.67	4807728.3	291.85	FO
913	644952.44	4807727.92	291.57	FO	914	644951.37	4807728.85	292.01	FO	915	644953.36	4807728.79	291.75	FO	916	644952.46	4807729.46	291.99	FO
917	644951.88	4807731.15	292.55	FO	918	644951	4807731.11	292.64	FO	919	644949.59	4807733.15	293.41	FO	920	644947.82	4807733.43	293.72	FO
921	644948.67	4807735.7	294.26	FO	922	644949.65	4807736.43	294.47	FO	923	644951.27	4807736.31	294.19	FO	924	644953	4807736.81	294.11	FO
925	644954.07	4807737.28	294.16	FO	926	644955.02	4807737.41	294.24	FO	927	644955.43	4807738.63	294.55	FO	928	644954.04	4807736.46	293.86	FO
929	644954.28	4807736.01	293.72	FO	930	644955.25	4807735.08	293.34	FO	931	644953.38	4807734.89	293.47	FO	932	644952.75	4807734.03	293.29	FO
933	644951.93	4807733.41	293.25	FO	934	644951.8	4807733.56	293.26	FO	935	644949.83	4807734.5	293.76	FO	936	644953.9	4807732.51	292.77	FO
937	644954.18	4807733.19	292.94	FO	938	644954.35	4807733.54	293.02	FO	939	644954.87	4807733.27	292.96	FO	940	644955.48	4807733.43	292.87	FO
941	644956.03	4807734.78	293.19	FO	942	644956.31	4807734.14	293	FO	943	644957.19	4807733.16	292.6	FO	944	644953.16	4807731.25	292.52	FO
945	644954.12	4807730.51	292.21	FO	946	644955.09	4807731.24	292.3	FO	947	644955.92	4807730.79	292.09	FO	948	644954.37	4807729.69	291.9	FO
949	644954.1	4807727.35	291.17	FO	950	644954.8	4807728.61	291.49	FO	951	644955.44	4807728.51	291.44	FO	952	644956.43	4807728.57	291.34	FO
953	644955.6	4807729.5	291.79	FO	954	644957.72	4807730.89	291.94	FO	955	644958.52	4807727.08	290.65	FO	956	644958.82	4807725.5	290.1	FO
957	644956.94	4807726.71	290.73	FO	958	644955.26	4807726.71	290.94	FO	959	644959.6	4807725.41	289.97	FO	960	644957.86	4807725.34	290.11	FO
961	644956.49	4807725.11	290.23	FO	962	644947.63	4807721.86	290.28	FO	963	644941.02	4807733.49	294.65	FO	964	645068.11	4807722.65	275.42	Pv
965	645067.43	4807734.73	279.83	FO	966	645067.56	4807736.05	280.17	FO	967	645068.66	4807736.45	280.36	FO	968	645070.06	4807735.45	280	FO
969	645071.59	4807737.45	280.54	FO	970	645069.24	4807738.67	280.96	FO	971	645068	4807739.32	281.22	FO	972	645067.38	4807740.63	281.76	FO
973	645067.15	4807741.34	281.98	FO	974	645070.9	4807740.71	281.45	FO	975	645072.74	4807739.03	280.98	FO	976	645072.1	4807741.12	281.61	FO
977	645072.43	4807742.04	281.83	FO	978	645070.15	4807741.95	281.98	FO	979	645070.21	4807742.4	281.99	FO	980	645068.98	4807741.67	281.85	FO
981	645068.08	4807743.03	282.31	FO	982	645066.44	4807743.34	282.54	FO	983	645067.34	4807744.52	282.77	FO	984	645065.31	4807744.41	282.8	FO
985	645069.38	4807743.88	282.48	FO	986	645071.56	4807745.12	282.67	FO	987	645069.28	4807746.01	283.17	FO	988	645065.96	4807746.57	283.44	FO
989	645065.91	4807746.99	283.5	FO	990	645065.72	4807748.36	283.85	FO	991	645073.08	4807741.84	281.76	FO	992	645065.04	4807749.16	284.09	FO
993	645066.07	4807749.19	284.1	FO	994	645067.84	4807748.36	283.83	FO	995	645069.3	4807748.55	283.7	FO	996	645070.99	4807749.41	283.96	FO
997	645070.55	4807747.97	283.61	FO	998	645071.94	4807747.75	283.42	FO	999	645073.61	4807747.56	283.27	FO	1000	645072.75	4807748.94	283.64	FO

Tabla C.6: Coordenadas puntos control terreno (año 2004) (parte 6).

ID	X	Y	Z	Clase	ID	X	Y	Z	Clase	ID	X	Y	Z	Clase	ID	X	Y	Z	Clase
1001	645073.76	4807749.51	283.6	FO	1002	645074.65	4807749.14	283.51	FO	1003	645076.53	4807749.03	283.15	FO	1004	645077.02	4807748.77	283.15	FO
1005	645077.76	4807748.72	283.03	FO	1006	645078.68	4807749.42	282.81	FO	1007	645080.26	4807751.12	284.12	FO	1008	645080.32	4807747.75	282.66	FO
1009	645075.86	4807746.8	283.03	FO	1010	645078.55	4807747.6	283.02	FO	1011	645077.88	4807747.82	283.06	FO	1012	645079.39	4807747.17	282.98	FO
1013	645077.4	4807746.56	282.91	FO	1014	645076.23	4807745.39	282.77	FO	1015	645074.45	4807745.15	282.68	FO	1016	645074.32	4807746.5	283.04	FO
1017	645072.38	4807745.96	282.87	FO	1018	645073.08	4807744.38	282.44	FO	1019	645074.91	4807743.49	282.2	FO	1020	645075.11	4807742.04	281.8	FO
1021	645075.26	4807741.81	281.67	FO	1022	645076.51	4807742.96	282.04	FO	1023	645077.79	4807743.79	282.09	FO	1024	645078.29	4807742.23	281.64	FO
1025	645078.48	4807742.78	281.83	FO	1026	645078.97	4807742.4	281.61	FO	1027	645081	4807742.44	281.65	FO	1028	645078.4	4807741.14	281.38	FO
1029	645079.2	4807740.69	281.2	FO	1030	645077.7	4807740.12	281.33	FO	1031	645075.48	4807739.27	280.87	FO	1032	645076.11	4807738.37	280.69	FO
1033	645075.17	4807737.68	280.61	FO	1034	645077.58	4807738.79	280.74	FO	1035	645077.97	4807738.93	280.74	FO	1036	645079.08	4807738.89	280.71	FO
1037	645078.59	4807736.91	280.11	FO	1038	645076.79	4807736.22	279.96	FO	1039	645077.1	4807735.97	280.07	FO	1040	645082.26	4807736.07	279.78	FO
1041	645073.78	4807735.87	279.93	FO	1042	645073.49	4807736.07	279.98	FO	1043	645075.09	4807735.44	279.73	FO	1044	645081.67	4807737.17	280.21	FO
1045	645081.42	4807738.86	280.45	FO	1046	645080.89	4807738.8	280.41	FO	1047	645080.5	4807740.36	280.92	FO	1048	645080.93	4807744.93	282.36	FO
1049	645079.12	4807745.73	282.57	FO	1050	644644.64	4808314.09	354.2	FO	1051	644653.43	4808377.54	361.53	FO	1052	644670.77	4808280.25	360.17	FO
1053	644665.23	4808379.98	366.84	FO	1054	644667.07	4808379.7	367.66	FO	1055	644667.27	4808377.9	367.71	FO	1056	644669.51	4808378.94	368.81	FO
1057	644669.59	4808378.66	368.8	FO	1058	644669.6	4808376.83	368.81	FO	1059	644671.98	4808378.17	370.13	FO	1060	644671.7	4808375.82	369.93	FO
1061	644669.24	4808374.99	368.58	FO	1062	644671.74	4808373.92	369.81	FO	1063	644667.08	4808376.14	367.52	FO	1064	644666.26	4808372.63	367.09	FO
1065	644668.02	4808372.29	368.01	FO	1066	644669.8	4808372.2	368.88	FO	1067	644669.52	4808370.18	368.71	FO	1068	644671.26	4808371.17	369.47	FO
1069	644672.7	4808371.26	370.32	FO	1070	644674.25	4808370.71	371.01	FO	1071	644673.06	4808369.17	370.29	FO	1072	644671.33	4808369.76	369.42	FO
1073	644668.13	4808370.24	368	FO	1074	644666.19	4808371.07	366.9	FO	1075	644666	4808369.08	366.87	FO	1076	644667.97	4808368.42	367.78	FO
1077	644669.83	4808368.23	368.63	FO	1078	644671.6	4808367.6	369.55	FO	1079	644670.04	4808366	368.69	FO	1080	644666.31	4808366.77	366.89	FO
1081	644668.2	4808366.13	367.7	FO	1082	644666.55	4808365.49	366.96	FO	1083	644673.66	4808367.46	370.5	FO	1084	644675.29	4808366.68	371.23	FO
1085	644674.8	4808368.37	371.08	FO	1086	644677.11	4808367.64	372.1	FO	1087	644677.44	4808369.7	372.58	FO	1088	644678.38	4808368.76	373.14	FO
1089	644678.57	4808366.68	372.82	FO	1090	644675.83	4808369.58	371.62	FO	1091	644674.36	4808372.99	371.04	FO	1092	644672.78	4808380.2	370.45	FO
1093	644674.88	4808379.03	371.54	FO	1094	644676.08	4808379	372.2	FO	1095	644674.61	4808377.21	371.45	FO	1096	644674.42	4808375.12	371.24	FO
1097	644676.58	4808375.01	372.4	FO	1098	644676.7	4808377.3	372.53	FO	1099	644679.18	4808375.05	373.55	FO	1100	644676.74	4808381.63	372.48	FO
1101	644679.03	4808382.08	373.84	FO	1102	644679.96	4808366.11	373.41	FO	1103	644666.22	4808365.14	366.83	FO	1104	644729.07	4808305.88	379.51	FO
1105	644729.01	4808305.34	379.41	FO	1106	644723.56	4808300.94	376.89	FO	1107	644725.11	4808301.67	377.79	FO	1108	644726.66	4808299.36	377.31	FO
1109	644726.71	4808302.47	378.26	FO	1110	644728.08	4808301.54	378.2	FO	1111	644727.89	4808303.79	378.71	FO	1112	644730.37	4808304.26	379.38	FO
1113	644731.2	4808308.44	380.82	FO	1114	644734.37	4808305.95	380.87	FO	1115	644734.19	4808304.52	380.5	FO	1116	644736.86	4808306.48	381.62	FO
1117	644734.87	4808303.05	380.26	FO	1118	644733.19	4808302.2	379.58	FO	1119	644732.01	4808300.62	378.93	FO	1120	644731.28	4808298.77	378.17	FO
1121	644729.47	4808300.35	378.05	FO	1122	644728.38	4808298.86	377.56	FO	1123	644733.14	4808298.06	378.33	FO	1124	644734.22	4808296.05	378.07	FO
1125	644735.45	4808297.75	378.93	FO	1126	644737.77	4808298.8	379.7	FO	1127	644736.53	4808300.35	379.95	FO	1128	644738.05	4808301.66	380.66	FO
1129	644737.44	4808303.25	380.88	FO	1130	644741.83	4808301.51	381.5	FO	1131	644735.13	4808301.59	379.9	FO	1132	644732.82	4808311.87	382.2	FO
1133	644743.42	4808301.32	381.86	FO	1134	644736.7	4808293.68	378.09	FO	1135	645193.17	4807758.01	264.93	Pv	1136	645153.98	4807771.61	276.84	FO
1137	645151.79	4807765.96	276.11	FO	1138	645152.34	4807769.26	276.93	FO	1139	645152.32	4807772.51	277.53	FO	1140	645152.06	4807771.19	277.32	FO
1141	645153.33	4807774.94	277.85	FO	1142	645152.78	4807774.82	277.96	FO	1143	645152.64	4807774.36	277.91	FO	1144	645152.12	4807773.95	277.98	FO
1145	645152.02	4807775.19	278.17	FO	1146	645151.52	4807774.23	278.37	FO	1147	645150.73	4807770.08	277.31	FO	1148	645150.86	4807769	277.04	FO
1149	645150.05	4807768.09	277.13	FO	1150	645148.9	4807766.76	277.02	FO	1151	645149.01	4807769.66	277.68	FO	1152	645149.37	4807771.87	278.14	FO
1153	645147.73	4807769.76	278.16	FO	1154	645146.96	4807768.51	277.96	FO	1155	645146.37	4807767.4	277.8	FO	1156	645145.58	4807767.34	277.92	FO
1157	645145.71	4807769.34	278.41	FO	1158	645146.98	4807769.33	278.09	FO	1159	645146.46	4807770.27	278.46	FO	1160	645146.82	4807771.52	278.97	FO
1161	645150.28	4807775.43	278.61	FO	1162	645150.69	4807776.7	278.91	FO	1163	645149.41	4807775.78	278.96	FO	1164	645148.81	4807774.84	279.06	FO
1165	645145.73	4807772.64	279.27	FO	1166	645145.43	4807771.42	278.99	FO	1167	645144.46	4807771.15	279.1	FO	1168	645143.91	4807769.94	278.95	FO
1169	645144.06	4807767.72	278.45	FO	1170	645142.4	4807769.07	279.12	FO	1171	645142.03	4807769.94	279.45	FO	1172	645144.47	4807772.68	279.57	FO
1173	645145.75	4807775.17	279.87	FO	1174	645146.37	4807776.16	279.93	FO	1175	645146.2	4807778.12	280.32	FO	1176	645145.29	4807776.13	280.16	FO
1177	645145.24	4807775.36	280.02	FO	1178	645144.03	4807775.69	280.44	FO	1179	645143.8	4807775.08	280.31	FO	1180	645142.83	4807773.54	280.17	FO
1181	645141.53	4807771.79	280.01	FO	1182	645140.71	4807772.07	280.36	FO	1183	645138.45	4807771.64	280.93	FO	1184	645140.39	4807775.23	281.06	FO
1185	645140.17	4807776.3	281.51	FO	1186	645141.72	4807779.32	281.86	FO	1187	645143.4	4807777.23	280.97	FO	1188	645137.12	4807768.64	280.55	FO
1189	645141.7	4807780.68	282.18	FO	1190	645157.29	4807777.35	277.37	FO	1191	644578.56	4808470.45	378.7	Mto	1192	644622.78	4808534.55	394.15	FO
1193	644631.36	4808538.17	394.06	FO	1194	644623.88	4808545.54	397.08	FO	1195	644625.83	4808543.51	396.3	FO	1196	644627.69	4808541.04	395.42	FO
1197	644629.59	4808538.76	394.38	FO	1198	644627.37	4808535.33	393.6	FO	1199	644625.16	4808532.98	392.99	FO	1200	644623.65	4808532.06	392.84	FO

Tabla C.7: Coordenadas puntos control terreno (año 2004) (parte 7).

ID	X	Y	Z	Clase	ID	X	Y	Z	Clase	ID	X	Y	Z	Clase	ID	X	Y	Z	Clase
1201	644619.4	4808534	394.31	FO	1202	644617.66	4808536	395.12	FO	1203	644615.97	4808537.89	395.7	FO	1204	644613.62	4808539.83	396.42	FO
1205	644616.6	4808540.88	396.5	FO	1206	644618.35	4808539.78	395.99	FO	1207	644619.9	4808537.51	395.23	FO	1208	644621.58	4808535.78	394.59	FO
1209	644624.72	4808534.85	393.99	FO	1210	644621.89	4808539.63	395.61	FO	1211	644620.15	4808541.67	396.36	FO	1212	644618.23	4808543.24	397.01	FO
1213	644620.49	4808545.28	397.37	FO	1214	644622.13	4808543.81	396.79	FO	1215	644623.8	4808541.82	396.07	FO	1216	644625.23	4808539.96	395.36	FO
1217	644622.44	4808549.53	398.43	FO	1218	644529.04	4808211.04	349.95	Mto	1219	644548.52	4808188.08	346.38	Ed	1220	644542.22	4808189.84	346.99	Ed
1221	644533.24	4808192.22	347.83	Ed	1222	644532.25	4808188.82	348.07	Ed	1223	644528.72	4808190.18	348.3	Ed	1224	644523.03	4808192.15	349.28	Ed
1225	644524.99	4808199.16	348.73	Ed	1226	644522.15	4808201.72	350.86	Ed	1227	644520.48	4808183.73	348.85	Ed	1228	644526.21	4808182.21	347.95	Ed
1229	644526.16	4808181.33	347.79	Ed	1230	644531.5	4808179.69	347.56	Ed	1231	644531.87	4808180.57	347.63	Ed	1232	644539.71	4808177.56	347.18	Ed
1233	644546.95	4808176.72	346.61	Ed	1234	644522.59	4808196.72	349.03	Ed	1235	644520.56	4808198.48	350.16	Ed	1236	644580.33	4808074.98	342.76	Ed
1237	644554.03	4808094.88	342.65	Ed	1238	644545.81	4808092.51	344.22	Ed	1239	644541.92	4808090.43	344.98	Ed	1240	644539.46	4808081.12	348.15	Ed
1241	644535.12	4808079.78	349.27	Ed	1242	644537.91	4808071.58	349.18	Ed	1243	644542.3	4808072.26	348.24	Ed	1244	644539.71	4808069.3	349.05	Ed
1245	644584.34	4808058.53	343.18	Ed	1246	644543.7	4808071.23	348.13	Ed	1247	644546.41	4808077.95	346.81	Ed	1248	644542.16	4808072.14	349	Ed
1249	644559.88	4808070.92	345.83	Ed	1250	644596.76	4808074.58	340.44	Ed	1251	644591.28	4808069.36	341.84	Ed	1252	644585.73	4808066.8	342.9	Ed
1253	644589.13	4808046.34	343.07	Ed	1254	644587.46	4808054.45	342.76	Ed	1255	644587.15	4808058.15	343.01	Ed	1256	644595.11	4808063.23	342.25	Ed
1257	644600.62	4808058.77	342.55	Ed	1258	644593.76	4808054.59	342.66	Ed	1259	644595.1	4808052.1	341.87	Ed	1260	644591.18	4808048.77	342.53	Ed
1261	644592.8	4808045.9	342.34	Ed	1262	644583.18	4808063.92	343.59	Ed	1263	644591.17	4808040.35	342.56	Ed	1264	644591.27	4808028.96	342.47	Ed
1265	644590.45	4808036.54	342.58	Ed	1266	644581.32	4808035.59	343.87	Ed	1267	644582.58	4808030.23	343.89	Ed	1268	644611.06	4808055.74	340.17	Ed
1269	644625.9	4808063.36	338.18	Ed	1270	644607.42	4808061.89	339.94	Ed	1271	644633.72	4808053.15	337.96	Pv	1272	644975.74	4808290.56	417.69	FO
1273	644975.12	4808286.24	416.57	FO	1274	645056.95	4808227.97	375.95	FO	1275	645017.03	4808123.67	372.89	FO	1276	645017.39	4808056.88	366.72	FO
1277	645139.12	4807923.06	306.84	FO	1278	645170.12	4808152.37	313.15	FO	1279	644874.34	4807689.75	291.21	Mto	1280	644878.44	4807727.77	299.41	FO
1281	644883.79	4807668.58	284.4	FO	1282	644882.8	4807669.47	284.61	FO	1283	644882.1	4807670.32	284.7	FO	1284	644882.08	4807672.71	284.99	FO
1285	644880.46	4807672.21	284.77	FO	1286	644877.8	4807678.33	285.84	FO	1287	644877.08	4807680.15	286.3	FO	1288	644877.04	4807678.32	285.8	FO
1289	644875.41	4807677.25	285.18	FO	1290	644874.14	4807677.2	284.85	FO	1291	644872.52	4807678.42	284.83	FO	1292	644869.32	4807676.43	283.23	FO
1293	644871.64	4807674.96	283.42	FO	1294	644873.24	4807673.39	283.36	FO	1295	644874.92	4807671.64	283.42	FO	1296	644877.91	4807672.84	284.39	FO
1297	644879.28	4807671.35	284.43	FO	1298	644878.2	4807670.97	284.25	FO	1299	644877.76	4807670.89	284.07	FO	1300	644879.91	4807669.12	284.2	FO
1301	644882.06	4807668.36	284.24	FO	1302	644883.13	4807667.96	284.27	FO	1303	644879.47	4807666.2	283.76	FO	1304	644879.9	4807668.15	284.09	FO
1305	644879.31	4807667.83	284.11	FO	1306	644878.75	4807668.09	283.82	FO	1307	644877.66	4807668.41	283.51	FO	1308	644877.05	4807670.43	283.92	FO
1309	644876.61	4807670.5	283.94	FO	1310	644874.33	4807670.25	282.91	FO	1311	644872.37	4807669.05	281.99	FO	1312	644873.76	4807668.17	282.29	FO
1313	644874.95	4807669.32	282.78	FO	1314	644875.7	4807666.38	282.63	FO	1315	644875.9	4807664.11	282.43	FO	1316	644875.45	4807664.58	282.38	FO
1317	644874.08	4807663.6	281.79	FO	1318	644872.91	4807664.58	281.31	FO	1319	644872.21	4807666.11	281.02	FO	1320	644871.89	4807667.29	281.41	FO
1321	644871.1	4807666.84	281.06	FO	1322	644870.04	4807665.66	280.46	FO	1323	644872.11	4807664.93	281.07	FO	1324	644872.89	4807663.43	281.35	FO
1325	644872.6	4807662.7	281.09	FO	1326	644872.18	4807662.46	280.95	FO	1327	644871.92	4807661.65	280.7	FO	1328	644884.66	4807668.68	284.36	FO
1329	644876.99	4807681.4	286.72	FO	1330	644865.2	4807674.25	281.15	FO										

Tabla C.8: Coordenadas puntos control terreno (año 2010) (parte 1).

ID	X	Y	Z	Clase	ID	X	Y	Z	Clase	ID	X	Y	Z	Clase	ID	X	Y	Z	Clase
1331	645100.07	4807956.99	322.3	FO	1332	645110.59	4807939.07	317.14	FO	1333	645097.44	4807942.67	321.35	FO	1334	645113.76	4807953.67	317.45	FO
1335	645114.33	4807951.03	317.01	FO	1336	645110.99	4807946.34	317.74	FO	1337	645108.82	4807944.04	318.12	FO	1338	645105.87	4807945	319.13	FO
1339	645108.21	4807947.6	318.75	FO	1340	645108.75	4807950.32	318.8	FO	1341	645105.7	4807951.07	319.82	FO	1342	645104.56	4807949.49	319.97	FO
1343	645100.75	4807945.48	320.68	FO	1344	645103.69	4807942.8	319.5	FO	1345	645109.31	4807940.38	317.68	FO	1346	644952.22	4807799.48	311.33	FO
1347	644954.79	4807785.36	307.05	FO	1348	644966.79	4807802.61	310.64	FO	1349	644969.32	4807788.28	306.61	FO	1350	644968.23	4807790.91	307.37	FO
1351	644965.73	4807793.63	308.25	FO	1352	644962.2	4807796.25	309.23	FO	1353	644959.14	4807796.27	309.48	FO	1354	644955.84	4807794.39	309.39	FO
1355	644954.27	4807793.72	309.38	FO	1356	644956.44	4807797	310.09	FO	1357	644958.77	4807797.39	309.92	FO	1358	644964.21	4807799.54	310.05	FO
1359	644965.02	4807789.23	307.17	FO	1360	644958.46	4807786.87	307.15	FO	1361	645133.17	4807909.32	307.37	FO	1362	645153	4807916.36	301.37	FO
1363	645139.16	4807923.11	306.59	FO	1364	645145.98	4807902.32	302.96	FO	1365	645139.12	4807919.72	306.45	FO	1366	645143.93	4807919.43	304.79	FO
1367	645146.81	4807917.23	303.68	FO	1368	645141.76	4807911.53	305.01	FO	1369	645138	4807913.86	306.41	FO	1370	645142.32	4807911	304.74	FO
1371	645137.43	4807915.02	306.65	FO	1372	645146.52	4807915.83	303.75	FO	1373	645143.9	4807916.14	304.63	FO	1374	645140.72	4807917.08	305.77	FO
1375	645139.69	4807917.13	306.1	FO	1376	644781.15	4807676.5	276.06	FO	1377	644764.99	4807676.18	280.15	FO	1378	644780	4807662.3	276.21	FO
1379	644764.96	4807661.68	279.52	FO	1380	644769.61	4807663.64	278.48	FO	1381	644768.07	4807666.2	278.93	FO	1382	644769.84	4807669.16	278.54	FO
1383	644772.81	4807667.49	277.76	FO	1384	644774.81	4807665.1	277.29	FO	1385	644777.8	4807665.33	276.66	FO	1386	644777.51	4807669.49	276.63	FO
1387	644775.51	4807669.99	277.24	FO	1388	644779.28	4807673.41	276.35	FO	1389	644771.48	4807667.02	278.11	FO	1390	644768.95	4807668.89	278.75	FO
1391	644568.94	4808544.92	404.5	FO	1392	644559.06	4808554.85	409.45	FO	1393	644568.71	4808564.2	410.9	FO	1394	644579.78	4808554.86	406.12	FO
1395	644576.5	4808554.6	406.53	FO	1396	644572.18	4808557.54	408.17	FO	1397	644569.7	4808559.89	409.32	FO	1398	644567.79	4808559.33	409.38	FO
1399	644565.37	4808557.49	409.19	FO	1400	644562.79	4808555.15	408.89	FO	1401	644565.43	4808554.1	408.1	FO	1402	644568.38	4808554.32	407.63	FO
1403	644571.47	4808554.77	407.4	FO	1404	644572.43	4808553.32	406.67	FO	1405	644568.11	4808550.67	406.51	FO	1406	644570.8	4808549.69	405.72	FO
1407	645022.24	4808053.32	364.61	FO	1408	645009.4	4808060.5	369.66	FO	1409	645016.09	4808073.26	369.04	FO	1410	645029.02	4808066.54	364.01	FO
1411	645027.08	4808063.35	364.52	FO	1412	645025.23	4808061.47	364.84	FO	1413	645024.24	4808059.7	365.01	FO	1414	645024.24	4808062.81	365.33	FO
1415	645021.49	4808061.86	366.05	FO	1416	645018.7	4808062.07	367.03	FO	1417	645020.41	4808064.74	366.75	FO	1418	645017.91	4808065.17	367.63	FO
1419	645016.38	4808067.71	368.41	FO	1420	645013.94	4808060.23	368.25	FO	1421	645016.13	4808058.39	367.35	FO	1422	644963.05	4808286.23	419.56	FO
1423	644975.56	4808278.34	414.66	FO	1424	644982.58	4808293.41	416.12	FO	1425	644969.22	4808299.21	421.13	FO	1426	644969.26	4808295.56	420.15	FO
1427	644969.74	4808292.2	419.23	FO	1428	644968.29	4808287.8	418.57	FO	1429	644969.19	4808285.58	417.85	FO	1430	644971.29	4808283.46	416.84	FO
1431	644972.95	4808286.32	417.01	FO	1432	644974.2	4808289.35	417.44	FO	1433	644973.25	4808293.84	418.77	FO	1434	644976.3	4808292.03	417.53	FO
1435	644976.04	4808288.56	416.76	FO	1436	644974.08	4808286.02	416.64	FO	1437	644548.22	4808523.29	401.52	FO	1438	644537.31	4808532.67	406.52	FO
1439	644546.75	4808542.99	408.15	FO	1440	644558.06	4808534.39	403.2	FO	1441	644552.73	4808534.6	404.23	FO	1442	644548.74	4808536.41	405.68	FO
1443	644546.7	4808538.95	406.82	FO	1444	644542.81	4808536.41	406.73	FO	1445	644545.06	4808534.25	405.64	FO	1446	644547.29	4808534.3	405.21	FO
1447	644547.89	4808531.59	404.19	FO	1448	644546.91	4808528.81	403.51	FO	1449	644549.36	4808527.44	402.58	FO	1450	644551.43	4808530.49	403.19	FO
1451	644551.13	4808532.9	404.06	FO	1452	645120.4	4807887.01	307.77	FO	1453	645118.3	4807882.92	307.66	FO	1454	645119.82	4807880.47	307.05	FO
1455	645120.9	4807885.03	307.42	FO	1456	645123.9	4807885.58	306.88	FO	1457	645126.94	4807885.76	306.19	FO	1458	645126.19	4807888.51	306.64	FO
1459	645126.54	4807882.75	305.99	FO	1460	645123.62	4807882.39	306.59	FO	1461	645121.97	4807880.53	306.61	FO	1462	645122.67	4807878.15	306.19	FO
1463	645114.76	4807878.84	307.87	FO	1464	645121.24	4807892.19	308.27	FO	1465	645134.07	4807886	304.65	FO	1466	645127.19	4807871.02	304.32	FO
1467	644872.03	4807661.61	280.34	FO	1468	644865.28	4807674.36	280.82	FO	1469	644877.2	4807681.59	287.2	FO	1470	644884.73	4807668.53	283.91	FO
1471	644876.53	4807678.82	285.4	FO	1472	644874.06	4807676.71	284.29	FO	1473	644873.39	4807674.12	283.26	FO	1474	644878.45	4807671.95	283.92	FO
1475	644880.24	4807672.77	284.39	FO	1476	644875.69	4807669.39	282.68	FO	1477	644874.39	4807666.86	281.82	FO	1478	644872.3	4807665.3	280.76	FO
1479	644875.05	4807663.68	281.64	FO	1480	644876.48	4807666.11	282.47	FO	1481	644879.29	4807666.97	283.39	FO	1482	645129.71	4808160.37	329.32	FO
1483	645117.64	4808168.57	335.92	FO	1484	645126.15	4808180.78	335.67	FO	1485	645137.55	4808173.25	329.59	FO	1486	645134.53	4808172.22	330.36	FO
1487	645131.56	4808169.57	330.91	FO	1488	645129.08	4808167.41	331.27	FO	1489	645127.02	4808168.35	332.31	FO	1490	645125.49	4808171.18	333.53	FO
1491	645127.65	4808173.75	333.28	FO	1492	645128.13	4808177.36	334.04	FO	1493	645124.7	4808175.28	334.8	FO	1494	645124.19	4808172.11	334.28	FO
1495	645124.34	4808169.81	333.61	FO	1496	645126.09	4808167.08	332.34	FO	1497	645091.22	4807880.23	312.69	FO	1498	645081.14	4807890.69	317.61	FO
1499	645090.81	4807902.72	317.45	FO	1500	645100.9	4807891.19	313.03	FO	1501	645098.01	4807891.43	313.55	FO	1502	645095.45	4807889.15	313.68	FO
1503	645093.73	4807892.06	314.65	FO	1504	645093.08	4807889.09	314.12	FO	1505	645093.73	4807885.88	313.4	FO	1506	645091.52	4807888.13	314.44	FO
1507	645090	4807886.55	314.28	FO	1508	645086.57	4807888.03	315.51	FO	1509	645086.01	4807891.82	316.51	FO	1510	645086.76	4807894.16	316.89	FO
1511	645090.69	4807883.07	313.4	FO	1512	645079.49	4807850.36	308.13	FO	1513	645087.78	4807838.33	304.85	FO	1514	645092.49	4807856.68	308.1	FO
1515	645099.45	4807843.23	304.59	FO	1516	645084.48	4807847.36	307.13	FO	1517	645086.29	4807844.12	306.15	FO	1518	645090.52	4807844.7	305.86	FO
1519	645089.47	4807843.18	305.69	FO	1520	645093.12	4807844.59	305.64	FO	1521	645096.51	4807844.55	305.27	FO	1522	645093.19	4807847.99	306.35	FO
1523	645089.51	4807847.75	306.7	FO	1524	645085.52	4807847.42	306.97	FO	1525	645082.32	4807848.69	307.49	FO	1526	645083.99	4807847.43	307.13	FO
1527	645065.18	4807749.2	283.97	FO	1528	645080.41	4807751.16	284.14	FO	1529	645067.51	4807734.65	279.72	FO	1530	645082.19	4807736.2	279.73	FO

Tabla C.9: Coordenadas puntos control terreno (año 2010) (parte 2).

ID	X	Y	Z	Clase	ID	X	Y	Z	Clase	ID	X	Y	Z	Clase	ID	X	Y	Z	Clase
1531	645073.84	4807740.95	281.38	FO	1532	645074.43	4807738.03	280.53	FO	1533	645069.62	4807736.05	280.08	FO	1534	645069.67	4807741.03	281.58	FO
1535	645069.61	4807744.68	282.64	FO	1536	645075.04	4807744.36	282.28	FO	1537	645066.56	4807746.34	283.21	FO	1538	645076.05	4807747.16	282.98	FO
1539	645075.54	4807740.48	281.17	FO	1540	645073.37	4807735.62	279.85	FO	1541	645072.32	4807736.56	280.15	FO	1542	644945.77	4807719.53	289.49	FO
1543	644960.87	4807725.14	289.46	FO	1544	644955.7	4807738.8	294.13	FO	1545	644940.19	4807733.44	294.53	FO	1546	644946.79	4807720.61	289.68	FO
1547	644945.84	4807726.29	291.5	FO	1548	644955.01	4807731.65	292.14	FO	1549	644954.05	4807725.93	290.51	FO	1550	644952.89	4807719.1	288.46	FO
1551	644959.52	4807722.21	288.74	FO	1552	644957.02	4807723.16	289.26	FO	1553	644680.12	4808366.21	372.87	FO	1554	644666.41	4808365.02	366.56	FO
1555	644679.19	4808382.08	373.42	FO	1556	644665.26	4808380.01	366.34	FO	1557	644667.24	4808375.78	367.24	FO	1558	644669.55	4808377	368.4	FO
1559	644671.53	4808378	369.43	FO	1560	644673.46	4808374.87	370.34	FO	1561	644675.6	4808373.15	371.32	FO	1562	644677.43	4808372.31	372.13	FO
1563	644672.94	4808371.39	369.99	FO	1564	644670.75	4808370.76	368.85	FO	1565	644671.25	4808367.95	368.98	FO	1566	644669.48	4808369.49	368.01	FO
1567	644668.46	4808367.55	367.52	FO	1568	644723.65	4808300.91	376.62	FO	1569	644736.76	4808293.68	377.81	FO	1570	644743.48	4808301.32	381.61	FO
1571	644732.88	4808311.85	381.85	FO	1572	644732.62	4808307.92	380.47	FO	1573	644735.22	4808305.72	380.45	FO	1574	644738.78	4808302.81	380.54	FO
1575	644739.15	4808300.61	380.18	FO	1576	644737.33	4808299.99	379.48	FO	1577	644734.9	4808302.39	379.56	FO	1578	644732.22	4808303.9	379.24	FO
1579	644730.08	4808305.13	379.02	FO	1580	644728.87	4808301.92	378.03	FO	1581	644731.41	4808299.81	377.92	FO	1582	644733.24	4808298.45	377.98	FO
1583	645029.3	4808584.2	466.2	FO	1584	645029.31	4808601.18	467.48	FO	1585	645044.4	4808584.16	468.32	FO	1586	645044.43	4808601.21	469.85	FO
1587	645037.06	4808586.1	467.61	FO	1588	645031.91	4808587.29	466.98	FO	1589	645034.81	4808590.74	467.74	FO	1590	645035.63	4808595.68	468.3	FO
1591	645011.15	4808574.09	461.95	FO	1592	645013.37	4808565.16	462.11	FO	1593	645010.53	4808558.84	461.21	FO	1594	645018.01	4808557.24	462.42	FO
1595	645022.68	4808551.89	462.58	FO	1596	645025.22	4808556.91	463.49	FO	1597	645022.83	4808560.78	463.45	FO	1598	645031.25	4808557.86	464.3	FO
1599	645040.2	4808553.64	464.68	Mto	1600	645043.58	4808559.93	465.75	Mto	1601	645041.84	4808566.93	466.47	Mto	1602	645035.03	4808565.56	465.63	Mto
1603	644612.65	4808539.7	396.21	FO	1604	644622.74	4808529.7	391.65	FO	1605	644622.49	4808549.61	398.13	FO	1606	644632.23	4808540.26	394.36	FO
1607	644626.72	4808541.29	395.39	FO	1608	644622.39	4808542.11	396	FO	1609	644620.37	4808536.32	394.7	FO	1610	644625.48	4808539.25	394.97	FO
1611	644609.13	4808556.06	401.98	FO	1612	644612.62	4808562.58	403.7	FO	1613	644606.78	4808563.14	404.59	FO	1614	644602.55	4808564.37	405.64	FO
1615	644605.35	4808560.65	403.96	FO	1616	644607.03	4808557.7	402.79	FO	1617	644605.07	4808553.54	401.75	FO	1618	644601.27	4808550.27	401.24	FO
1619	644597.54	4808546.44	400.51	Mto	1620	644592.64	4808549.09	401.97	Mto	1621	644586.59	4808552.4	403.94	Mto	1622	644583.62	4808545.19	402.09	Mto
1623	644584.25	4808539.68	400.17	FO	1624	644579.07	4808535.86	399.74	FO	1625	644576.46	4808530.63	398.54	FO	1626	644575.17	4808524.98	397.02	FO
1627	645150.65	4808146.85	317.8	FO	1628	645170.25	4808152.32	312.69	FO	1629	645158.6	4808160.12	318.3	FO	1630	645162.17	4808140.01	310.89	FO
1631	645153.72	4808148.04	316.77	FO	1632	645154.53	4808150.51	316.97	FO	1633	645155.9	4808153.77	317.34	FO	1634	645158.58	4808157.49	317.4	FO
1635	645160.47	4808157.03	316.54	FO	1636	645159.56	4808149.71	314.53	FO	1637	645158.94	4808146.67	313.97	FO	1638	645159.17	4808143.56	312.96	FO
1639	645161.69	4808142.39	311.7	FO	1640	645164.78	4808146.93	311.98	FO	1641	645163.09	4808147.62	312.75	FO	1642	644999.62	4807830.63	315.41	FO
1643	644996.24	4807844.63	319.36	FO	1644	645013.59	4807835.06	314.58	FO	1645	645009.37	4807847.94	318.71	FO	1646	645008.92	4807846.25	318.3	FO
1647	645009.01	4807844.13	317.71	FO	1648	645008.59	4807841.52	317.1	FO	1649	645008.62	4807838.97	316.31	FO	1650	645007.22	4807836.18	315.78	FO
1651	645004.5	4807834.29	315.66	FO	1652	645001.08	4807833.6	315.86	FO	1653	645000.36	4807836.38	316.77	FO	1654	645000.83	4807838.27	317.2	FO
1655	645000.96	4807839.74	317.58	FO	1656	644998.42	4807840.64	318.06	FO										

C.2 Selección de muestras de entrenamiento y validación

La selección de las muestras de entrenamiento y validación para cada cobertura se detalla a continuación:

Coberturas vías pavimentadas (*Pv*) y pistas de tierra (*Ps*). Como primer paso, las vías de comunicación se digitalizan tomando como información auxiliar la ortoimagen de la zona de estudio, obtenida en formato ráster a partir del centro de descargas de información geográfica de Galicia - CDIX (http://mapas.xunta.gal/visores/descargas/) y la cartografía de vías de comunicación, obtendida en formato vectorial a partir de la sede electrónica de catastro (http://www.sedecatastro.gob.es/). De esta forma se obtiene un *shapefile* con el eje central de las vías de la zona de estudio. Cada trazado se codificó como *1* si la vía es pavimentada y como *2* si se trata de pista forestal. Posteriormente, a partir de la función *spsample* incluida en el paquete *sp* (v.1.2-7) de R se generaron aleatoriamente n puntos sobre el trazado de las vías de comunicación. Cada uno de estos puntos representa el centro de un cuadrado de 2x2 píxeles (para la nube de puntos original, la resolución se estableció en 0.6 m). En la Figura C.1 se incluye el resultado de este proceso para las muestras de entrenamiento de las coberturas *Pv* y *Ps*.

Cobertura edificaciones (*Ed*). Como cartografía de referencia se emplea el *shapefile* de edificaciones en formato vectorial disponible en la sede electrónica de catastro (http://www.sedecatastro.gob.es/). A cada polígono se le aplica un *buffer* interior de 1 m para mitigar discrepancias planimétricas entre los datos LiDAR y la cartografía de edificaciones. Mediante la función *spsample* se generaron aleatoriamente n puntos en el interior de los polígonos que representan las edificaciones de referencia. En la Figura C.2 se incluye el resultado de este proceso para la muestra de entrenamiento de la cobertura *Ed* (color azul).

Coberturas suelo desnudo (*Sd*), vegetación baja (*Vb*) y vegetación arbustiva (*Vr*). Como cartografía de referencia se emplea el *shapefile* de recintos en formato vectorial disponible en

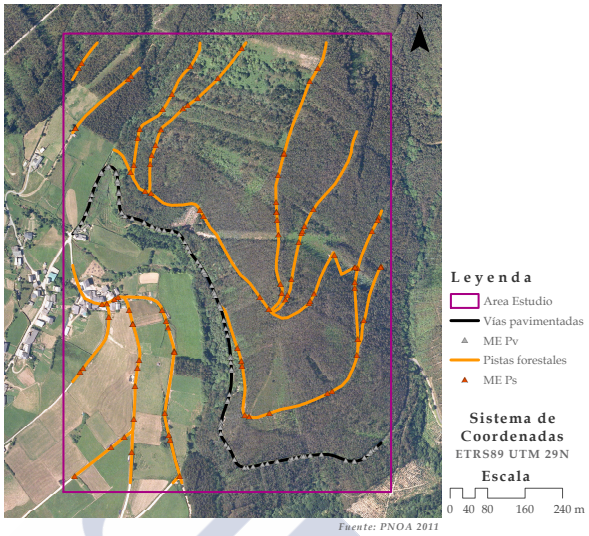

Figura C.1: Resultado gráfico de la digitalización de las vías de comunicación y la selección de las muestras de entrenamiento para las clases Pv y Ps.

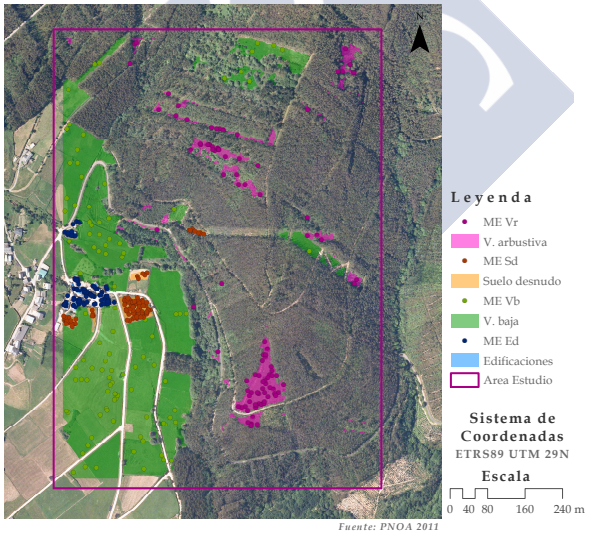

Figura C.2: Resultado gráfico de la selección de las muestras de entrenamiento para las clases Ed, Sd, Vb y Vr.

la sede electrónica de catastro (http://www.sedecatastro.gob.es/). Mediante fotointerpretación tomando como base la ortoimagen y la imagen de intensidad derivada de los datos LiDAR, se clasifican los recintos como *Vb*, *Vr* y *Sd*. Después de la clasificación, los recintos de cada clase de unen y al igual que en caso anterior a cada polígono se le aplica un *buffer* interior de 1 m. Finalmente, mediante la función *spsample* se generaron aleatoriamente n puntos en el interior de los recintos resultantes del proceso anterior. En la Figura C.2 se incluye el resultado de este proceso para las muestras de entrenamiento de las coberturas *Sd*, *Vb* y *Vr* (color naranja, verde y magenta, respectivamente).

Coberturas vegetación arbolada (*Va*) y vegetación mixta (*Vm*). Como cartografía de referencia se emplea el *shapefile* de recintos en formato vectorial disponible en la sede electrónica de catastro (http://www.sedecatastro.gob.es/). Se consideran recintos con vegetación arbolada (tanto *Va* como *Vm*) aquellos que no fueron clasificados como *Sd*, *Vb* y *Vr* ni aquellos que se intersecan con los polígonos de las edificaciones. A continuación, al igual que en el caso anterior, los recintos se fusionan y al resultado se le aplica un *buffer* interior de 1 m (zona sombreada en verde en la Figura C.3). Mediante la función *spsample* se generaron aleatoriamente n puntos en el interior de los polígonos resultantes del proceso anterior. Mediante fotointerpretación tomando como base la ortoimagen y la vista 3D de los datos LiDAR, se clasifican los puntos como *Va* y *Vm* hasta alcanzar el número de observaciones deseada. Finalmente, en la Figura C.3 se incluye el resultado de este proceso para las muestras de entrenamiento de las coberturas *Va* y *Vm* (color verde y rojo, respectivamente).

Finalmente, se tienen 200 observaciones por cobertura (cuadrados de 2x2 píxeles), donde el 50% pasa a formar parte de la muestra de entrenamiento y el 50% restante forman la muestra de validación. Para comprobar que las muestras no contienen errores de asignación de coberturas reales, se comprobó manualmente que a cada cuadrado se le asignara correctamente la cobertura del suelo. Para ello se tomó como base la ortoimagen y la imagen de intensidad derivada de los datos LiDAR. Durante el proceso de validación, a cada observación se le asignará como *cobertura estimada* la cobertura mayoritaria extraída

Figura C.3: Resultado gráfico de la selección de las muestras de entrenamiento para las clases Va y Vm.

de la clasificación.

C.3 Ejecución de *HyCLass* a partir de nubes con diferentes densidades de puntos.

En las siguientes figuras se incluyen el árbol de decisión de *HyClass* adaptando sus parámetros a las diferentes densidades de puntos: Figura C.4 - 4 ptos/m^2; Figura C.5 - 2 ptos/m^2 y Figura C.6 - 1 ptos/m^2.

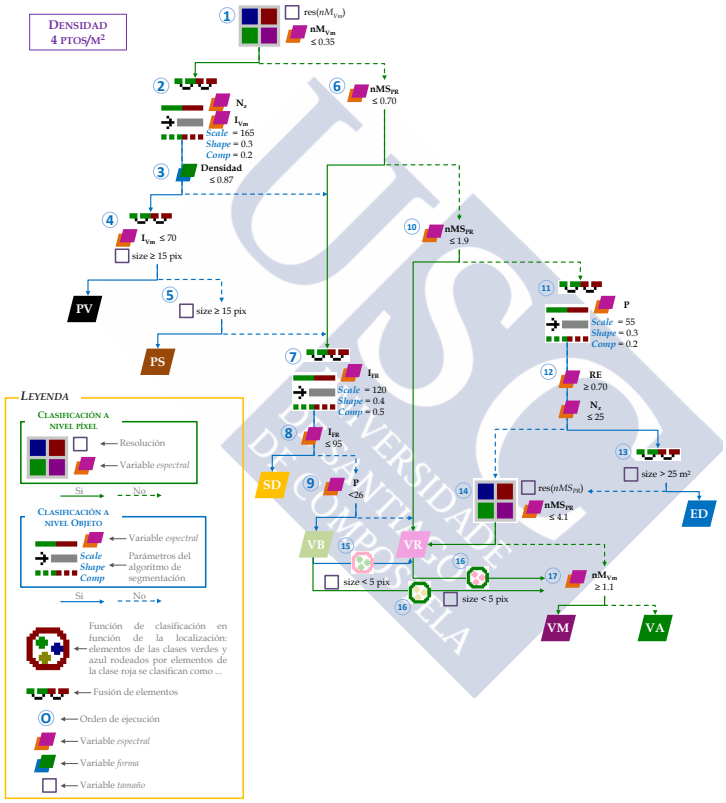

Figura C.4: Árbol de decisión de *HyClass*: parámetros adaptados a una densidad de 4 ptos/m^2.

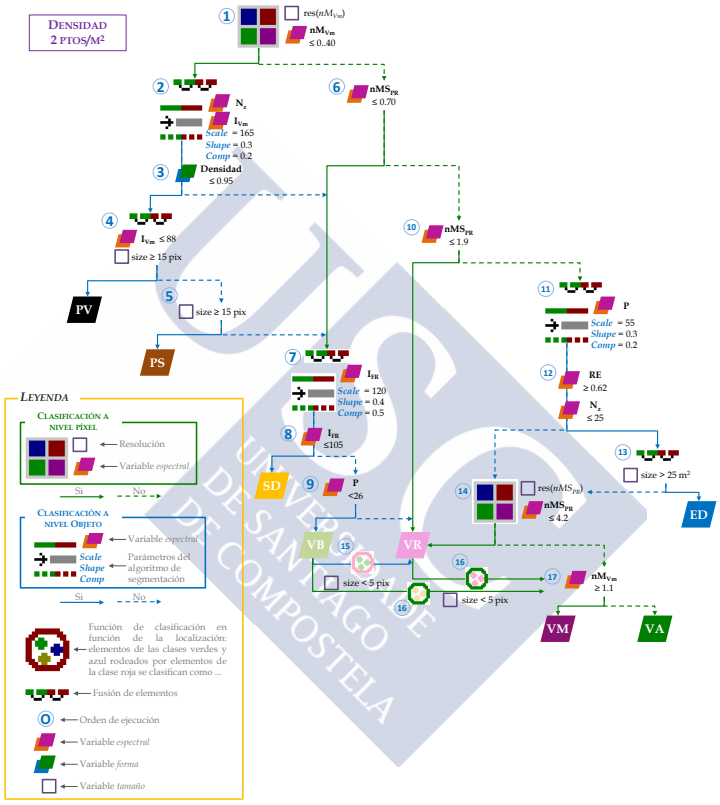

Figura C.5: Árbol de decisión de *HyClass*: parámetros adaptados a una densidad de 2 ptos/m^2.

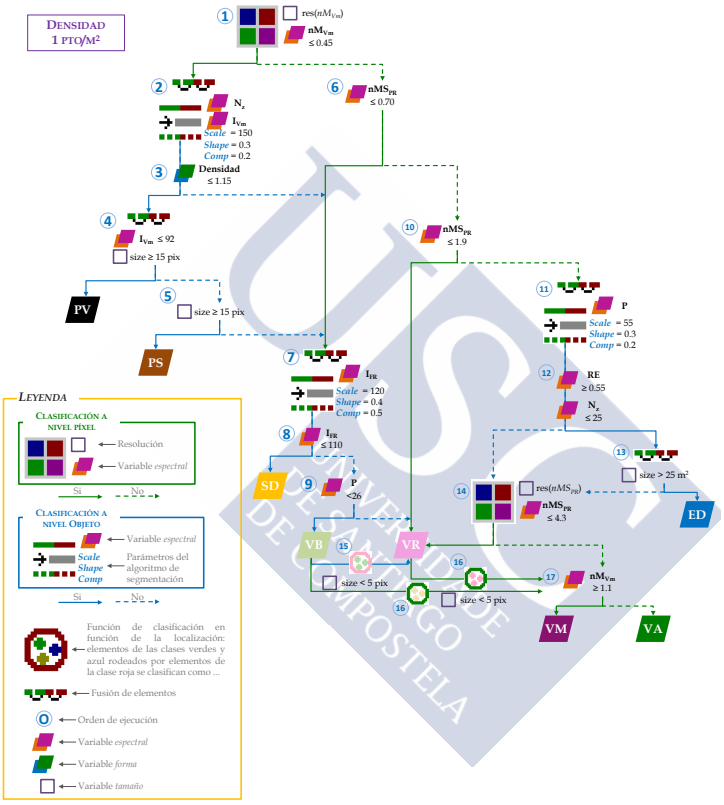

Figura C.6: Árbol de decisión de *HyClass*: parámetros adaptados a una densidad de 1 pto/m^2.

C.4 Resultados cuantitativos de la clasificación HyClass empleando nube de puntos con densidad reducida.

En las Tablas C.10 a C.12 se incluyen las matrices de confusión y los valores de precisión obtenidos para la clasificación de nivel 2 (8 coberturas) al emplear el método de clasificación *HyClass* y las nubes de puntos reducidas.

Tabla C.10: Matriz de confusión usando el método híbrido *HyClass* a partir de una nube de puntos con densidad de 4 ptos/m^2

	HyClass								
	Precisión (IC)= 92.37% (*90.26% - 94.07%*)								
	Desacuerdo = 7.63% Q = 3.42% A = 4.21%								
Referencia → **Clasificación ↓**	**Pv**	**Ps**	**Sd**	**Vb**	**Vr**	**Va**	**Vm**	**Ed**	***Usuario (%)***
Pv	96	1	0	0	0	0	0	0	98.97
Ps	0	87	7	0	1	2	1	0	88.78
Sd	0	0	93	0	0	0	0	0	100.00
Vb	0	1	0	99	8	0	0	0	91.67
Vr	2	3	0	1	86	0	0	0	93.48
Va	2	7	0	0	4	95	16	0	76.61
Vm	0	1	0	0	1	3	83	0	94.32
Ed	0	0	0	0	0	0	0	100	100.0
Productor (%)	96.0	87.0	93.00	99.0	86.0	95.0	83.0	100.0	

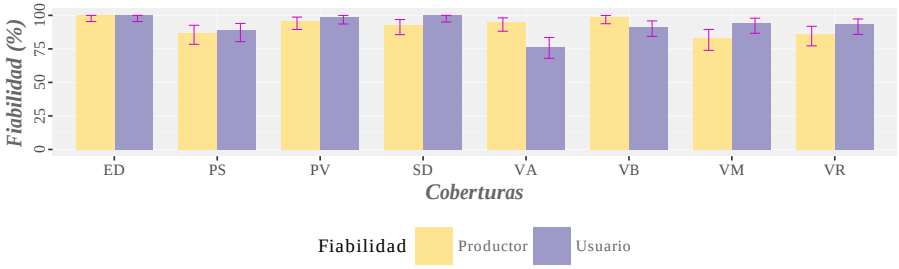

Tabla C.11: Matriz de confusión usando el método híbrido *HyClass* a partir de una nube de puntos con densidad de 2 ptos/m^2

				HyClass					
				Precisión (IC)= 88.12% (*85.63% - 90.24%*)					
				Desacuerdo = 11.88% Q = 2.90% A = 8.97%					
Referencia → **Clasificación ↓**	**Pv**	**Ps**	**Sd**	**Vb**	**Vr**	**Va**	**Vm**	**Ed**	***Usuario (%)***
Pv	97	1	0	0	0	0	0	0	98.98
Ps	0	72	0	1	6	0	0	5	85.71
Sd	0	3	99	0	0	0	0	0	97.06
Vb	1	6	1	96	7	0	0	0	86.49
Vr	0	6	0	3	85	2	1	0	87.63
Va	2	11	0	0	0	82	20	0	71.30
Vm	0	1	0	0	2	16	79	0	80.61
Ed	0	0	0	0	0	0	0	95	100.0
Productor (%)	97.0	72.0	99.00	96.0	85.0	82.0	79.0	95.0	

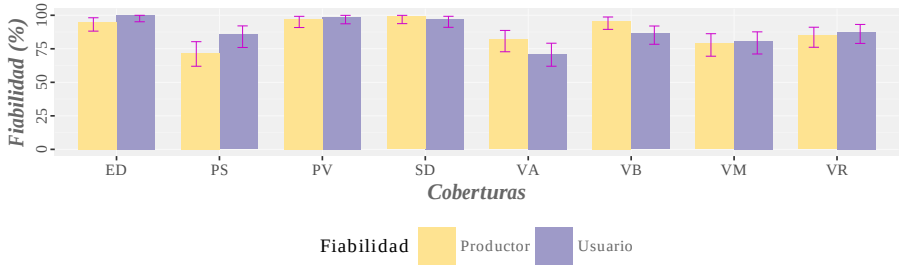

Tabla C.12: Matriz de confusión usando el método híbrido *HyClass* a partir de una nube de puntos con densidad de 1 pto/m^2

	HyClass **Precisión (IC)= 84.00% (*81.23% - 86.43%*) Desacuerdo = 16.00% Q = 5.49% A = 10.51%**								
Referencia → **Clasificación ↓**	**Pv**	**Ps**	**Sd**	**Vb**	**Vr**	**Va**	**Vm**	**Ed**	***Usuario (%)***
Pv	84	1	0	0	0	1	0	0	97.67
Ps	12	51	8	1	0	1	0	0	69.86
Sd	0	3	92	0	0	0	0	0	96.84
Vb	2	6	0	98	10	0	0	0	84.48
Vr	0	11	0	1	83	1	2	0	84.69
Va	2	24	0	0	4	87	15	2	64.93
Vm	0	4	0	0	2	10	83	4	80.58
Ed	0	0	0	0	1	0	0	94	98.95
Productor (%)	84.0	51.0	92.00	98.0	83.0	87.0	83.0	94.0	

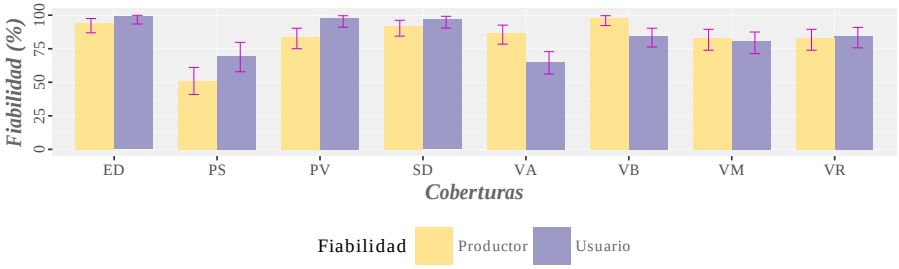

En la siguiente Tabla (Tabla C.13) se incluyen los errores por cantidad y debidos a la posición calculados a partir de los resultados de las clasificaciones de nivel 2 realizadas empleando el método de clasificación *HyClass*, la nube de puntos original y las nubes de puntos reducidas.

Tabla C.13: Medidas de desacuerdo (%) usando el método híbrido *HyClass* en función de la densidad de puntos (clasificación de nivel 2 - 8 coberturas)

	Original		4 ptos/m^2		2 ptos/m^2		1 pto/m^2	
	Q	A	Q	A	Q	A	Q	A
Pv	0.01	0.24	0.37	0.28	0.21	0.26	2.27	0.61
Ps	1.47	0.30	0.11	3.05	1.53	3.68	1.62	7.91
Sd	0.38	0.00	0.97	0.00	0.26	0.23	1.02	0.83
Vb	0.36	0.27	0.98	0.30	1.19	1.10	1.72	0.63
Vr	0.72	0.27	0.85	1.77	0.40	3.19	0.09	3.83
Va	0.95	0.26	2.43	1.48	1.33	4.74	2.86	3.48
Vm	0.09	0.79	1.12	1.54	0.12	4.74	0.81	3.47
Ed	0.15	0.00	0.00	0.00	0.77	0.00	0.57	0.28
Total	*2.06*	*1.06*	*3.42*	*4.21*	*2.90*	*8.97*	*5.49*	*10.51*

En las Tablas C.14 a C.17 se incluyen las matrices de confusión y los valores de precisión obtenidos para la clasificación de nivel 1 (5 coberturas) al emplear el método de clasificación *HyClass* y las nubes de puntos reducidas.

Tabla C.14: Matriz de confusión usando el método híbrido *HyClass* a partir de una nube de puntos con densidad de 8 pto/m^2 (clasificación nivel 1 - 5 coberturas)

			HyClass			
			Precisión (IC)= 99.40% (*98.10% - 99.84%*)			
			Desacuerdo = 0.60% Q = 0.40% A = 0.20%			
Referencia →						
Clasificación ↓	**Pv**	**Sd**	**VnA**	**Va**	**Ed**	***Usuario (%)***
Pv	99	0	0	0	0	100.00
Sd	0	99	0	0	1	99.00
VnA	0	1	100	0	0	99.01
Va	1	0	0	100	0	99.01
Ed	0	0	0	0	99	100.00
Productor (%)	99.00	99.00	100.00	100.00	99.00	

Tabla C.15: Matriz de confusión usando el método híbrido *HyClass* a partir de una nube de puntos con densidad de 4 pto/m^2 (clasificación nivel 1 - 5 coberturas)

			HyClass			
			Precisión (IC)= 97.00% (*94.99% - 98.25%*)			
			Desacuerdo = 3.00% Q = 0.98% A = 2.02%			
Referencia →						
Clasificación ↓	**Pv**	**Sd**	**VnA**	**Va**	**Ed**	***Usuario (%)***
Pv	96	0	0	0	0	100.00
Sd	0	96	1	2	0	96.97
VnA	2	4	95	0	0	94.06
Va	2	0	4	98	0	94.23
Ed	0	0	0	0	100	100.00
Productor (%)	96.00	96.00	95.00	98.00	100.00	

Tabla C.16: Matriz de confusión usando el método híbrido *HyClass* a partir de una nube de puntos con densidad de 2 pto/m^2 (clasificación nivel 1 - 5 coberturas)

HyClass						
Precisión (IC)= 96.40% (*94.26% - 97.79%*)						
Desacuerdo = 3.60% Q = 1.59% A = 2.01%						
Referencia →						
Clasificación ↓	**Pv**	**Sd**	**VnA**	**Va**	**Ed**	***Usuario (%)***
Pv	97	0	0	0	0	100.00
Sd	0	96	2	2	5	91.43
VnA	1	2	97	1	0	96.04
Va	2	2	1	97	0	95.10
Ed	0	0	0	0	95	100.00
Productor (%)	97.00	96.00	97.00	97.00	100.00	

Tabla C.17: Matriz de confusión usando el método híbrido *HyClass* a partir de una nube de puntos con densidad de 1 pto/m^2 (clasificación nivel 1 - 5 coberturas)

HyClass						
Precisión (IC)= 91.20% (*88.28% - 93.47%*)						
Desacuerdo = 8.80% Q = 4.58% A = 4.22%						
Referencia →						
Clasificación ↓	**Pv**	**Sd**	**VnA**	**Va**	**Ed**	***Usuario (%)***
Pv	84	0	0	1	0	100.00
Sd	12	85	0	1	0	86.73
VnA	2	9	96	2	0	88.07
Va	2	6	4	97	6	84.35
Ed	0	0	0	0	94	100.00
Productor (%)	84.00	85.00	96.00	97.00	94.00	

En la Tabla C.18 se incluyen los errores por cantidad y debidos a la posición calculados a partir de los resultados de las clasificaciones de nivel 1 realizadas empleando el método de clasificación *HyClass*, la nube de puntos original y las nubes de puntos reducidas.

Tabla C.18: Medidas de desacuerdo (%) usando el método híbrido *HyClass* en función de la densidad de puntos (clasificación de nivel 1 - 5 coberturas)

	Original		4 ptos/m^2		2 ptos/m^2		1 pto/m^2	
	Q	A	Q	A	Q	A	Q	A
Pv	0.20	0.00	0.79	0.00	0.61	0.00	3.41	0.00
Sd	0.00	0.40	0.19	1.23	0.96	1.63	0.05	5.72
VnA	0.20	0.00	0.22	1.98	0.22	1.19	1.82	1.50
Va	0.20	0.00	0.76	0.82	0.41	1.20	2.76	1.23
Ed	0.20	0.00	0.00	0.00	0.98	0.00	1.12	0.00
Total	*0.40*	*0.20*	*0.98*	*2.02*	*1.59*	*2.01*	*4.58*	*4.22*